NASA TECHNICAL MEMORANDUM

NASA TM 73,238

(NASA-TM-X-73238) LASER VELOCIMETER MEASUREMENTS OF TWO-BLADED HELICOPTER ROTOR FLOW FIELDS (NASA) 158 p HC A08/MF A01 CSCL 01A

N77-25088

Unclas G3/02 30395

NASA TM 73,238

LASER VELOCIMETER MEASUREMENTS OF TWO-BLADED HELICOPTER ROTOR FLOW FIELDS

James C. Biggers, Albert Lee, Kenneth L. Orloff
Ames Research Center
Moffett Field, Calif. 94035

and

Opal J. Lemmer
Ames Directorate, USAAMRDL
Ames Research Center
Moffett Field, Calif. 94035

May 1977

1. Report No.	2. Government Accession No.	3. Recipient's Catalog No.
NASA TM 73,238		

4. Title and Subtitle

LASER VELOCIMETER MEASUREMENTS OF TWO-BLADED HELICOPTER ROTOR FLOW FIELDS

5. Report Date

6. Performing Organization Code

7. Author(s)

James C. Biggers,* Albert Lee,** Kenneth L. Orloff,* and Opal J. Lemmer†

8. Performing Organization Report No.

A-7017

9. Performing Organization Name and Address

*Ames Research Center, NASA and
†Ames Directorate, USAAMRDL
Ames Research Center, Moffett Field, CA 94035

10. Work Unit No.

505-10-21

11. Contract or Grant No.

12. Sponsoring Agency Name and Address

National Aeronautics and Space Administration
Washington, D.C. 20546

13. Type of Report and Period Covered

Technical Memorandum

14. Sponsoring Agency Code

15. Supplementary Notes

**Beam Engineering Co., Inc.
Sunnyvale, Calif. 94086

16. Abstract

This report presents data from a wind tunnel investigation of the flow fields around helicopter rotors. A 2-component laser velocimeter was used to measure the velocity fields of two 2.1 m diameter rotors. A minicomputer-based online data system is described which monitored, reduced, and plotted the results. Tip vortices constitute the primary disturbances in the flow field, but present theories do not predict vortex positions and velocity distributions with sufficient accuracy. Therefore, the measurements in this experiment were concentrated near the vortices, and data were obtained from which vortices and their interactions with a following blade may be studied. The results presented herein provide a base for developing improved rotor wake theories.

17. Key Words (Suggested by Author(s))	18. Distribution Statement
Helicopter Rotor Flow Field Helicopter Inflow Helicopter Rotor Aerodynamics Laser Velocimeter	Unlimited STAR Category 02

19. Security Classif. (of this report)	20. Security Classif. (of this page)	21. No. of Pages	22. Price*
Unclassified	Unclassified	157	$6.25

LASER VELOCIMETER MEASUREMENTS OF TWO-BLADED HELICOPTER ROTOR FLOW FIELDS

James C. Biggers, Albert Lee,* Kenneth L. Orloff
Ames Research Center

Opal J. Lemmer
Ames Directorate, USAAMRDL

SUMMARY

This report presents data from a wind tunnel investigation of the flow fields around helicopter rotors. A 2-component laser velocimeter was used to measure the velocity fields of two 2.1 m diameter rotors. A minicomputer-based online data system is described which monitored, reduced, and plotted the results. Tip vortices constitute the primary disturbances in the flow field, but present theories do not predict vortex positions and velocity distributions with sufficient accuracy. Therefore, the measurements in this experiment were concentrated near the vortices, and data were obtained from which vortices and their interactions with a following blade may be studied. The results presented herein provide a base for developing improved rotor wake theories.

*Beam Engineering Co., Inc., Sunnyvale, Calif. 94086

LIST OF SYMBOLS

a_o	blade precone angle
A_{1_s}	lateral cyclic pitch
a_{1_s}	longitudinal flapping angle relative to shaft
B_{1_s}	longitudinal cyclic pitch
b	number of blades
b_{1_s}	lateral flapping angle relative to shaft
c	blade chord
C_{L_R}/σ	rotor lift coefficient, LIFT/$\rho(\Omega R)^2 bcR$
M_t	rotational tip Mach number
N	rotor rotational speed, rpm
q	tunnel dynamic pressure, $1/2\rho V^2$
R	rotor radius
ΩR	tip speed
U	streamwise velocity component normalized with tip speed, positive downstream
V	free-stream velocity
$V/\Omega R$	tip speed ratio
W	vertical velocity component normalized with tip speed, positive upward
X	distance downstream from hub center
Y	distance toward advancing side from hub center

Z	distance above hub center
α_s	shaft tilt from vertical, positive for top aft
α_{TPP}	tip path plane angle-of-attack, positive leading edge up
$\theta_{0.75}$	collective pitch angle at 0.75R radial station
θ_1	blade twist, from hub center to tip
ρ	air density
σ	rotor solidity, $bc/\Pi R$
ψ	rotor azimuth
Ω	rotor rotational speed, Rad/sec

INTRODUCTION

Previous investigations of helicopter flow fields using a laser velocimeter (LV) have been reported in references 1-4. This new device offers the opportunity to greatly improve knowledge of the complicated flow fields of helicopter rotors. References 1-3 reported methods of application for the LV and data acquisition and analysis techniques being developed. Reference 4 demonstrated that the LV may be used to deduce the lift loading along a rotor blade. It also showed the ability of the LV to measure the detailed velocity structure of model rotor tip vortices.

The blade tip vortices constitute the primary disturbances in the rotor wake, and contribute significantly to the dynamic loads and acoustic characteristics of the helicopter. Various sophisticated theories have been developed to calculate the velocities in the wake, the vortex positions, and the resulting dynamic loads. These have been compared to measured loads, but it is not known whether the discrepancies are due to nonlinear and 3-dimensional effects or to inaccuracies in the predicted vortex characteristics. It is, therefore, desirable to obtain accurate measurements of the rotor wake, the vortex positions, and the vortex characteristics. The present investigation was undertaken to begin to fulfill these requirements. A laser velocimeter was used because of its ability to make accurate, nonintrusive flowfield measurements.

A new data system was developed, based on the requirements for higher speed data acquisition with online processing and plotting, as outlined in reference 4. It was also felt that a system based on a minicomputer could operate interactively with the experimenter to provide monitoring and control of the investigation. The software and new hardware to perform these functions is described herein.

The earlier experiments (refs. 3 and 4) and part of the present one used zero-twist blades. However, blade twist has a significant effect on blade loading, and hence on the tip vortices. Therefore, the present investigation also utilized blades having about 11 deg of negative linear twist. These blades are more representative of current helicopters, and these results should then be more useful to the industry.

LASER VELOCIMETER (LV) AND SIGNAL PROCESSING

The LV used in this investigation is the same instrument as is described in references 3 and 4, but with certain improvements. An acousto-optic modulator (Bragg cell) has been incorporated into the channel of the velocimeter which senses vertical velocity in the wind tunnel. The Bragg cell was inserted into the optical path of one of the pair of beams. The cell causes the frequency of the output beam to be shifted by the magnitude of the acoustic frequency used to excite the cell, in this case, 40 MHz. Then, where the pair of beams cross, in the tunnel at the focal volume, the backscattered light is shifted by the same frequency. This means that with zero vertical velocity in the wind tunnel, the output from the "vertical" photomultiplier is 40 MHz. This provides for directional sensitivity and a very accurate measurement of even a zero value for this velocity component. The measured velocity components (streamwise and vertical) remain uncoupled and rotation of the LV about its optical axis to avoid directional ambiguity is not required as in the previous investigations.

Improved counter-type processing electronics have now been used to handle the LV signals. These new units incorporate a multi-level detection concept which checks the quality and shape of each burst signal (in addition to a periodicity check) before validation and transfer of the data. This feature has greatly improved the data processing rate and nearly eliminated the possibility of processing spurious noise signals.

Another significant improvement in this investigation has been the incorporation of a high-speed minicomputer with the peripherals required for compatibility with the LV signal processors and other electronics. The digital outputs of the counter type processors are now accepted on a non-multiplexed basis which noticably reduces the time required to collect any given number of velocity samples. In addition, the computer system is capable of accepting a number of analog inputs which are digitized in a software-specified sequence. In this experiment, the X, Y, and Z locations of the LV focal volume were analog inputs as well as the tunnel dynamic pressure and rotor RPM. The computer was instructed to test the q and RPM while acquiring LV data to insure the correct flapping position of the rotor blade during the "data window." If these values were found to be outside of prescribed limits, then the LV data acquisition was inhibited and a CRT terminal message was displayed to the operator until the values returned within these limits. This feature greatly reduced scatter in the data due to inconsistent blade flapping position. In all, the data acquisition time in this latest series of experiments has been reduced by nearly one order of magnitude as compared to the time required for the investigation reported in reference 4.

DATA ACQUISITION, REDUCTION, AND PRESENTATION

A PDP 11/05 minicomputer with four floppy disk drives and a Tektronix 4014-1 CRT terminal with a hard copy unit were used in this investigation. A block diagram of the data system is shown on Figure 1. It was possible to store all of the data from this test on one floppy disk.

The software program used to acquire and process the incoming information provided the experimenter with computer control over data gathering and display. The Tektronix Graphics Terminal software has several features that have made this possible. The "Write-Thru" mode enabled informative messages to appear on the CRT screen but not on the hard copy. This allowed the engineer to monitor tunnel conditions and LV focal point location from the CRT terminal.

Extensive use was also made of a software feature which allows the program to treat any keyboard character as a special interrupt input that does not appear on the CRT screen. The character is stored and, at the appropriate time, the program interrogates the system to see if any keyboard entries have been made, then takes the indicated action. These actions are shown schematically in Figure 2.

Data were displayed as plotted points on suitably labeled axes along with computed and costant test information (run number, computed advance ratio, tip speed, etc.). As each point was taken, the velocity components were plotted on the screen and the experimenter was asked, via a "write-thru" message on the CRT, if this was a point that was reasonable or if for some reason the data should be acquired again to insure repeatability. If the response (a keyboard character) was positive ("Y"), it was written on the disk; if not ("N"), it was discarded. If the screen became cluttered with discarded points, the letter "R" entered at the keyboard caused the old plot to be erased and a new plot of only saved points to be produced. Data gathering could then be continued. Also, if the axes scaling could not accommodate the data being acquired, the letter "A" entered at the keyboard caused all scaling information to be printed out with instructions on how to change it. Plots were then redrawn with the new scaling and all data acquired thus far were replotted. It was not necessary for the experimenter to halt the program in the middle of a run because the range which the data might span had been misjudged. Additionally, these data plots could be redrawn at a later time with the same program using any scaling desired.

Use of the minicomputer and the software described above allowed the experimenters to concentrate the measurements more in the area where the vortices were located. Large step sizes were used during the first part of a traverse. The approximate position of the vortex was then obvious from the online plot. Small step sizes were then used in the vicinity of the vortex to define its position and velocity structure. It is estimated that ten times as many measurements would have been required to obtain the same information on the vortices without the online features of this data system.

ROTORS AND OPERATING CONDITIONS

For this investigation, a two-bladed teetering rotor system was operated in the 7- by 10-Foot Wind Tunnel of the U. S. Army Air Mobility Research and Development Laboratory, Ames Directorate. Figure 3 is a photograph of the test setup, showing the laser beams being projected into the test section from the observation window on the left. The test setup is shown schematically in Figure 4, which also illustrates the coordinate system used.

Two sets of blades were used, one with zero twist blades and the other with -11 deg twist blades. Both sets are made of balsa wood covered with fiberglass and have aluminum spars. The same hub was used for both sets of blades. The blade properties and test conditions are tabulated below. No force measurements were made in the tests of zero twist blades. However, the same operating conditions were repeated for reference 5; and the rotor lift coefficient was, therefore, quoted in the table below.

Blade Properties	Zero-Twist Blades	-11 deg Twist Blades
Number of blades, b	2	2
Hub precone angle, a_o	1.5 deg	1.5 deg
Rotor radius, R	1.066 m	1.045 m
Blade chord, c	0.1080 m	0.0762 m
Rotor solidity, σ	0.0644	0.0464
Blade twist, θ_1	0.0 deg	-10.89 deg (nominal -11 deg)

Blade Properties	Zero-Twist Blades	-11 deg Twist Blades
Blade taper ratio	1.0	1.0
Airfoil	NACA 0012	NACA 0012
Flapping hinge undersling	0.0086R	0.0086R

Operating Conditions, Zero-Twist Blades	
Advance ratio, $V/\Omega R$	0.18
Rotor rotational speed, N	600 rpm
Rotor tip speed, ΩR	67 m/sec
Rotational tip mach number, M_t	0.20
Shaft angle-of-attack, α_s	-10.0 deg
Collective pitch, $\theta_{.75}$	8.5 deg
Cyclic pitch relative to shaft, A_{1_s}, B_{1_s}	0.0
Longitudinal flapping, [illegible]$_s$	3.40 deg (ref. 4)
Lateral flapping, b_{1_s}	1.55 deg (ref. 3)
Rotor lift coefficient, C_{L_R}/σ	0.074 (ref. 5)

Operating Conditions, -11 deg Twist Blades	
Tip speed ratio, $V/\Omega R$	0.137, 0.18
Rotor rotational speed, N	600, 1000 rpm
Rotor tip speed, ΩR	65.5 m/sec
	109 m/sec
Rotational tip mach number, M_t	0.19[illegible], 0.226

Operating Conditions, -11 deg Twist Blades (cont)

Shaft angle-of-attack, α_s	-0.5, -10.0 deg	
Collective pitch, $\theta_{.75}$	2.94 to 10.1 deg	
Cyclic pitch relative to shaft, a_{1_s}, b_{1_s}	0.0	
Longitudinal flapping, a_{1_s}	4.5 deg	for α_s = -10 deg and $\theta_{.75}$ = 10.1 deg*
Lateral flapping b_{1_s}	3.5 deg	
Rotor lift coefficient, C_{L_R}/σ	.0923	

*Flapping and force measurements are not available for the other conditions

RESULTS

Velocity distributions of the rotor flowfield at various operating conditions were measured by traversing the LV focal volume along the X, Y, or Z coordinates, and recording the vertical and streamwise velocity components. Each measurement was obtained by taking the mean of 20 samples, strobed when the rotor was at the specified azimuth. The measurements then represent a mean instantaneous velocity in this periodic flow environment. The velocities have been normalized by the rotor tip speed, and the positions have been normalized by blade chord. It should be noted that the two sets of blades have different aspect ratios, so the blade tips are at 9.88 chords for the zero-twist blades and at 13.71 chords for the twisted blades.

Data from the zero twist blades are presented in Figures 5-1 through 5-14. These data were all at the same operating conditions and strobing azimuth, as indicated in Table I and on the figures. Table I summarizes the data on the zero twist blades, and may be used as an index to the plots. Although not included here, the 300 rpm operating condition presented in references 3 and 4 was repeated to verify that the revised LV and data system produced the same results as the previous system. Excellent repeatability was found.

The majority of the present investigation was devoted to the -11° linear twist blades, and these results are presented in Figures 6 through 16. Many traverses were made, at strobing azimuths from 50.6

to 90 deg. At each azimuth, several traverses were made to locate the vortex, followed by one or more traverses through the core of the vortex. The plots are summarized in Table II, which may be used as an index. The traverses through the cores may be recognized by the higher peak velocities and the minimum variations in the streamwise velocity profiles. For example, Figures 7-12 through 7-15 show the results of a series of traverses strobing at an azimuth of 90 deg, giving the velocity distributions in the vicinity of the blade and the proceding vortex. Figure 7-13 gives the velocity distribution through the vortex core. From these results it is apparent that the vortex core is located at X = 0.76C, Y = 11.3C, and Z = -0.39C. The peak rotational velocity, one-half of the peak-to-peak velocity, is 0.12 times the tip speed.

The extent of these flow surveys was limited to the ranges given in the figures due to the limited size of the wind tunnel observation window. Also, only one side of the rotor disk could be surveyed due to the restricted operating range of the LV. For surveys of the retreating side of the rotor, a set of blades must be used which rotate opposite to the ones used here, because there is space for the LV only on one side of the test section.

In spite of the limitations discussed above, this set of results should be very useful in checking and improving methods for predicting the details of the rotor flow field.

REFERENCES

1. Sullivan, John P.: An Experimental Investigation of Vortex Rings and Helicopter Wakes Using a Laser Doppler Velocimeter. M.I.T. Aerophysics Laboratory TR-183, June 1973.

2. Landgrebe, A. J. and Johnson, B. V.: Measurement of Model Helicopter Rotor Flow Velocities with a Laser Doppler Velocimeter. Tech. Note, J. Amer. Heli. Soc., Vol. 19, No. 3, July 1974.

3. Biggers, James C. and Orloff, Kenneth L.: Laser Velocimeter Measurements of the Helicopter Rotor - Induced Flow Field. J. Amer. Heli. Soc., Vol. 20, No. 1, January 1975.

4. Biggers, James C.; Chu, Sing; and Orloff, Kenneth L.: Laser Velocimeter Measurements of Rotor Blade Loads and Tip Vortex Rollup. Preprint No. 900, 31st Annual National Forum of the Amer. Heli. Soc., Washington, D.C., May 1975.

5. Dadone, L. U. and Fukushima, T.: Investigation of Rotor Blade Element Airloads for a Teetering Rotor in the Blade Stall Regime NASA CR-137534-A, October 1975.

TABLE 1

TEST PARAMETERS OF THE FLOWFIELD MEASUREMENTS (ZERO-TWIST BLADES)

Zero-twist Blade				Traverses					
Plot #	N (rpm)	V/ΩR	$\theta_{0.75}$ (deg)	α_s (deg)	ψ (deg)	Traversing x/c	y/c	z/c	Run No.
5-1	600	0.18	8.5	-10	90	-2.00	7.0	Var.	5
5-2	600	0.18	8.5	-10	90	-2.55	7.0	Var.	8
5-3	600	0.18	8.5	-10	90	-2.81	7.0	Var.	6
5-4	600	0.18	8.5	-10	90	-2.55	Var.	-0.86	9
5-5	600	0.18	8.5	-10	90	-1.28	7.78	Var.	11
5-6	600	0.18	8.5	-10	90	-1.49	7.79	Var.	10
5-7	600	0.18	8.5	-10	90	0	Var.	-0.61	17
5-8	600	0.18	8.5	-10	90	1.75	4.98	Var.	18
5-9	600	0.18	8.5	-10	90	1.73	Var.	-1.71	19
5-10	600	0.18	8.5	-10	90	1.99	7.56	Var.	12
5-11	600	0.18	8.5	-10	90	1.99	9.01	Var.	13
5-12	600	0.18	8.5	-10	90	1.99	9.10	Var.	15
5-13	600	0.18	8.5	-10	90	1.99	Var.	-0.47	16
5-14	600	0.18	8.5	-10	90	1.99	Var.	-0.49	14

TABLE 2

TEST PARAMETERS OF THE FLOWFIELD MEASUREMENTS
(-11 DEG TWIST BLADES)

Plot #	N (rpm)	$V/\Omega R$	$\theta_{0.75}$ (deg)	α_s (deg)	ψ (deg)	Traversing x/c	y/c	z/c	Run No.
6-1	600	0.18	8.5	-10	90	-3.54	9.90	Var.	103
6-2	600	0.18	8.5	-10	90	-3.54	10.00	Var.	104
6-3	600	0.18	8.5	-10	90	-3.54	Var.	-0.80	101
6-4	600	0.18	8.5	-10	90	-3.54	Var.	-0.85	102
7-1	600	0.18	10.1	-10	90	-3.50	10.00	Var.	105
7-2	600	0.18	10.1	-10	90	-3.50	Var.	-0.76	107
7-3	600	0.18	10.1	-10	90	-3.52	Var.	-0.80	106
7-4	600	0.18	10.1	-10	90	-2.00	Var.	-0.64	114
7-5	600	0.18	10.1	-10	90	-1.98	10.96	Var.	108
7-6	600	0.18	10.1	-10	90	-1.40	Var.	-0.49	118
7-7	600	0.18	10.1	-10	90	-1.40	11.26	Var.	115
7-8	600	0.18	10.1	-10	90	-1.00	Var.	-0.51	117
7-9	600	0.18	10.1	-10	90	-1.00	Var.	-0.56	116
7-10	600	0.18	10.1	-10	90	-1.00	Var.	-0.61	110
7-11	600	0.18	10.1	-10	90	-0.99	11.49	Var.	109
7-12	600	0.18	10.1	-10	90	-0.76	Var.	-0.39	128
7-13	600	0.18	10.1	-10	90	-0.74	Var.	-0.39	131
7-14	600	0.18	10.1	-10	90	-0.75	Var.	-0.45	127
7-15	600	0.18	10.1	-10	90	-0.75	Var.	-0.49	113
7-16	600	0.18	10.1	-10	90	-0.48	Var.	-0.41	112
7-17	600	0.18	10.1	-10	90	-0.50	Var.	-0.46	125
7-18	600	0.18	10.1	-10	90	-0.50	Var.	-0.53	123
7-19	600	0.18	10.1	-10	90	-0.50	11.39	Var.	120
7-20	600	0.18	10.1	-10	90	-0.49	11.57	Var.	111
7-21	600	0.18	10.1	-10	90	-0.50	11.60	Var.	119
7-22	600	0.18	10.1	-10	90	-0.50	11.68	Var.	122
7-23	600	0.18	10.1	-10	90	0.00	Var.	-0.24	129
7-24	600	0.18	10.1	-10	90	1.30	Var.	-0.39	143
7-25	600	0.18	10.1	-10	90	1.25	Var.	-0.45	130
7-26	600	0.18	10.1	-10	90	1.20	Var.	-0.50	138
7-27	600	0.18	10.1	-10	90	1.20	Var.	-0.60	137

TABLE 2 (CONT)

Plot #	N (rpm)	V/ΩR	$\epsilon_{0.75}$ (deg)	α_s (deg)	ψ (deg)	Traversing x/c	y/c	z/c	Run No.
7-28	600	0.18	10.1	-10	90	1.59	Var.	-0.32	147
7-29	600	0.18	10.1	-10	90	1.60	Var.	-0.41	145
7-30	600	0.18	10.1	-10	90	1.59	Var.	-0.45	144
7-31	600	0.18	10.1	-10	90	1.59	Var.	-0.49	139
7-32	600	0.18	10.1	-10	90	1.69	Var.	-0.48	155
7-33	600	0.18	10.1	-10	90	1.84	Var.	-0.47	153
7-34	600	0.18	10.1	-10	90	2.19	Var.	-0.27	148
7-35	600	0.18	10.1	-10	90	2.21	Var.	-0.57	142
7-36	600	0.18	10.1	-10	90	2.19	Var.	-0.60	141
7-37	600	0.18	10.1	-10	90	2.50	Var.	-0.50	133
7-38	600	0.18	10.1	-10	90	2.50	Var.	-0.92	135
7-39	600	0.18	10.1	-10	90	3.51	Var.	-0.07	149
7-40	600	0.18	10.1	-10	90	4.84	Var.	-0.00	191
7-41	600	0.18	10.1	-10	90	4.84	Var.	-0.13	191w
7-42	600	0.18	10.1	-10	90	4.83	Var.	-0.25	189
7-43	600	0.18	10.1	-10	90	4.82	Var.	-0.35	190
8-1	600	0.18	10.1	-10	77.3	1.01	Var.	-0.34	159
8-2	600	0.18	10.1	-10	77.3	1.01	Var.	-0.37	160
8-3	600	0.18	10.1	-10	77.3	1.01	Var.	-0.39	158
8-4	600	0.18	10.1	-10	77.3	1.01	Var.	-0.42	157
8-5	600	0.18	10.1	-10	77.3	1.01	12.34	Var.	156
8-6	600	0.18	10.1	-10	77.3	1.50	Var.	-0.26	165
8-7	600	0.18	10.1	-10	77.3	1.50	Var	-0.30	164
8-8	600	0.18	10.1	-10	77.3	1.50	Var.	-0.35	163
8-9	600	0.18	10.1	-10	77.3	1.50	Var.	-0.38	[illegible]
8-10	600	0.18	10.1	-10	77.3	1.50	12.37	Var.	161
8-11	600	0.18	10.1	-10	77.3	1.64	Var.	-0.26	[illegible]
8-12	600	0.18	10.1	-10	77.3	1.64	Var.	-0.29	[illegible]
8-13	600	0.18	10.1	-10	77.3	1.64	Var.	-0.36	[illegible]
8-14	600	0.18	10.1	-10	77.3	1.64	12.30	Var.	[illegible]

TABLE 2 (CONT)

Plot #	N (rpm)	V/ΩR	$\theta_{0.75}$ (deg)	α_s (deg)	ψ (deg)	Traversing x/c	y/c	z/c	Run No.
8-15	600	0.18	10.1	-10	77.3	1.99	Var.	-0.25	168
8-16	600	0.18	10.1	-10	77.3	2.00	Var.	-0.28	169
8-17	600	0.18	10.1	-10	77.3	1.99	Var.	-0.31	170
8-18	600	0.18	10.1	-10	77.3	1.99	12.44	Var.	167
8-19	600	0.18	10.1	-10	77.3	2.48	Var.	-0.26	172
8-20	600	0.18	10.1	-10	77.3	2.49	Var.	-0.32	171
8-21	600	0.18	10.1	-10	77.3	2.51	12.47	Var.	166
8-22	600	0.18	10.1	-10	77.3	4.28	Var.	-0.12	182
8-23	600	0.18	10.1	-10	77.3	4.28	Var.	-0.21	180
8-24	600	0.18	10.1	-10	77.3	4.27	Var.	-0.29	181
8-25	600	0.18	10.1	-10	77.3	4.28	Var.	-0.30	173
8-26	600	0.18	10.1	-10	77.3	4.28	13.25	Var.	179
9-1	600	0.18	10.1	-10	70.3	1.34	Var.	-0.24	184
9-2	600	0.18	10.1	-10	70.3	1.34	Var.	-0.31	183
9-3	600	0.18	10.1	-10	70.3	1.35	Var.	-0.5	186
9-4	600	0.18	10.1	-10	70.3	1.35	12.78	Var.	185
9-5	600	0.18	10.1	-10	70.3	3.67	Var.	-0.24	174
9-6	600	0.18	10.1	-10	70.3	4.01	Var.	-0.20	175
9-7	600	0.18	10.1	-10	70.3	3.99	Var.	-0.25	176
10.1	600	0.18	10.1	-10	60.5	3.56	Var.	-0.17	177
10.2	600	0.18	10.1	-10	60.5	3.57	Var.	-0.20	178
11-1	1000	0.137	4.67	-0.5	74.5	1.43	Var.	0.59	208
11-2	1000	0.137	4.67	-0.5	74.5	1.43	Var.	0.49	207
11-3	1000	0.137	4.67	-0.5	74.5	1.43	Var.	0.31	206
11-4	1000	0.137	4.67	-0.5	74.5	1.43	Var.	0.21	205
11-5	1000	0.137	4.67	-0.5	74.5	1.41	Var.	0.01	204
11-6	1000	0.137	4.67	-0.5	74.5	1.41	Var.	-0.20	201
11-7	1000	0.137	4.67	-0.5	74.5	1.42	Var.	-0.45	202
11-8	1000	0.137	4.67	-0.5	74.5	1.41	Var.	-0.59	203
12-1	1000	0.137	4.67	-0.5	64.7	Var.	8.50	0.29	211
12-2	1000	0.137	4.67	-0.5	64.7	Var.	8.50	0.01	210
12-3	1000	0.137	4.67	-0.5	64.7	Var.	8.49	-0.16	212
12-4	1000	0.137	4.67	-0.5	64.7	4.00	Var.	0.48	209

TABLE 2 (CONT)

Plot #	N (rpm)	$V/\Omega R$	$\theta_{0.75}$ (deg)	α_s (deg)	ψ (deg)	Traversing x/c	y/c	z/c	Run No.
13-1	1000	0.137	2.94	-0.5	90	2.83	Var.	0.39	236
13-2	1000	0.137	2.94	-0.5	90	2.83	Var.	0.30	235
13-3	1000	0.137	2.94	-0.5	90	2.82	Var.	-0.36	237
14-1	1000	0.137	2.94	-0.5	64.7	2.00	Var.	0.41	234
14-2	1000	0.137	2.94	-0.5	64.7	1.99	Var.	0.34	232
14-3	1000	0.137	2.94	-0.5	64.7	1.99	Var.	0.31	233
14-4	1000	0.137	2.94	-0.5	64.7	4.00	Var.	0.51	226
14-5	1000	0.137	2.94	-0.5	64.7	4.00	Var.	0.35	228
14-6	1000	0.137	2.94	-0.5	64.7	4.01	Var.	0.30	229
14-7	1000	0.137	2.94	-0.5	64.7	4.00	Var.	0.26	230
14-8	1000	0.137	2.94	-0.5	64.7	4.00	Var.	0.20	231
14-9	1000	0.137	2.94	-0.5	64.7	4.01	Var.	-0.01	227
15-1	1000	0.137	2.94	-0.5	60.5	Var.	7.49	0.49	217
15-2	1000	0.137	2.94	-0.5	60.5	Var.	7.48	0.29	216
15-3	1000	0.137	2.94	-0.5	60.5	Var.	7.50	0.00	215
15-4	1000	0.137	2.94	-0.5	60.5	Var.	7.49	-0.31	214
15-5	1000	0.137	2.94	-0.5	60.5	Var.	7.49	-0.59	218
15-6	1000	0.137	2.94	-0.5	60.5	Var.	7.49	-0.79	219
15-7	1000	0.137	2.94	-0.5	60.5	Var.	5.98	-0.41	213
16-1	1000	0.137	2.94	-0.5	50.6	Var.	7.48	0.30	221
16-2	1000	0.137	2.94	-0.5	50.6	Var.	7.49	-0.01	222
16-3	1000	0.137	2.94	-0.5	50.6	Var.	7.49	-0.29	220
16-4	1000	0.137	2.94	-0.5	50.6	Var.	7.48	-0.50	223
16-5	1000	0.137	2.94	-0.5	50.6	4.00	8.23	Var.	224

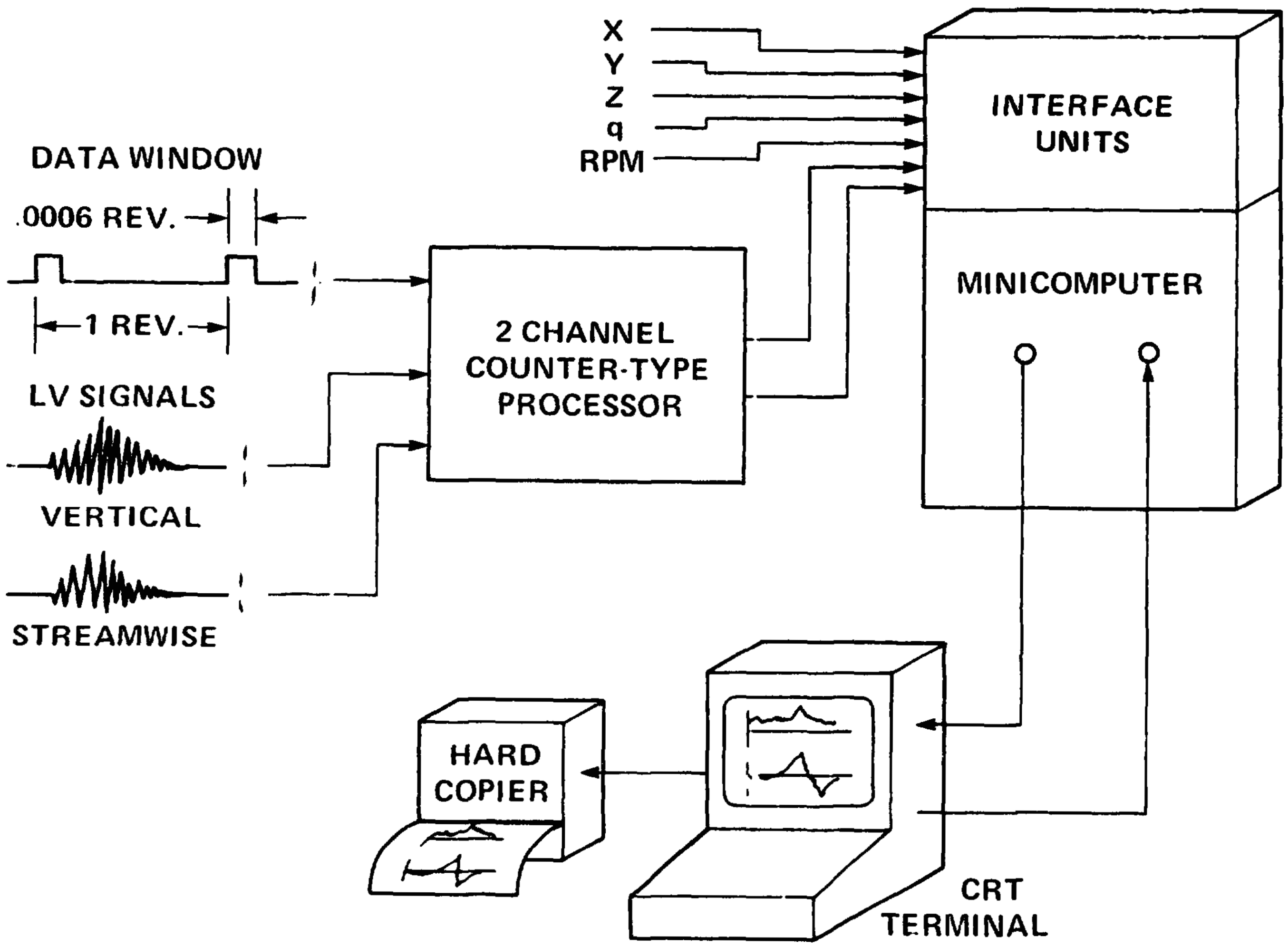

Figure 1. Block diagram of data processing system.

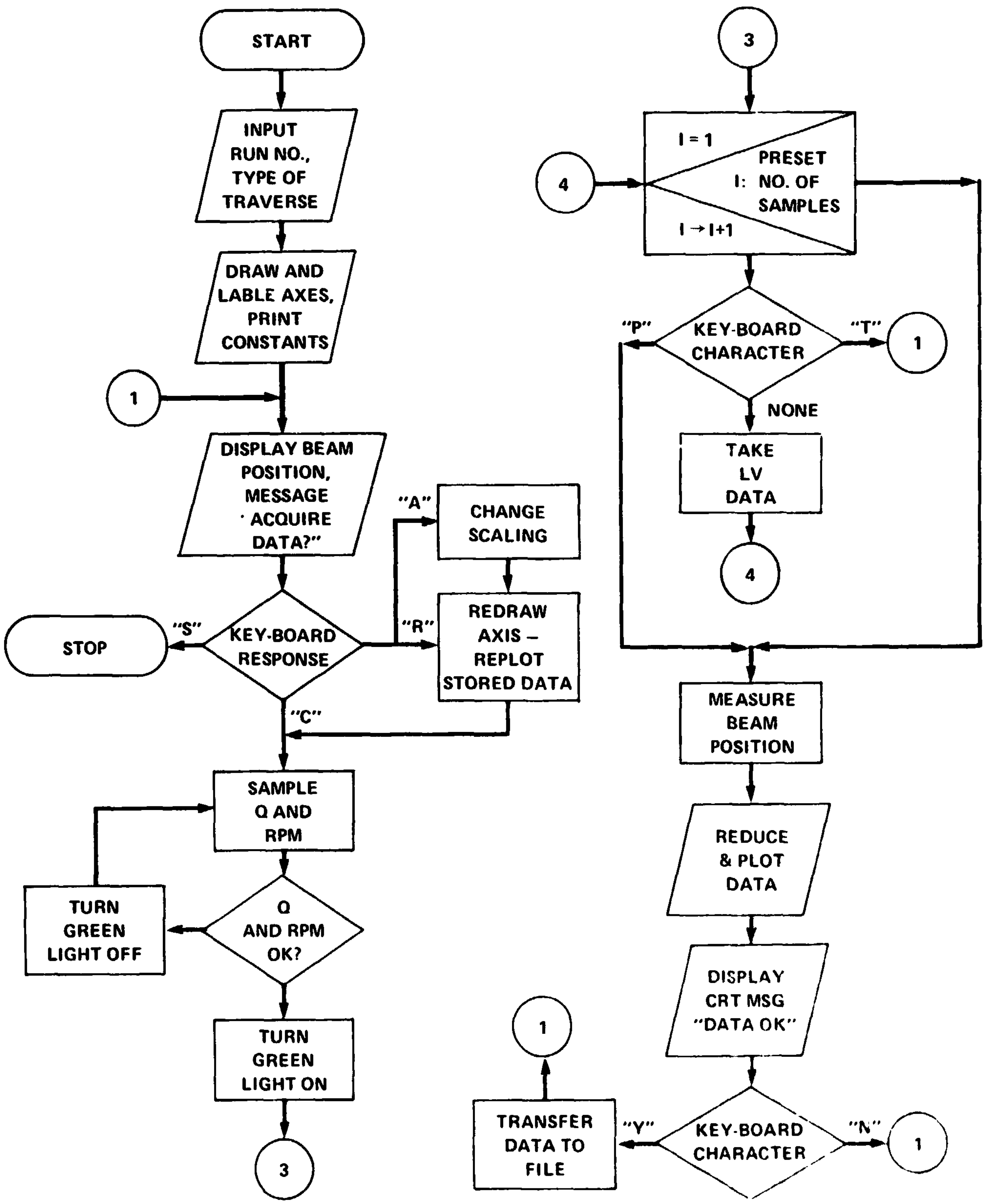

Figure 2. Minicomputer software flow chart.

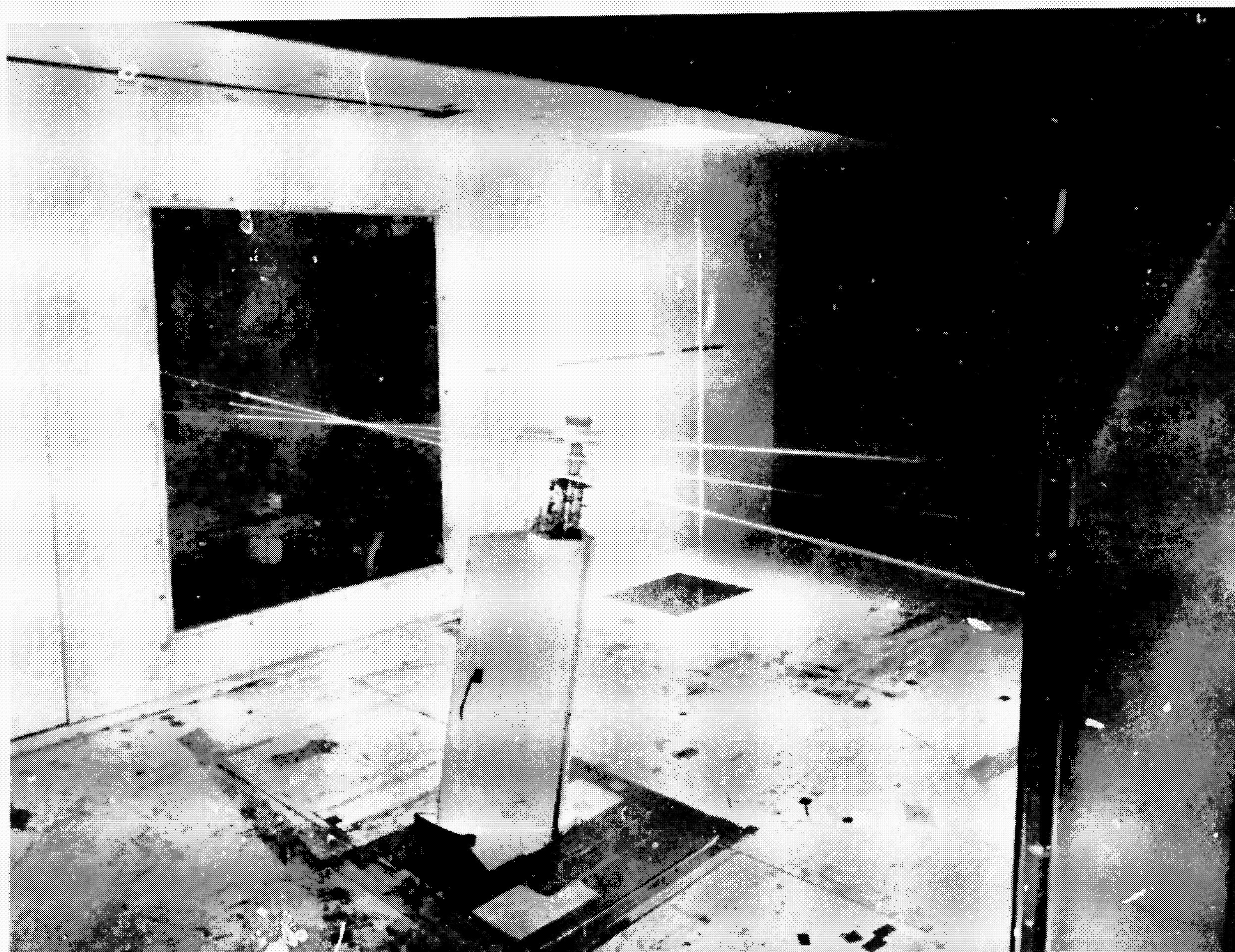

Figure 3. Rotor and laser velocimeter in operation.

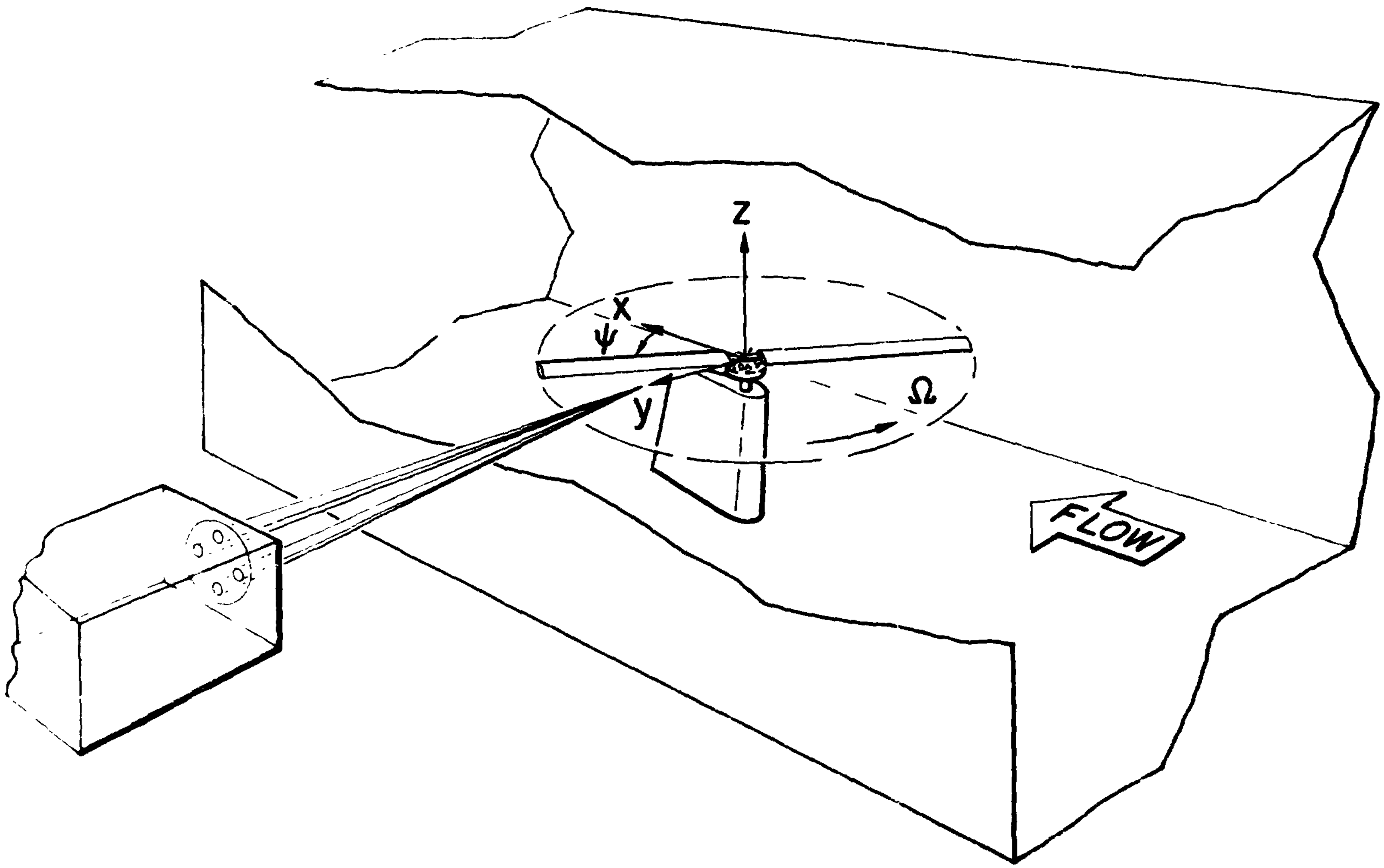

Figure 4. Coordinate system.

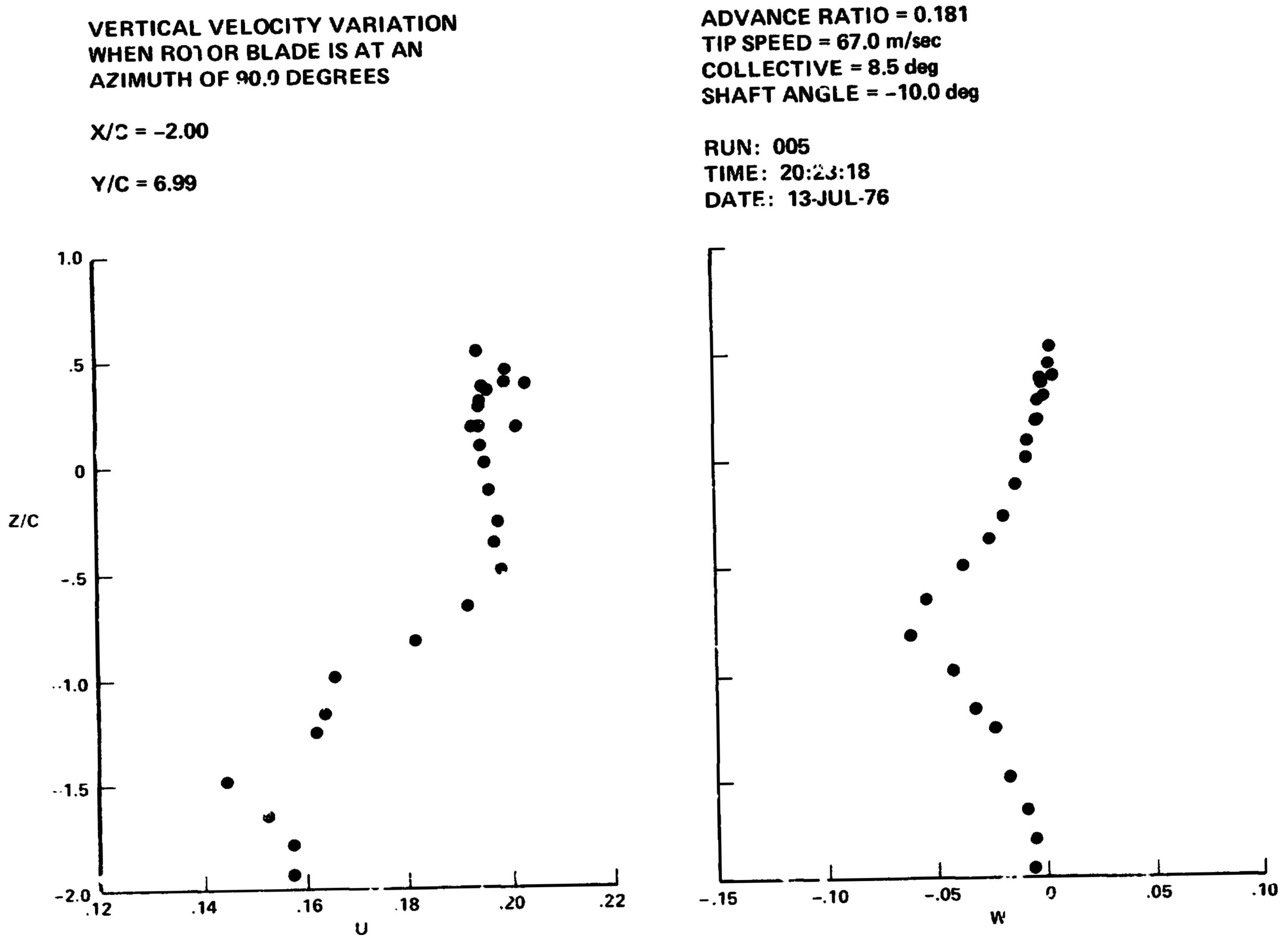

5-1. Vertical traverse, x/c = -2.00, y/c = 7.00

Figure 5. Flowfield velocities from the zero-twist blades.

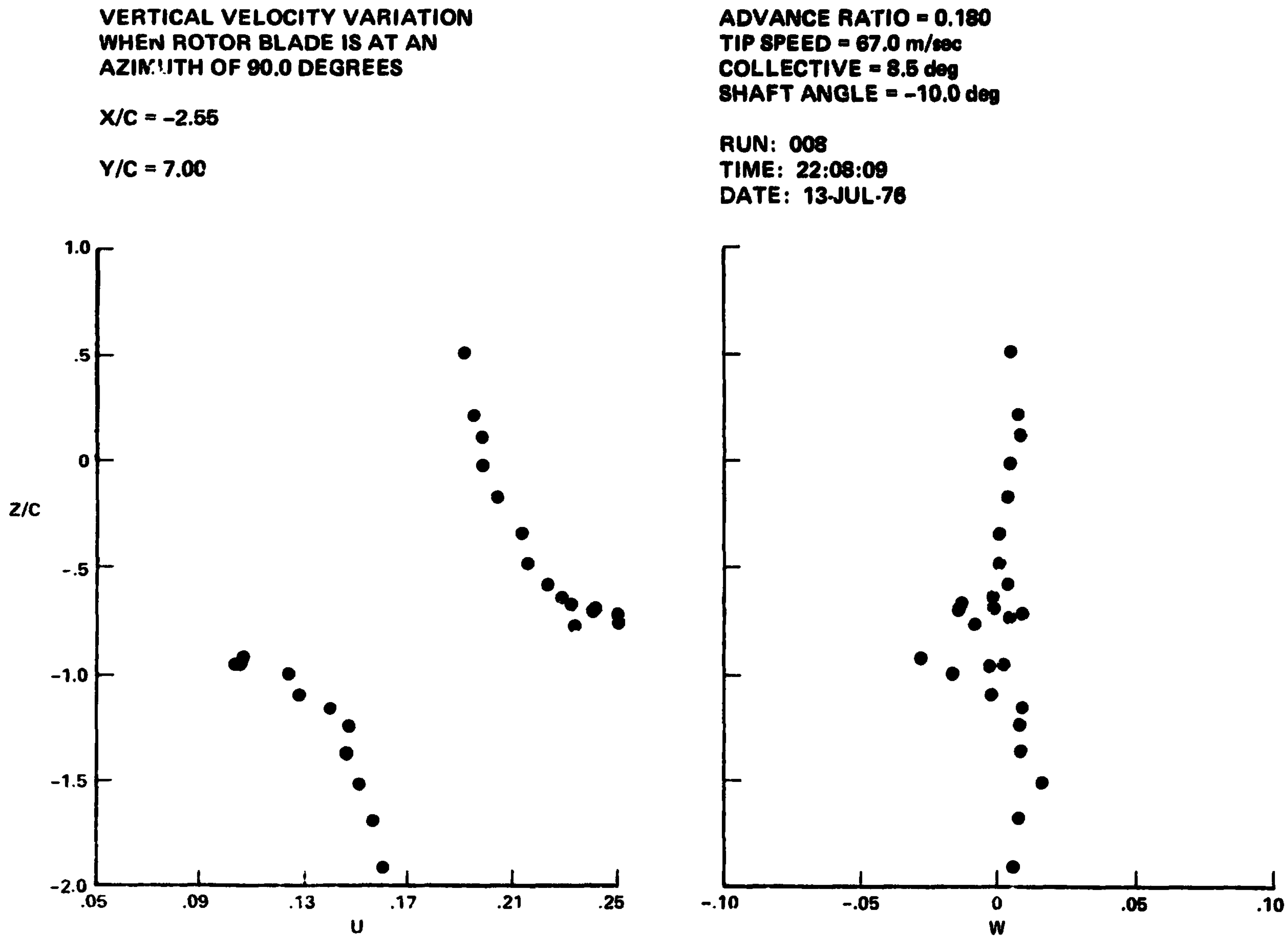

5-2. Vertical traverse, x/c = -2.55, y/c = 7.00

Figure 5. (Continued)

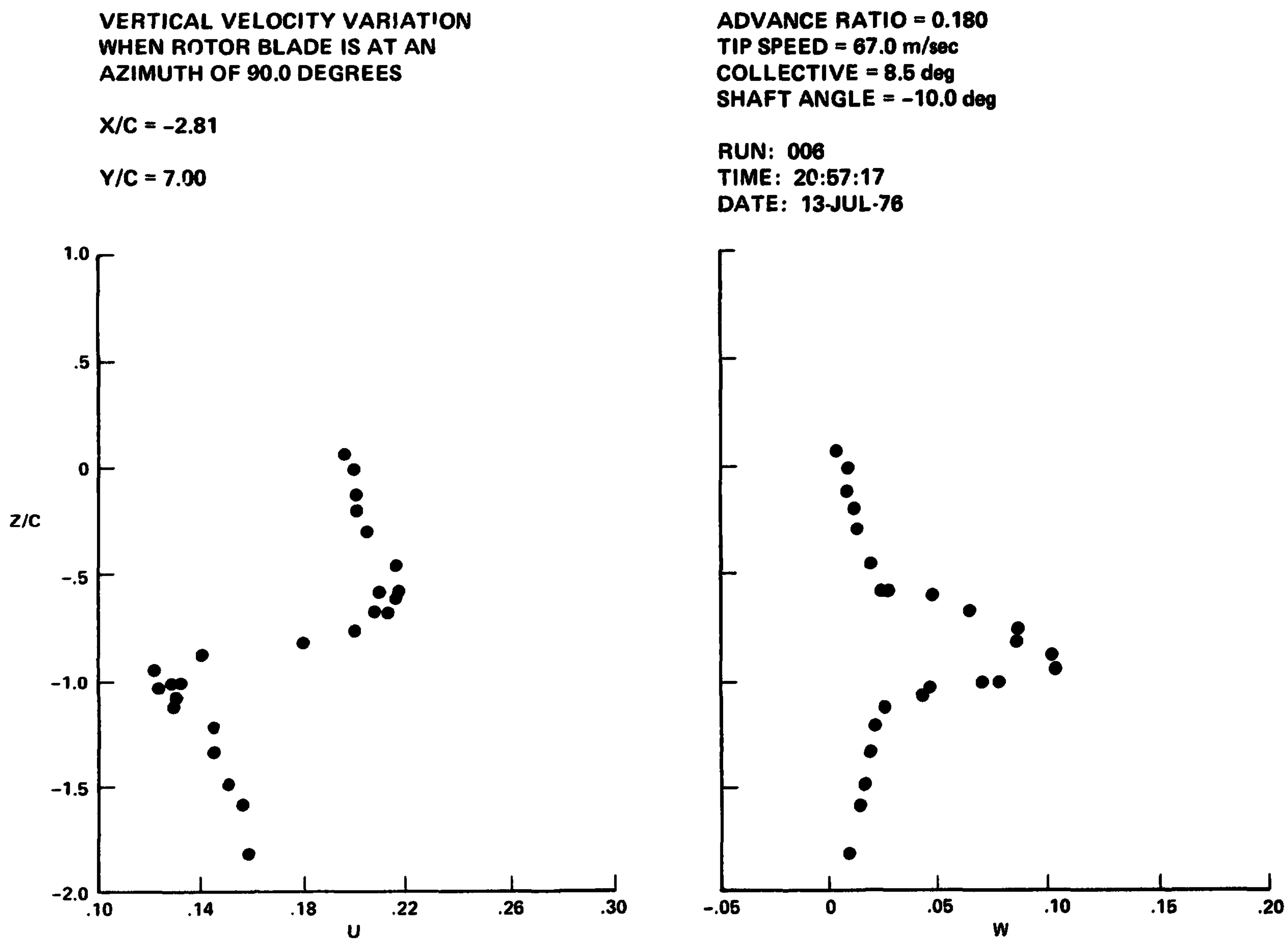

5-3. Vertical traverse, x/c = -2.81, y/c = 7.00

Figure 5. (Continued)

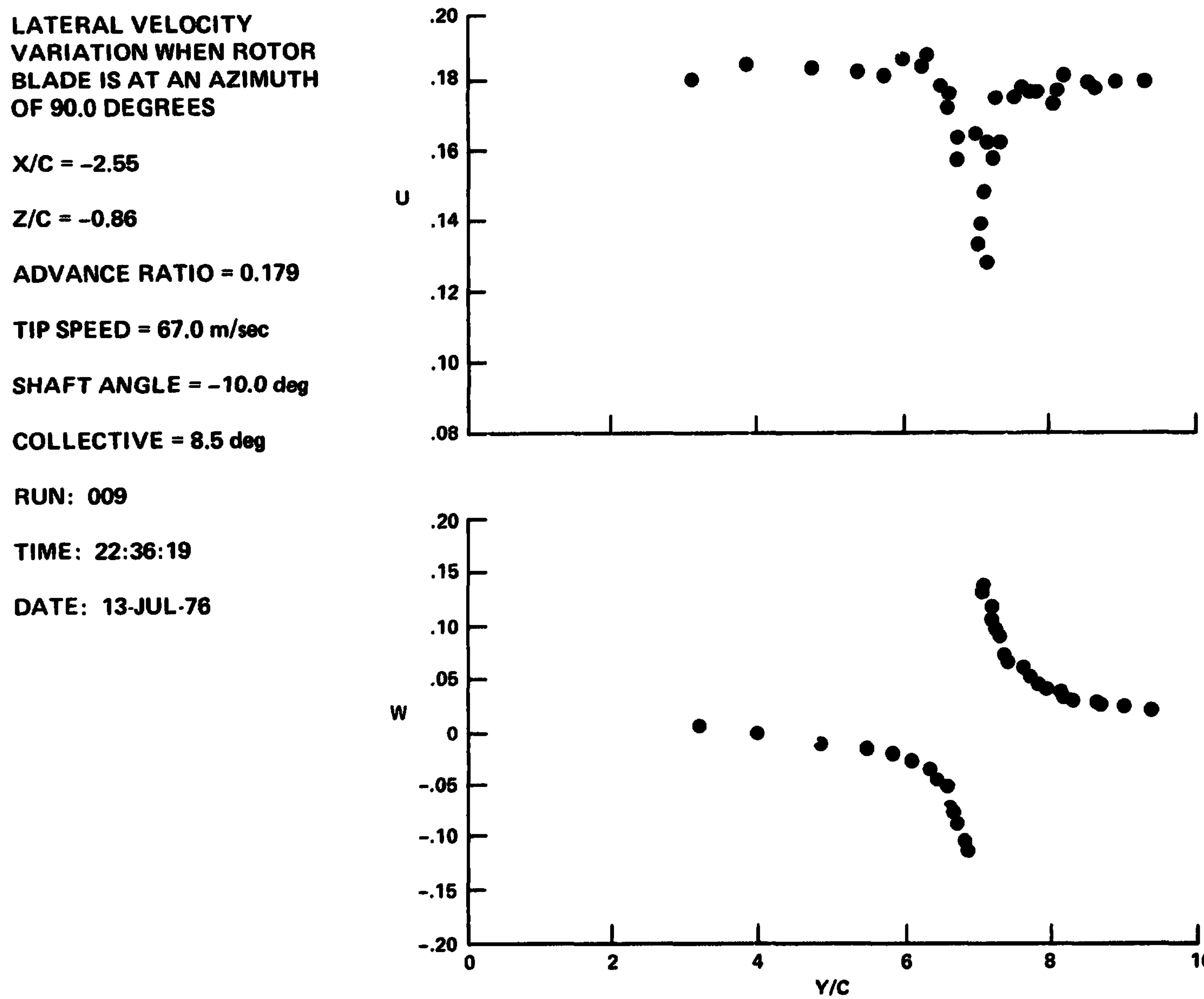

5-4. Lateral traverse, x/c = -2.55, z/c = -0.86

Figure 5. (Continued)

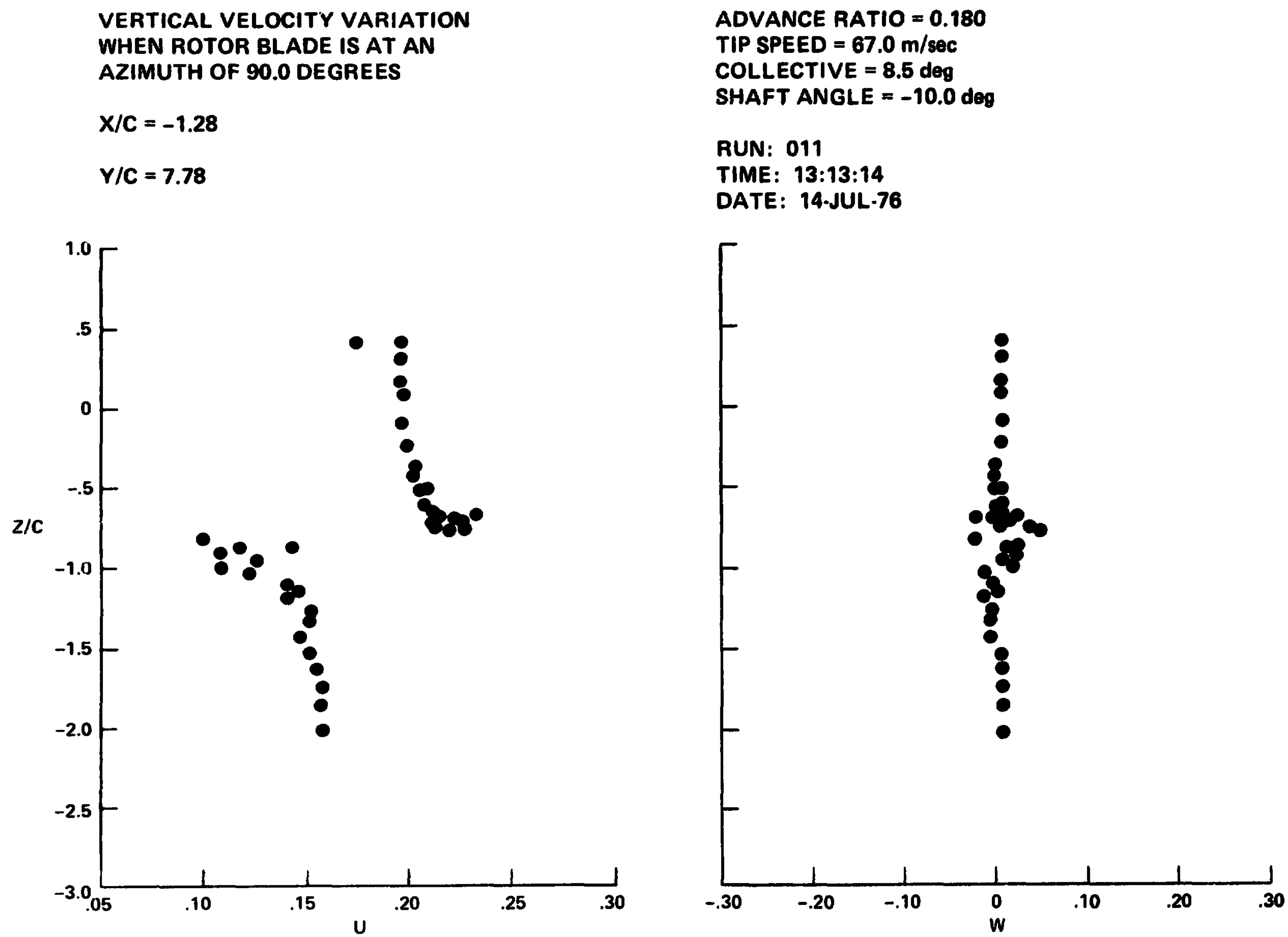

5-5. Vertical traverse, x/c = -1.28, y/c = 7.78

Figure 5. (Continued)

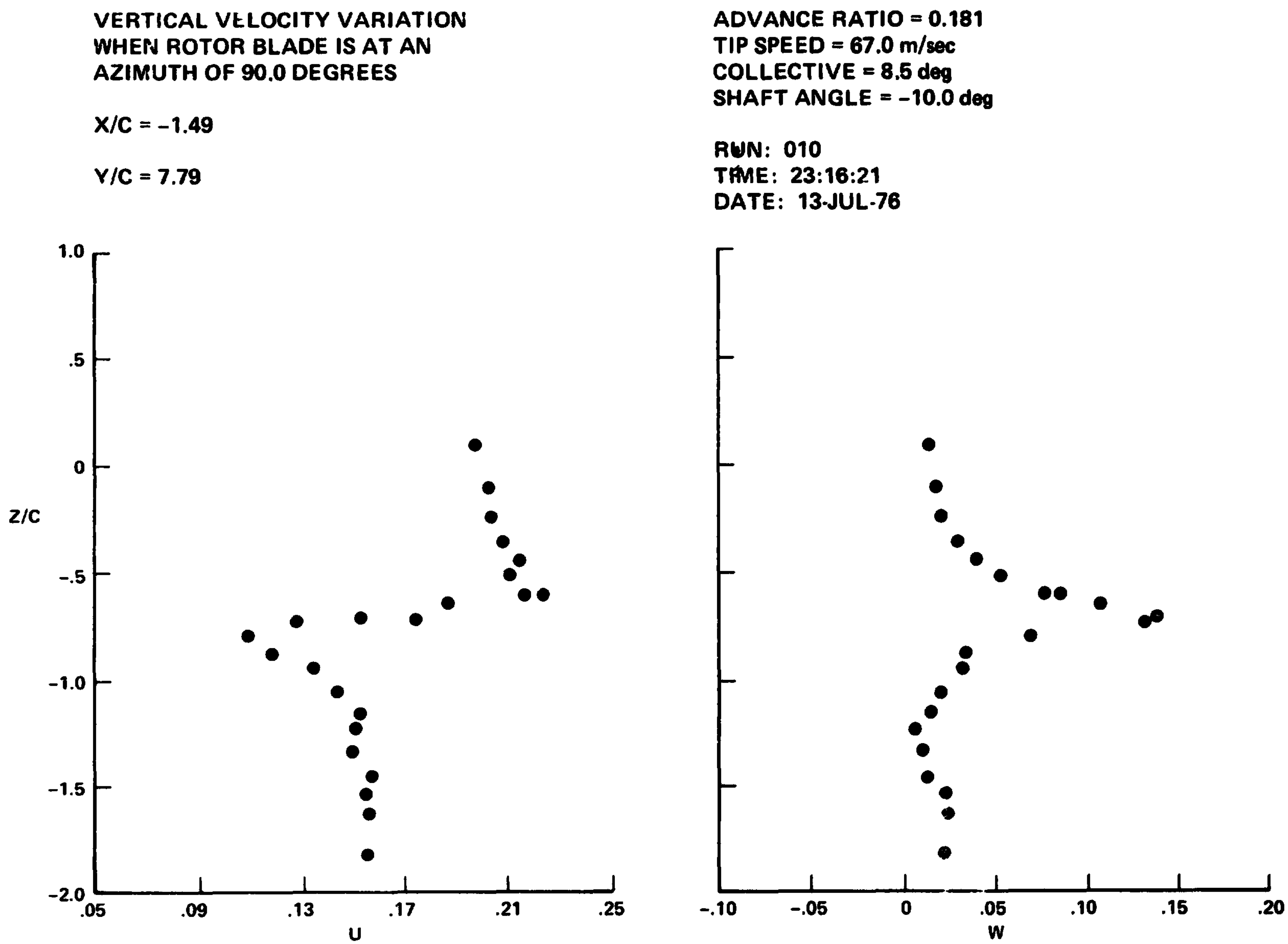

5-6. Vertical traverse, x/c = -1.49, y/c = 7.79

Figure 5. (Continued)

LATERAL VELOCITY
VARIATION WHEN ROTOR
BLADE IS AT AN AZIMUTH
OF 90.0 DEGREES

X/C = 0.00

Z/C = -0.61

ADVANCE RATIO = 0.180

TIP SPEED = 67.0 m/sec

SHAFT ANGLE = -10.0 deg

CCLLECTIVE = 8.5 deg

RUN: 017

TIME: 18:23:10

DATE: 14-JUL-76

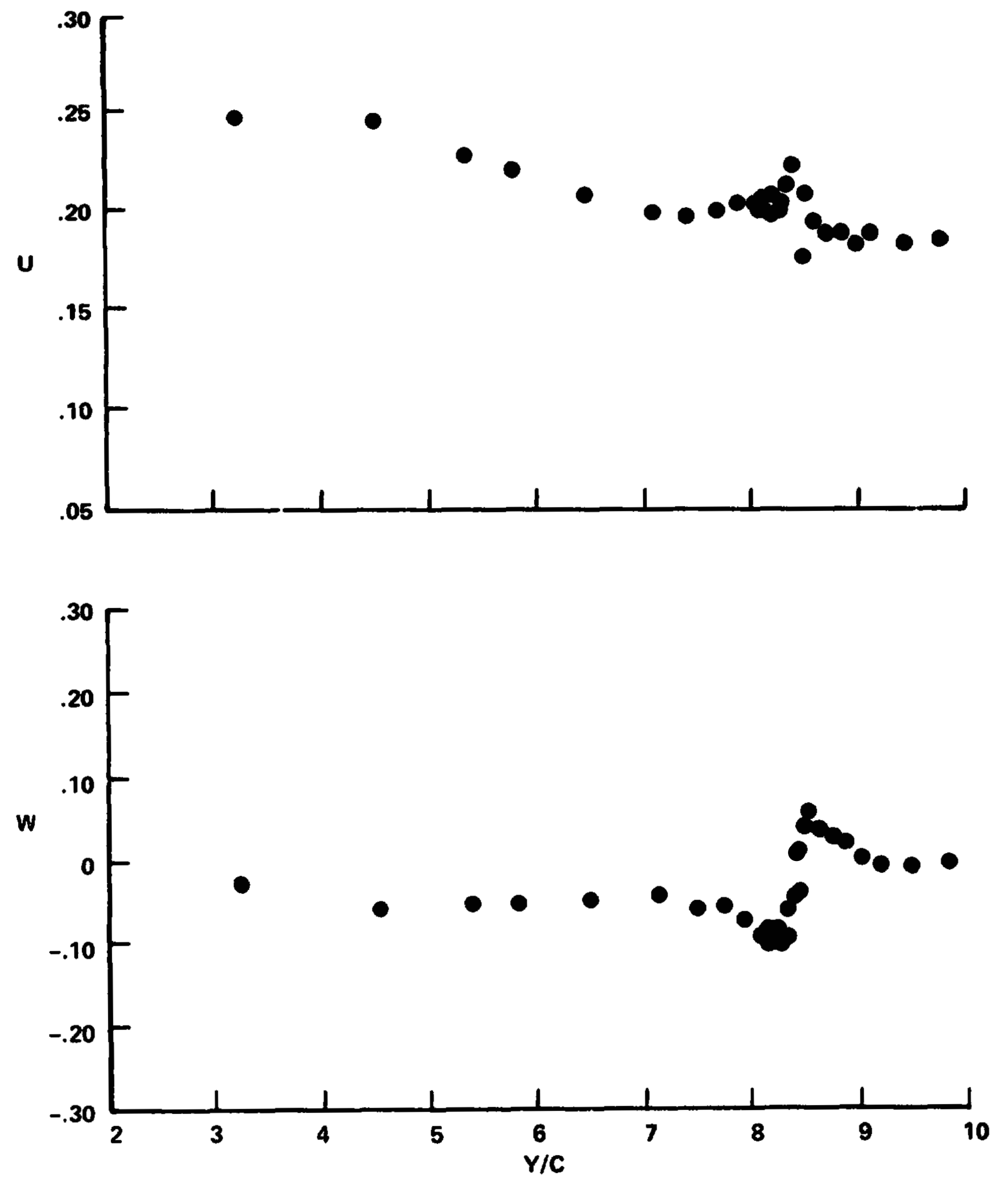

5-7. Lateral traverse, x/c = 0.00, z/c = -0.61

Figure 5. (Continued)

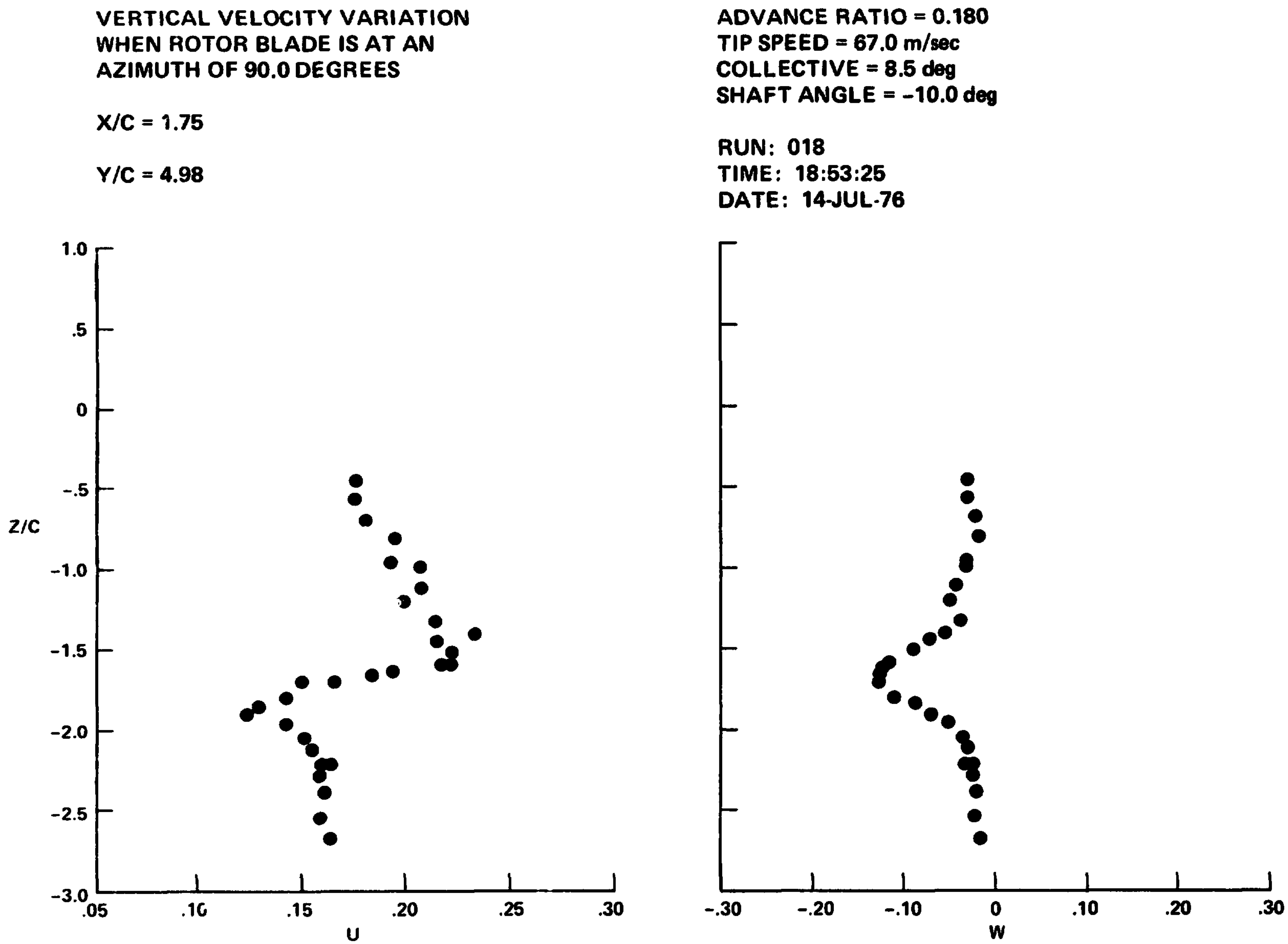

5-8. Vertical traverse, x/c = 1.75, y/c = 4.98

Figure 5. (Continued)

LATERAL VELOCITY VARIATION WHEN ROTOR BLADE IS AT AN AZIMUTH OF 90.0 DEGREES

X/C = 1.73

Z/C = -1.71

ADVANCE RATIO = 0.183

TIP SPEED = 67.0 m/sec

SHAFT ANGLE = -10.0 deg

COLLECTIVE = 8.5 deg

RUN: 019

TIME: 20:50:10

DATE: 14-JUL-76

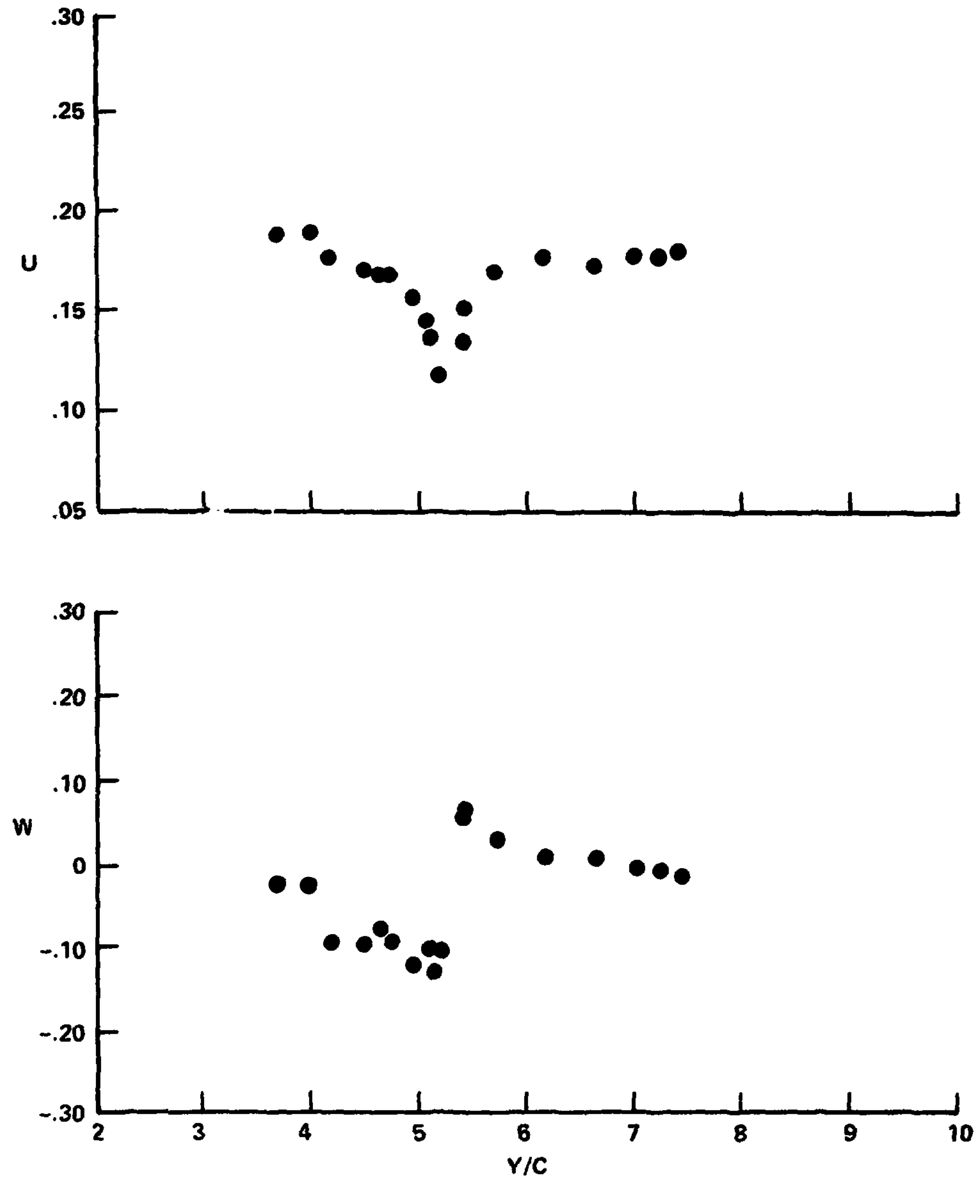

5-9. Lateral traverse, x/c = 1.73, z/c = -1.71

Figure 5. (Continued)

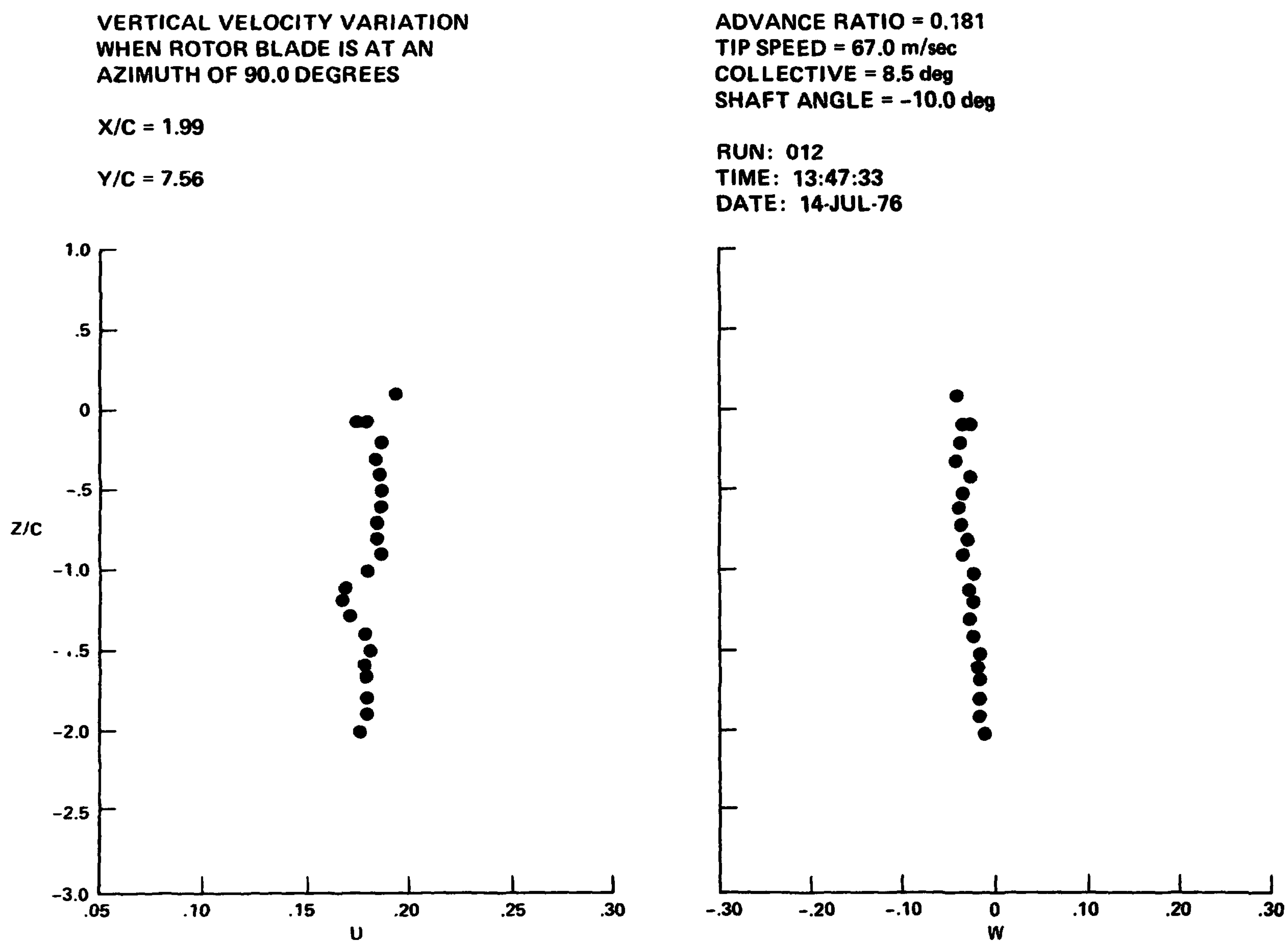

5-10. Vertical traverse, x/c = 1.99, y/c = 7.56

Figure 5. (Continued)

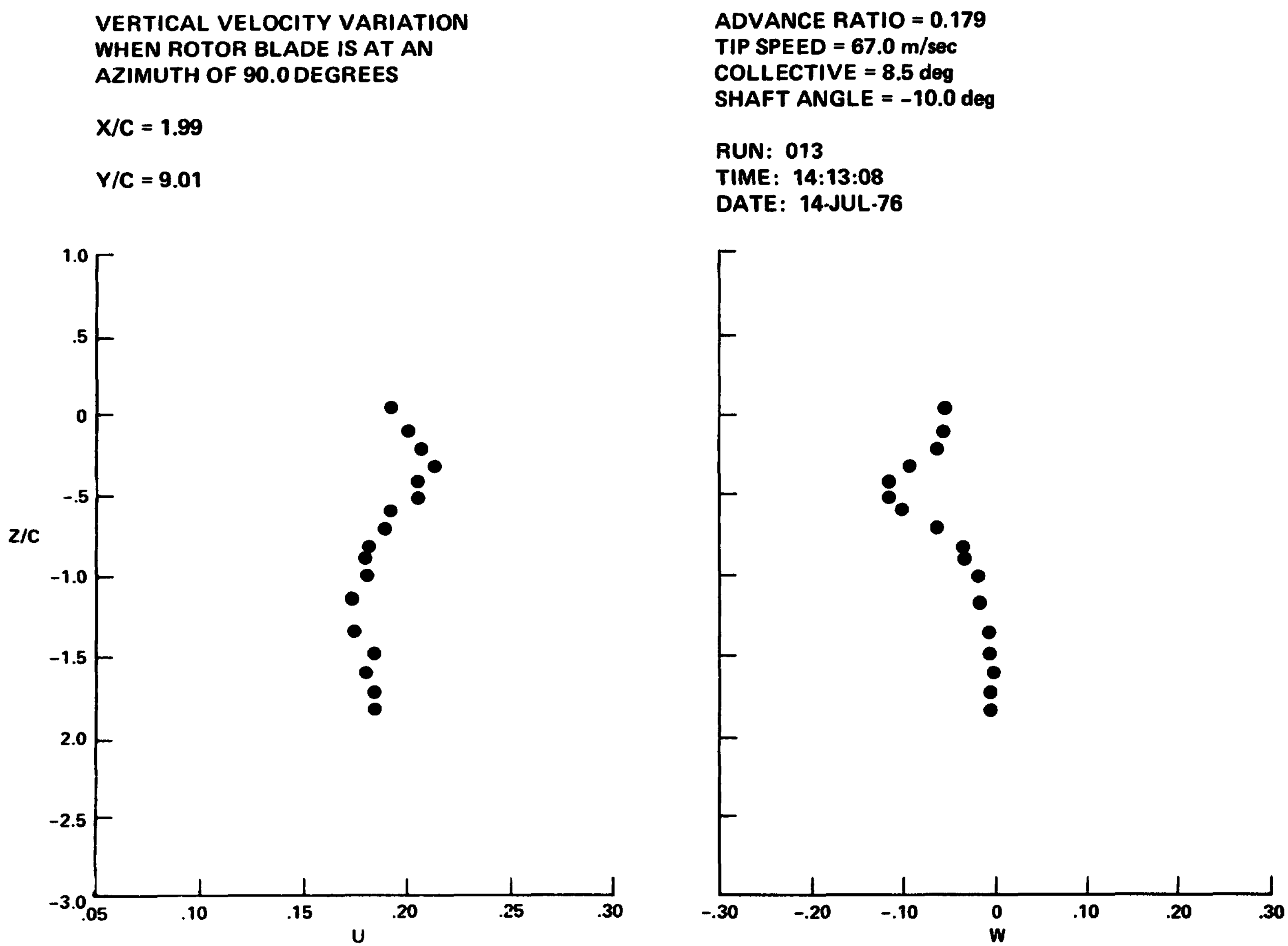

5-11. Vertical traverse, x/c = 1.99, y/c = 9.01

Figure 5. (Continued)

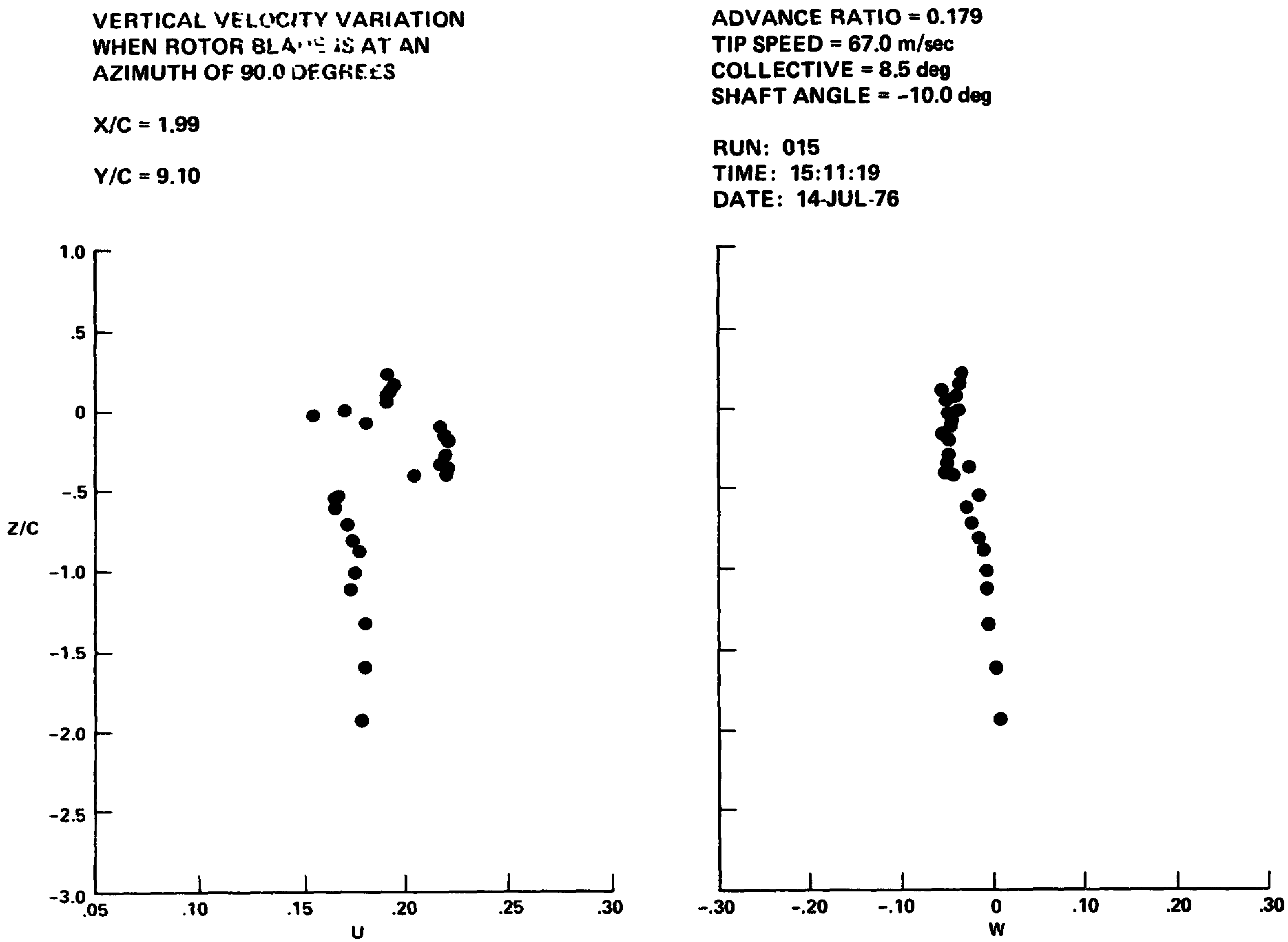

5-12. Vertical traverse, x/c = 1.99, y/c = 9.10

Figure 5. (Continued)

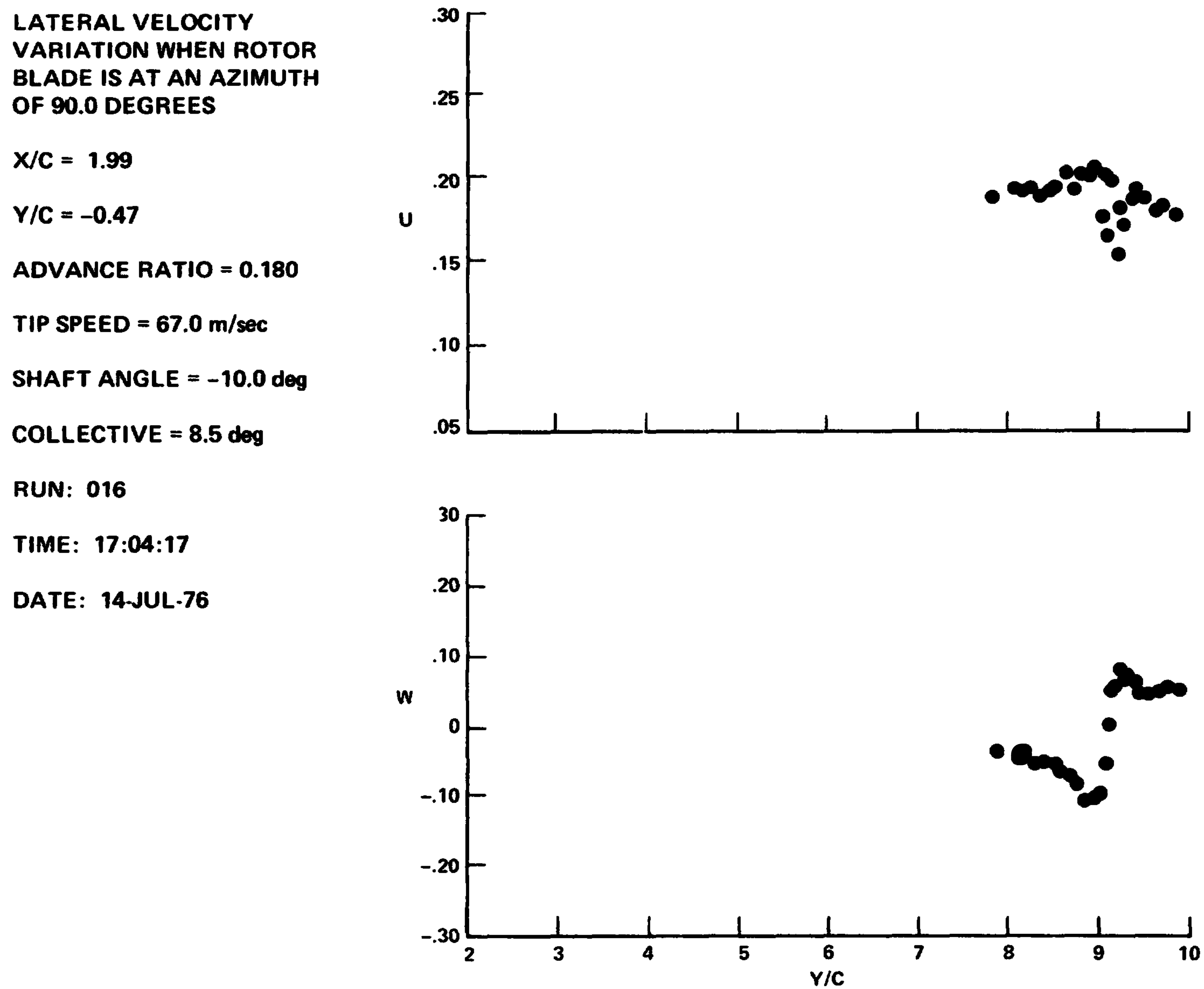

5-13. Lateral traverse, x/c = 1.99, z/c = –0.47

Figure 5. (Continued)

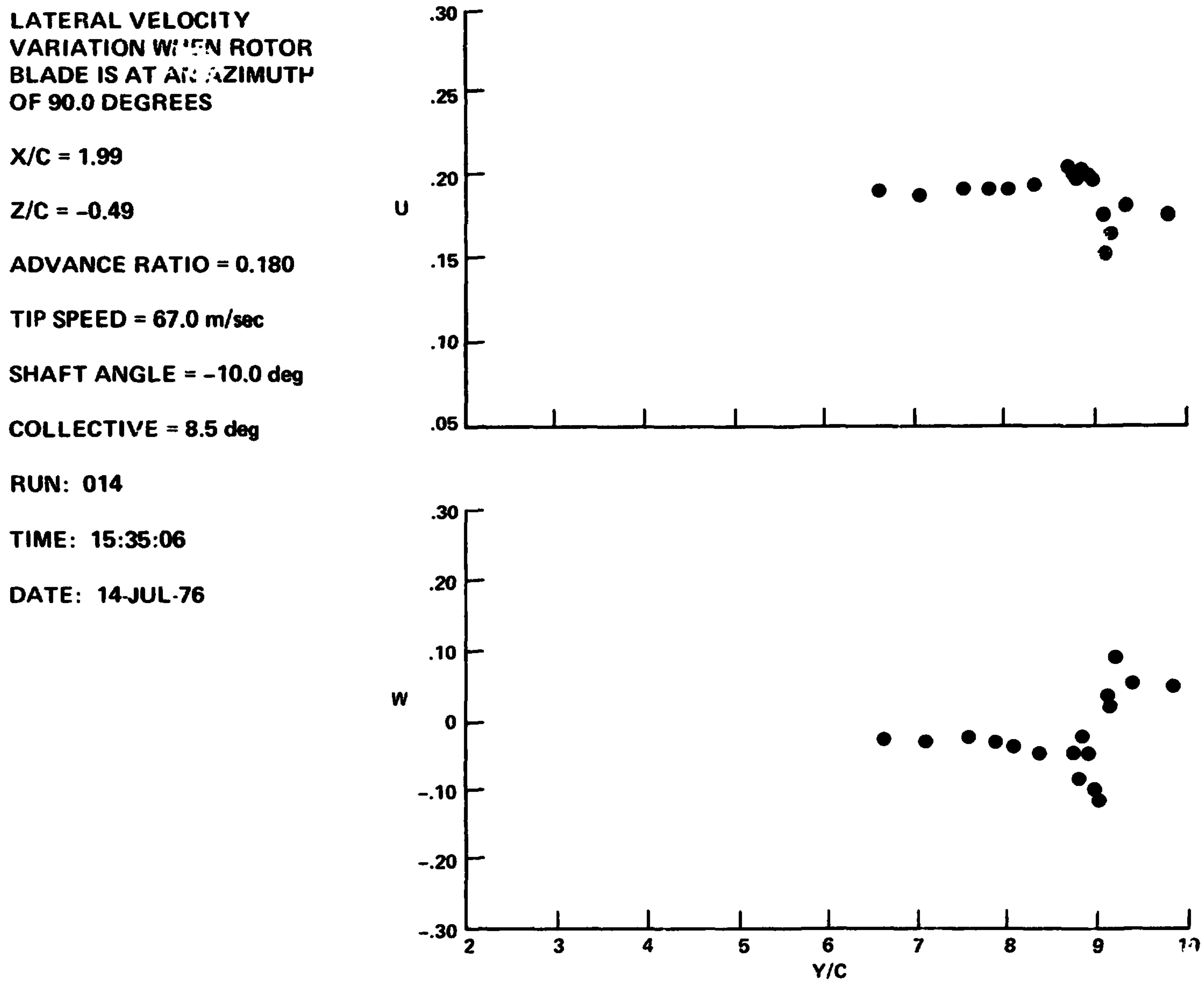

5.14. Lateral traverse, x/c = 1.99, z/c = –0.49

Figure 5. (Concluded)

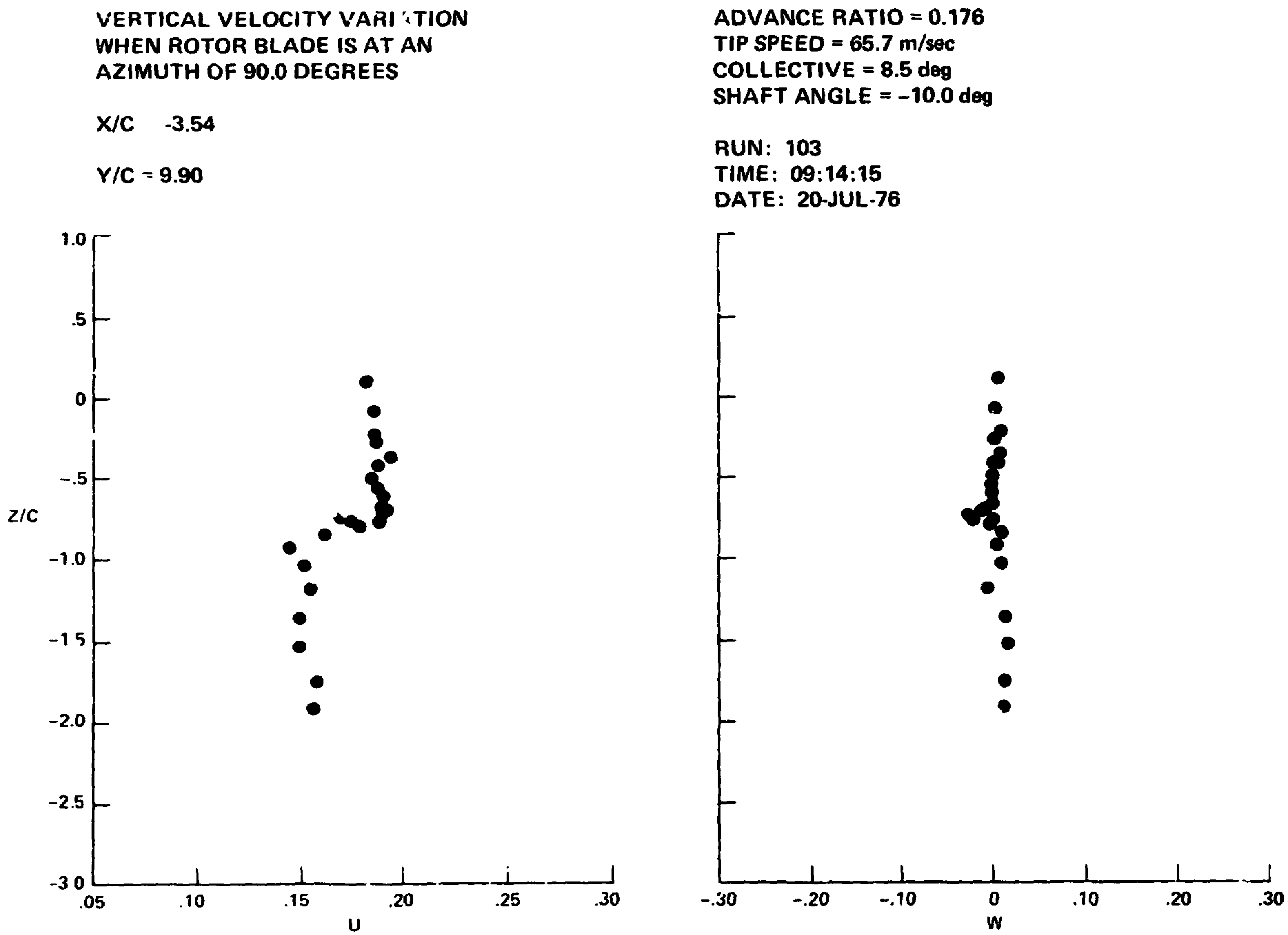

6-1. Vertical traverse, x/c = -3.54, y/c = 9.90

Figure 6. Flowfield velocities from the -11° twist blades, $V/\Omega R = 0.18$, $\theta_{0.75R} = 8.5$, $\psi = 90°$, N = 600.

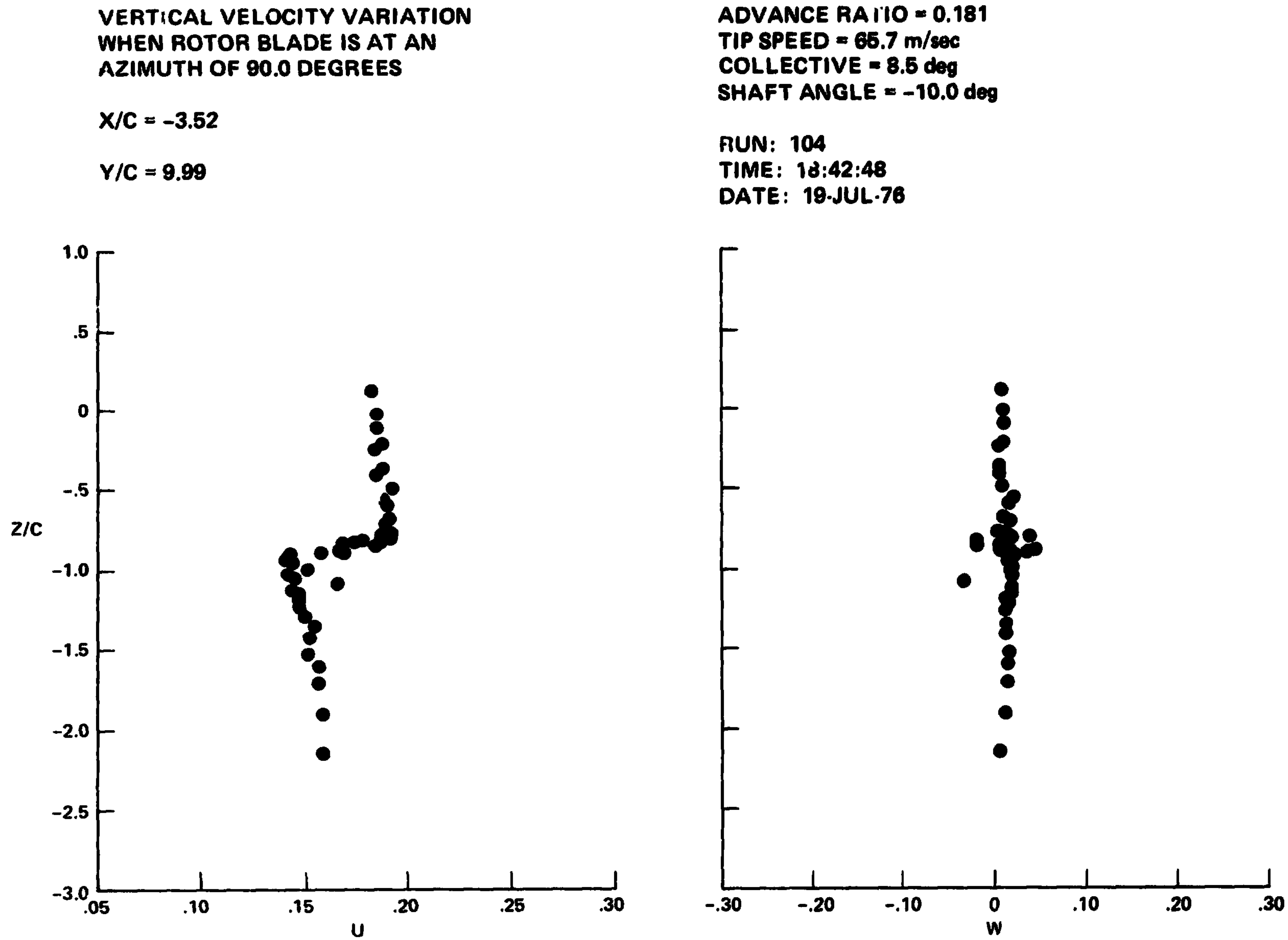

6-2. Vertical traverse, x/c = -3.54, y/c = 10.00

Figure 6. (Continued)

LATERAL VELOCITY VARIATION WHEN ROTOR BLADE IS AT AN AZIMUTH OF 90.0 DEGREES

X/C = –3.54

Z/C - –0.80

ADVANCE RATIO = 0.179

TIP SPEED = 65.7 m/sec

SHAFT ANGLE = –10.0 deg

COLLECTIVE = 8.5 deg

RUN: 101

TIME: 09:12:41

DATE: 20-JUL-76

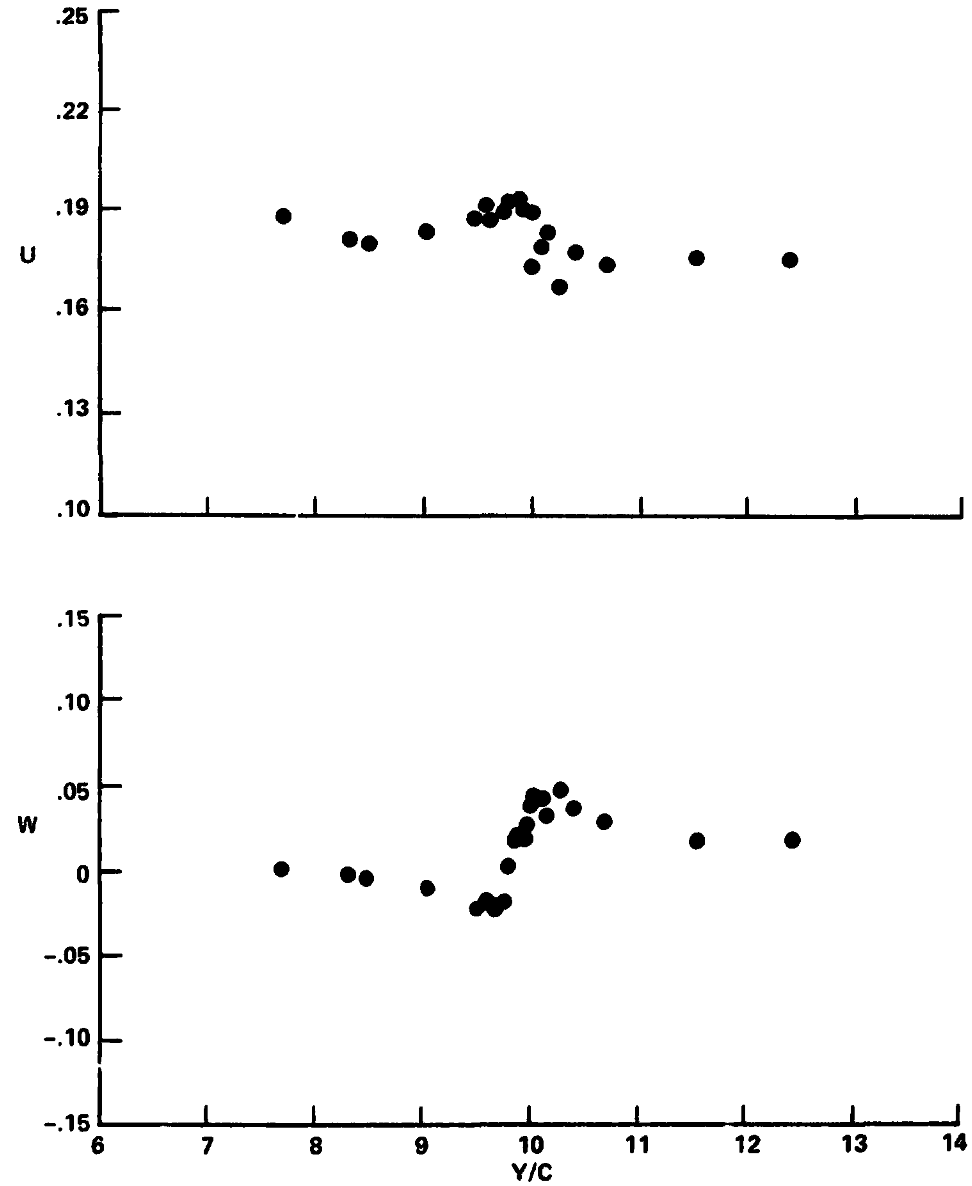

6-3. Lateral traverse, x/c = -3.54, z/c = -0.80

Figure 6. (Continued)

LATERAL VELOCITY VARIATION WHEN ROTOR BLADE IS AT AN AZIMUTH OF 90.0 DEGREES

X/C = -3.54

Z/C = -0.85

ADVANCE RATIO = 0.177

TIP SPEED = 65.7 m/sec

SHAFT ANGLE = -10.0 deg

COLLECTIVE = 8.5 deg

RUN: 102

TIME: 18:36:54

DATE: 19-JUL-76

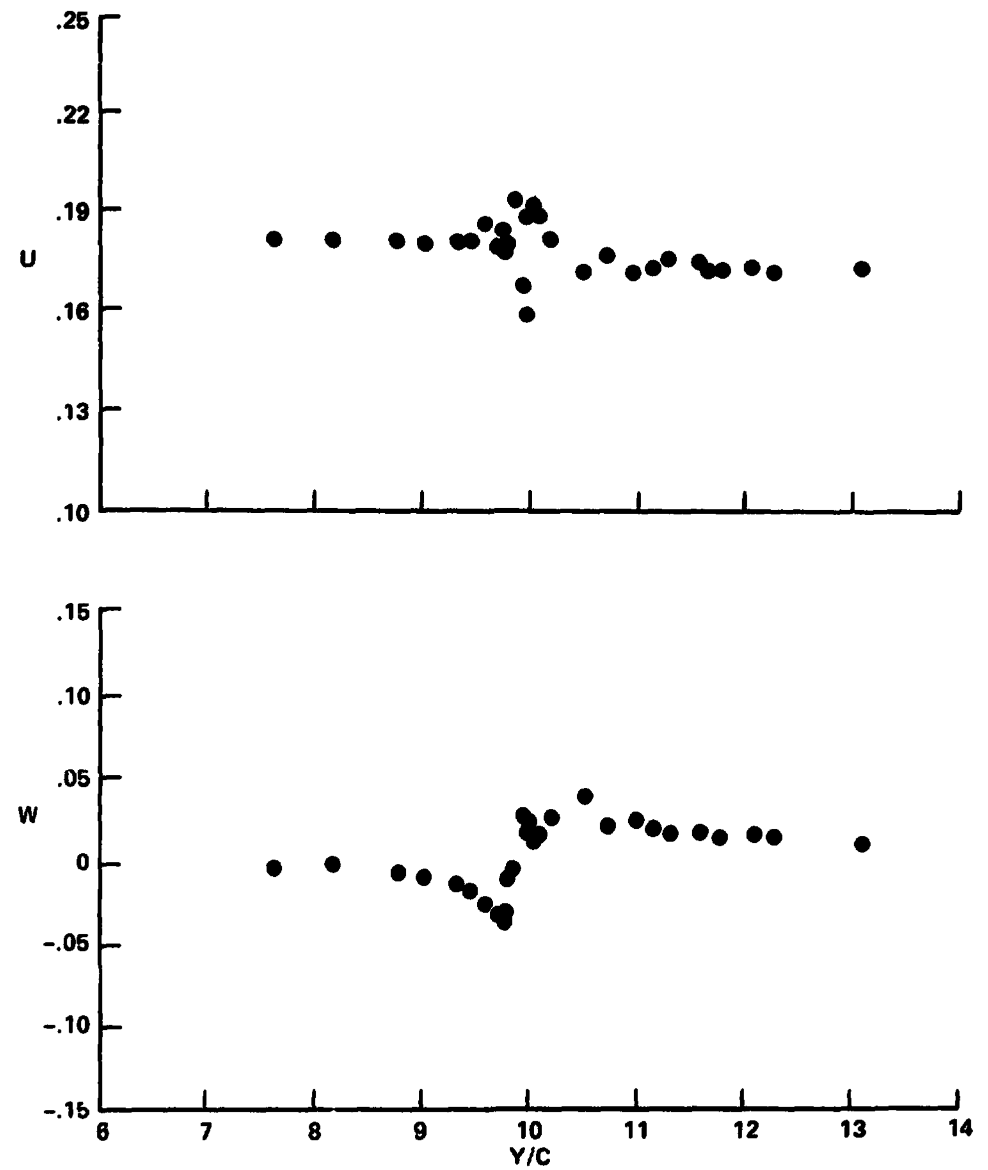

6-4. Lateral traverse, x/c = -3.54, z/c = -0.85

Figure 6. (Concluded)

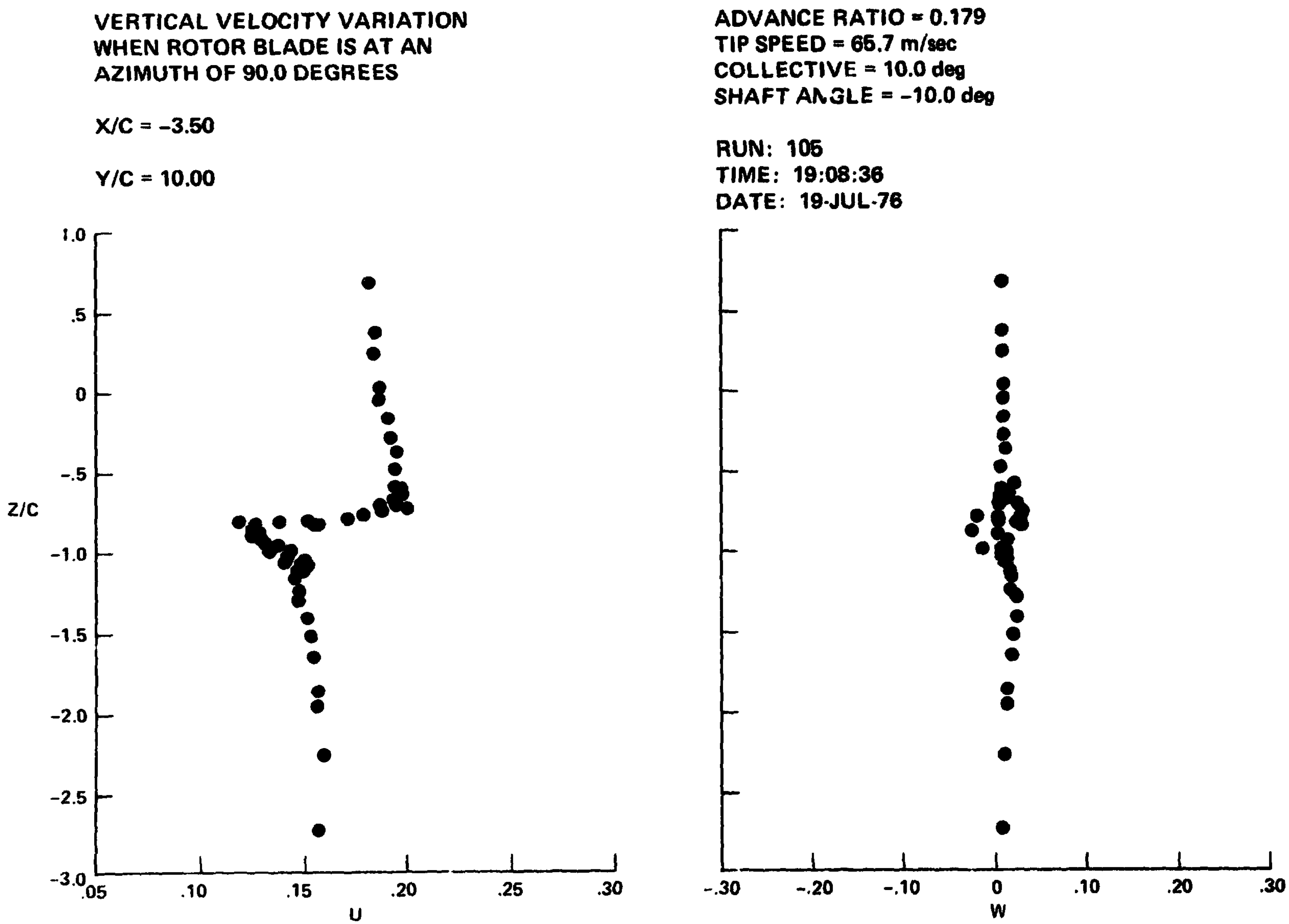

7-1. Vertical traverse, x/c = -3.50, y/c = 10.00

Figure 7. Flowfield velocities from the -11° twist blades, $V/\Omega R = 0.18$, $\theta_{0.75R} = 10.1^{\circ}$, $\psi = 90^{\circ}$, $N = 600$.

LATERAL VELOCITY VARIATION WHEN ROTOR BLADE IS AT AN AZIMUTH OF 90.0 DEGREES

X/C = -3.50

Z/C = -0.76

ADVANCE RATIO = 0.181

TIP SPEED = 65.7 m/sec

SHAFT ANGLE = -10.0 deg

COLLECTIVE = 10.1 deg

RUN: 107

TIME: 19:47:24

DATE: 19-JUL-76

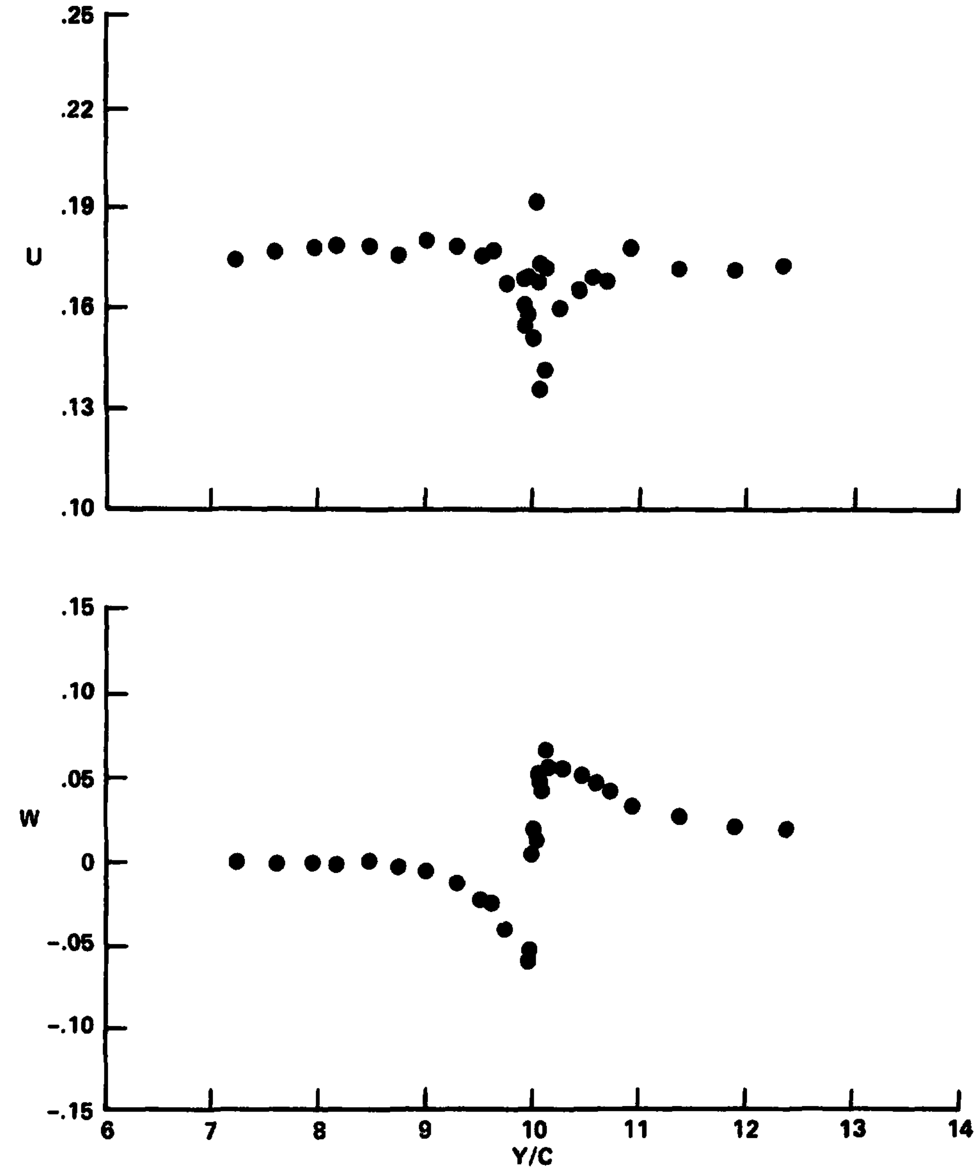

7-2. Lateral traverse, x/c = -3.50, z/c = -0.76

Figure 7. (Continued)

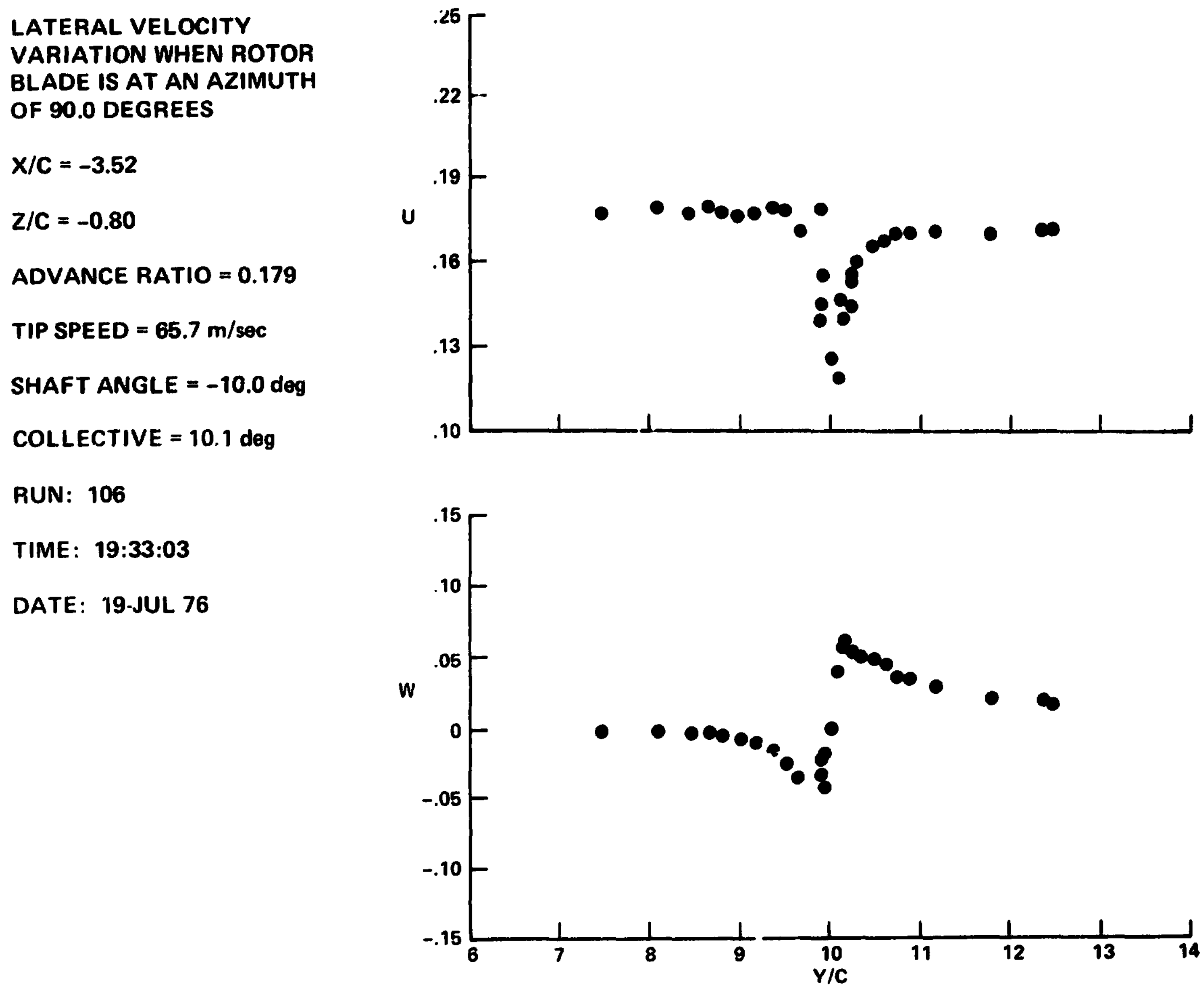

7-3. Lateral traverse, x/c = -3.50, z/c = -0.80

Figure 7. (Continued)

LATERAL VELOCITY VARIATION WHEN ROTOR BLADE IS AT AN AZIMUTH OF 90.0 DEGREES

X/C = -2.00

Z/C = -0.64

ADVANCE RATIO = 0.180

TIP SPEED = 65.7 m/sec

SHAFT ANGLE = -10.0 deg

COLLECTIVE = 10.1 deg

RUN: 114

TIME: 19:23:08

DATE: 20-JUL-76

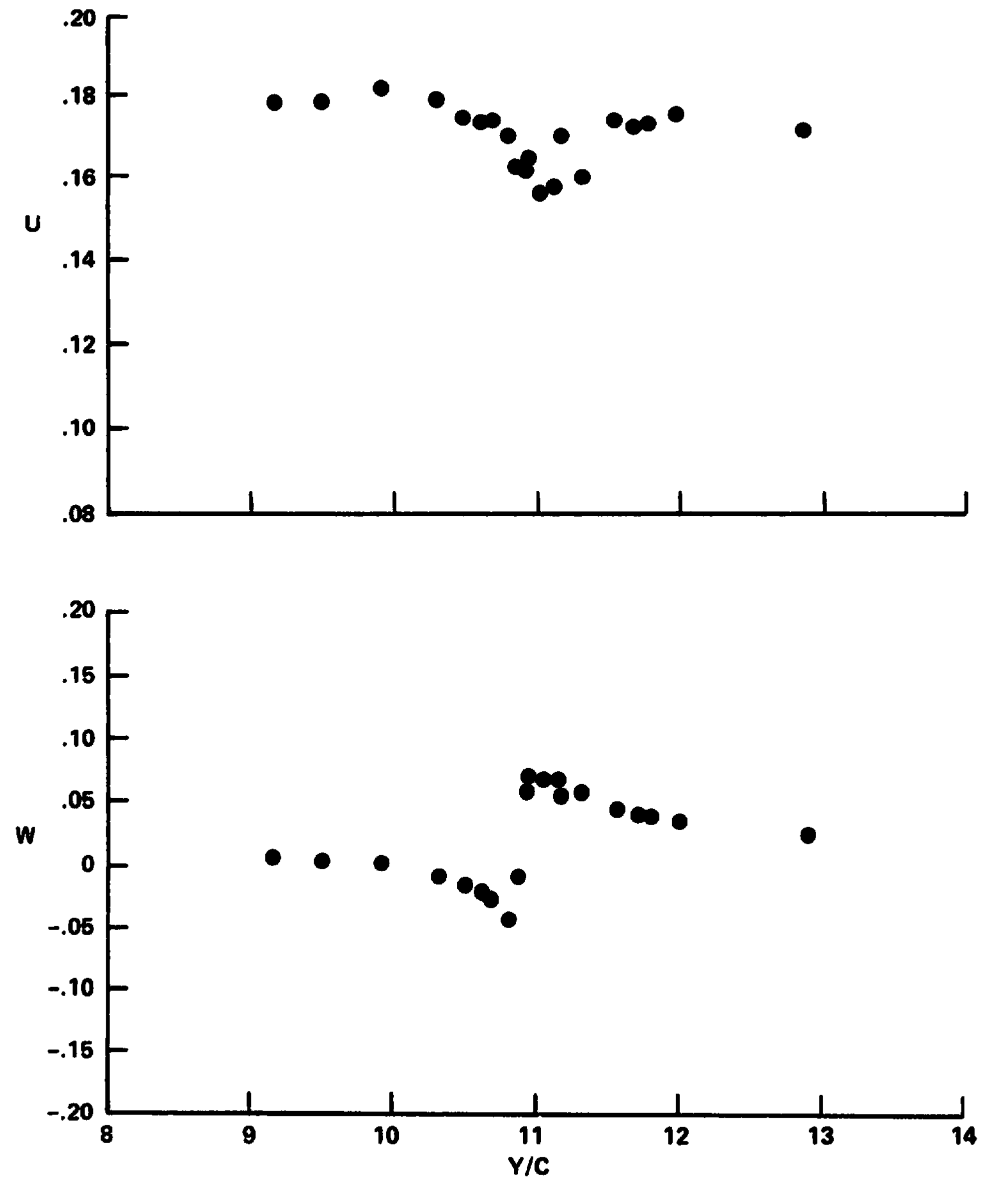

7-4. Lateral traverse, x/c = -2.00, z/c = -0.64

Figure 7. (Continued)

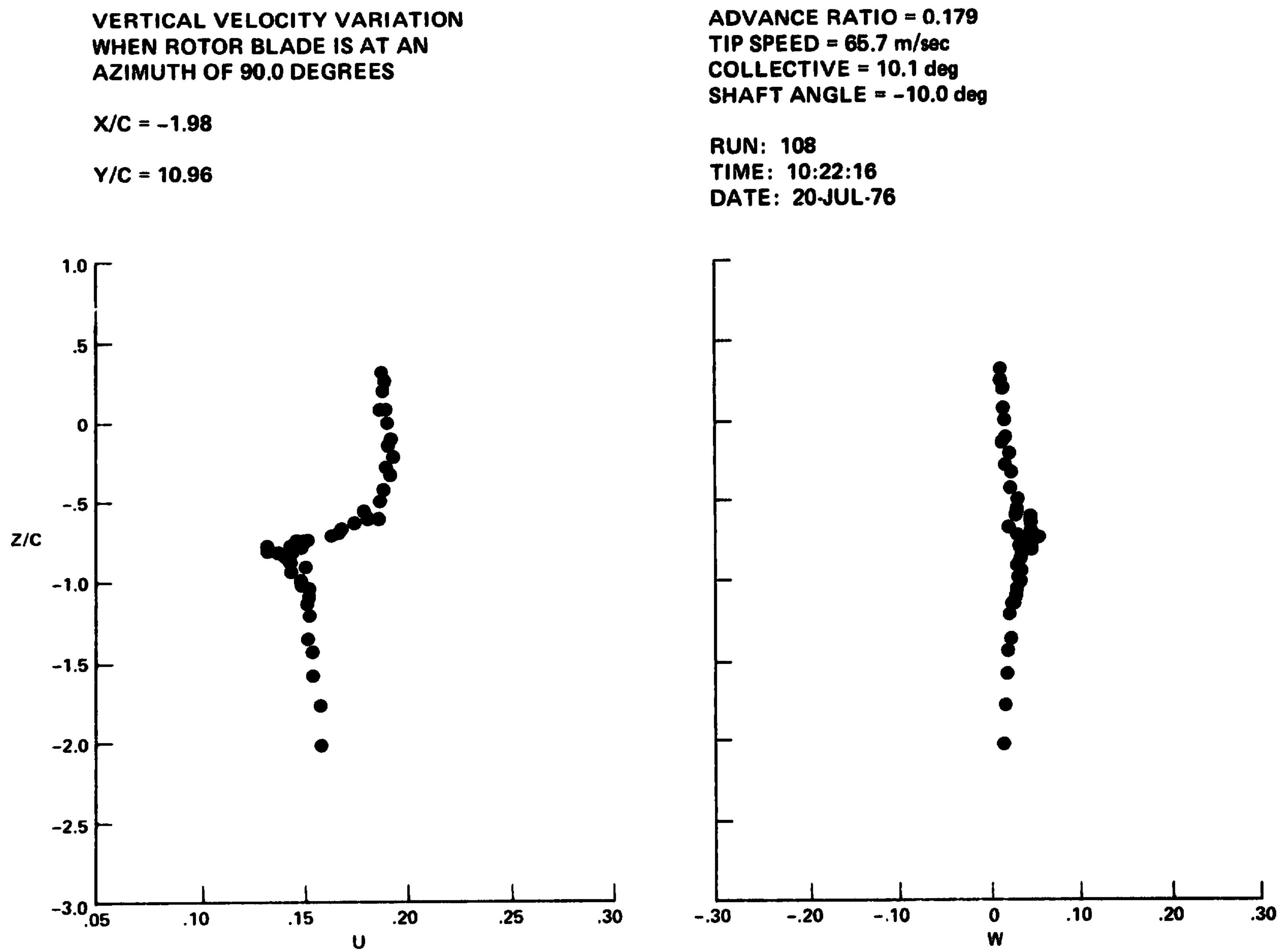

7-5. Vertical traverse, x/c = -1.98, y/c = 10.96

Figure 7. (Continued)

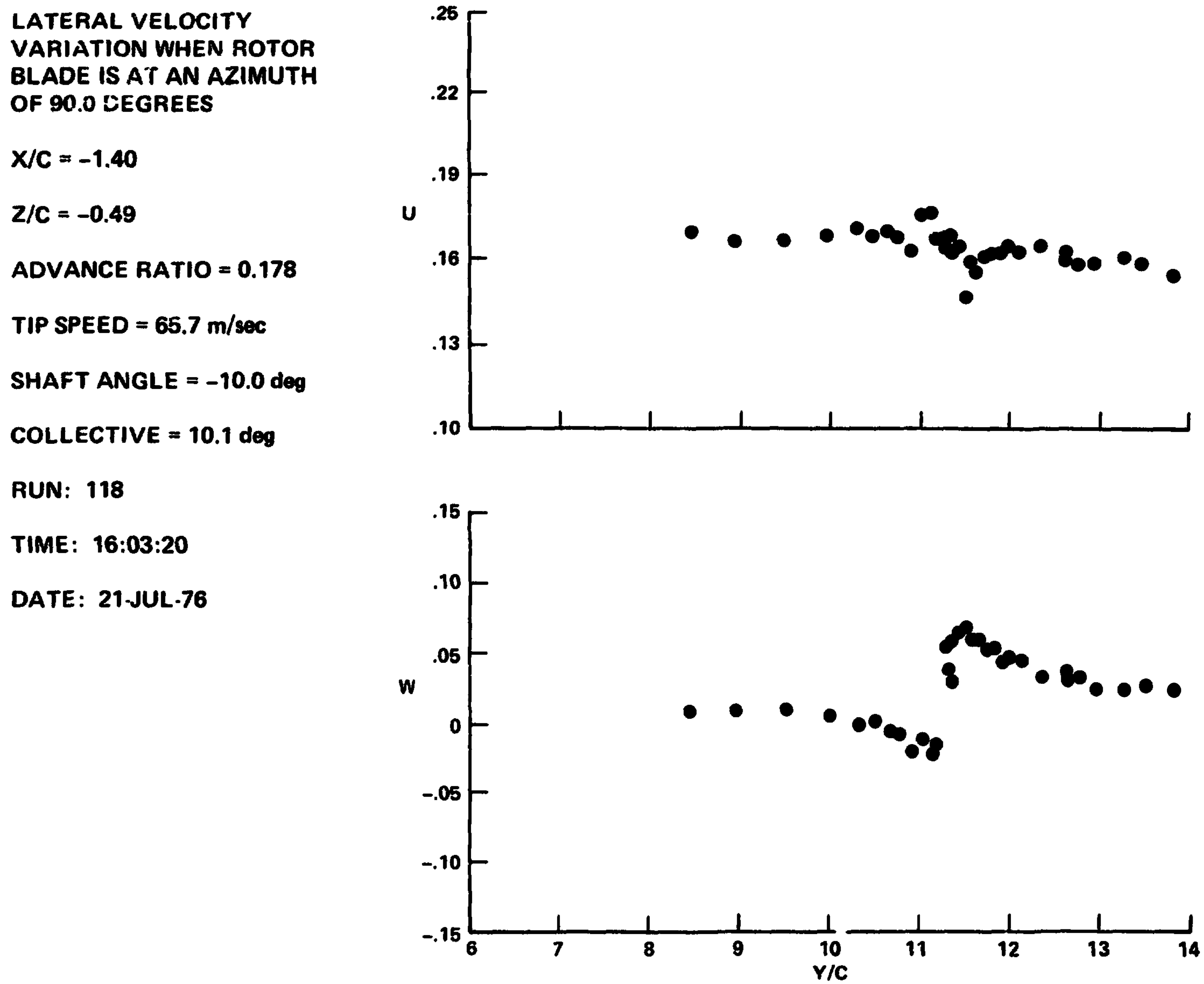

7-6. Lateral traverse, x/c = -1.40, z/c = -0.49

Figure 7. (Continued)

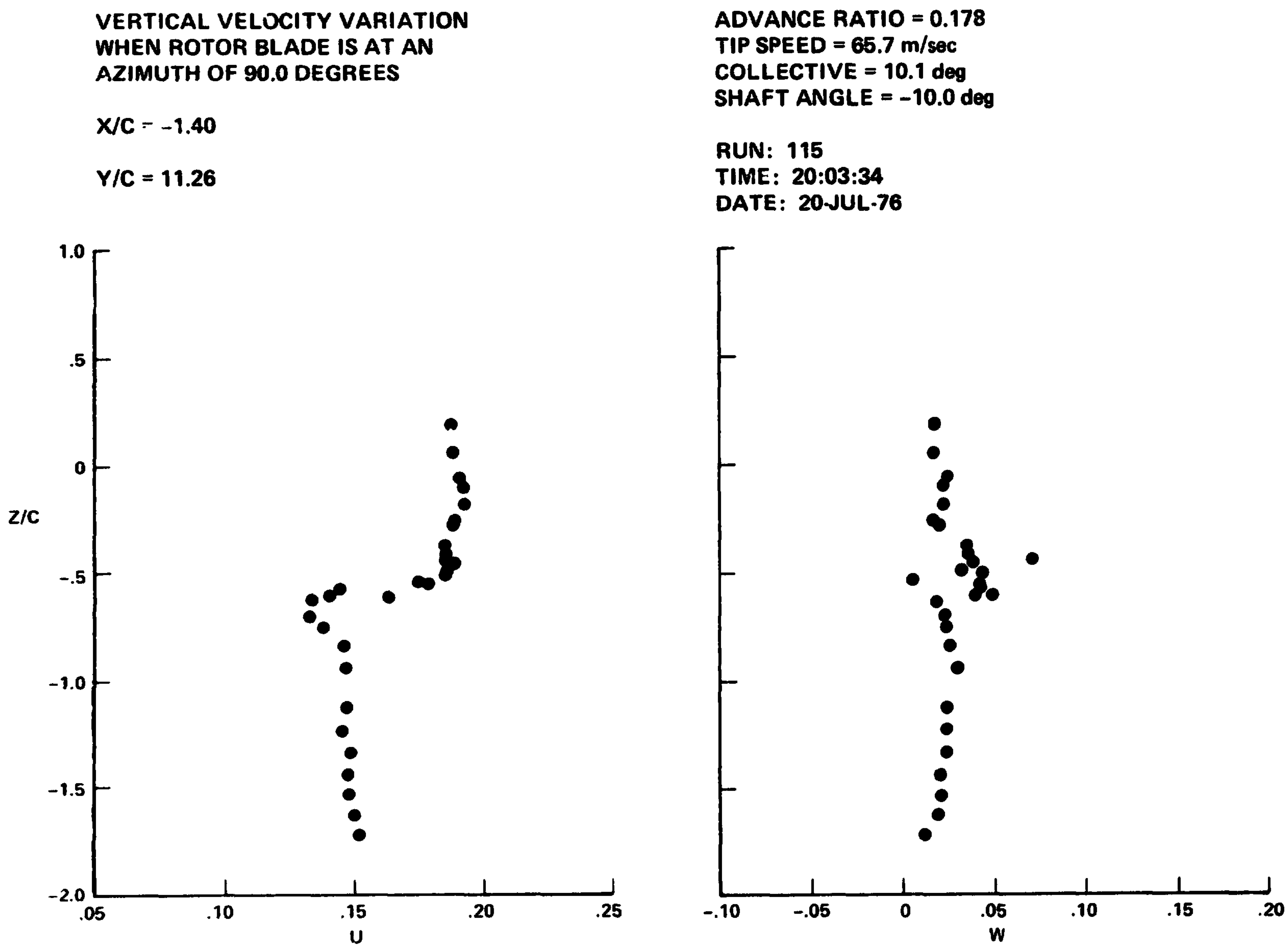

7-7. Vertical traverse, x/c = -1.40, y/c = 11.26

Figure 7. (Continued)

LATERAL VELOCITY VARIATION WHEN ROTOR BLADE IS AT AN AZIMUTH OF 90.0 DEGREES

X/C = -0.99

Z/C = -0.51

ADVANCE RATIO = 0.178

TIP SPEED = 65.7 m/sec

SHAFT ANGLE = -10.0 deg

COLLECTIVE = 10.1 deg

RUN: 117

TIME: 14:55:01

DATE: 21-JUL-76

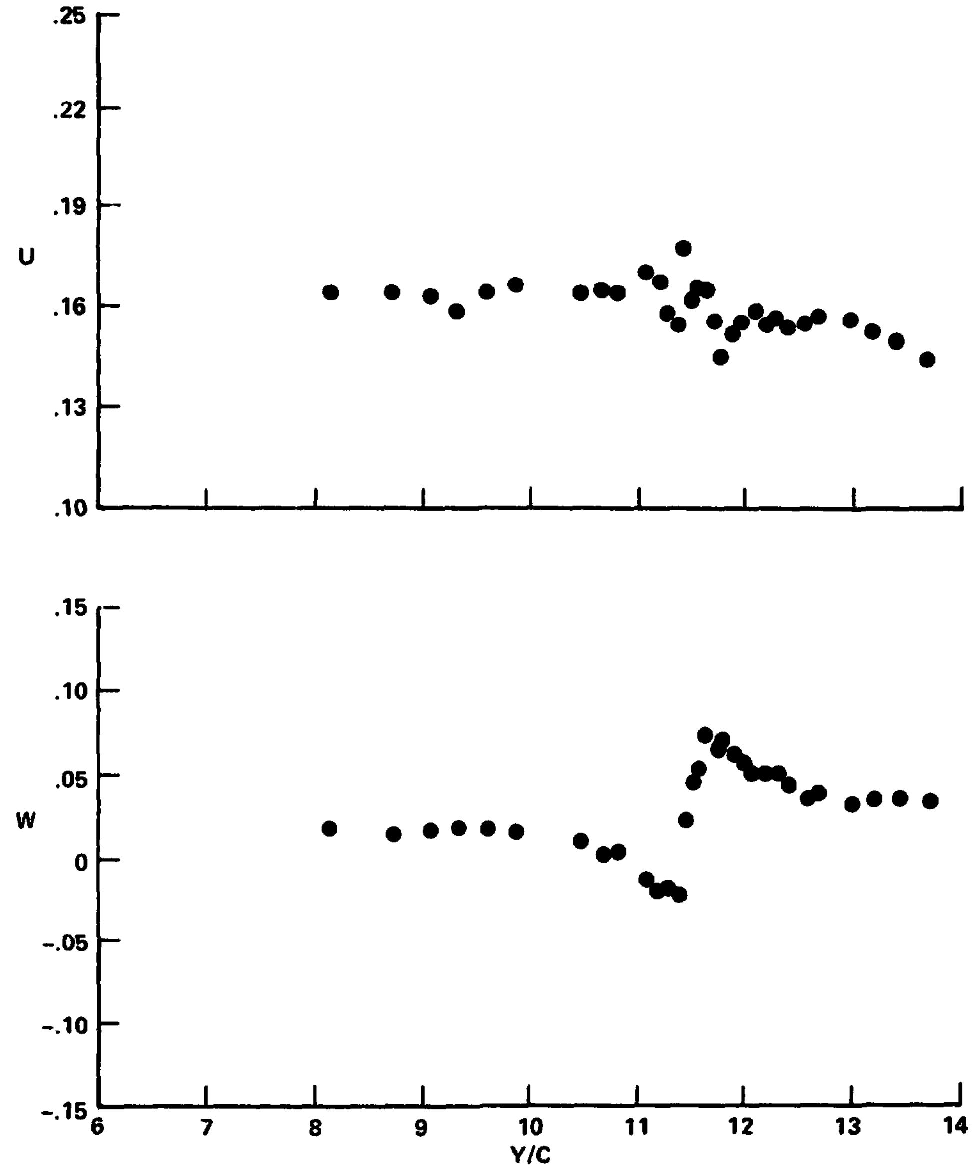

7-8. Lateral traverse, x/c = -1.00, z/c = -0.51

Figure 7. (Continued)

LATERAL VELOCITY VARIATION WHEN ROTOR BLADE IS AT AN AZIMUTH OF 90.0 DEGREES

X/C = -1.00

Z/C = -0.56

ADVANCE RATIO = 0.176

TIP SPEED = 65.7 m/sec

SHAFT ANGLE = -10.0 deg

COLLECTIVE = 10.1 deg

RUN: 116

TIME: 14:23:55

DATE: 21-JUL-76

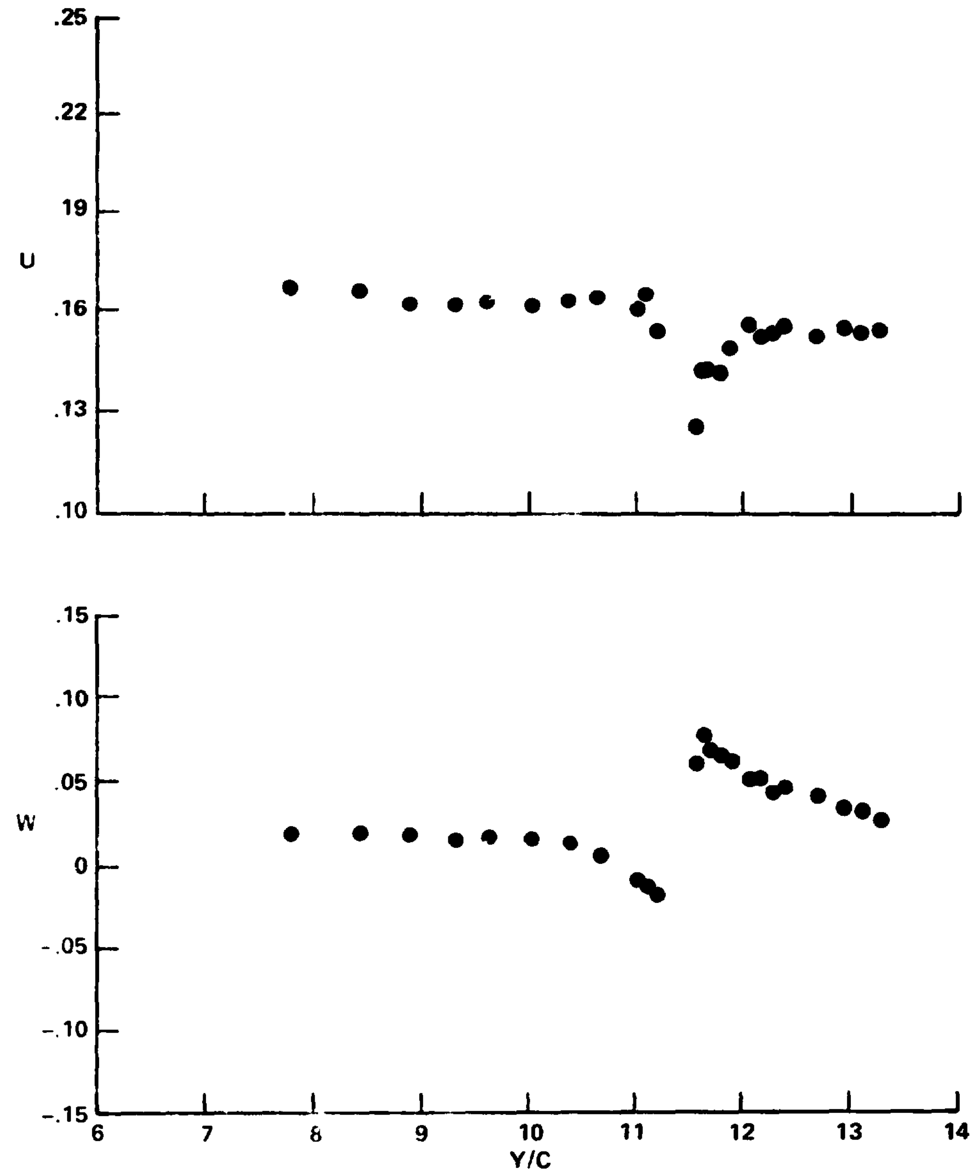

7-9. Lateral traverse, x/c = -1.00, z/c = -0.56

Figure 7. (Continued)

LATERAL VELOCITY VARIATION WHEN ROTOR BLADE IS AT AN AZIMUTH OF 90.0 DEGREES

X/C = -1.00

Z/C = -0.61

ADVANCE RATIO = 0.1?

TIP SPEED = 65.7 m/sec

SHAFT ANGLE = -10.0 deg

COLLECTIVE = 10.1 deg

RUN: 110

TIME: 11:28:25

DATE: 20-JUL-76

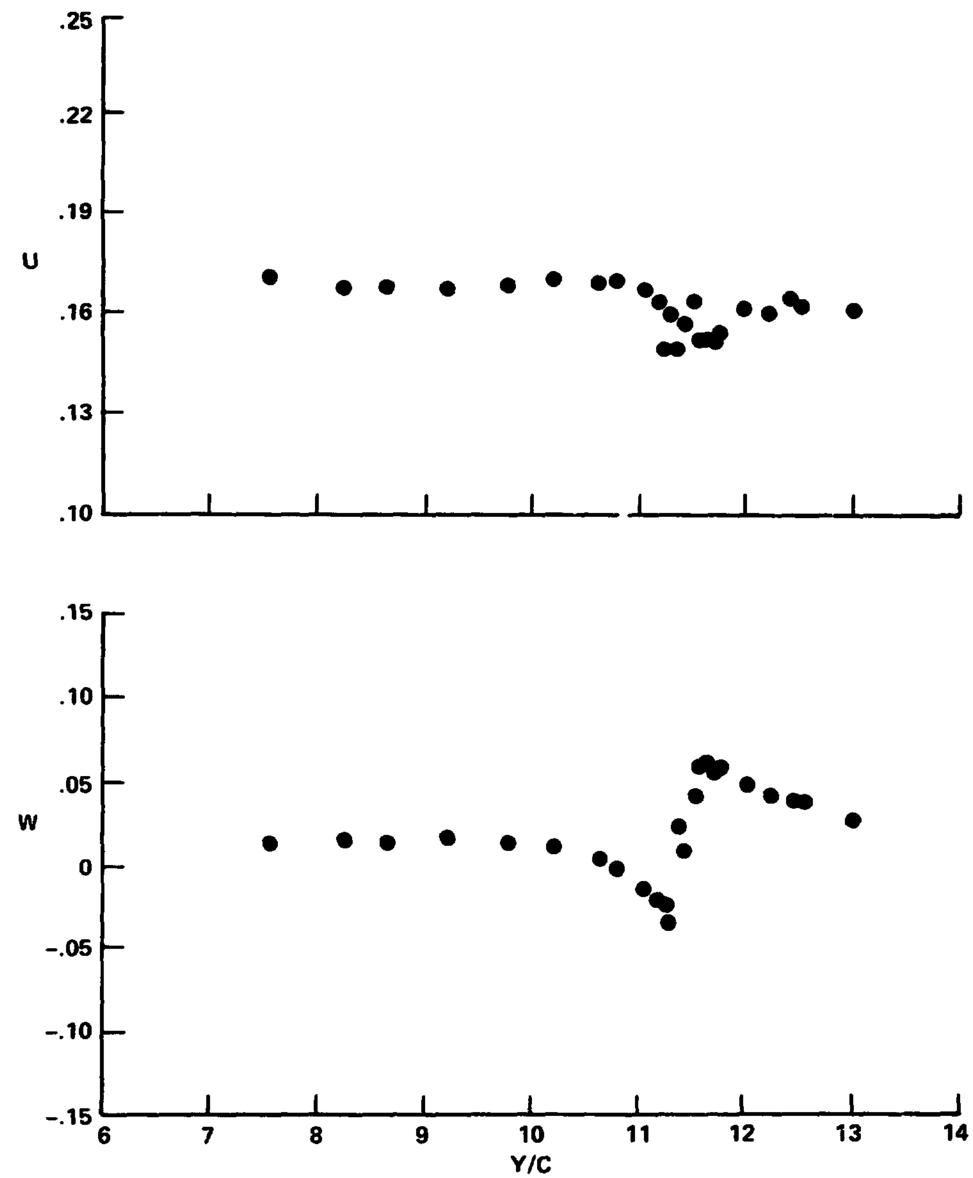

7-10. Lateral traverse, x/c = -1.00, z/c = -0.61

Figure 7. (Continued)

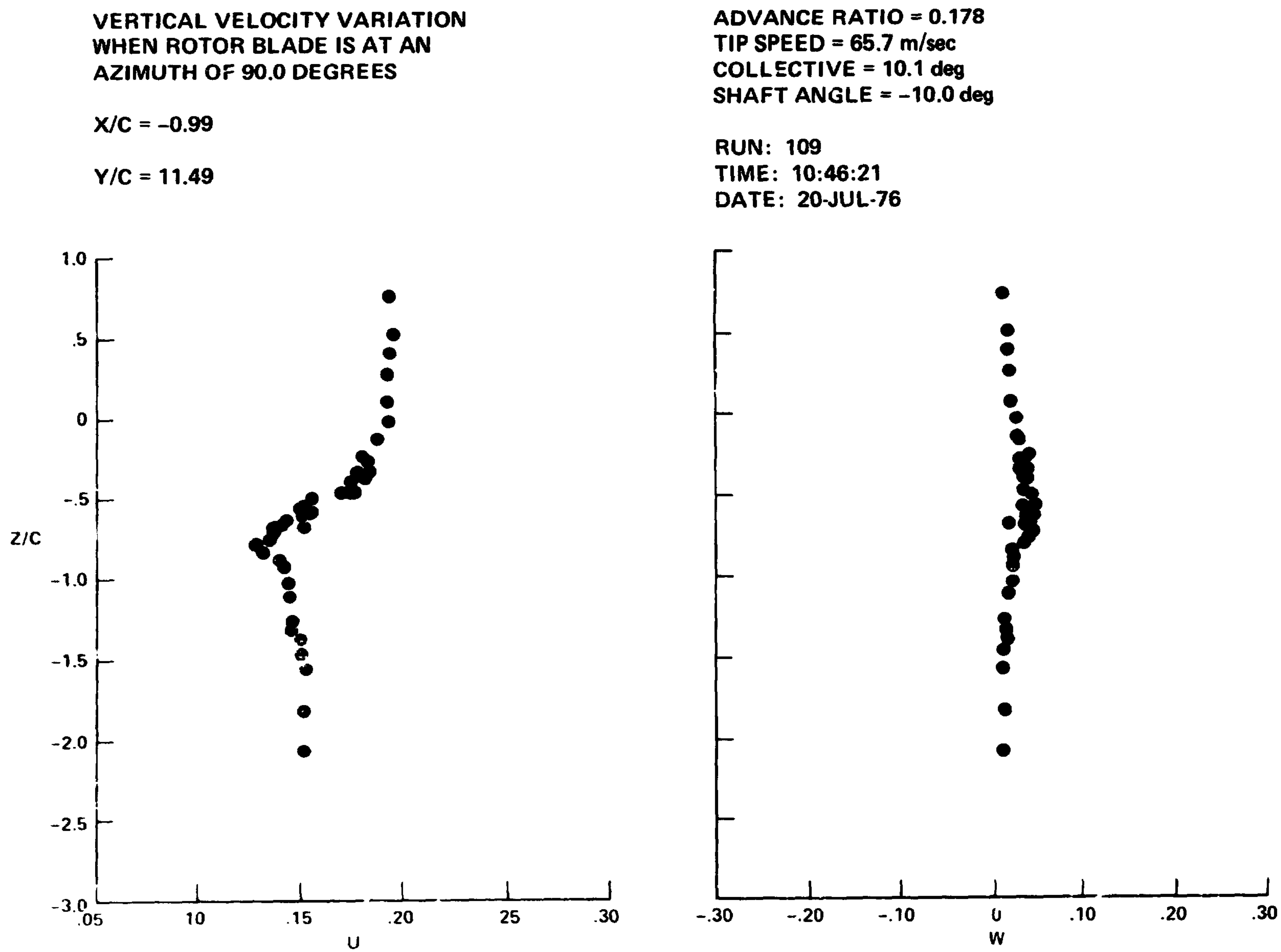

7-11. Vertical traverse, x/c = -1.00, y/c = 11.49

Figure 7. (Continued)

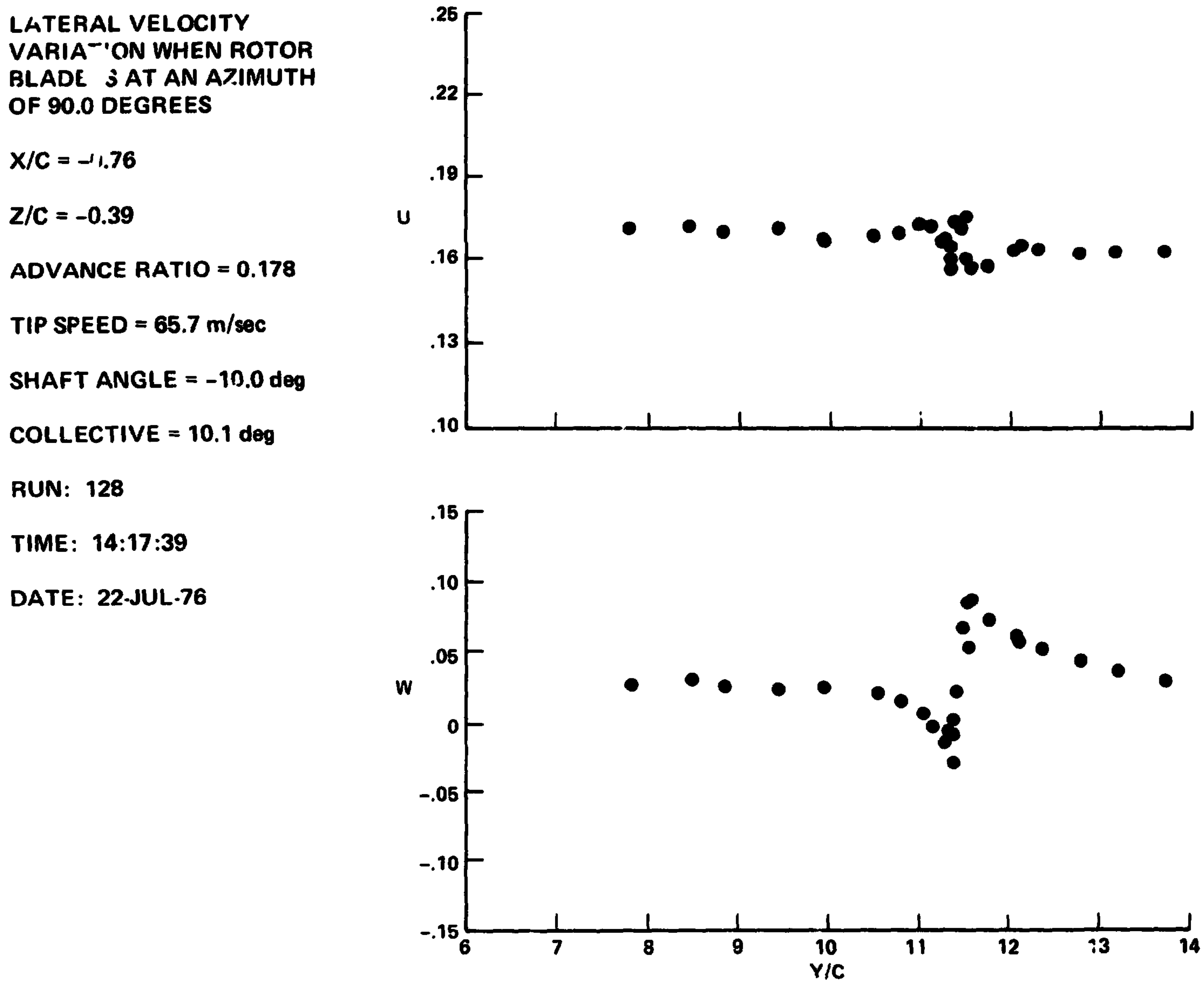

7-12. Lateral traverse, x/c = -0.75, z/c = -0.34

Figure 7. (Continued)

LATERAL VELOCITY
VARIATION WHEN ROTOR
BLADE IS AT AN AZIMUTH
OF 90.0 DEGREES

X/C = -0.74

Z/C = -0.39

ADVANCE RATIO = 0.178

TIP SPEED = 65.7 m/sec

SHAFT ANGLE = -10.0 deg

COLLECTIVE = 10.1 deg

RUN: 131

TIME: 13:22:29

DATE: 26-JUL-76

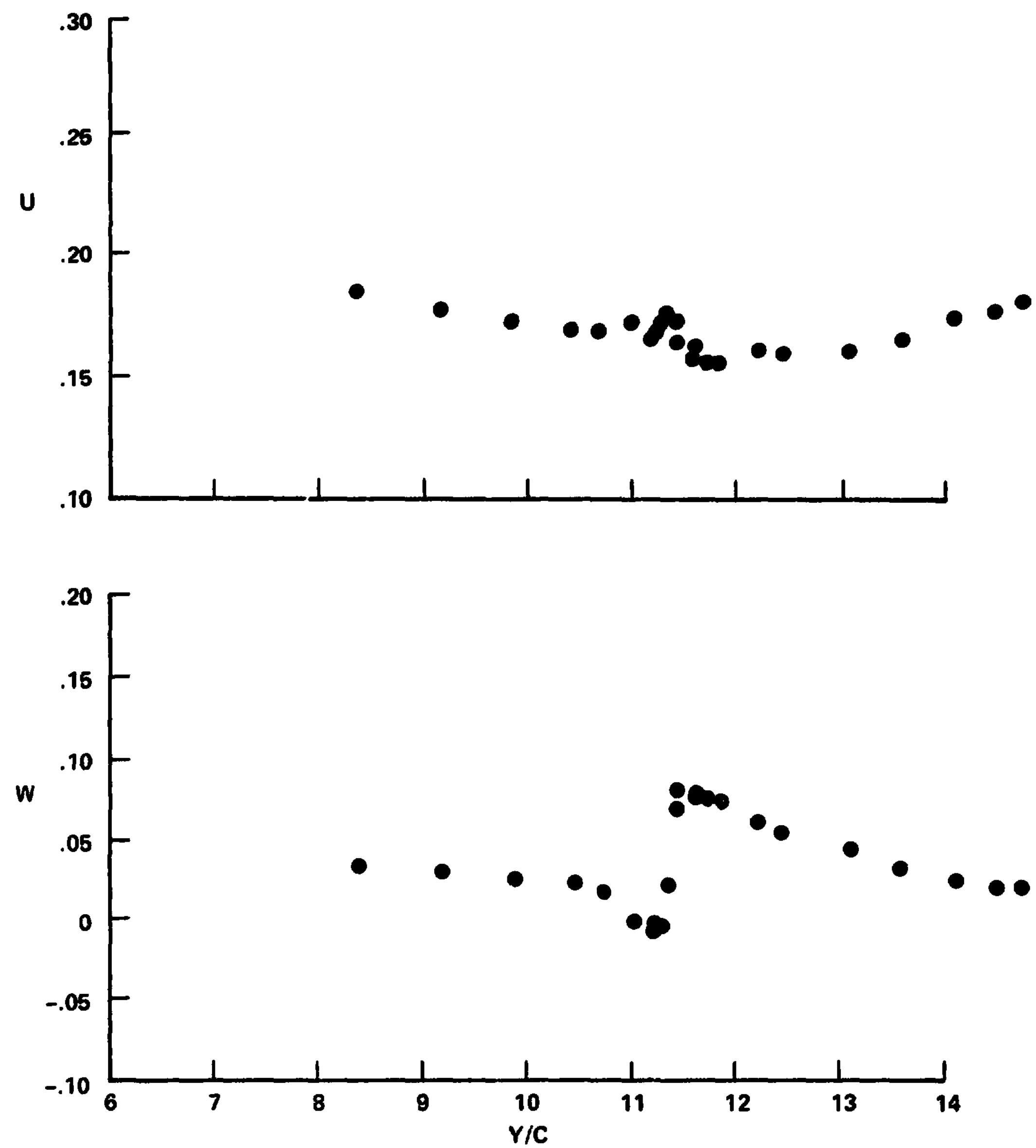

7-13. Lateral traverse, x/c = -0.75, z/c = -0.39

Figure 7. (Continued)

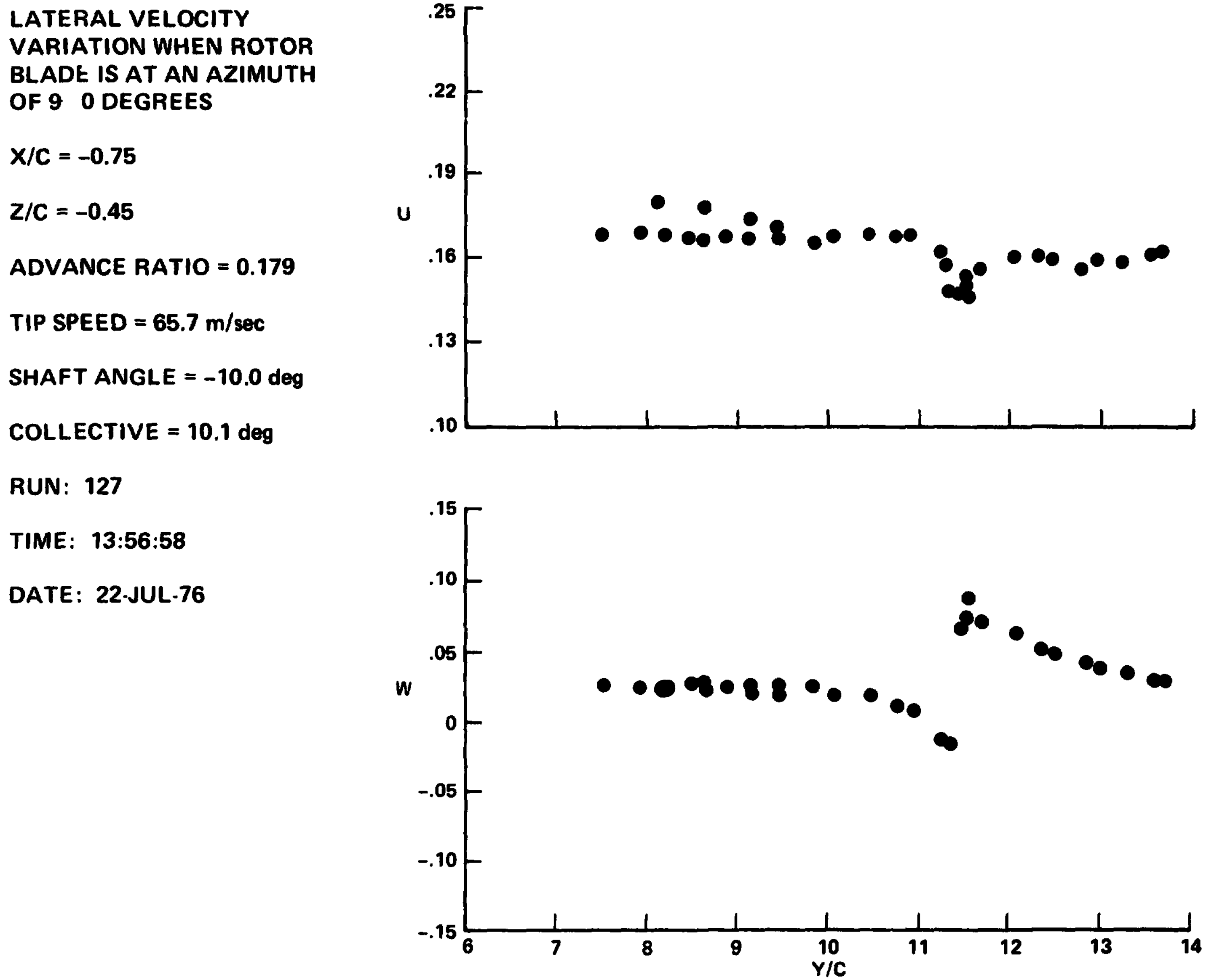

7-14. Lateral traverse, x/c = –0.75, z/c = –0.45

Figure 7. (Continued)

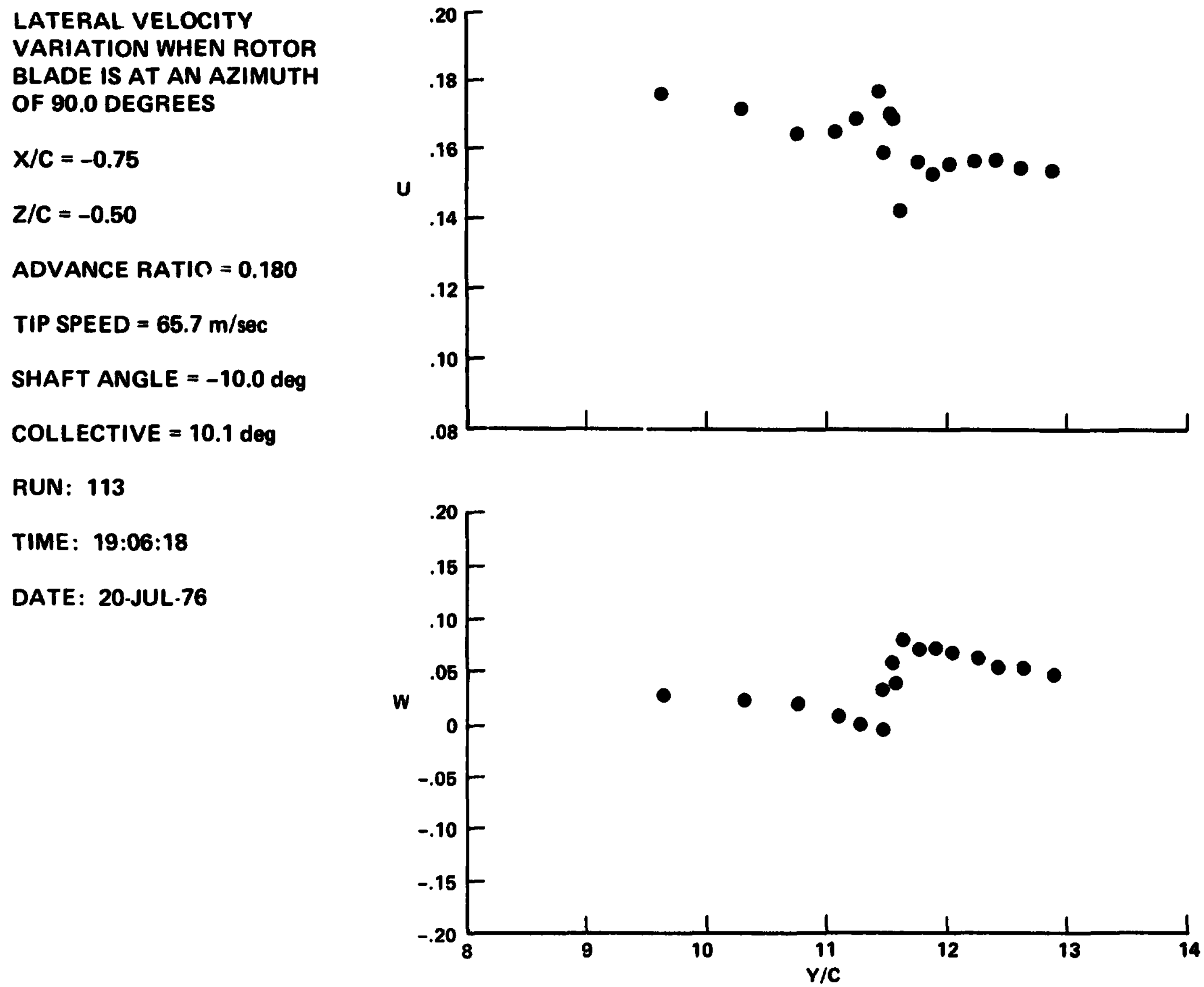

7-15. Lateral traverse, x/c = -0.75, z/c = -0.49

Figure 7. (Continued)

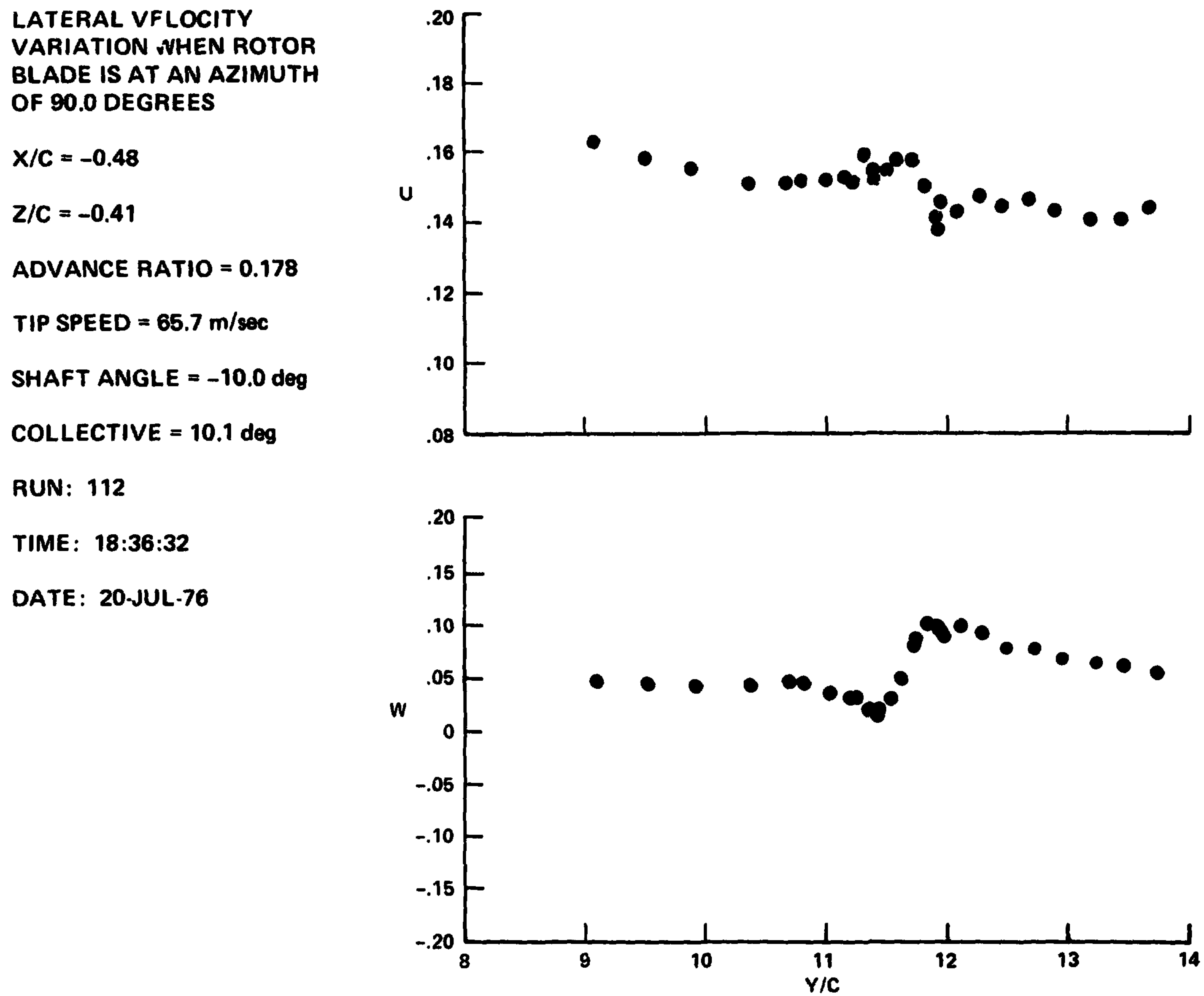

7-16. Lateral traverse, x/c = -0.48, z/c = -0.41

Figure 7. (Continued)

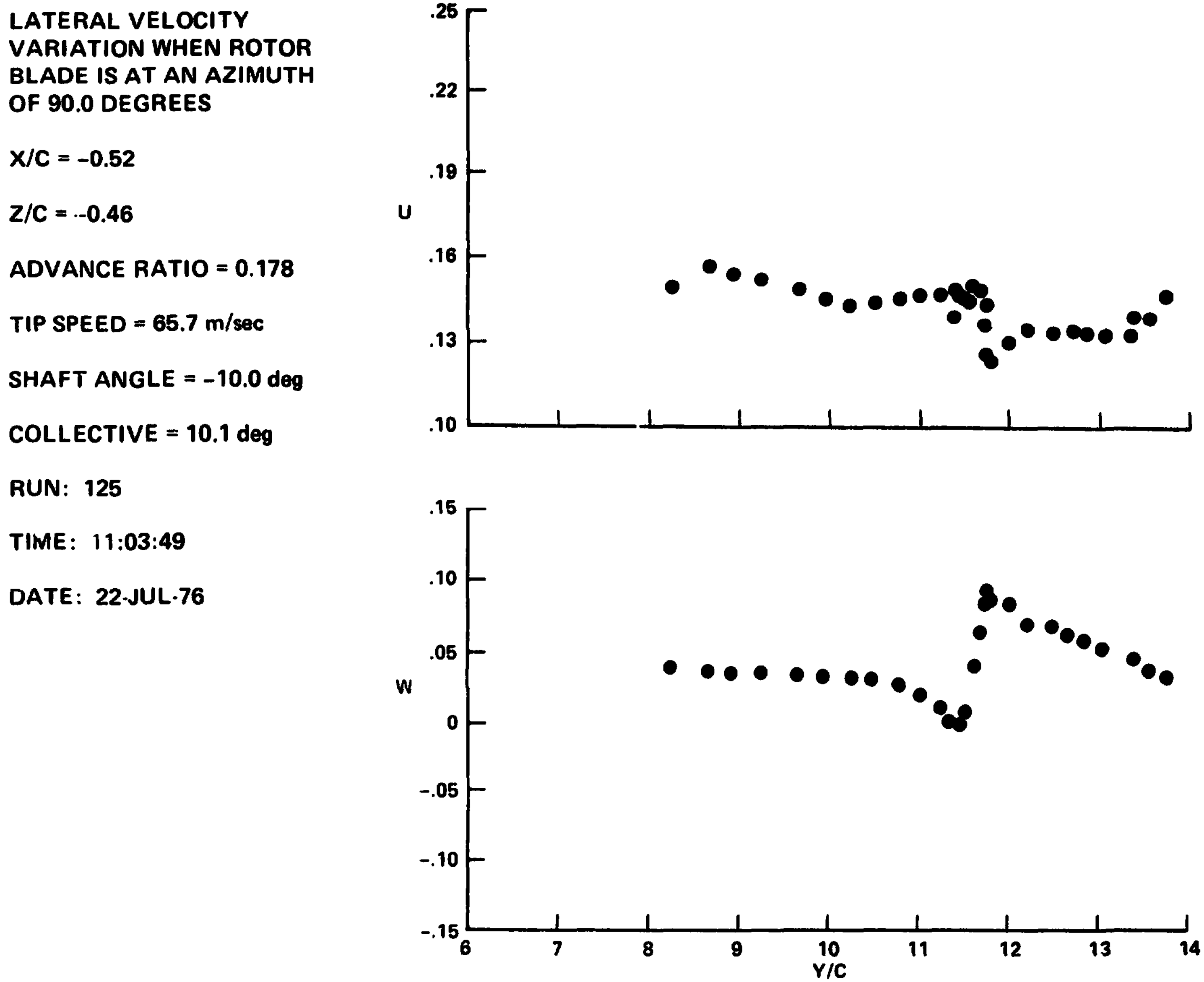

7-17. Lateral traverse, x/c = -0.50, z/c = -0.45

Figure 7. (Continued)

LATERAL VELOCITY VARIATION WHEN ROTOR BLADE IS AT AN AZIMUTH OF 90.0 DEGREES

X/C = -0.52

Z/C = -0.53

ADVANCE RATIO = 0.177

TIP SPEED = 65.7 m/sec

SHAFT ANGLE = -10.0 deg

COLLECTIVE = 10.1 deg

RUN: 123

TIME: 18:13:39

DATE: 21-JUL-76

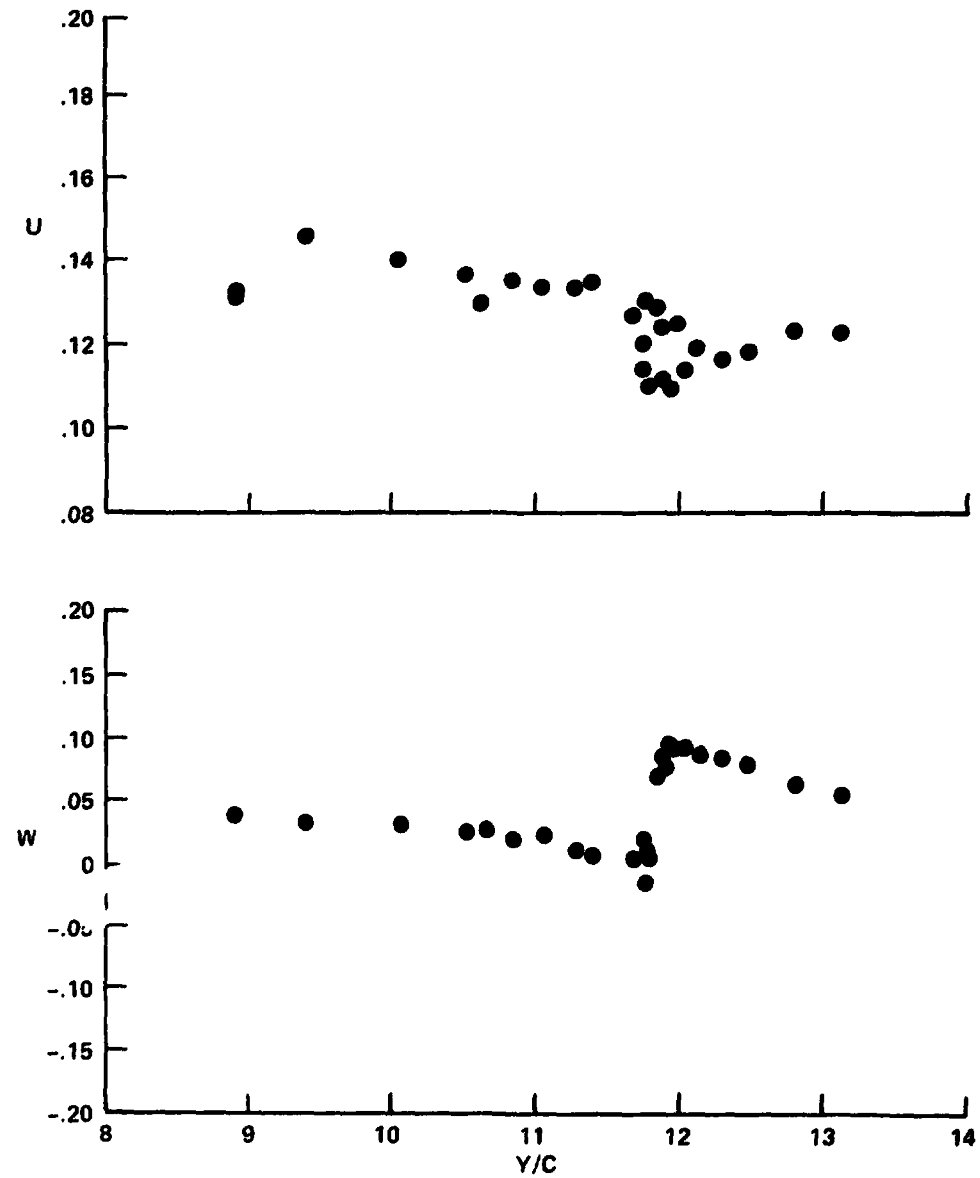

7-18. Lateral traverse, x/c = -0.50, z/c = -0.53

Figure 7. (Continued)

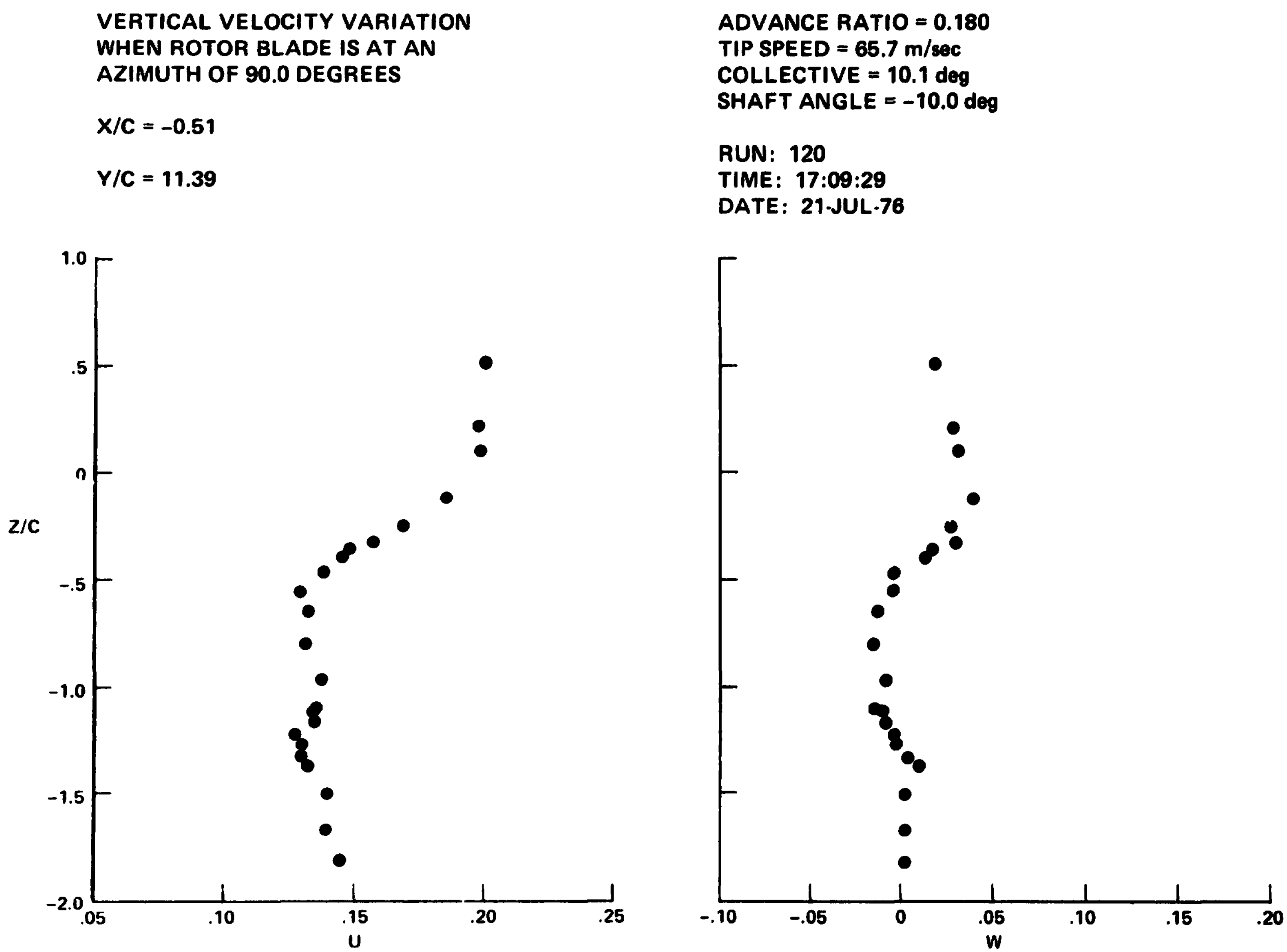

7-19. Vertical traverse, x/c = -0.50, y/c = 11.39

Figure 7. (Continued)

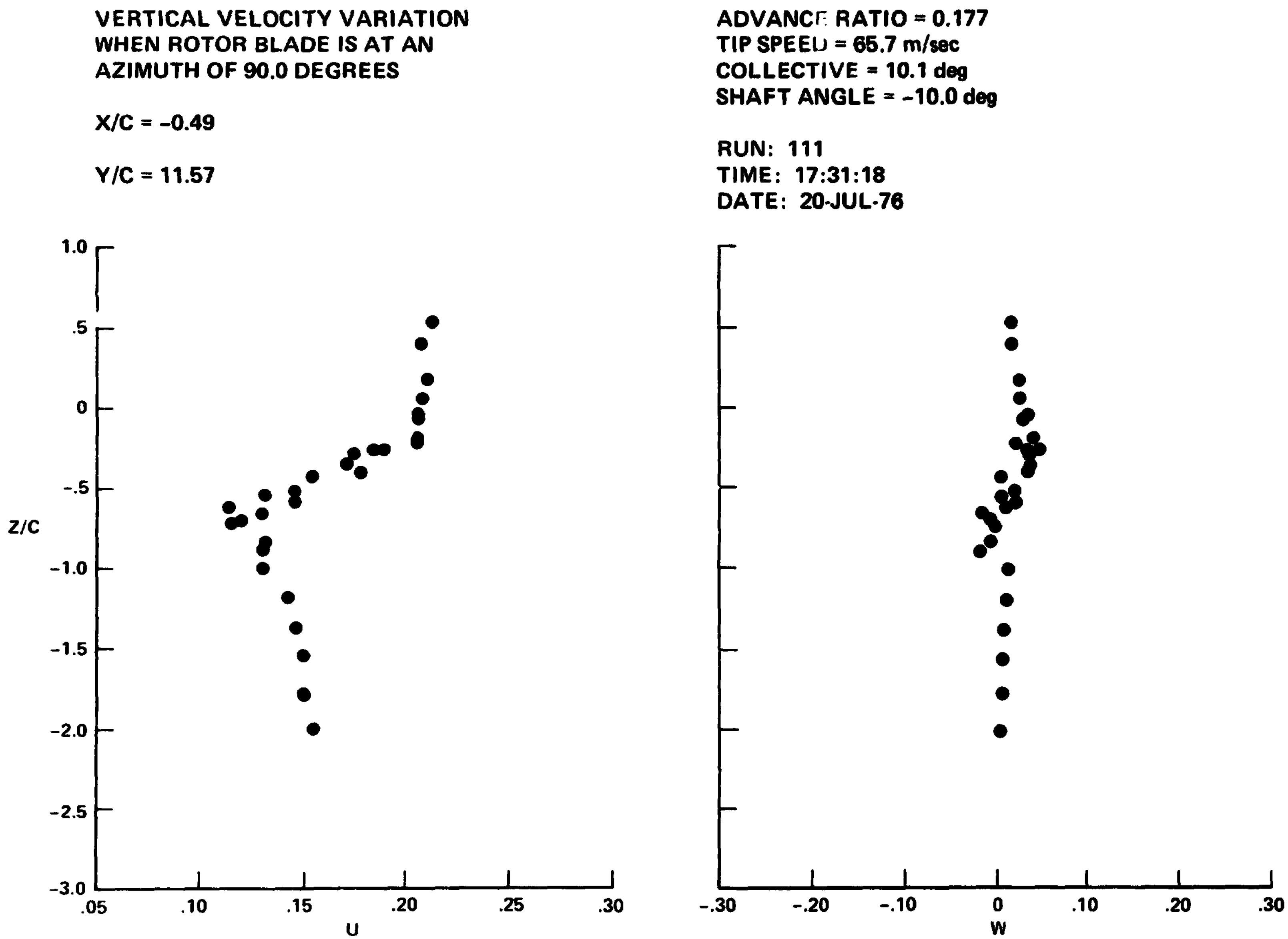

7-20. Vertical traverse, x/c = -0.50, y/c = 11.57

Figure 7. (Continued)

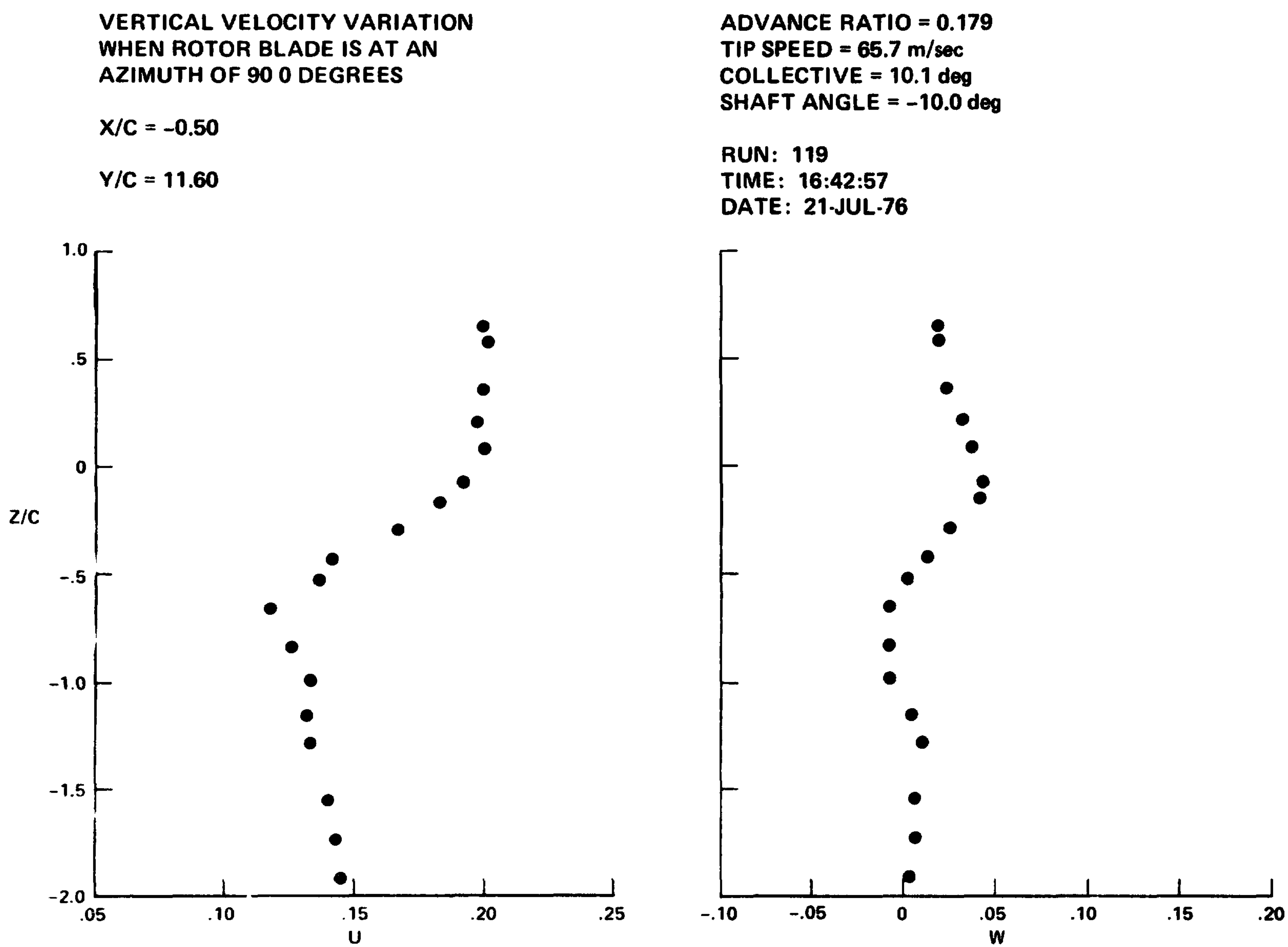

7-21. Vertical traverse, x/c = -0.50, y/c = 11.60

Figure 7. (Continued)

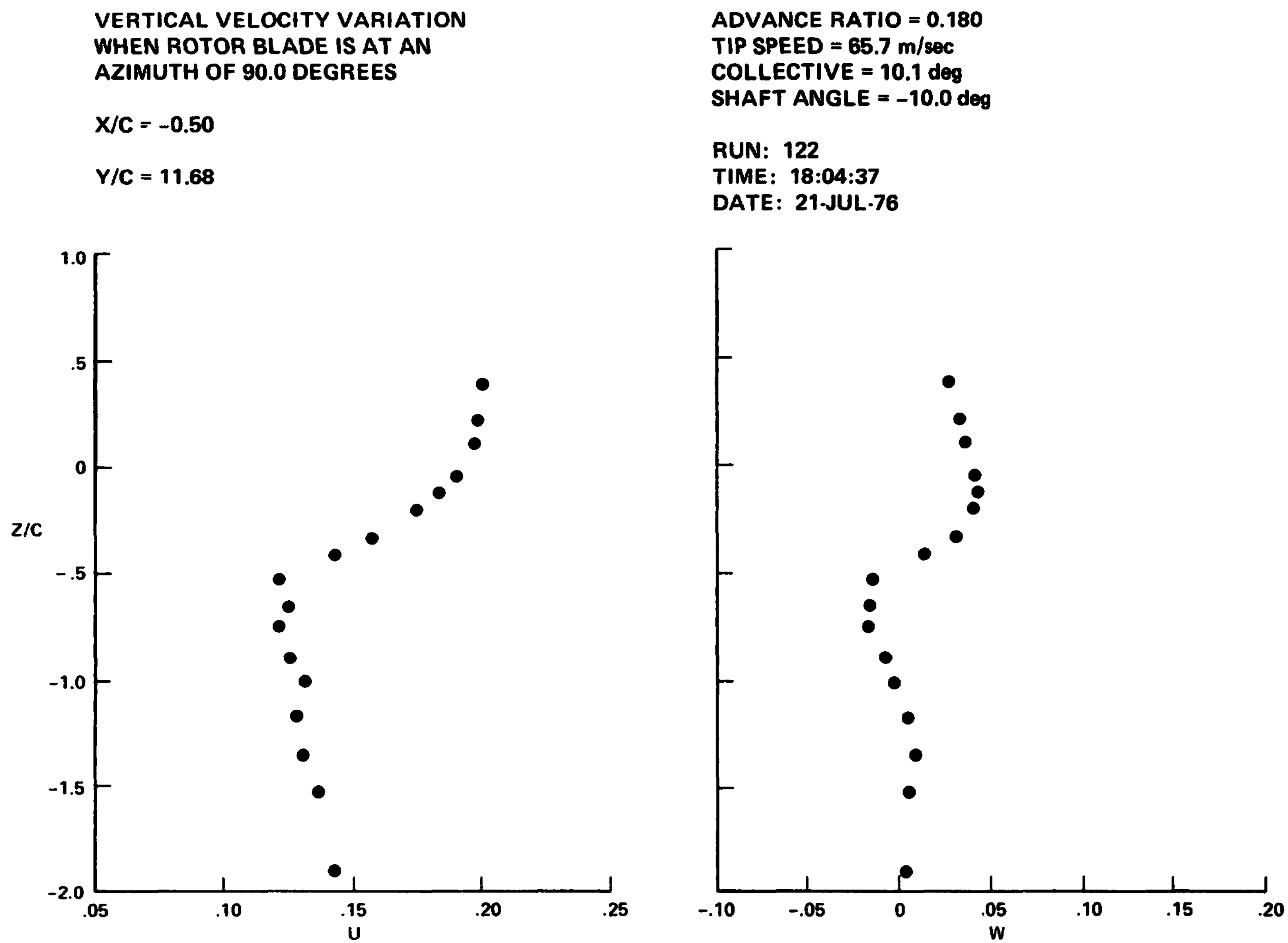

7-22. Vertical traverse, x/c = -0.50, y/c = 11.68

Figure 7. (Continued)

LATERAL VELOCITY VARIATION WHEN ROTOR BLADE IS AT AN AZIMUTH OF 90.0 DEGREES

X/C = -0.00

Z/C = -0.24

ADVANCE RATIO = 0.18

TIP SPEED = 65.7 m/sec

SHAFT ANGLE = -10.0 deg

COLLECTIVE = 10.1 deg

RUN: 129

TIME: 15:12:09

DATE: 22-JUL-76

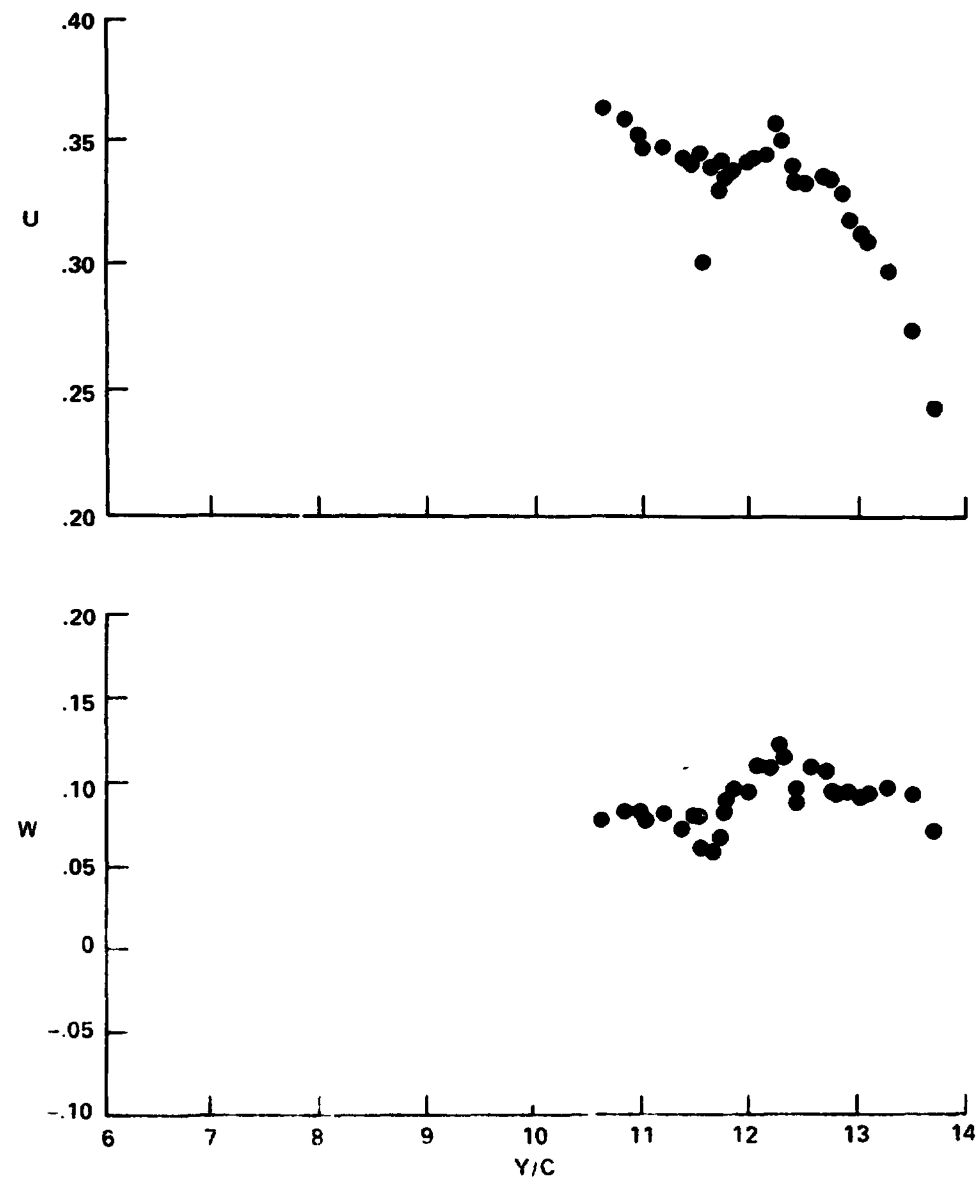

7-23. Lateral traverse, x/c = 0.00, z/c = -0.24

Figure 7. (Continued)

LATERAL VELOCITY VARIATION WHEN ROTOR BLADE IS AT AN AZIMUTH OF 90.0 DEGREES

X/C = 1.30

Z/C = -0.39

ADVANCE RATIO = 0.180

TIP SPEED = 65.7 m/sec

SHAFT ANGLE = -10.0 deg

COLLECTIVE = 10.1 deg

RUN: 143

TIME: 10:10:01

DATE: 27-JUL-76

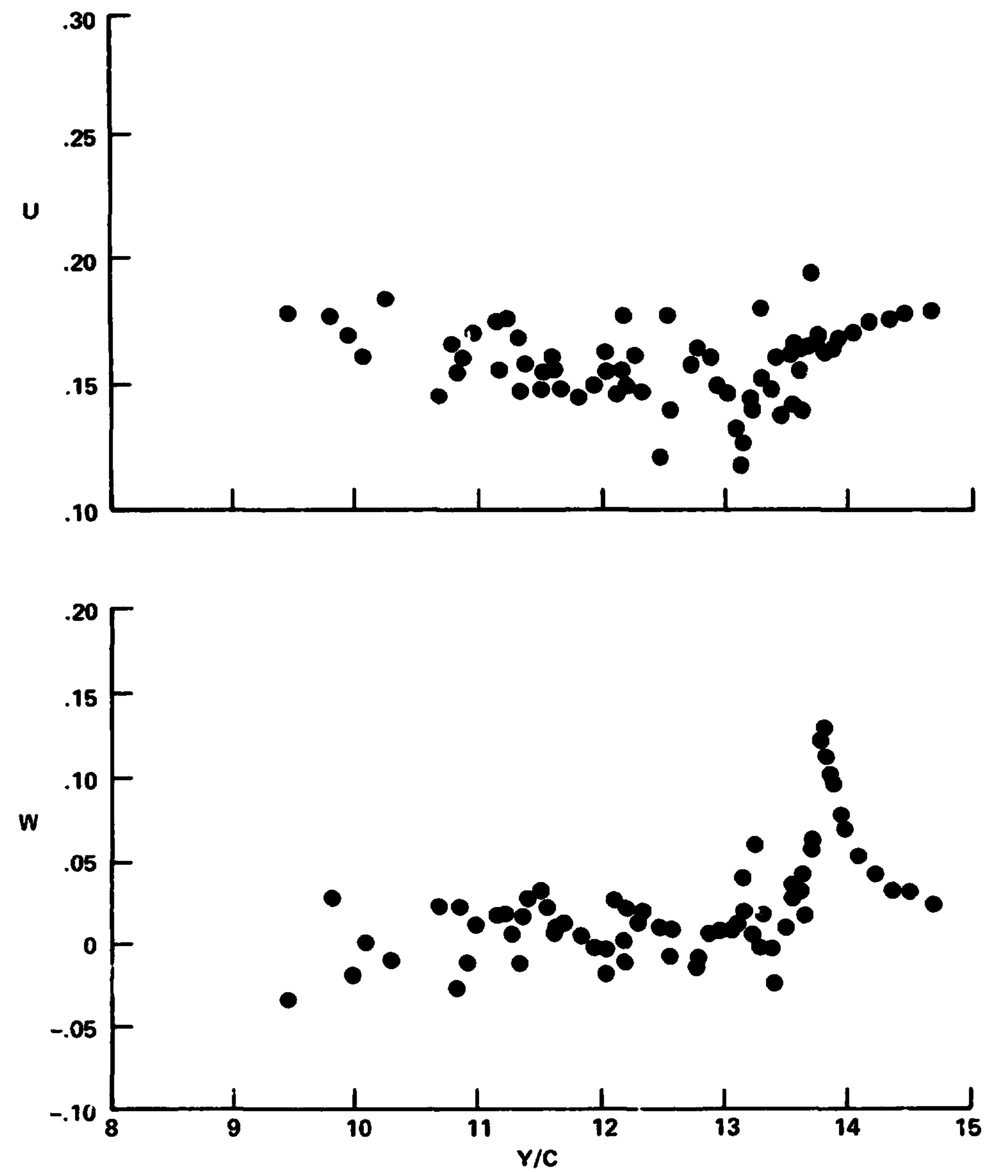

7-24. Lateral traverse, x/c = 1.30, z/c = -0.39

Figure 7. (Continued)

LATERAL VELOCITY
VARIATION WHEN ROTOR
BLADE IS AT AN AZIMUTH
OF 90.0 DEGREES

X/C = 1.25

Z/C = -0.45

ADVANCE RATIO = 0.180

TIP SPEED = 65.7 m/sec

SHAFT ANGLE = -10.0 deg

COLLECTIVE = 10.1 deg

RUN: 130

TIME: 16:50:19

DATE: 22-JUL-76

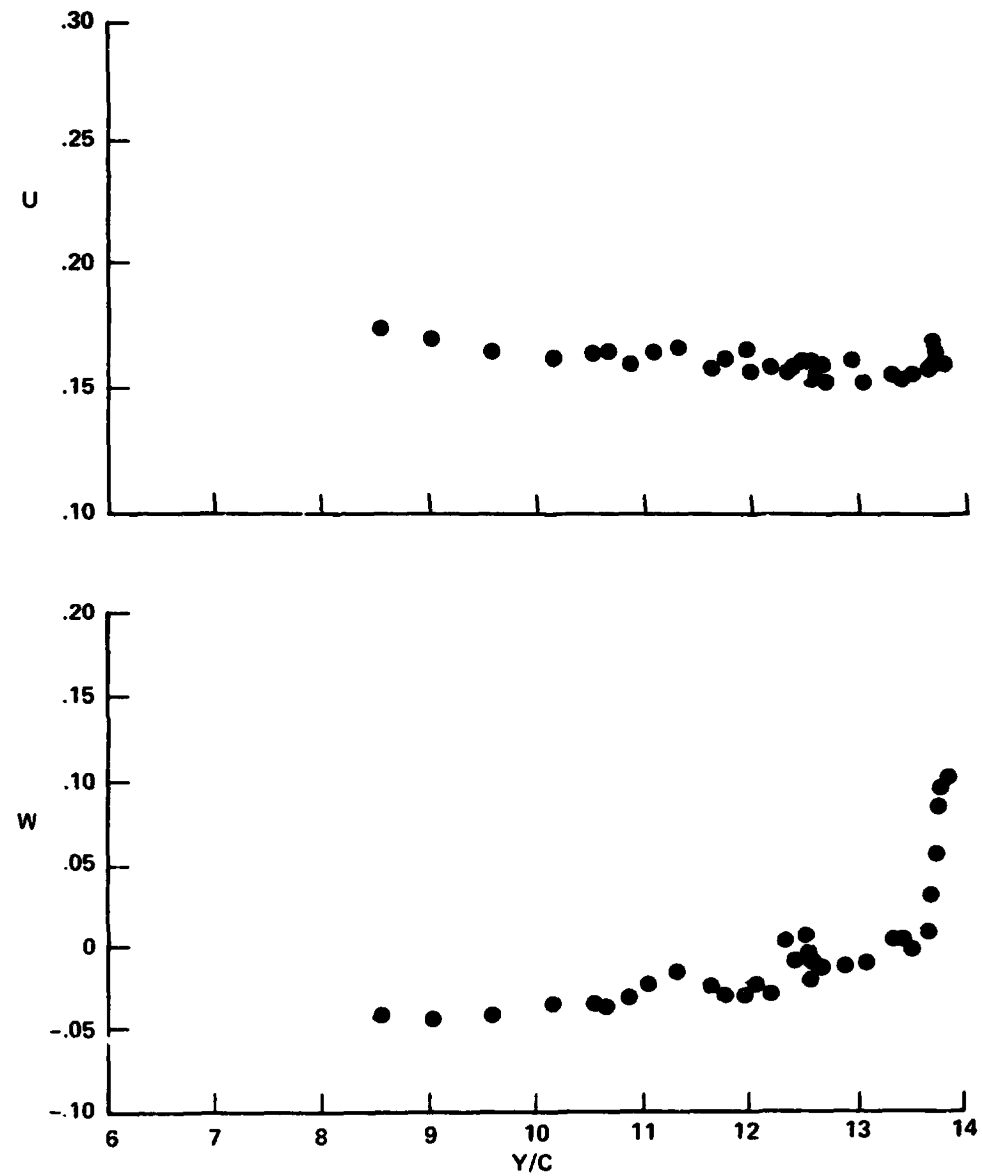

7-25. Lateral traverse, x/c = 1.25, z/c = -0.45

Figure 7. (Continued

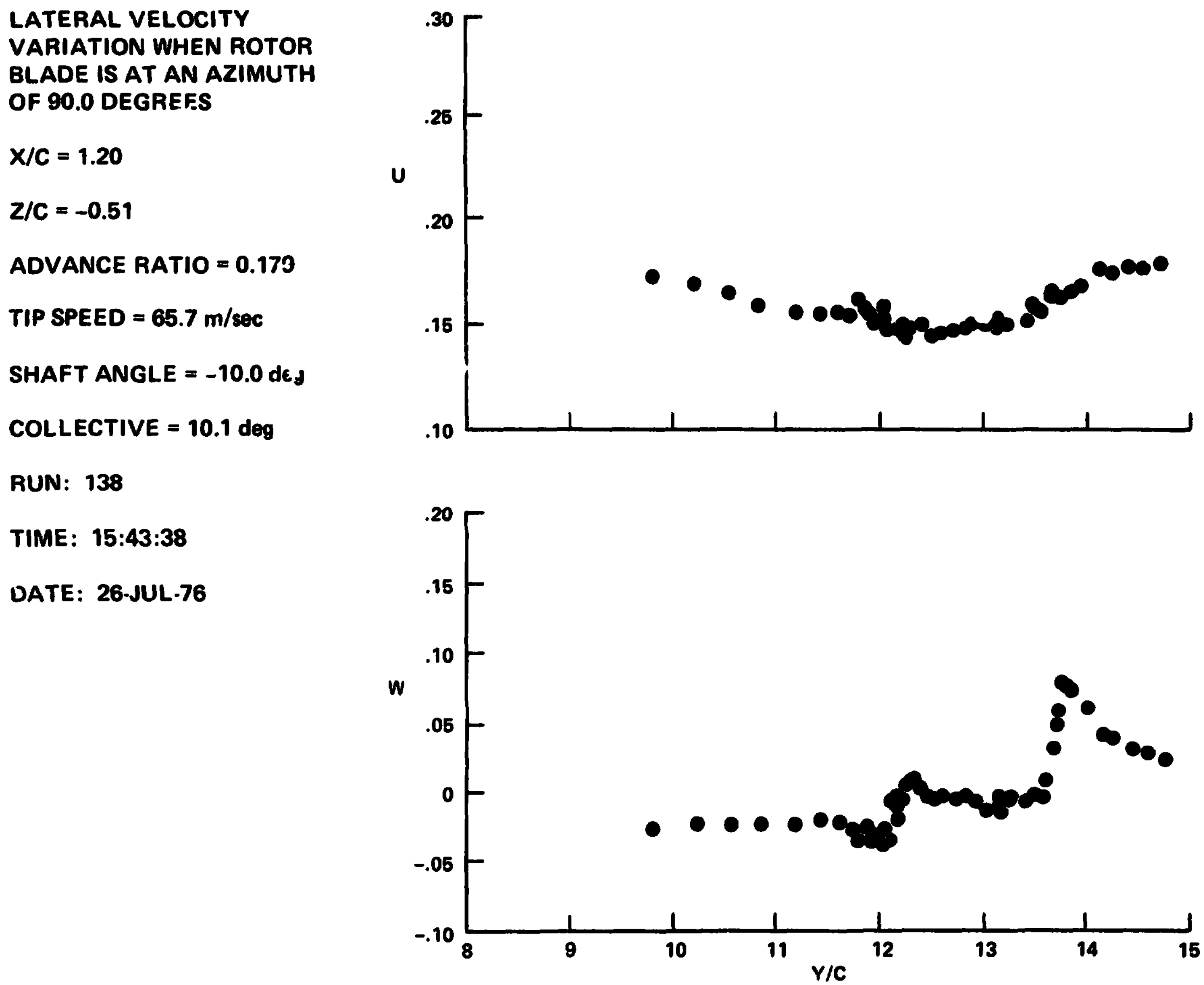

7-26. Lateral traverse, x/c = 1.20, z/c = -0.50

Figure 7. (Continued)

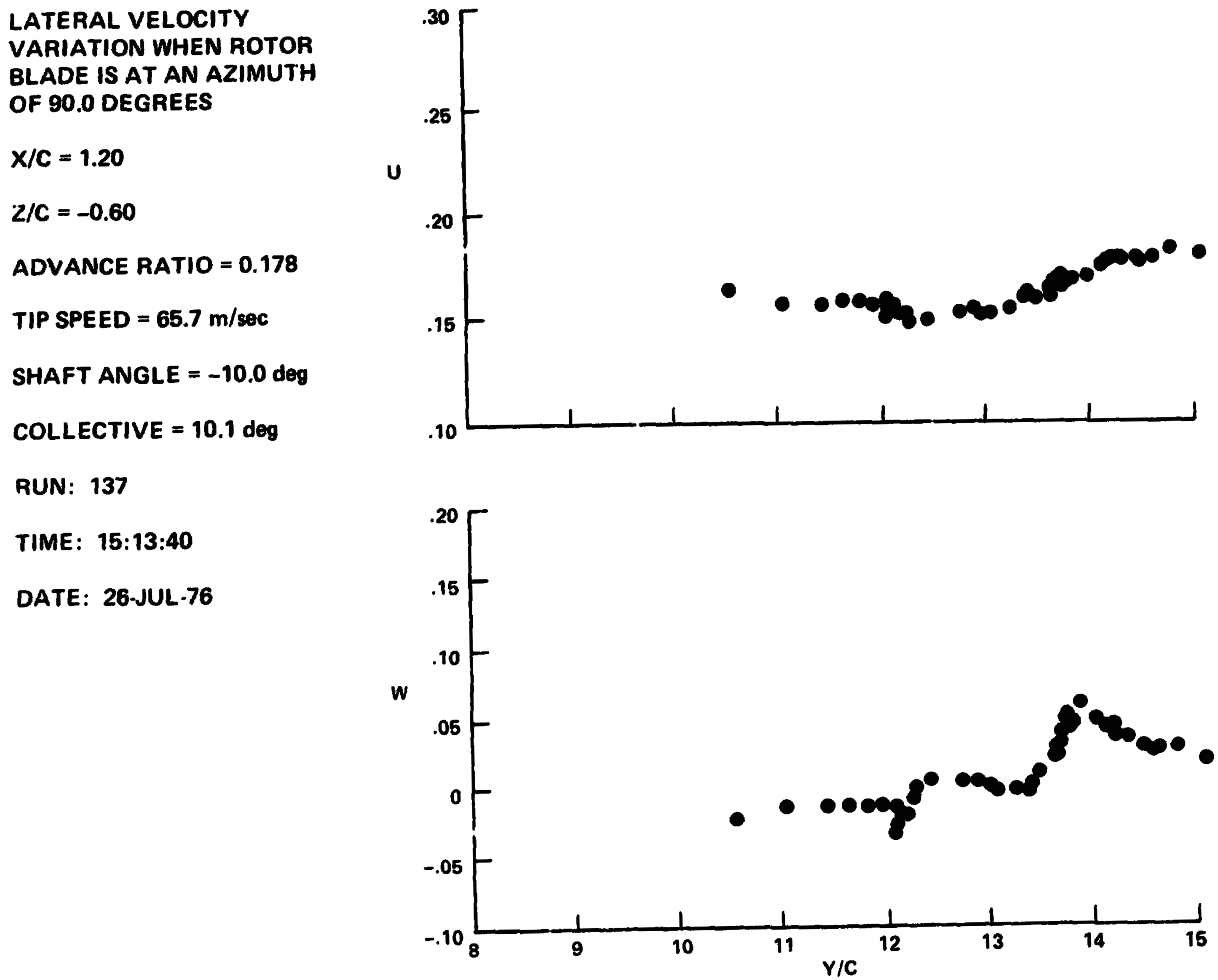

7-27. Lateral traverse, x/c = 1.20, z/c = -0.60

Figure 7. (Continued)

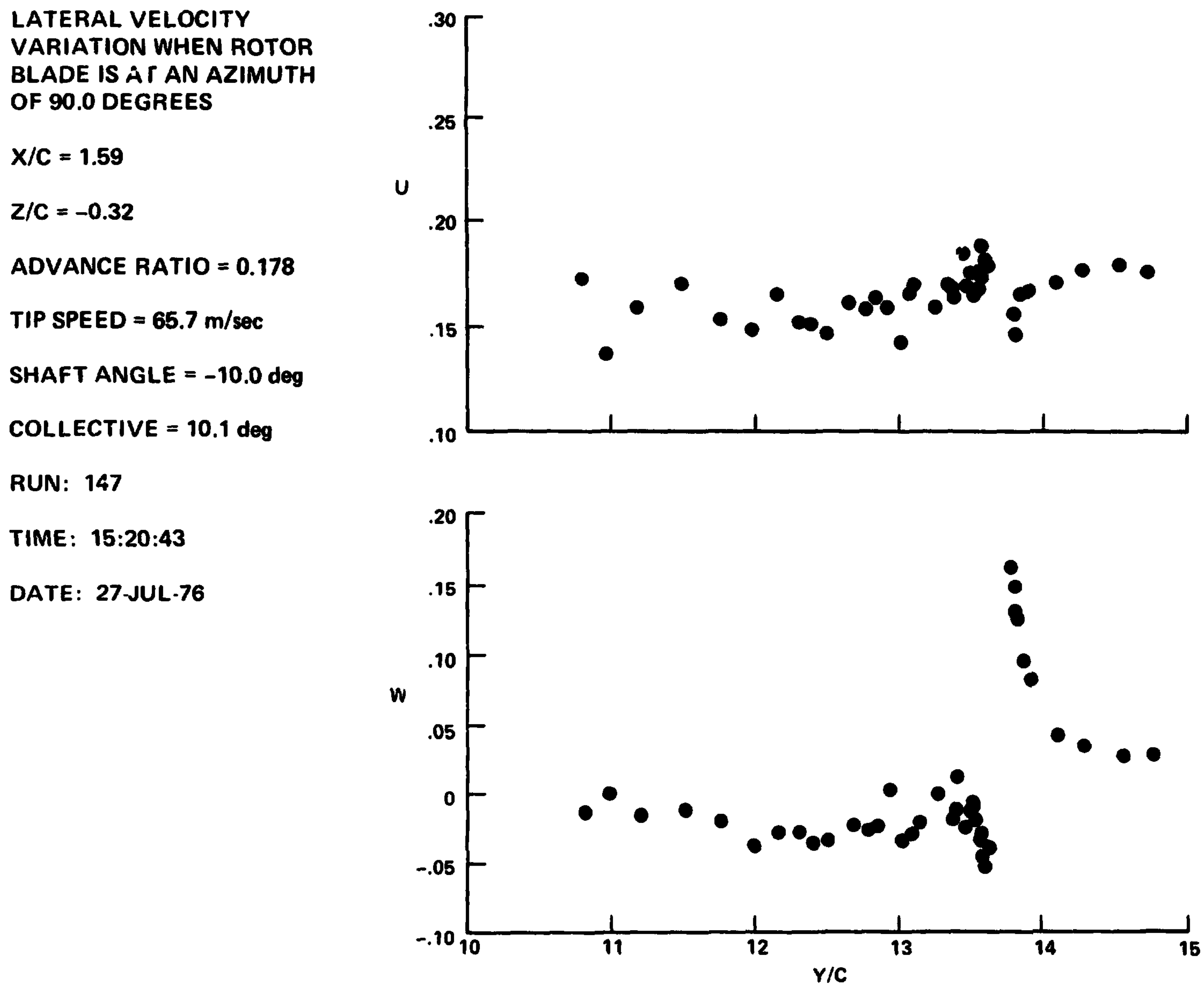

7-28. Lateral traverse, x/c = 1.59, z/c = -0.32

Figure 7. (Continued)

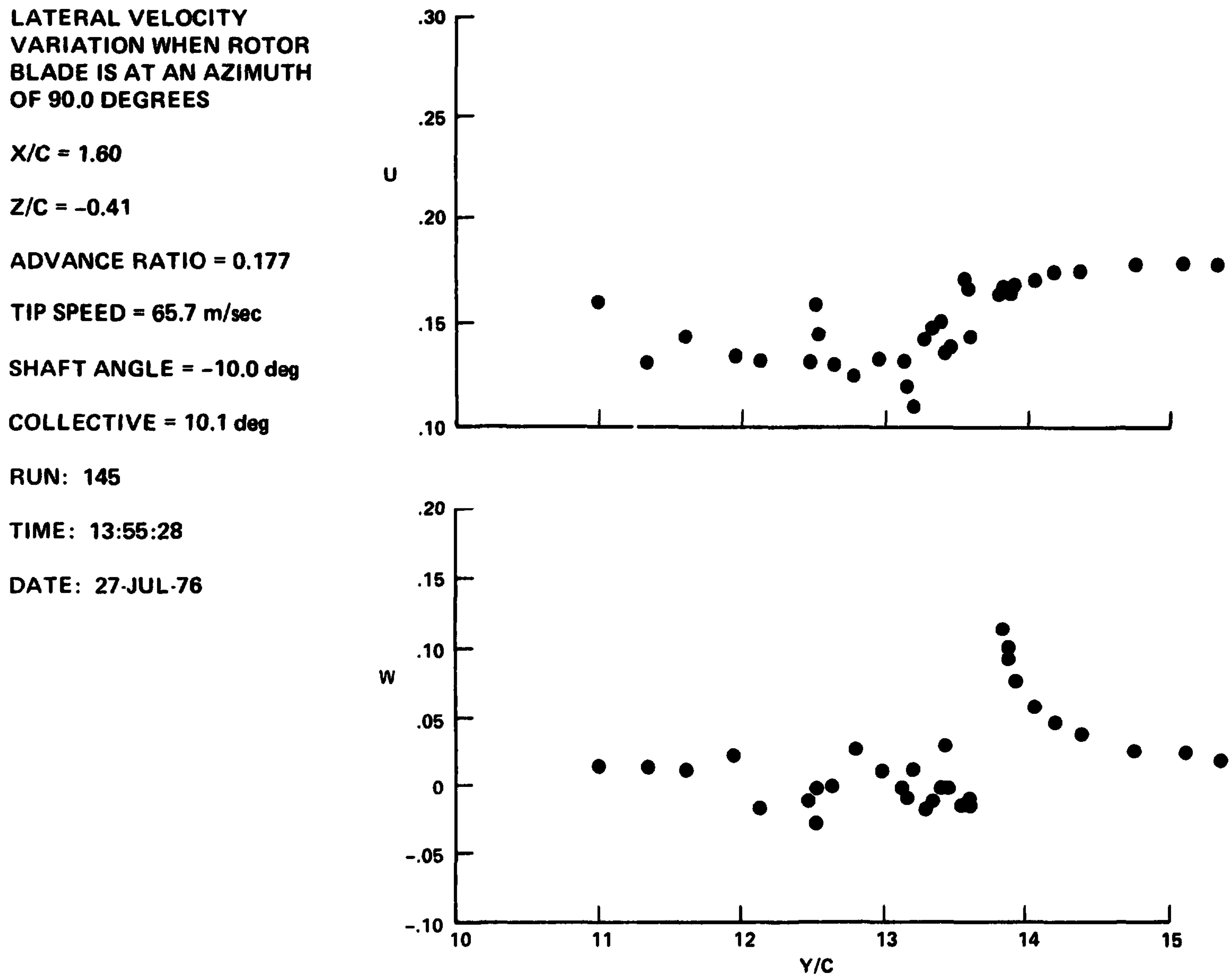

7-29. Lateral traverse, x/c = 1.60, z/c = −0.41

Figure 7. (Continued)

LATERAL VELOCITY VARIATION WHEN ROTOR BLADE IS AT AN AZIMUTH OF 90.0 DEGREES

X/C = 1.59

Z/C = -0.45

ADVANCE RATIO = 0.181

TIP SPEED = 65.7 m/sec

SHAFT ANGLE = -10.0 deg

COLLECTIVE = 10.1 deg

RUN: 144

TIME: 11:09:15

DATE: 27-JUL-76

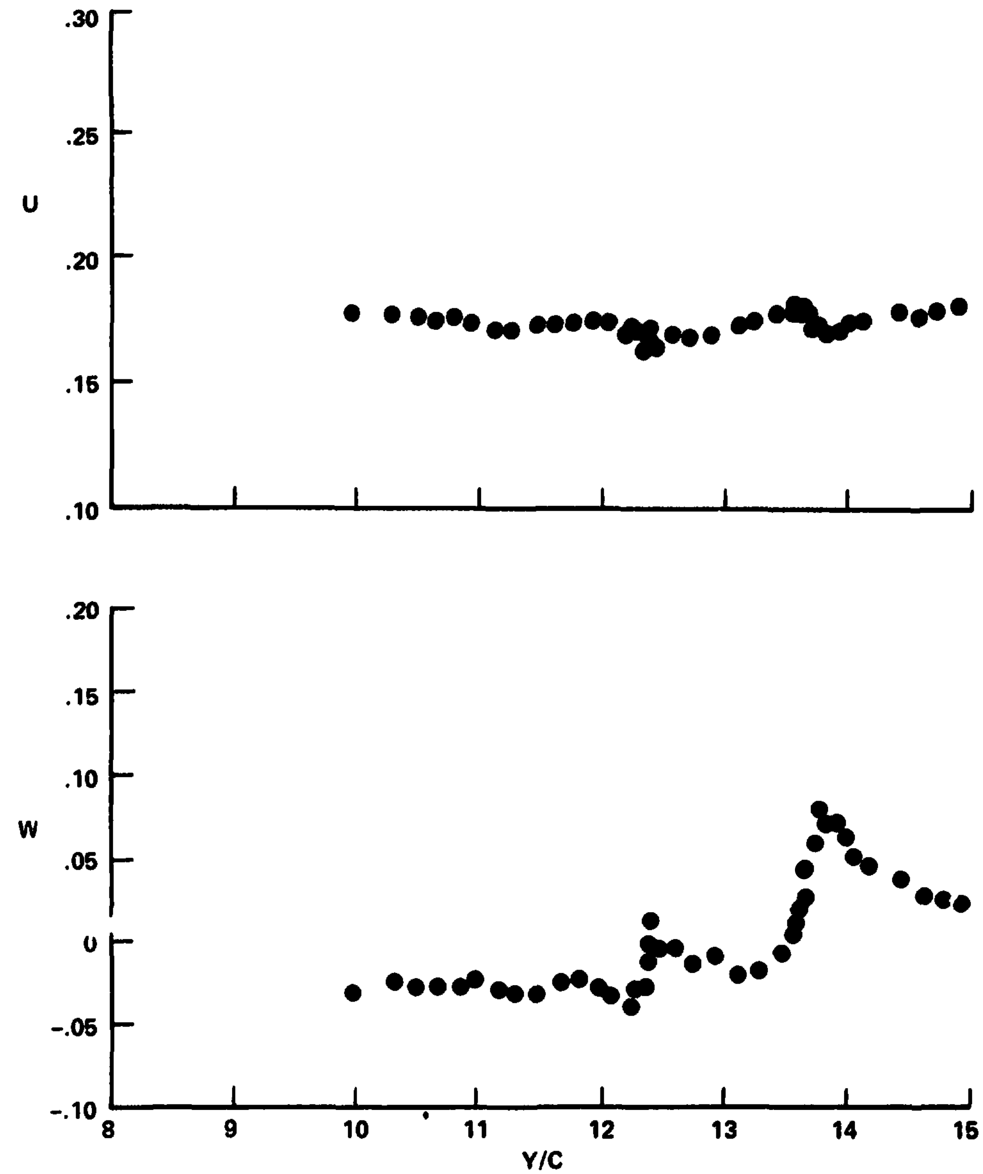

7-30. Lateral traverse, x/c = 1.59, z/c = -0.45

Figure 7. (Continued)

LATERAL VELOCITY VARIATION WHEN ROTOR BLADE IS AT AN AZIMUTH OF 90.0 DEGREES

X/C = 1.59

Z/C = -0.49

ADVANCE RATIO = 0.179

TIP SPEED = 65.7 m/sec

SHAFT ANGLE = -10.0 deg

COLLECTIVE = 10.1 deg

RUN: 139

TIME: 16:16:20

DATE: 26-JUL-73

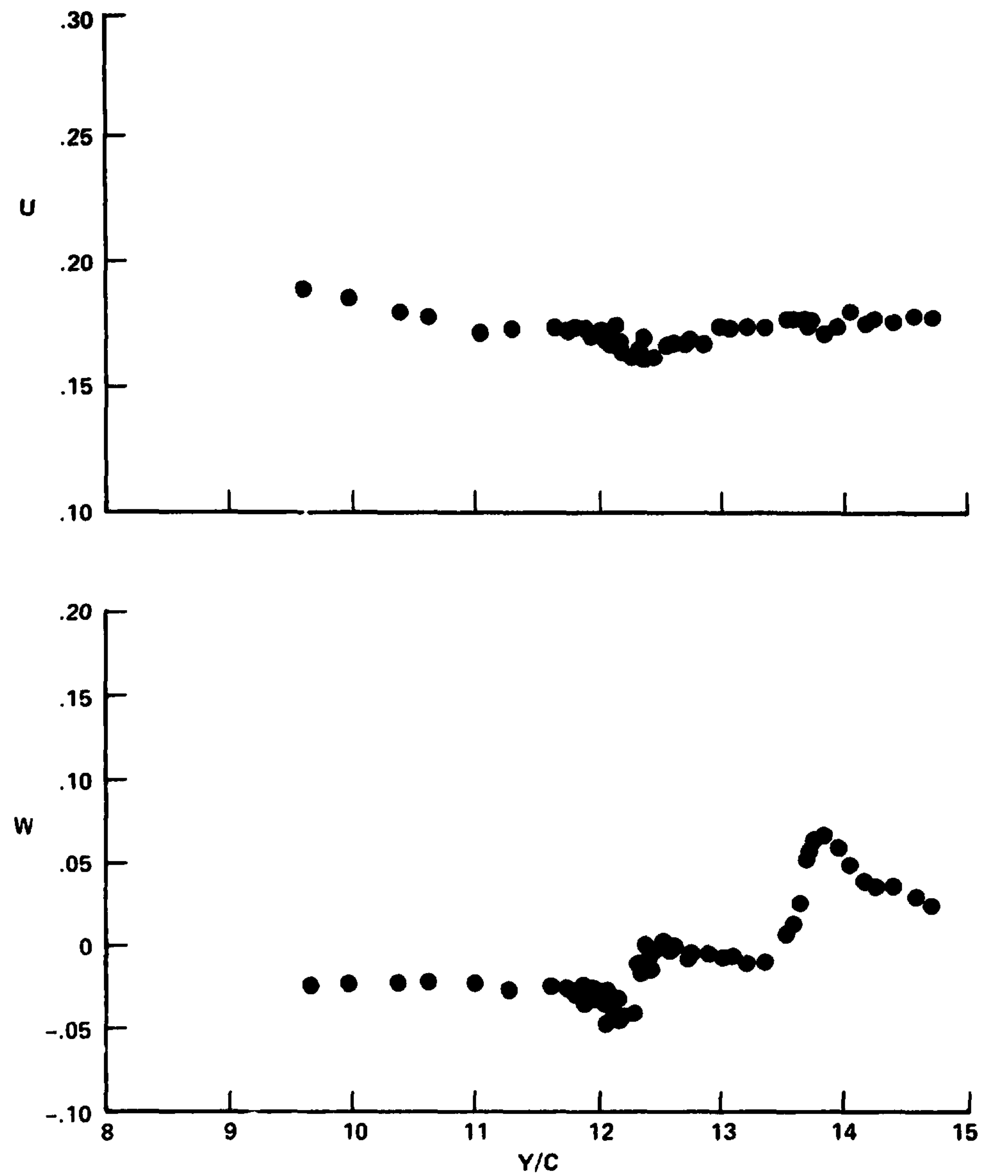

7-31. Lateral traverse, x/c = 1.59, z/c = -0.49

Figure 7. (Continued)

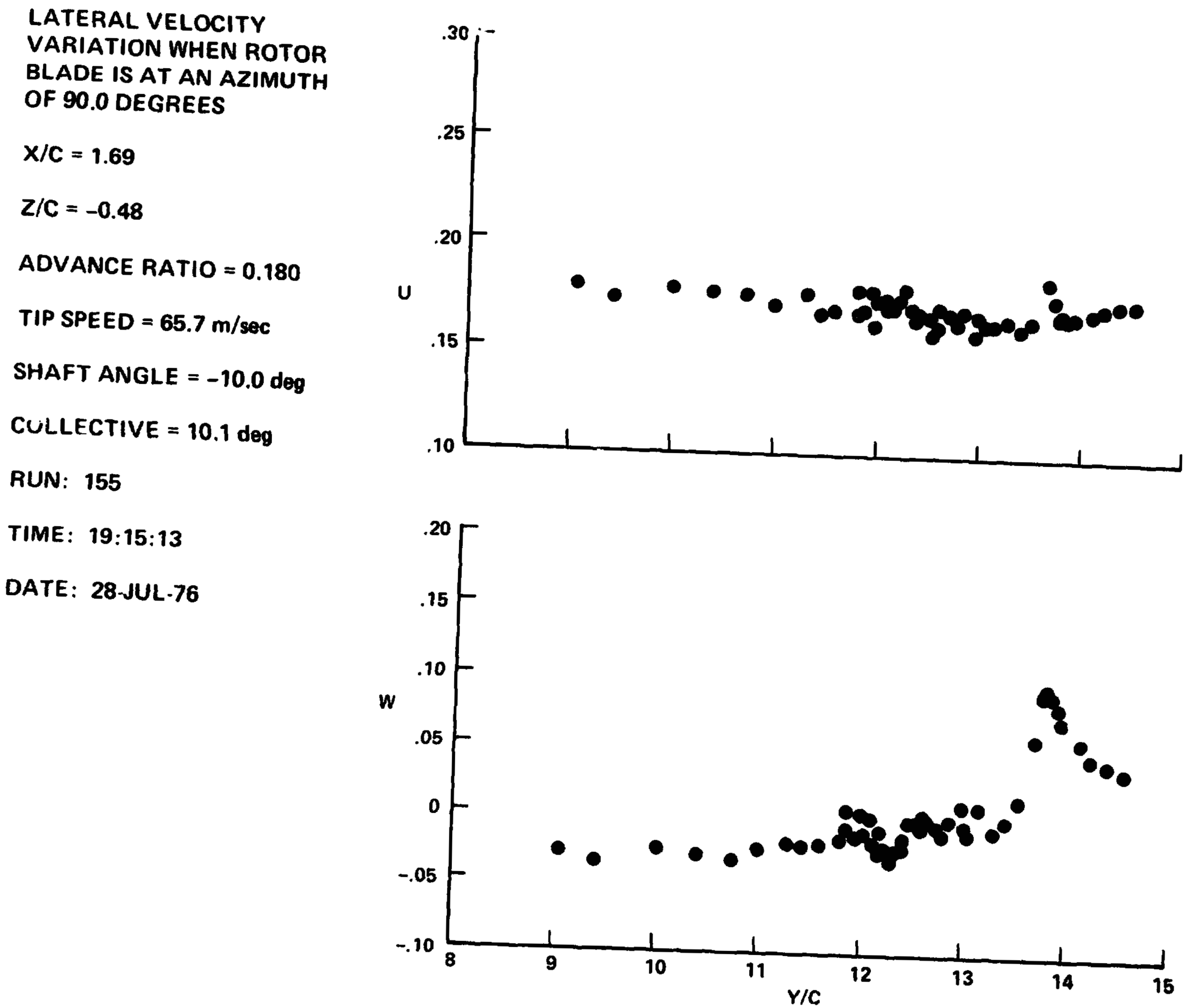

7-32. Lateral traverse, x/c = 1.69, z/c = -0.48

Figure 7. (Continued)

LATERAL VELOCITY VARIATION WHEN ROTOR BLADE IS AT AN AZIMUTH OF 90.0 DEGREES

X/C = 1.84

Z/C = –0.47

ADVANCE RATIO = 0.174

TIP SPEED = 65.7 m/sec

SHAFT ANGLE = –10.0 deg

COLLECTIVE = 10.1 deg

RUN: 153

TIME: 17:48:25

DATE: 28-JUL-76

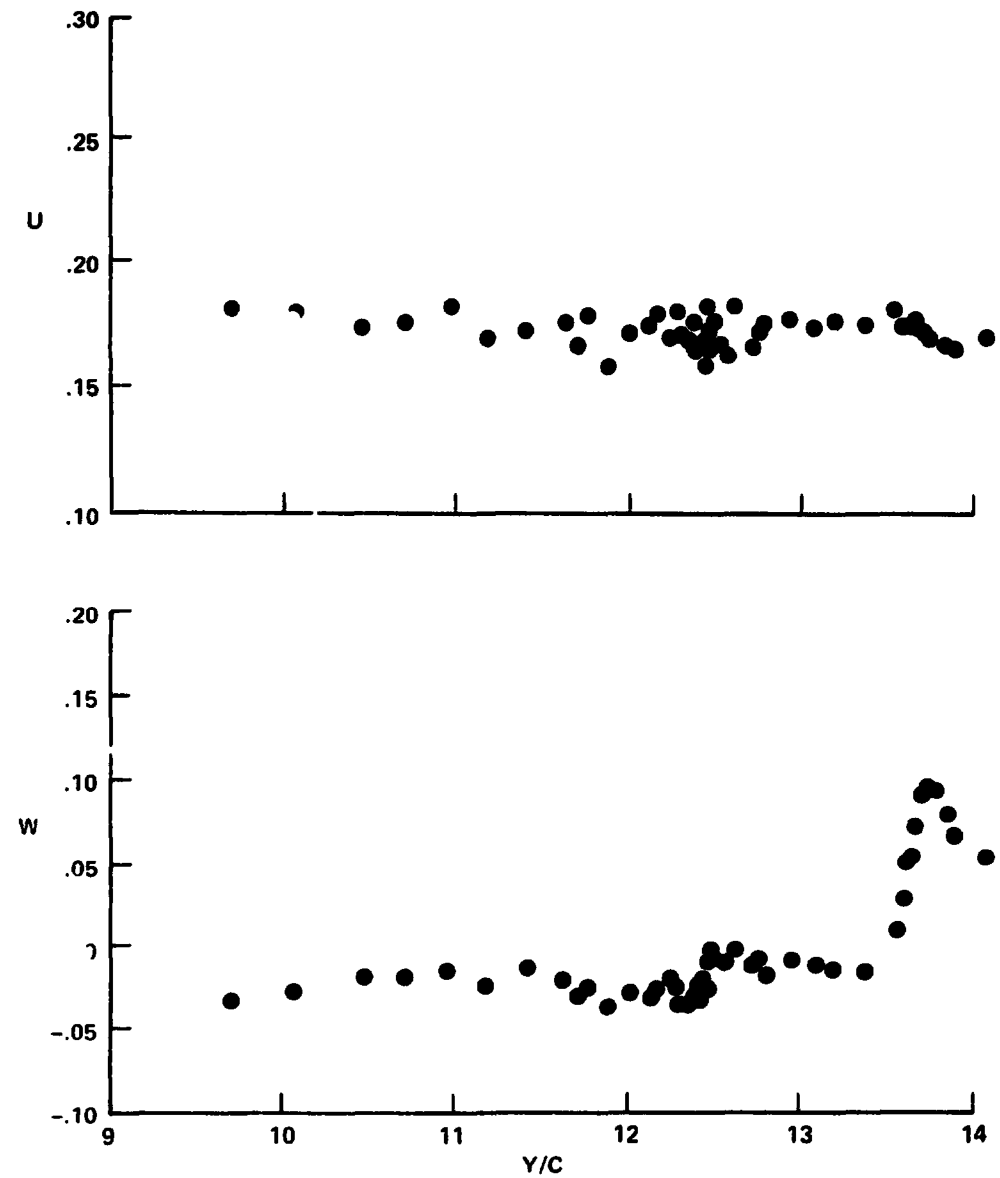

7-33. Lateral traverse, x/c = 1.84, z/c = -0.47

Figure 7. (Continued)

LATERAL VELOCITY VARIATION WHEN ROTOR BLADE IS AT AN AZIMUTH OF 90.0 DEGREES

X/C = 2.19

Z/C = −0.27

ADVANCE RATIO = 0.180

TIP SPEED = 65.7 m/sec

SHAFT ANGLE = −10.0 deg

COLLECTIVE = 10.1 deg

RUN: 148

TIME: 16:50:31

DATE: 27-JUL-76

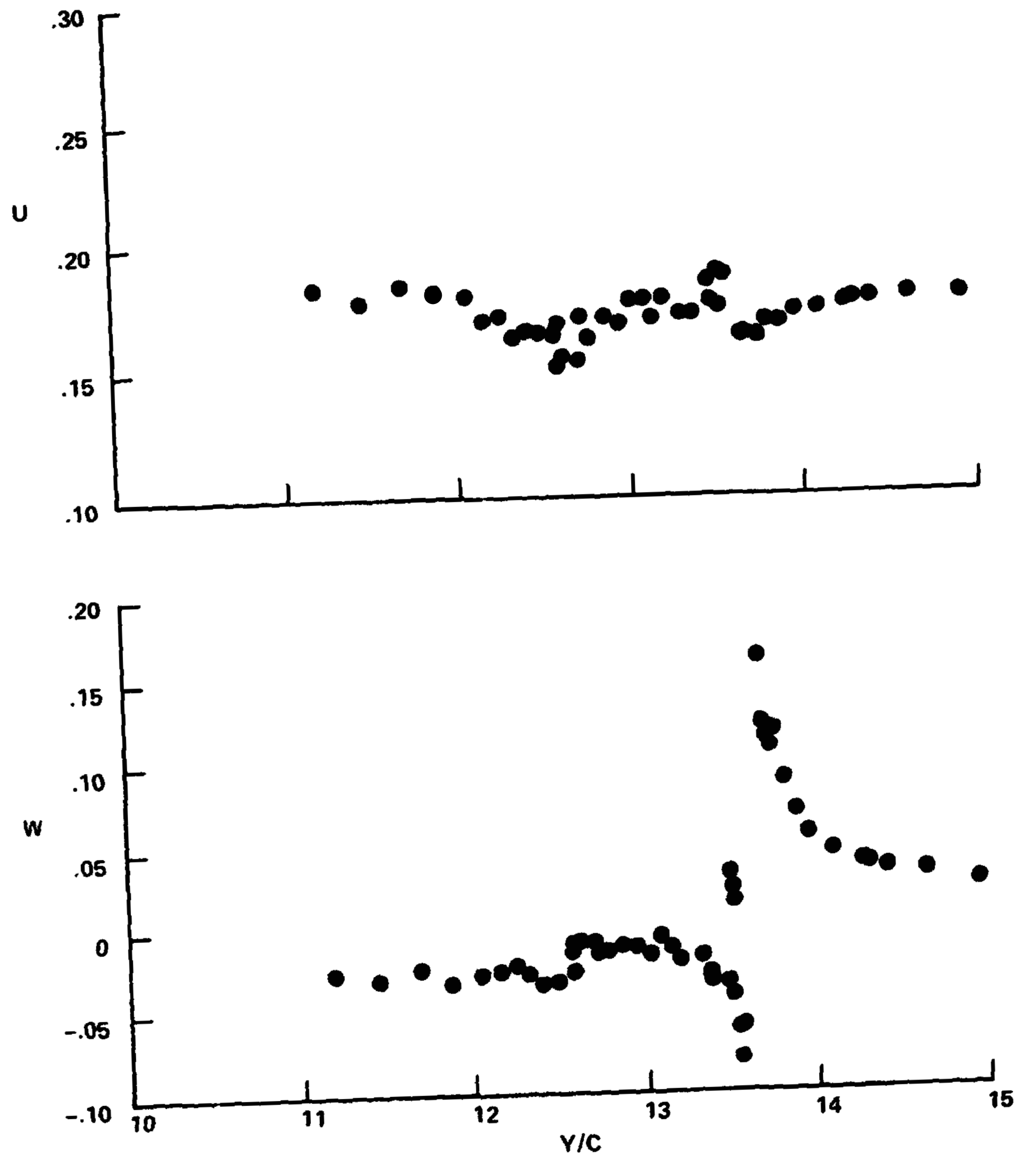

7-34. Lateral traverse, x/c = 2.19, z/c = −0.27

Figure 7. (Continued)

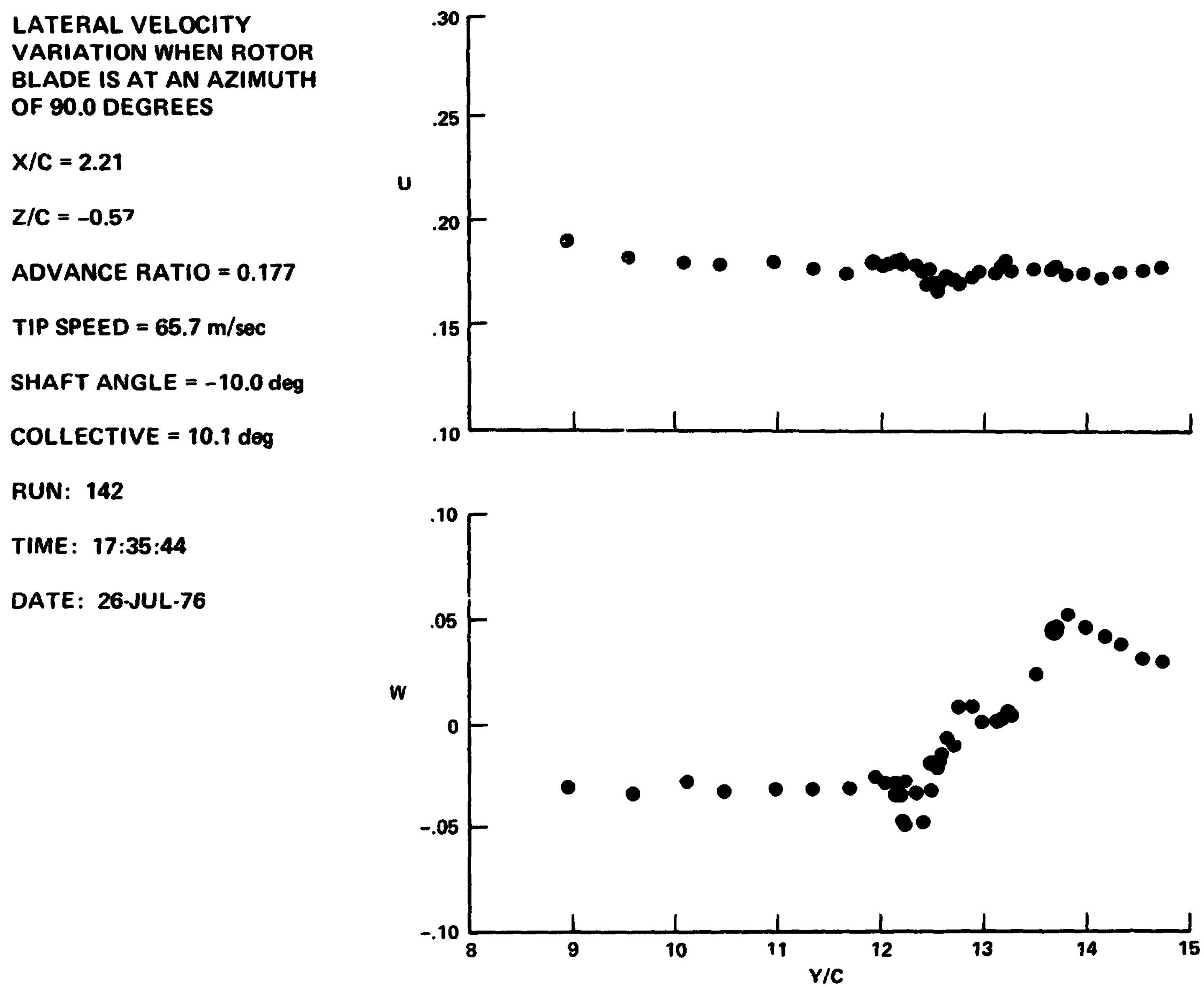

7-35. Lateral traverse, x/c = 2.21, z/c = -0.57

Figure 7. (Continued)

LATERAL VELOCITY VARIATION WHEN ROTOR BLADE IS AT AN AZIMUTH OF 90.0 DEGREES

X/C = 2.19

Z/C = -0.60

ADVANCE RATIO = 0.18

TIP SPEED = 65.7 m/sec

SHAFT ANGLE = -10.0 deg

COLLECTIVE = 10.1 deg

RUN: 141

TIME: 16:56:07

DATE: 26-JUL-76

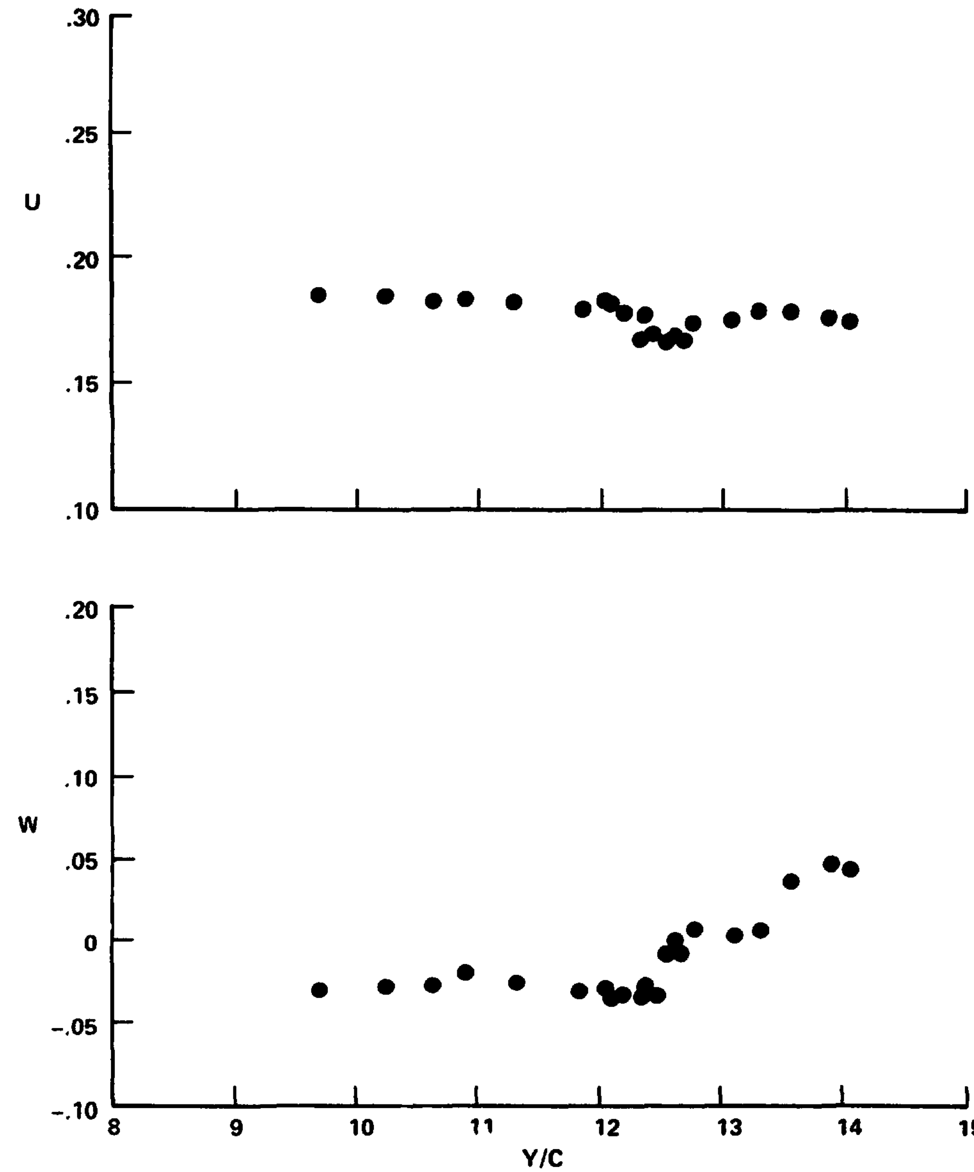

7-36. Lateral traverse, x/c = 2.19, z/c = -0.60

Figure 7. (Continued)

LATERAL VELOCITY VARIATION WHEN ROTOR BLADE IS AT AN AZIMUTH OF 90.0 DEGREES

X/C = 2.49

Z/C = –0.50

ADVANCE RATIO = 0.180

TIP SPEED = 65.7 m/sec

SHAFT ANGLE = –10.0 deg

COLLECTIVE = 10.1 deg

RUN: 133

TIME: 13:53:04

DATE: 26-JUL-76

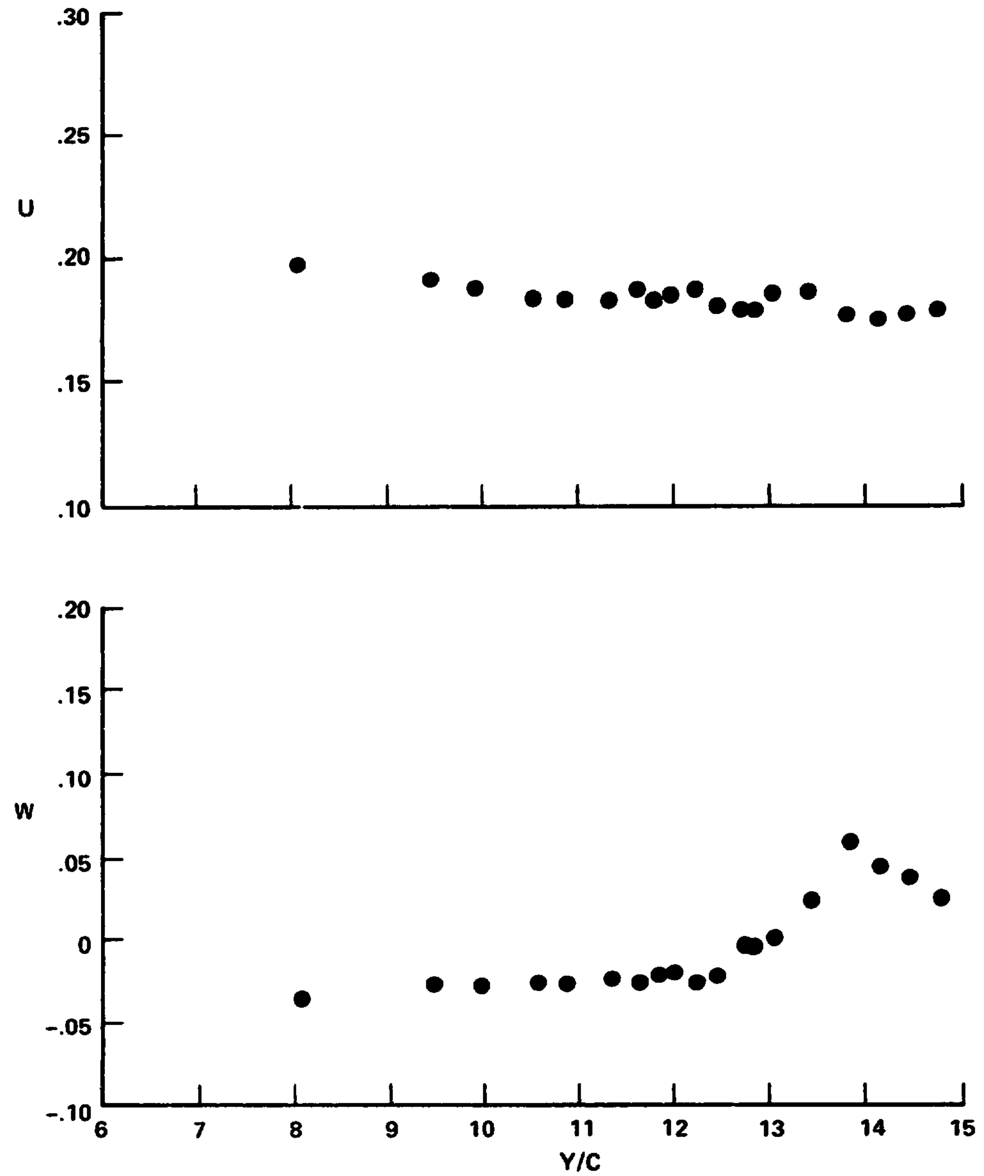

7-37. Lateral traverse, x/c = 2.50, z/c = –0.50

Figure 7. (Continued)

LATERAL VELOCITY VARIATION WHEN ROTOR BLADE IS AT AN AZIMUTH OF 90.0 DEGREES

X/C = 2.50

Z/C = –0.92

ADVANCE RATIO = 0.178

TIP SPEED = 65.7 m/sec

SHAFT ANGLE = –10.0 deg

COLLECTIVE = 10.1 deg

RUN: 135

TIME: 14:17:09

DATE: 26-JUL-76

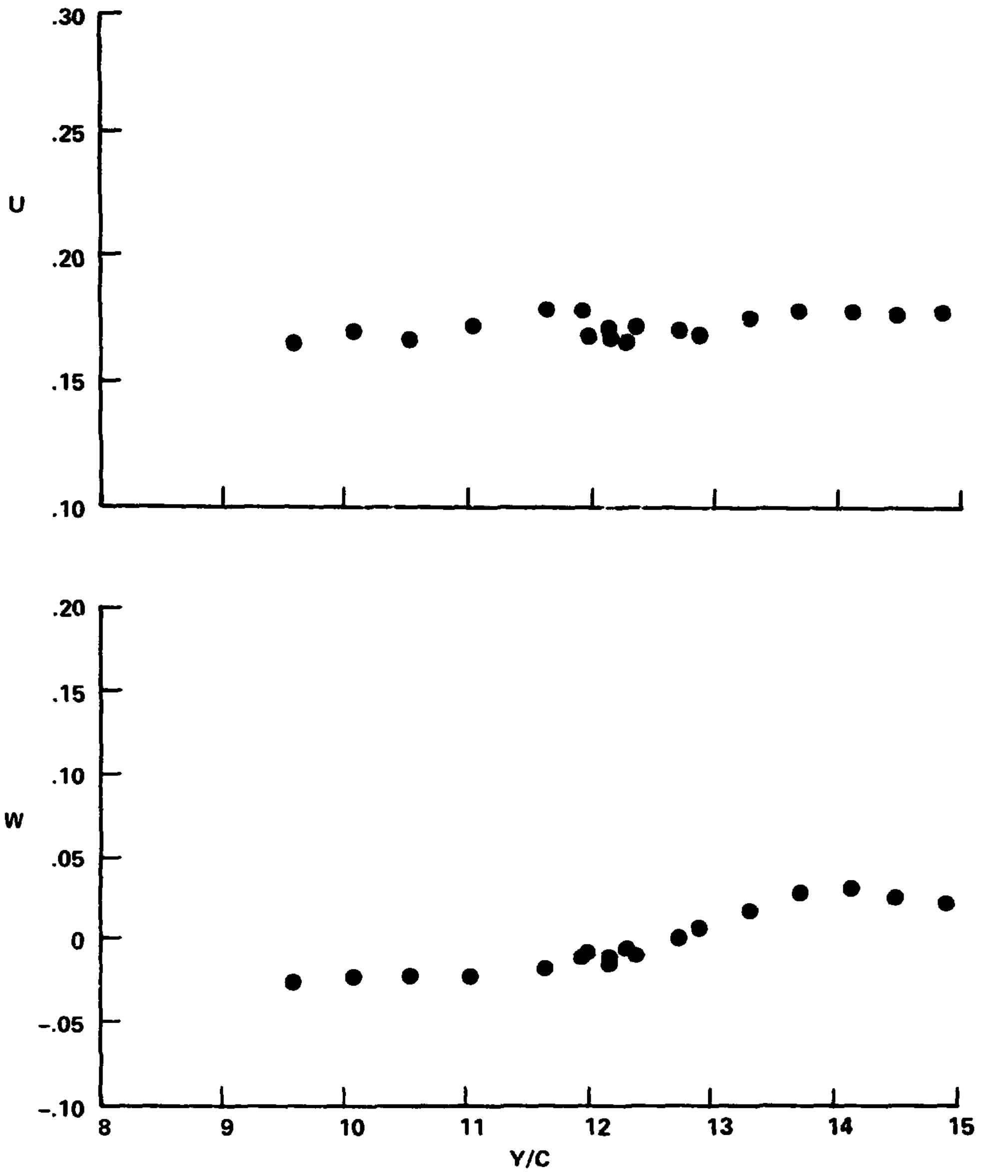

7-38. Lateral traverse, x/c = 2.50, z/c = –0.92

Figure 7. (Continued)

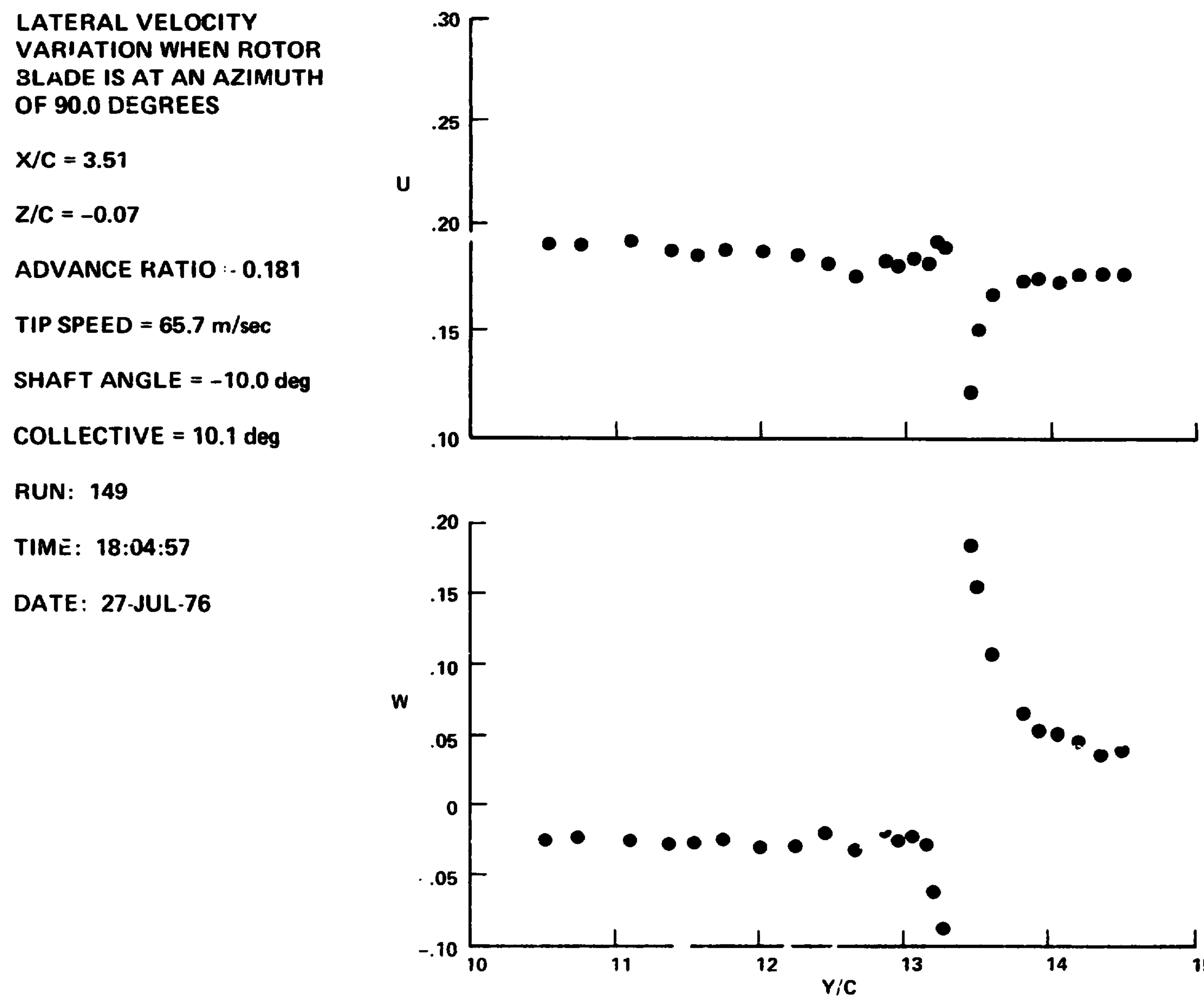

7-39. Lateral traverse, x/c = 3.51, z/c = -0.07

Figure 7. (Continued)

LATERAL VELOCITY
VARIATION WHEN ROTOR
BLADE IS AT AN AZIMUTH
OF 90.0 DEGREES

X/C = 4.84

Z/C = -0.00

ADVANCE RATIO = 0.178

TIP SPEED = 65.7 m/sec

SHAFT ANGLE = -10.0 deg

COLLECTIVE = 10.1 deg

RUN: 191

TIME: 15:09:43

DATE: 02-AUG-76

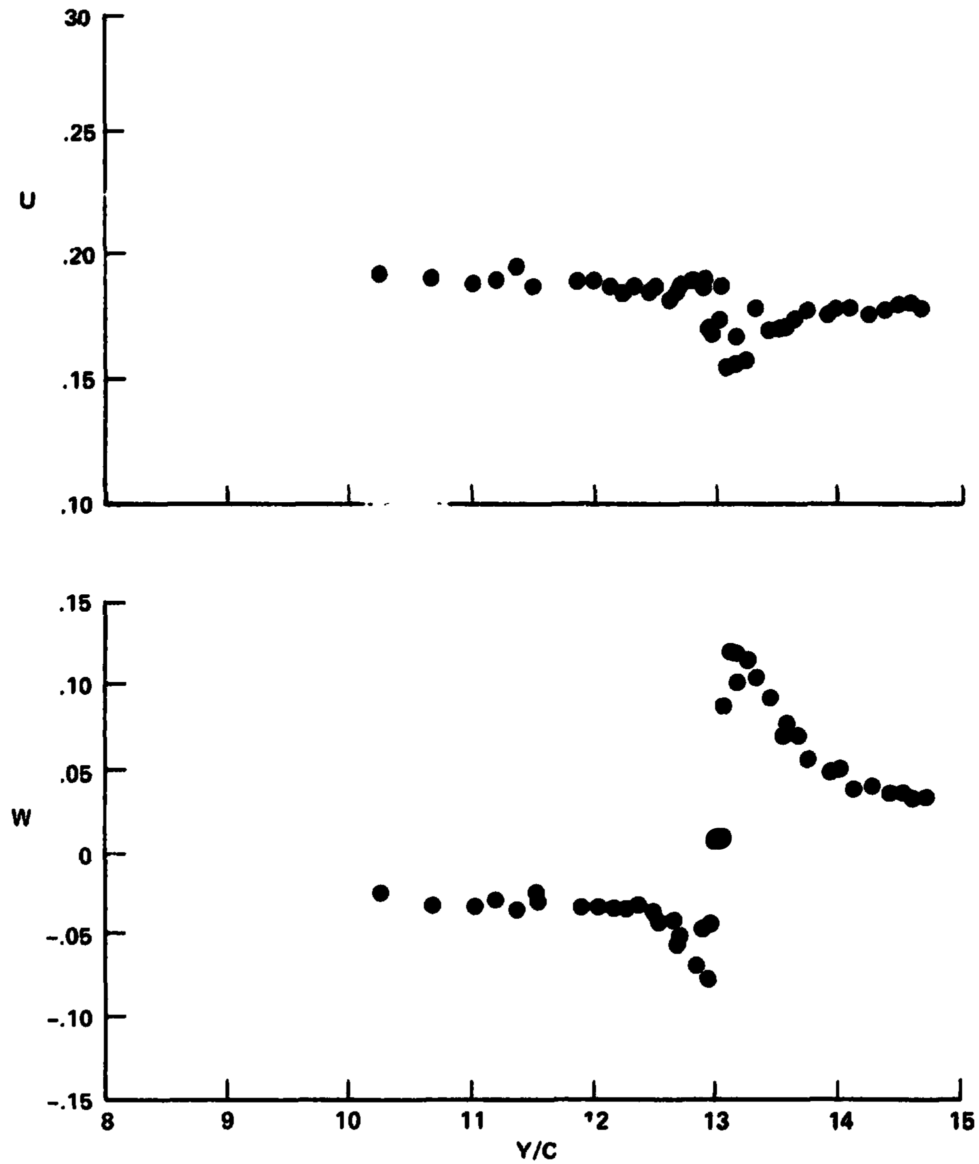

7-40. Lateral traverse, x/c = 4.84, z/c = 0.00

Figure 7. (Continued)

LATERAL VELOCITY VARIATION WHEN ROTOR BLADE IS AT AN AZIMUTH OF 90.0 DEGREES

X/C = 4.84

Z/C = -0 13

ADVANCE RATIO = 0.179

TIP SPEED = 65.7 m/sec

SHAFT ANGLE = -10.0 deg

COLLECTIVE = 10.1 deg

RUN: 191 W

TIME: 14:40:36

DATE: 02-AUG-76

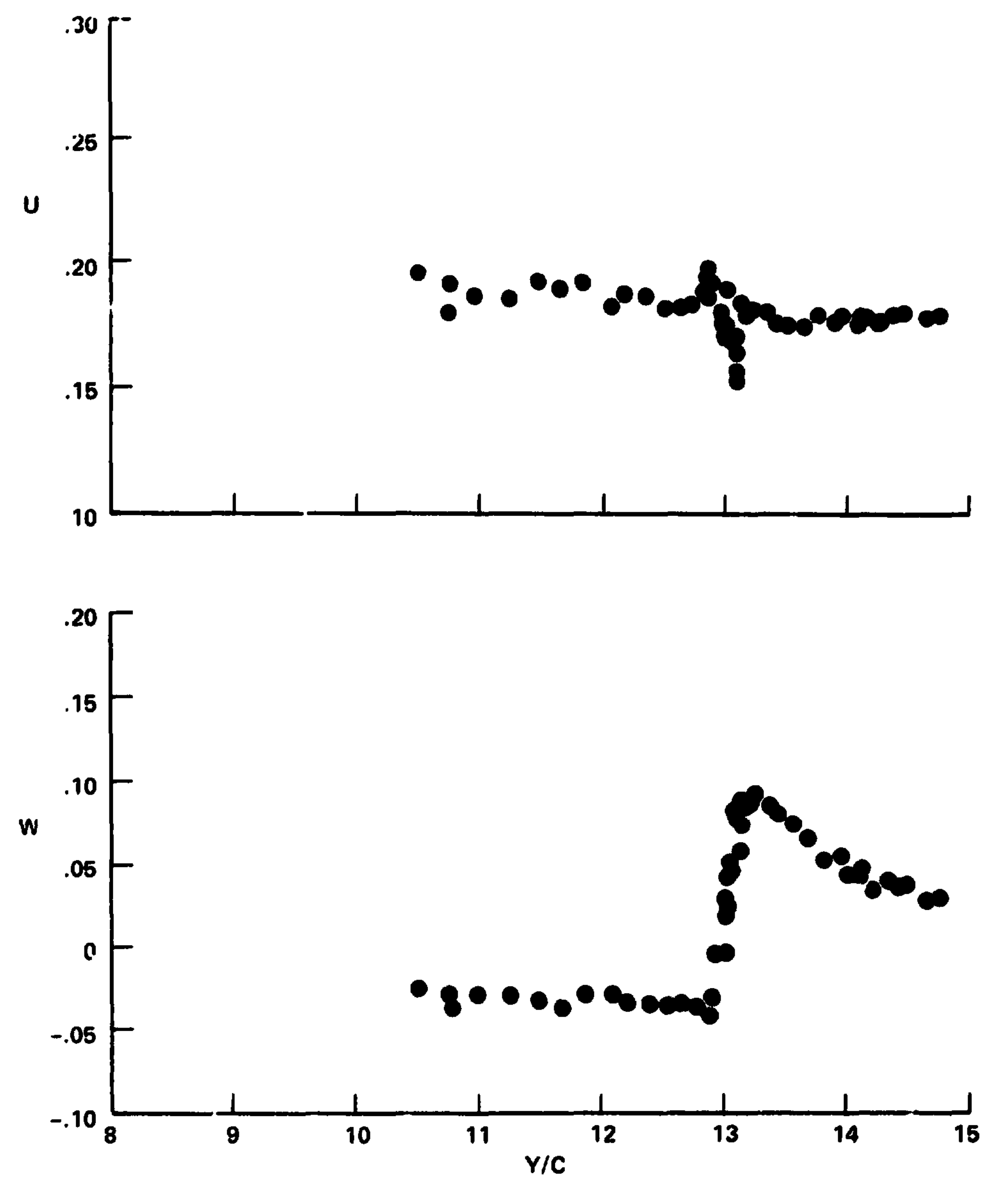

7-41. Lateral traverse, x/c = 4.84, z/c = -0.13

Figure 7. (Continued)

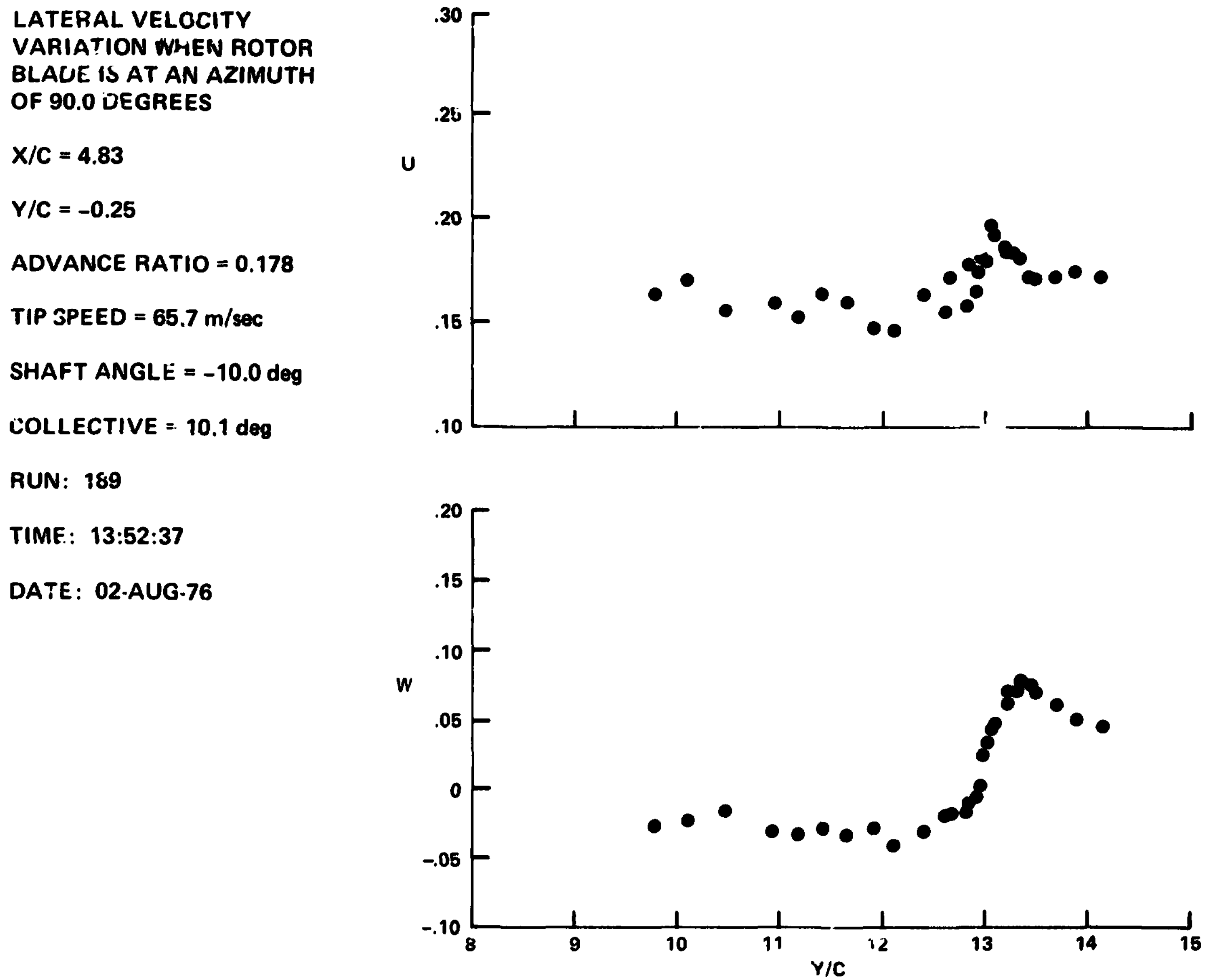

7-42. Lateral traverse, x/c = 4.83, z/c = -0.25

Figure 7. (Continued)

LATERAL VELOCITY
VARIATION WHEN ROTOR
BLADE IS AT AN AZIMUTH
OF 90.0 DEGREES

X/C = 4.82

Y/C = -0.35

ADVANCE RATIO = 0.179

TIP SPEED = 65.7 m/sec

SHAFT ANGLE = -10.0 deg

COLLECTIVE = 10.1 deg

RUN: 190

TIMF: 14:18:20

DATE: 02-AUG-76

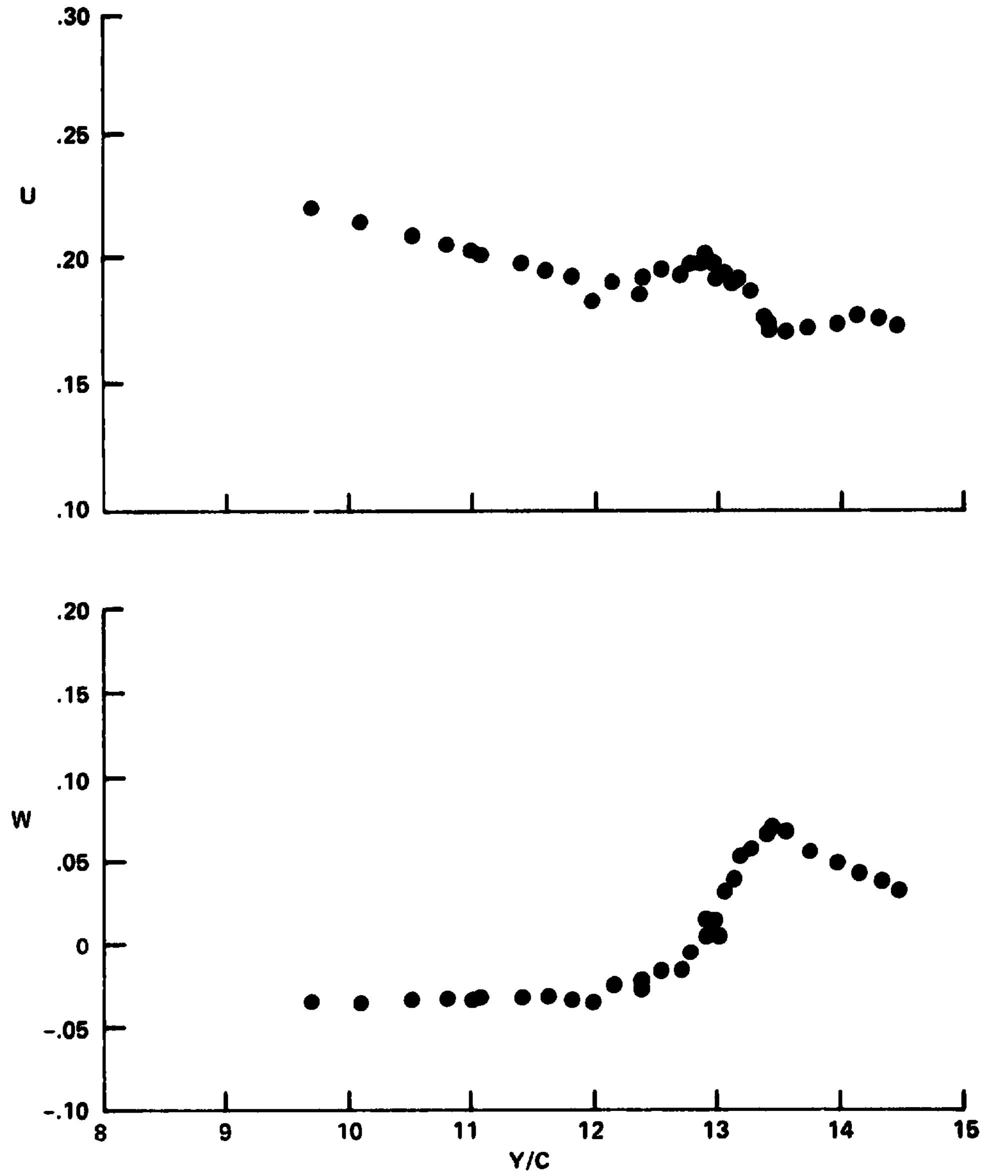

7-43. Lateral traverse, x/c = 4.82, z/c = -0.35

Figure 7. (Concluded)

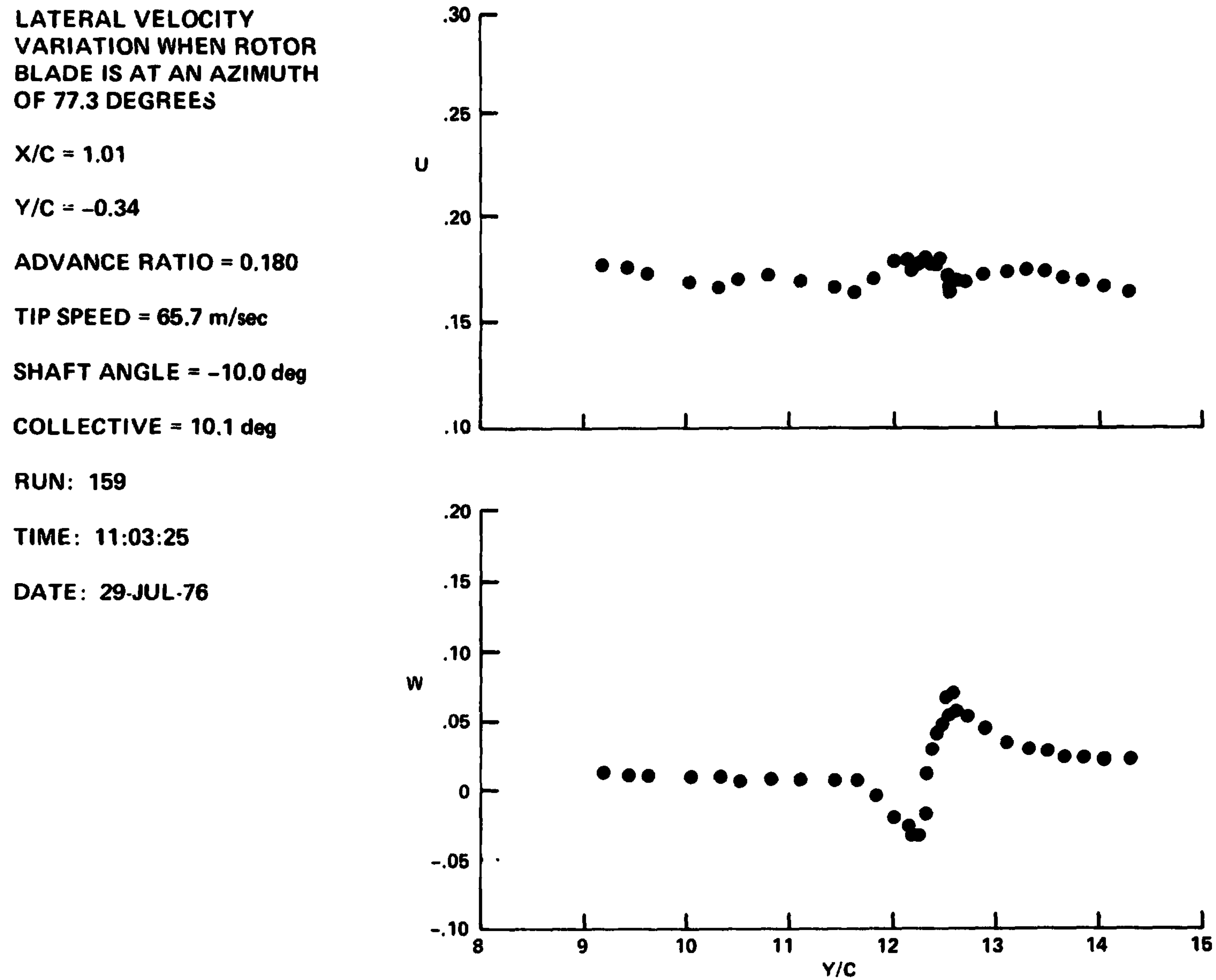

8-1. Lateral traverse, x/c = 1.01, z/c = -0.34

Figure 8. Flowfield velocities from the -11° twist blades, $V/\Omega R = 0.18$, $\theta_{0.75R} = 10.1^\circ$, $\psi = 77.3^\circ$, N = 600.

LATERAL VELOCITY VARIATION WHEN ROTOR BLADE IS AT AN AZIMUTH OF 77.3 DEGREES

X/C = 1.01

Y/C = −0.37

ADVANCE RATIO = 0.178

TIP SPEED = 65.7 m/sec

SHAFT ANGLE = −10.0 deg

COLLECTIVE = 10.1 deg

RUN: 160

TIME: 11:13:42

DATE: 29-JUL-76

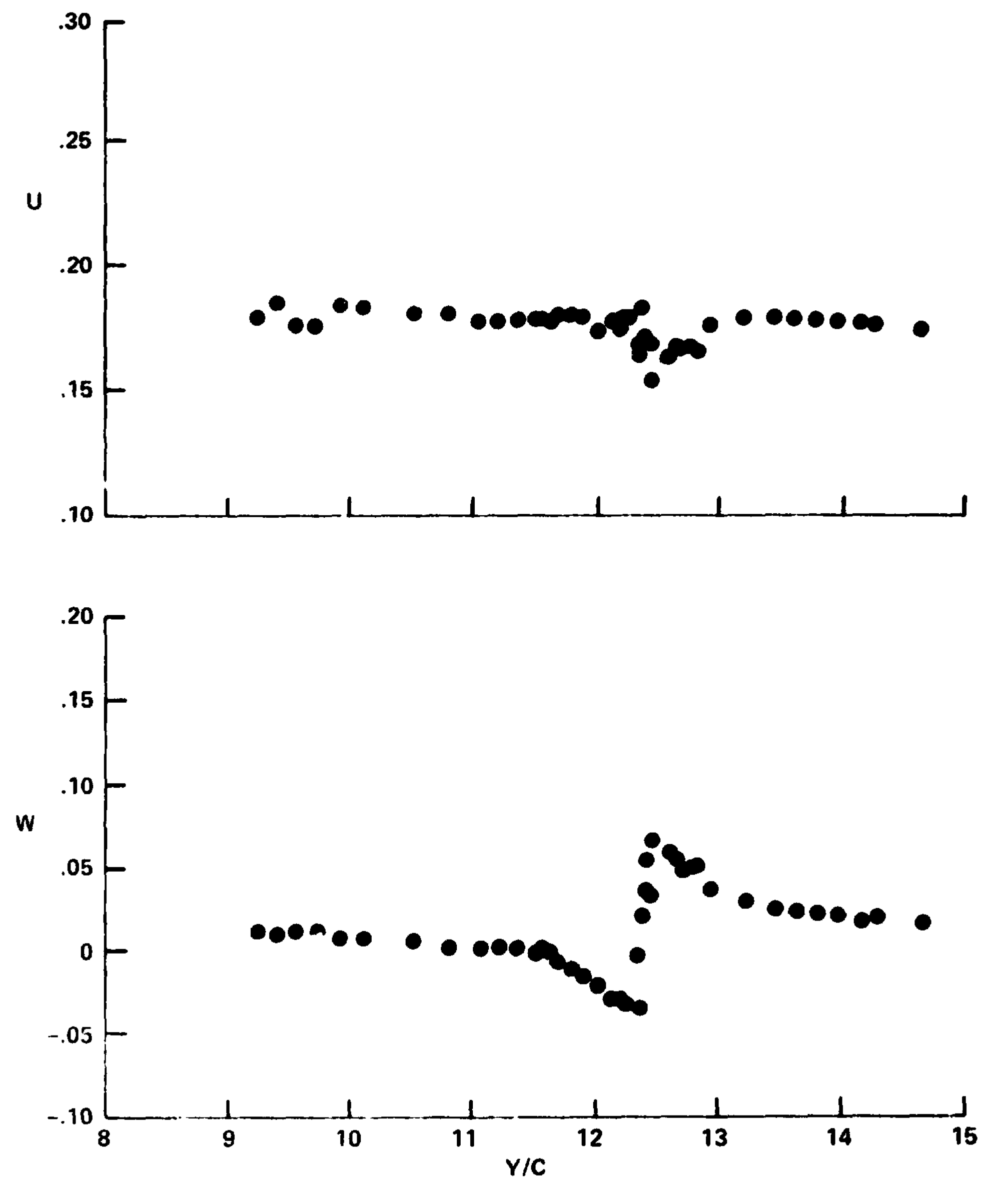

8-2. Lateral traverse, x/c = 1.01, z/c = −0.37

Figure 8. (Continued)

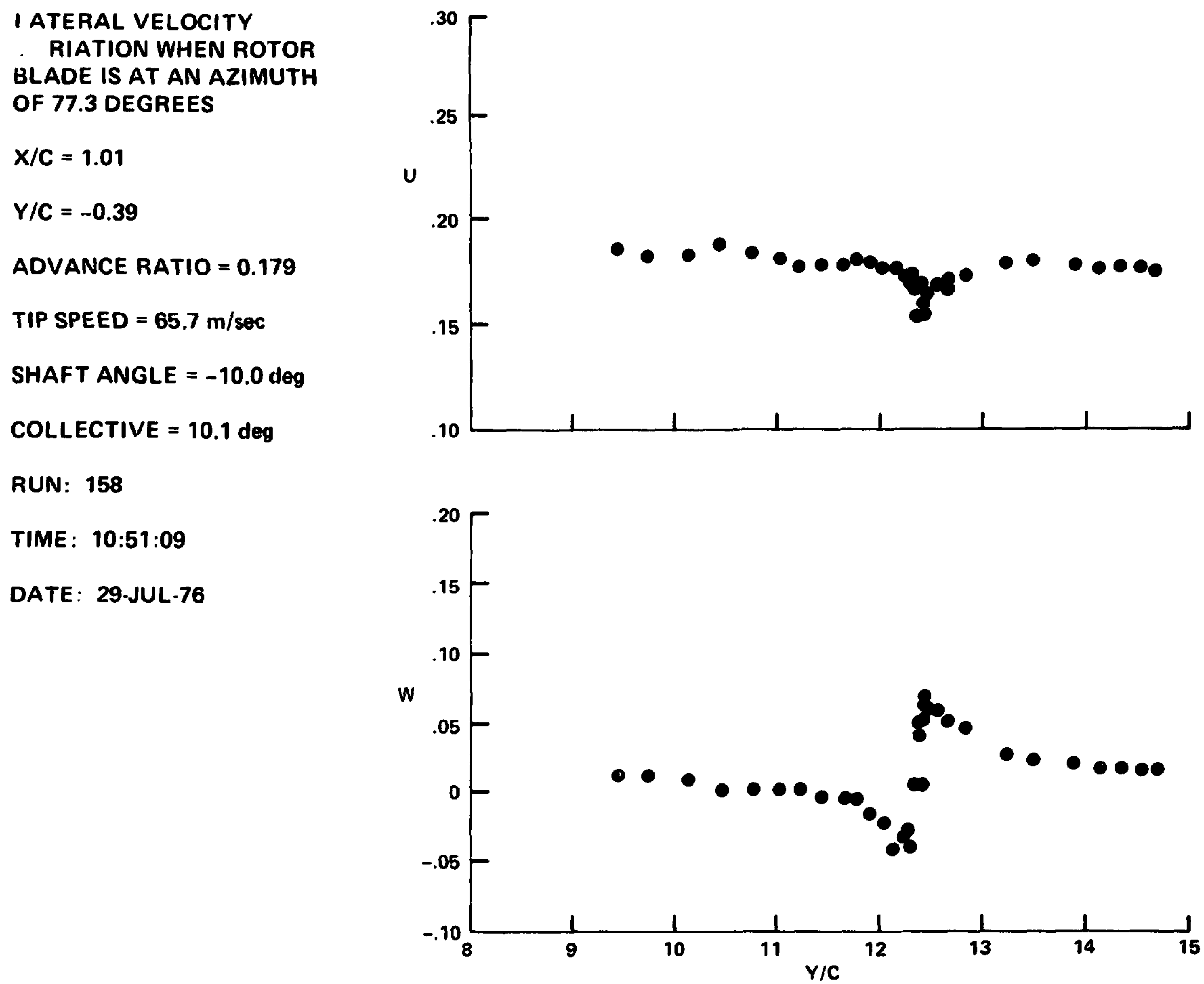

8-3. Lateral traverse, x/c = 1.01, z/c = -0.39

Figure 8. (Continued)

LATERAL VELOCITY VARIATION WHEN ROTOR BLADE IS AT AN AZIMUTH OF 77.3 DEGREES

X/C = 1.01

Y/C = −0.42

ADVANCE RATIO = 0.178

TIP SPEED = 65.7 m/sec

SHA.˙ .\NGLE = −10.0 deg

COLLECTIVE = 10.1 deg

RUN: 157

TIME: 10:40:29

DATE: 29-JUL-76

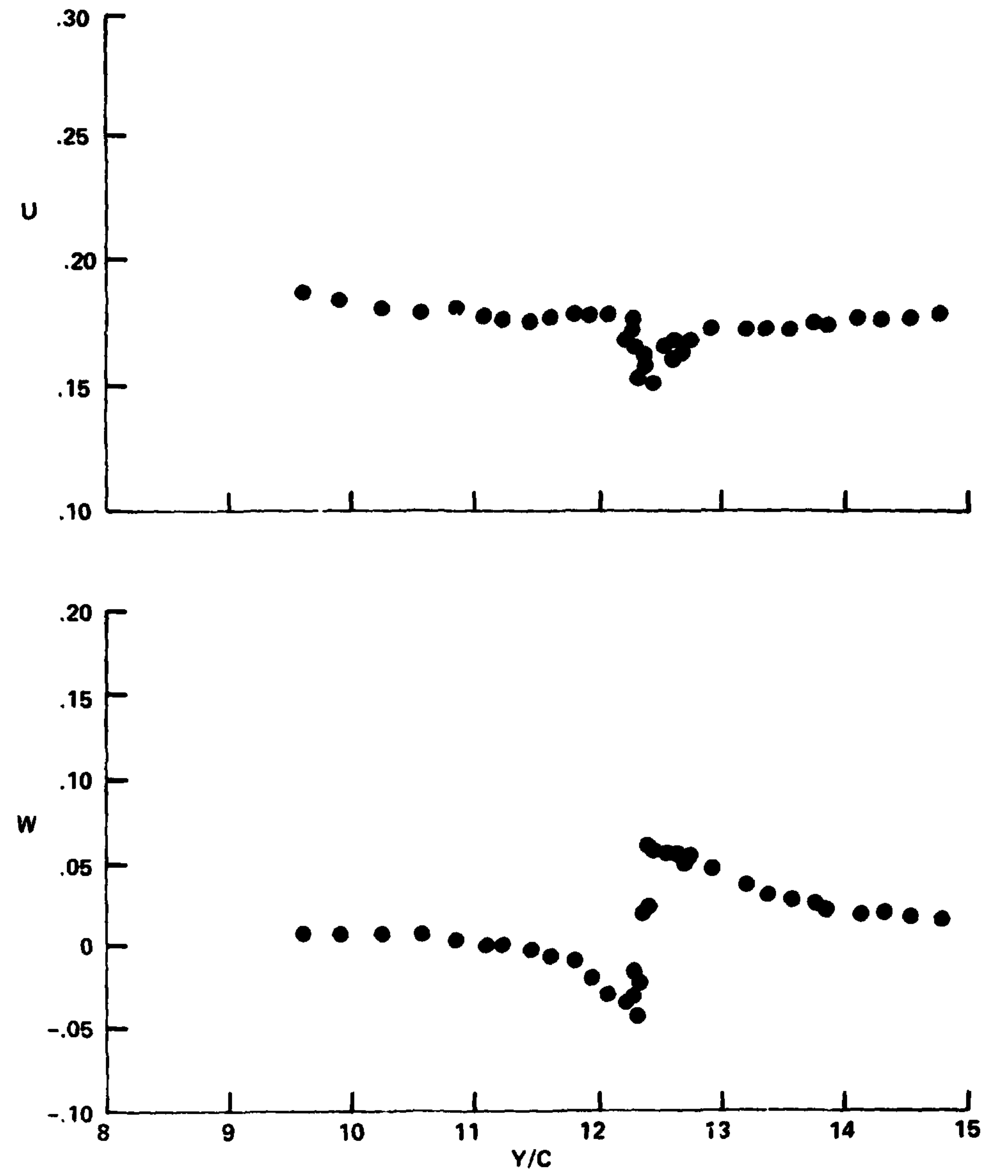

8-4. Lateral traverse, x/c = 1.01, z/c = −0.42

Figure 8. (Continued)

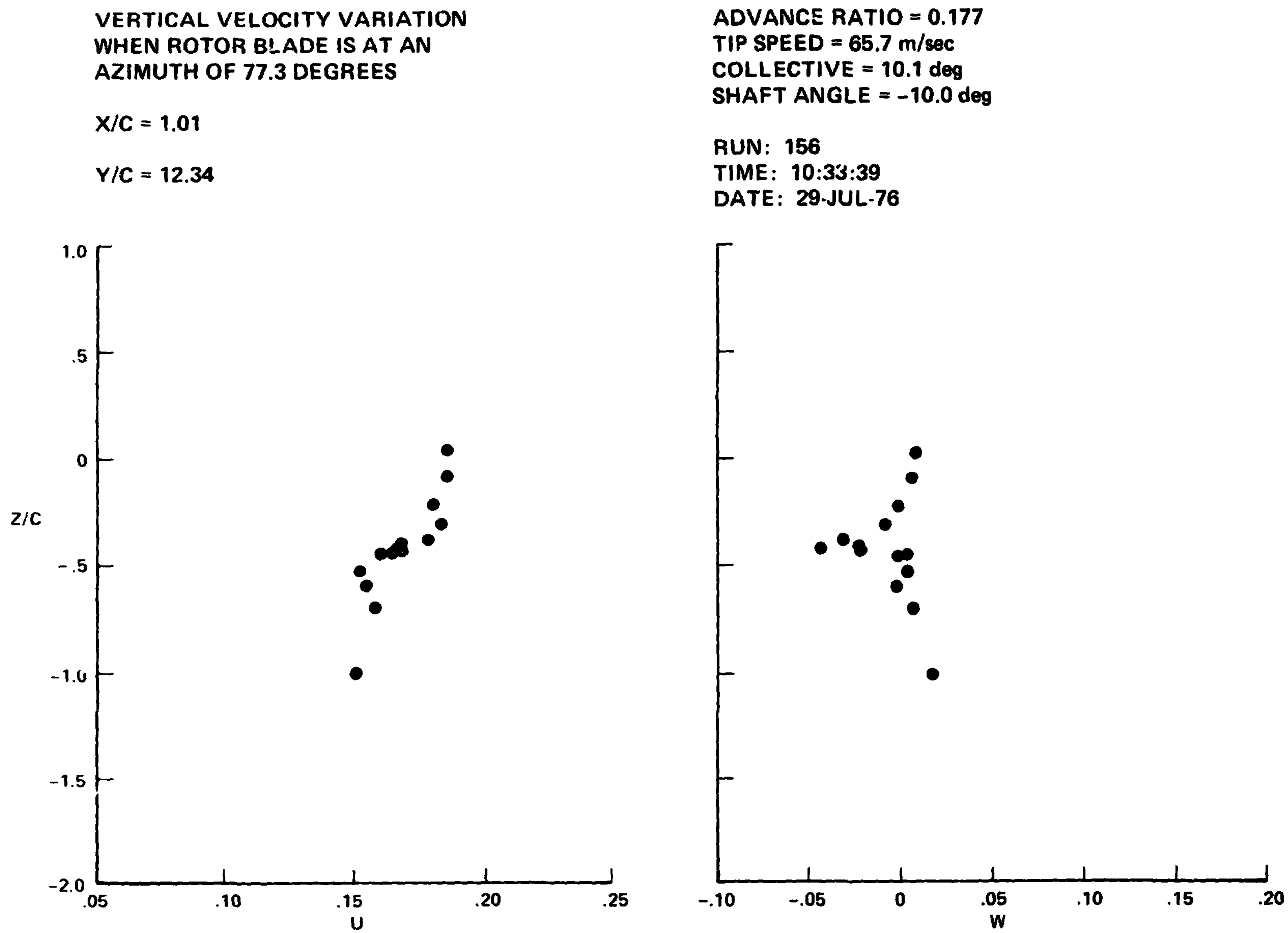

8-5. Vertical traverse, x/c = 1.01, y/c = 12.34

Figure 8. (Continued)

LATERAL VELOCITY VARIATION WHEN ROTOR BLADE IS AT AN AZIMUTH OF 77.3 DEGREES

X/C = 1.50

Y/C = –0.26

ADVANCE RATIO = 0.178

TIP SPEED = 65.7 m/sec

SHAFT ANGLE = –10.0 deg

COLLECTIVE = 10.1 deg

RUN: 165

TIME: 15:07:25

DATE: 29-JUL-76

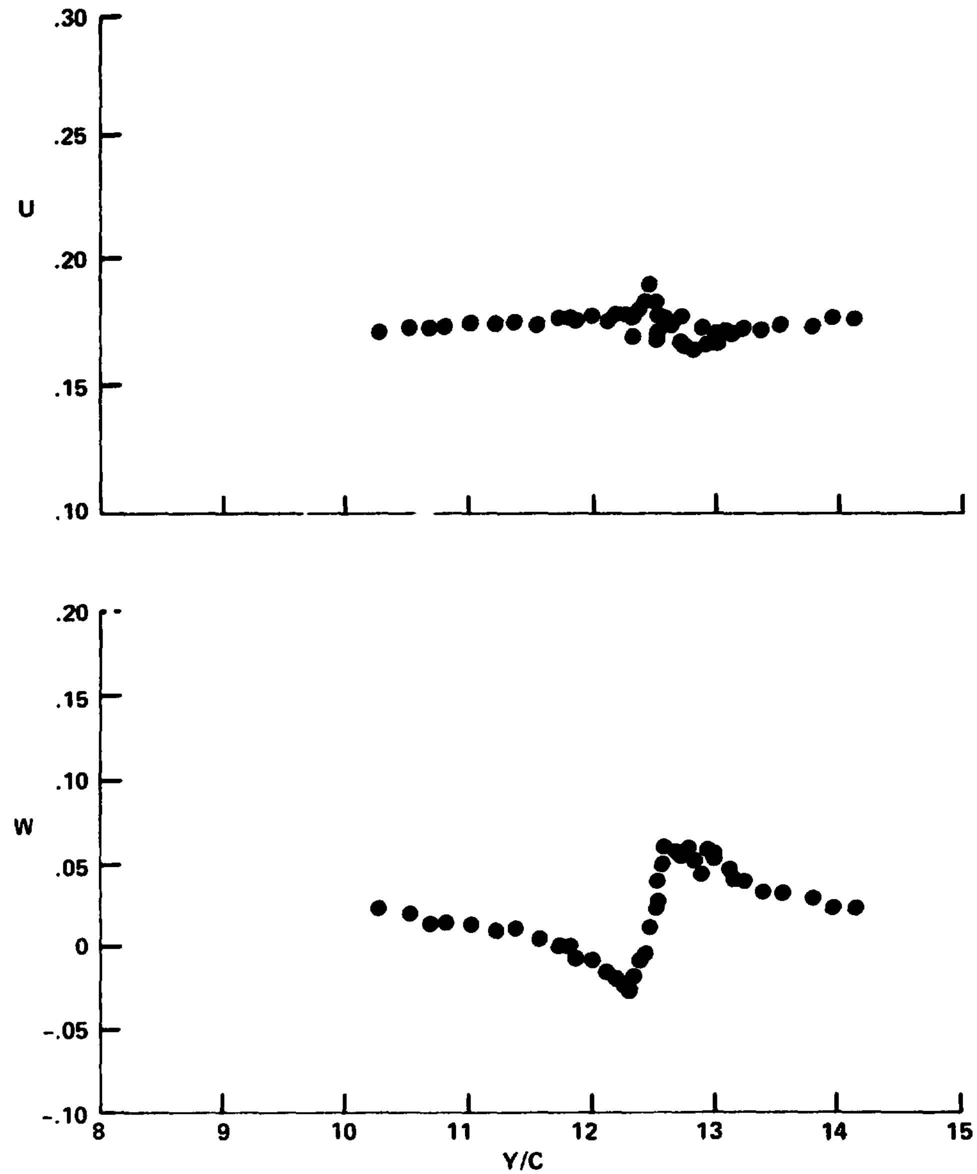

8-6. Lateral traverse, x/c = 1.50, z/c = −0.26

Figure 8. (Continued)

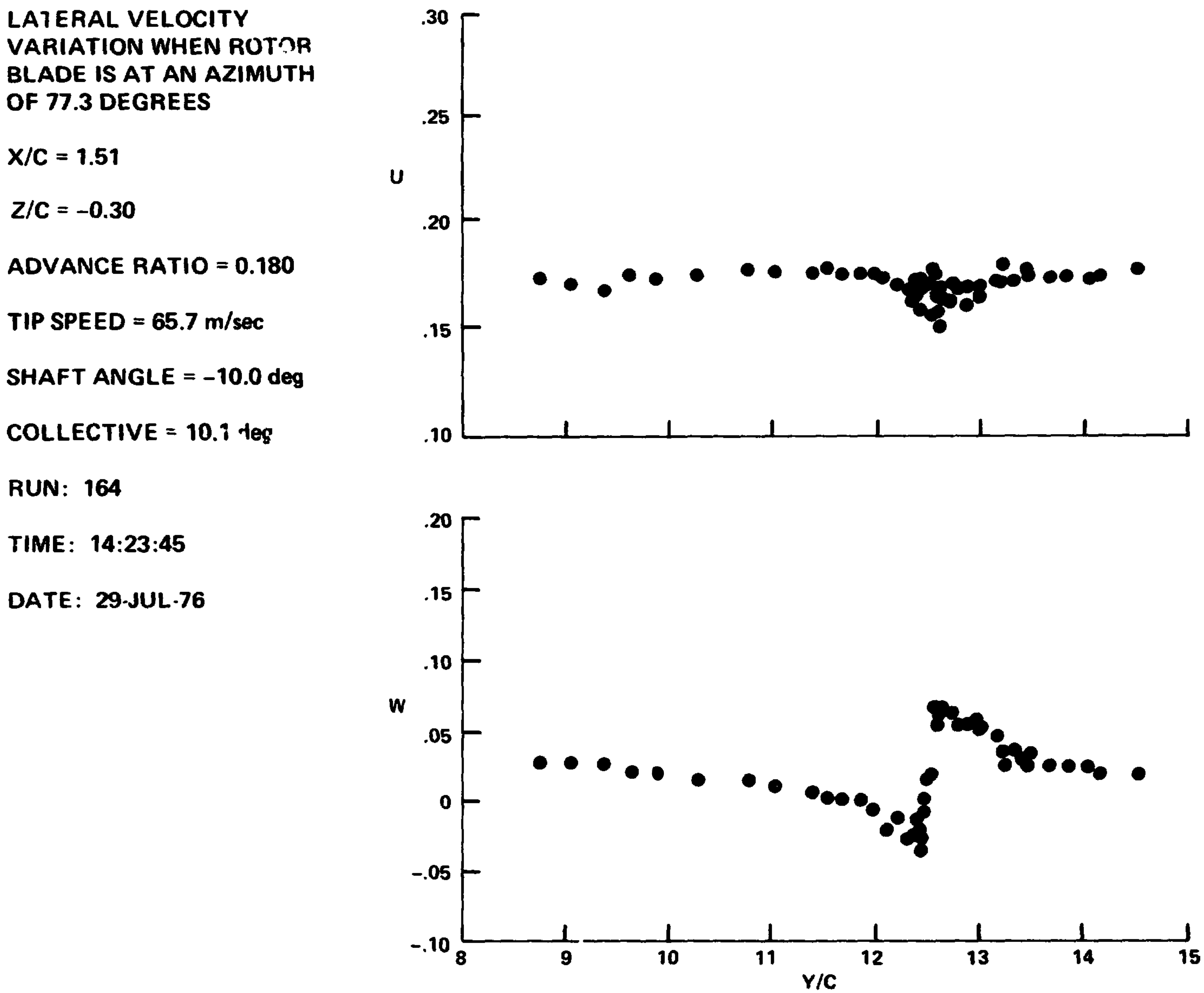

8-7. Lateral traverse, x/c = 1.50, z/c = -0.30

Figure 8. (Continued)

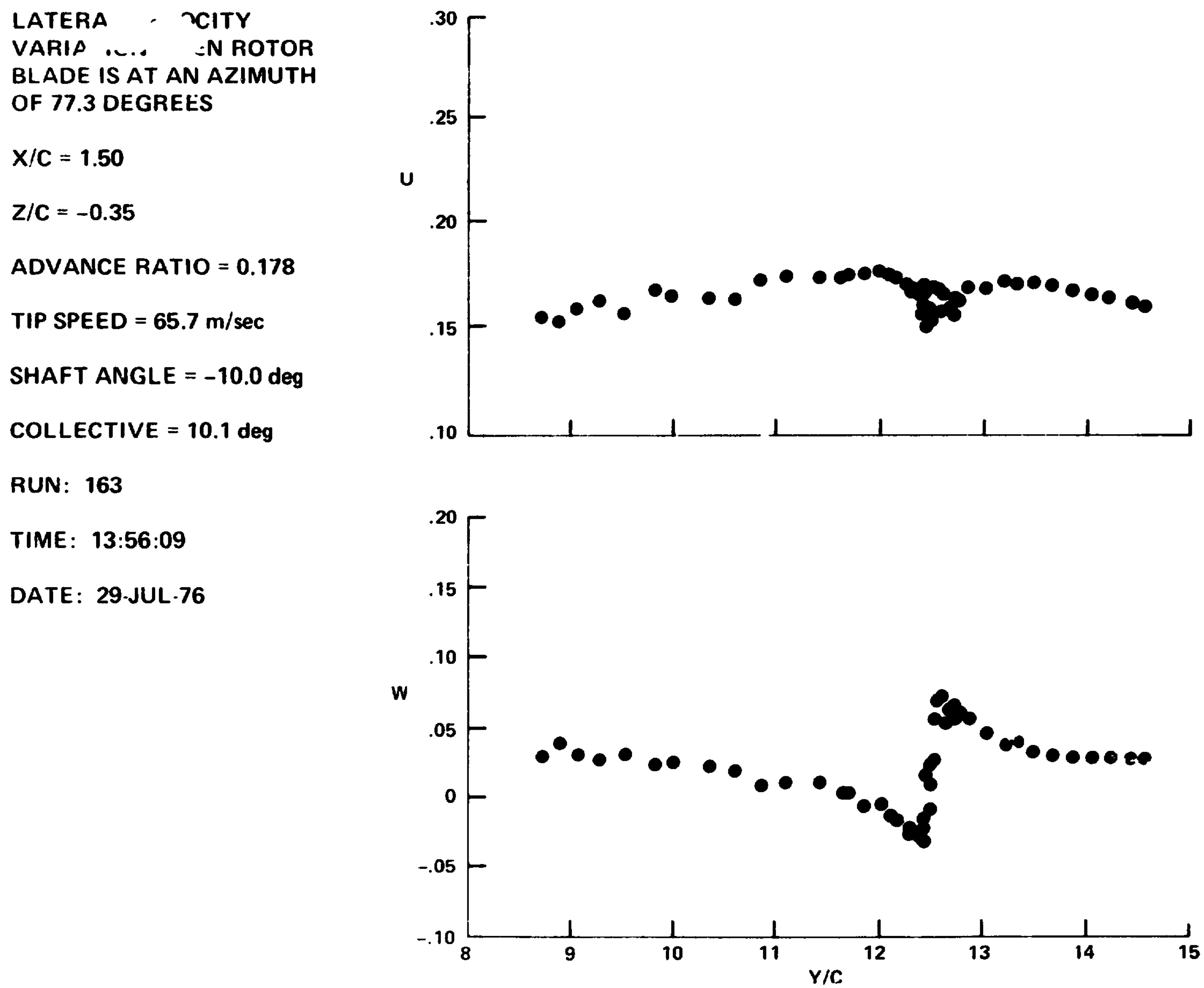

8-8. Lateral traverse, x/c = 1.50, z/c = -0.35

Figure 8. (Continued)

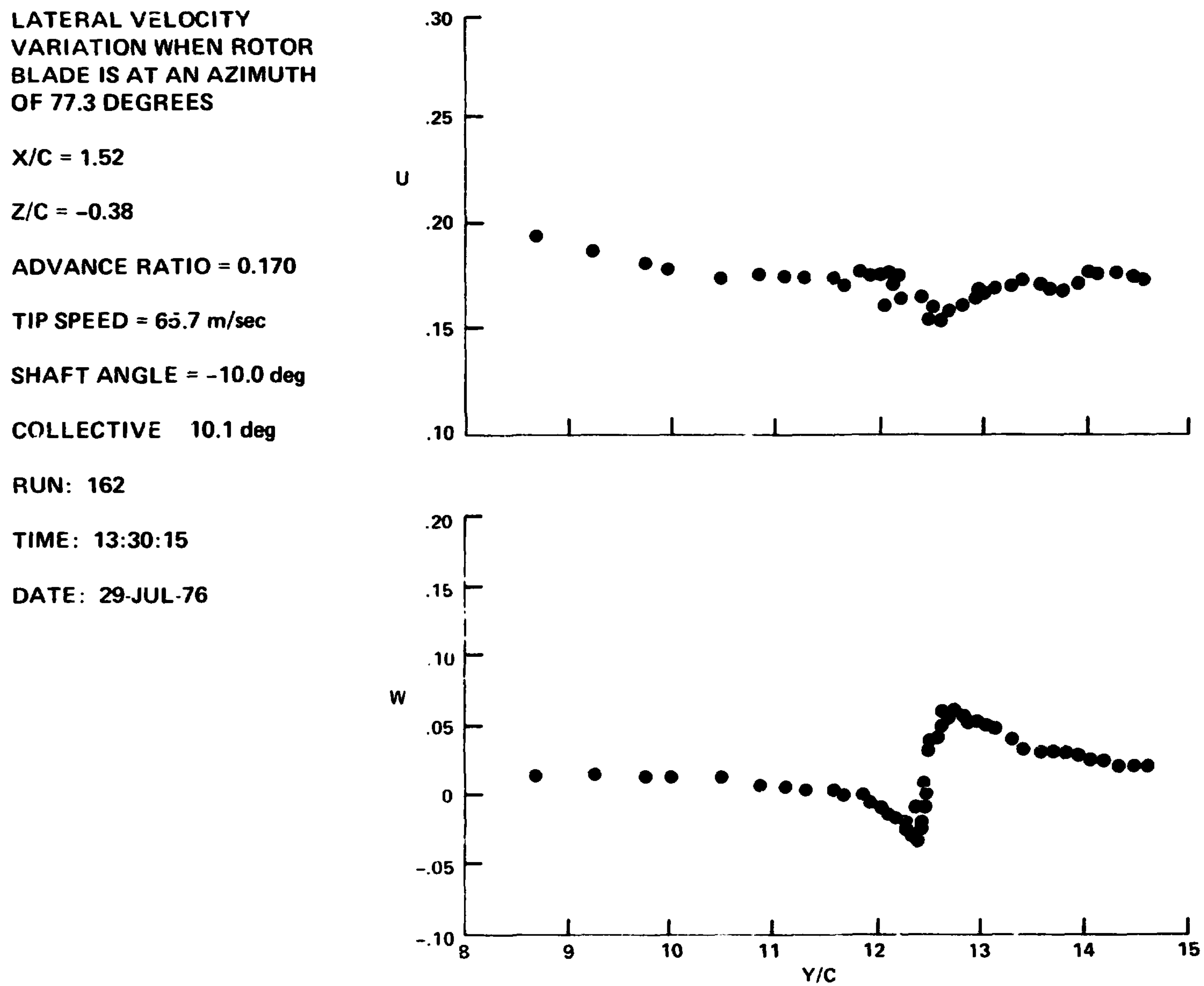

8-9. Lateral traverse, x/c = 1.50, z/c = -0.38

Figure 8. (Continued)

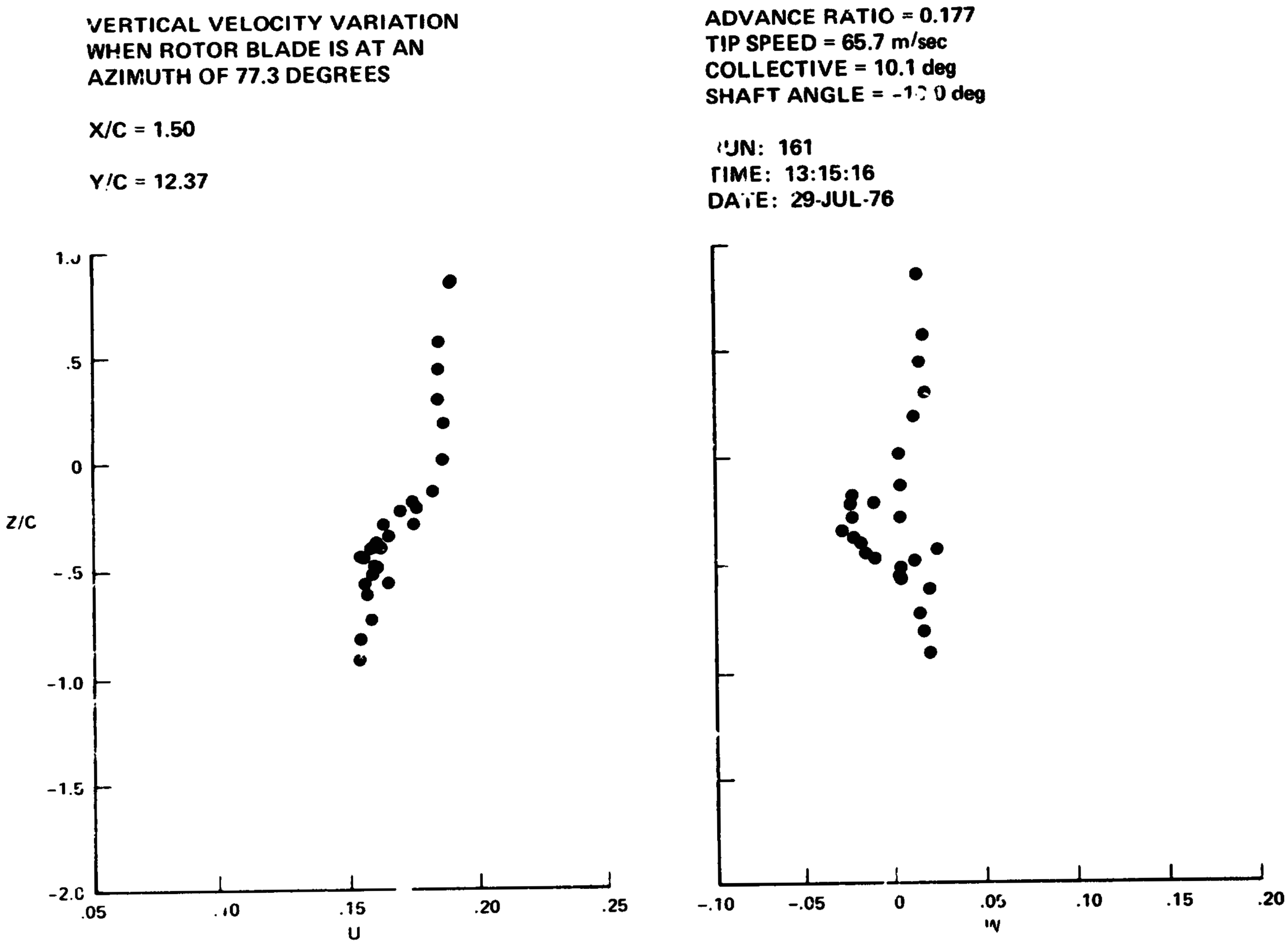

8-10. Vertical traverse, x/c = 1.50, y/c = 12.37

Figure 8. (Continued)

LATERAL VELOCITY VARIATION WHEN ROTOR BLADE IS AT AN AZIMUTH OF 77.3 DEGREES

X/C = 1.64

Z/C = –0.26

ADVANCE RATIO = 0.179

TIP SPEED = 65.7 m/sec

SHAFT ANGLE = –10.0 deg

COLLECTIVE = 10.1 deg

RUN: 194

TIME: 18:21:44

DATE: 02-AUG-76

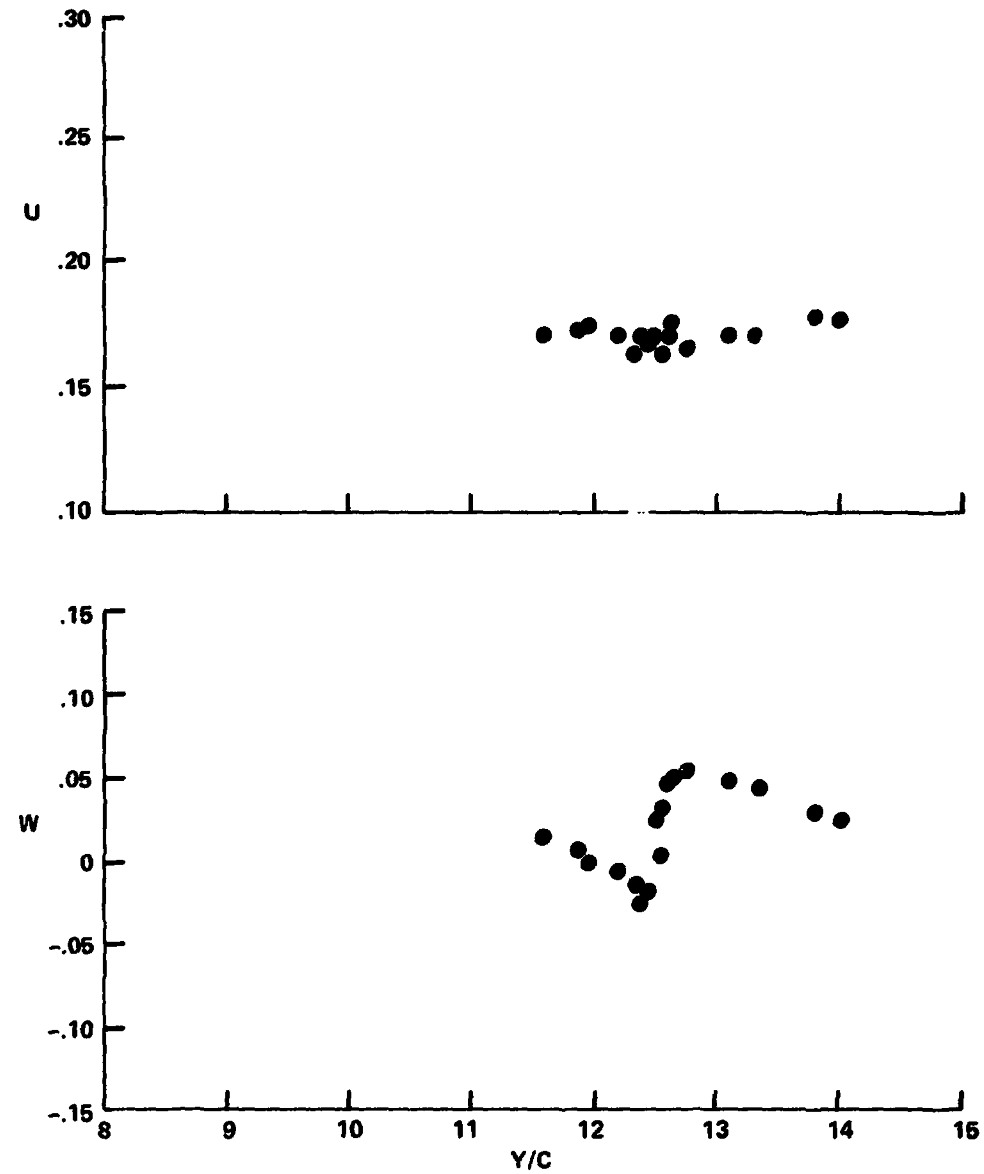

8-11. Lateral traverse, x/c = 1.64, z/c = –0.26

Figure 8. (Continued)

LATERAL VELOCITY
VARIATION WHEN ROTOR
BLADE IS AT AN AZIMUTH
OF 77.3 DEGREES

X/C = 1.64

Z/C = −0.29

ADVANCE RATIO = 0.177

TIP SPEED = 65.7 m/sec

SHAFT ANGLE = −10.0 deg

COLLECTIVE = 10.1 deg

RUN: 192

TIME: 17:54:54

DATE: 02-AUG-76

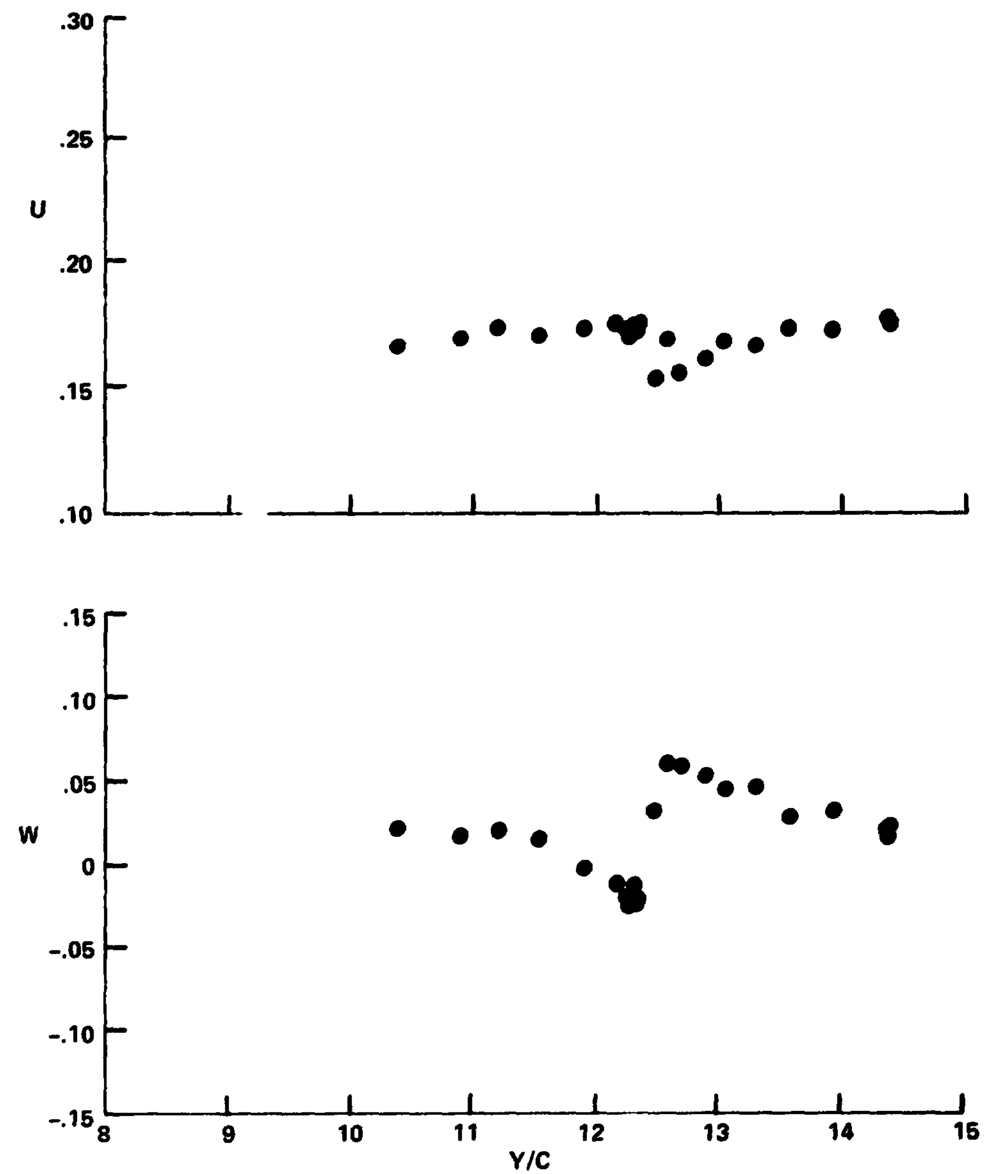

8-12. Lateral traverse, x/c = 1.64, z/c = −0.29

Figure 8. (Continued)

LATERAL VELOCITY VARIATION WHEN ROTOR BLADE IS AT AN AZIMUTH OF 77.3 DEGREES

X/C = 1.64

Z/C = –0.36

ADVANCE RATIO = 0.177

TIP SPEED = 65.7 m/sec

SHAFT ANGLE = –10.0 deg

COLLECTIVE = 10.1 deg

RUN: 195

TIME: 18:51:15

DATE: 02-AUG-76

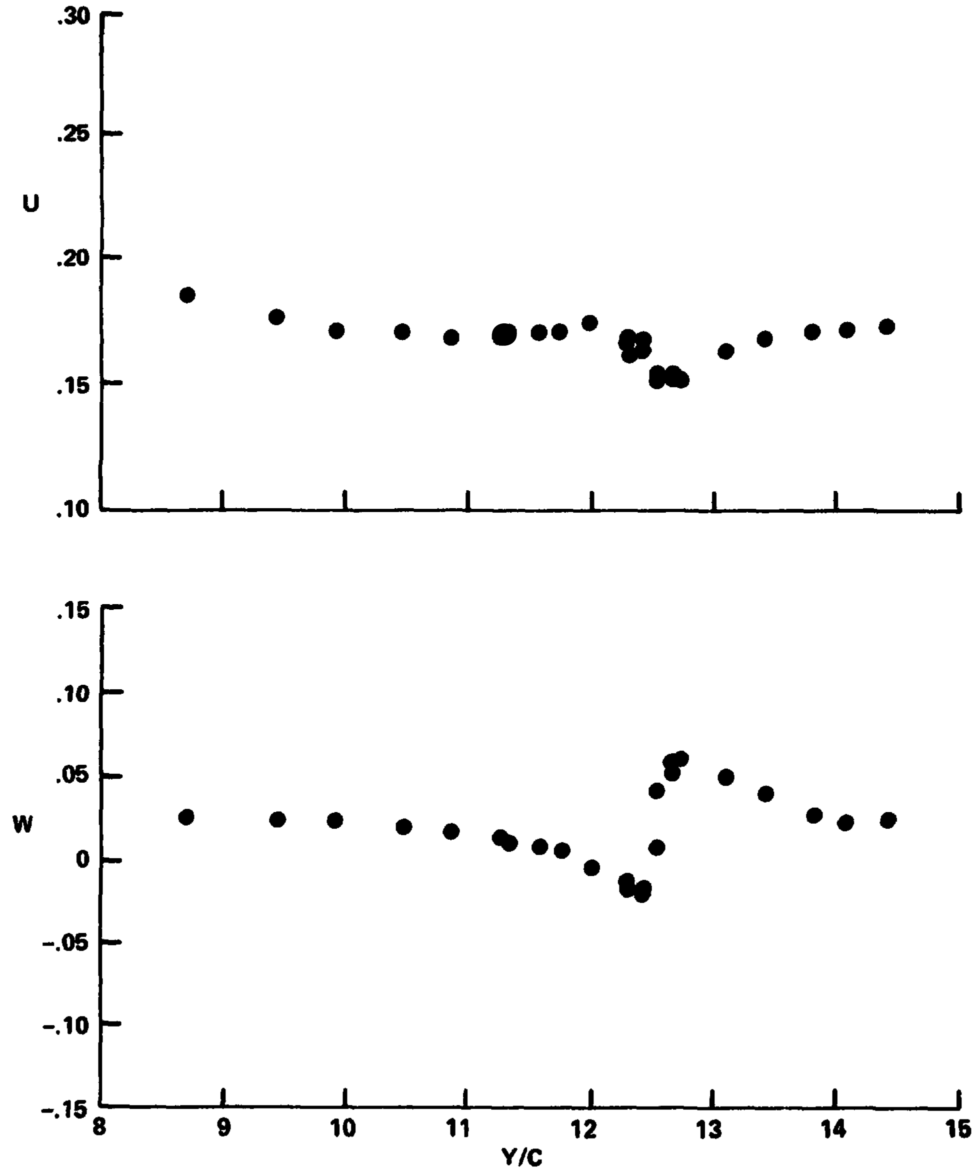

8-13. Lateral traverse, x/c = 1.64, z/c = –0.36

Figure 8. (Continued)

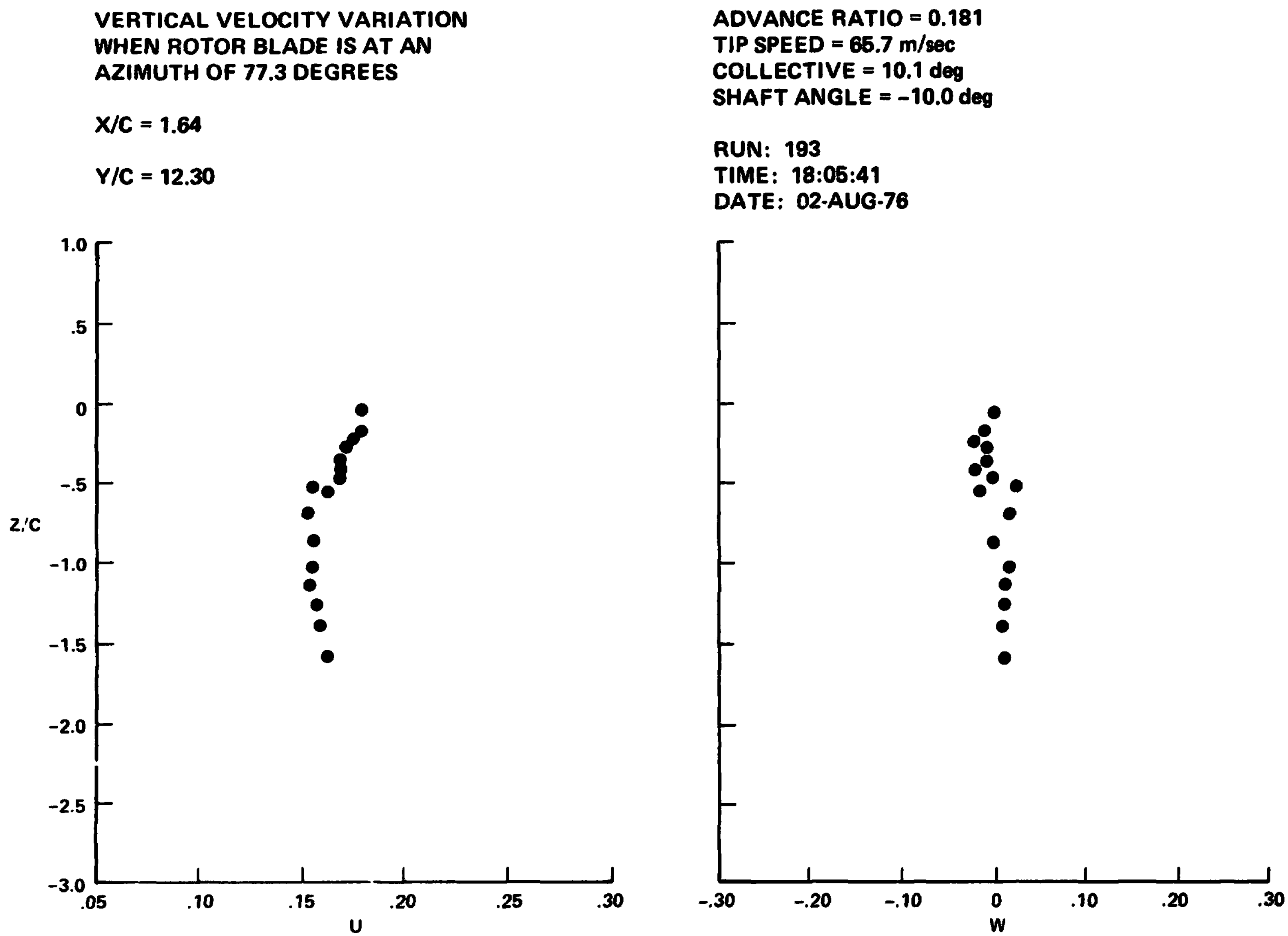

8-14. Vertical traverse, x/c = 1.64, y/c = 12.30

Figure 8. (Continued)

LATERAL VELOCITY VARIATION WHEN ROTOR BLADE IS AT AN AZIMUTH OF 77.3 DEGREES

X/C = 2.00

Z/C = –0.26

ADVANCE RATIO = 0.179

TIP SPEED = 65.7 m/sec

SHAFT ANGLE = –10.0 deg

COLLECTIVE = 10.1 deg

RUN: 168

TIME: 16:40:53

DATE: 29-JUL-76

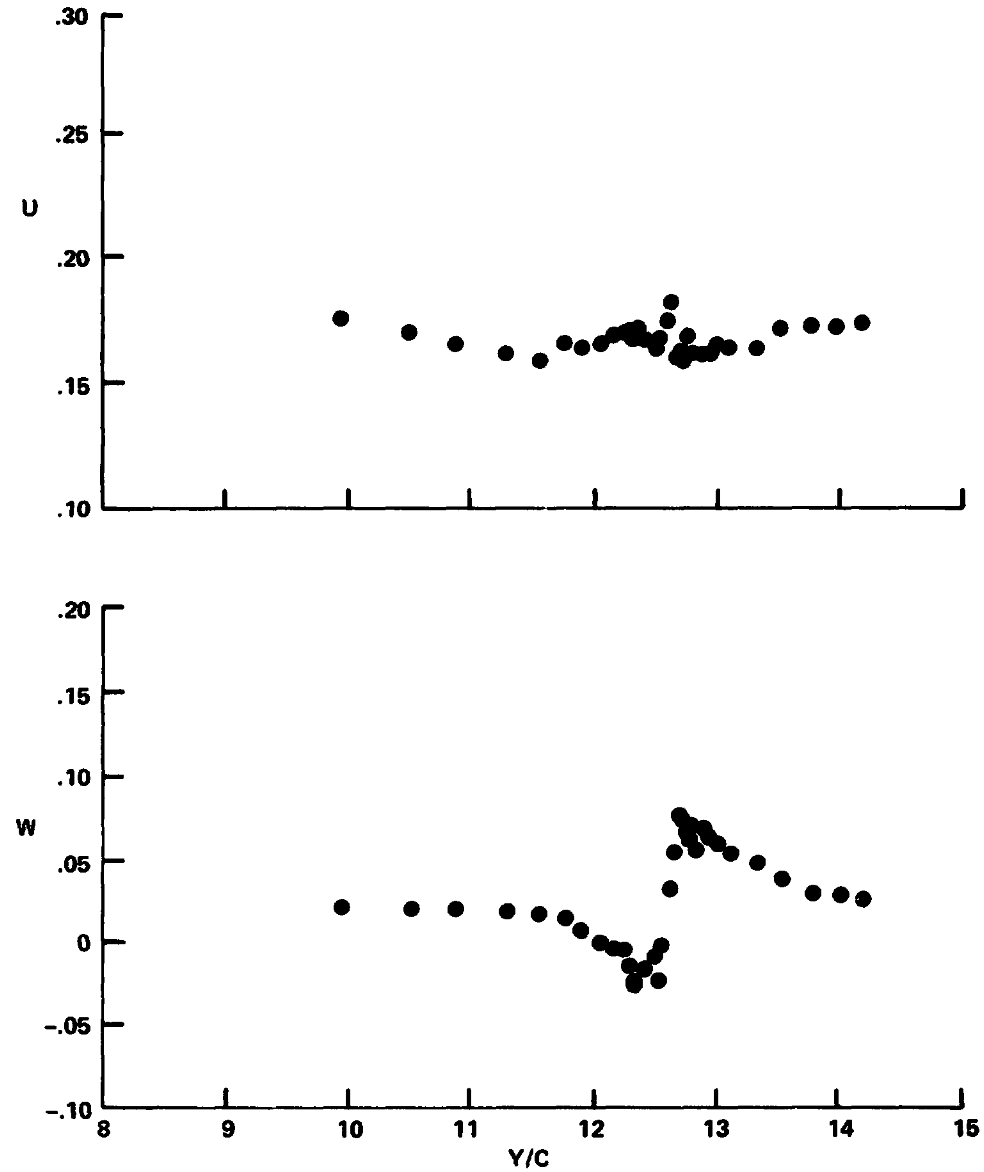

8-15. Lateral traverse, x/c = 1.99, z/c = -0.25

Figure 8. (Continued)

LATERAL VELOCITY VARIATION WHEN ROTOR BLADE IS AT AN AZIMUTH OF 77.3 DEGREES

X/C = 2.00

Z/C = −0.28

ADVANCE RATIO = 0.178

TIP SPEED = 65.7 m/sec

SHAFT ANGLE = −10.0 deg

COLLECTIVE = 10.1 deg

RUN: 169

TIME: 17:03:16

DATE: 29-JUL-76

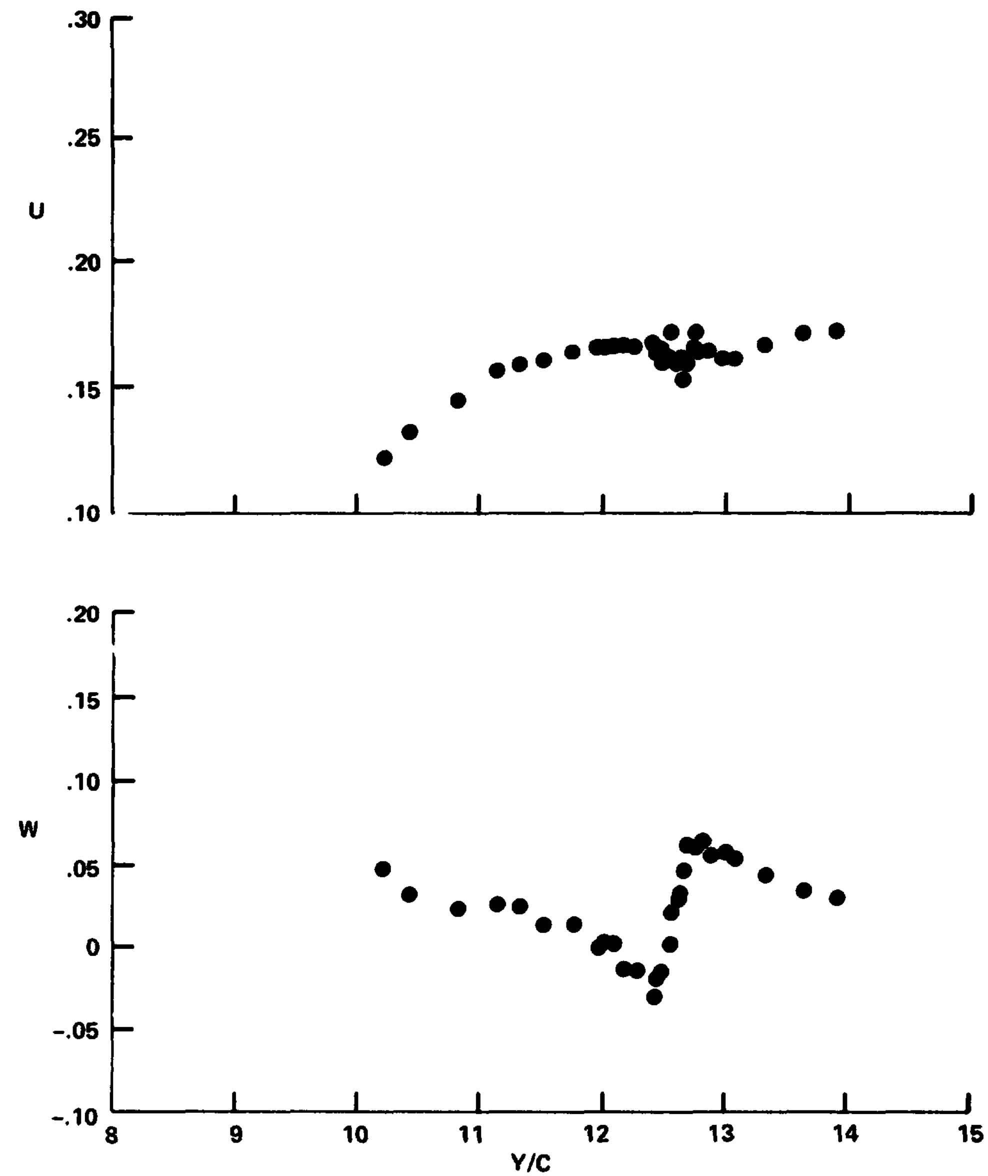

8-16. Lateral traverse, x/c = 1.99, z/c = -0.28

Figure 8. (Continued)

LATERAL VELOCITY VARIATION WHEN ROTOR BLADE IS AT AN AZIMUTH OF 77.3 DEGREES

X/C = 1.99

Z/C = −0.31

ADVANCE RATIO = 0.179

TIP SPEED = 65.7 m/sec

SHAFT ANGLE = −10.0 deg

COLLECTIVE = 10.1 deg

RUN: 170

TIME: 17:27:13

DATE: 29-JUL-76

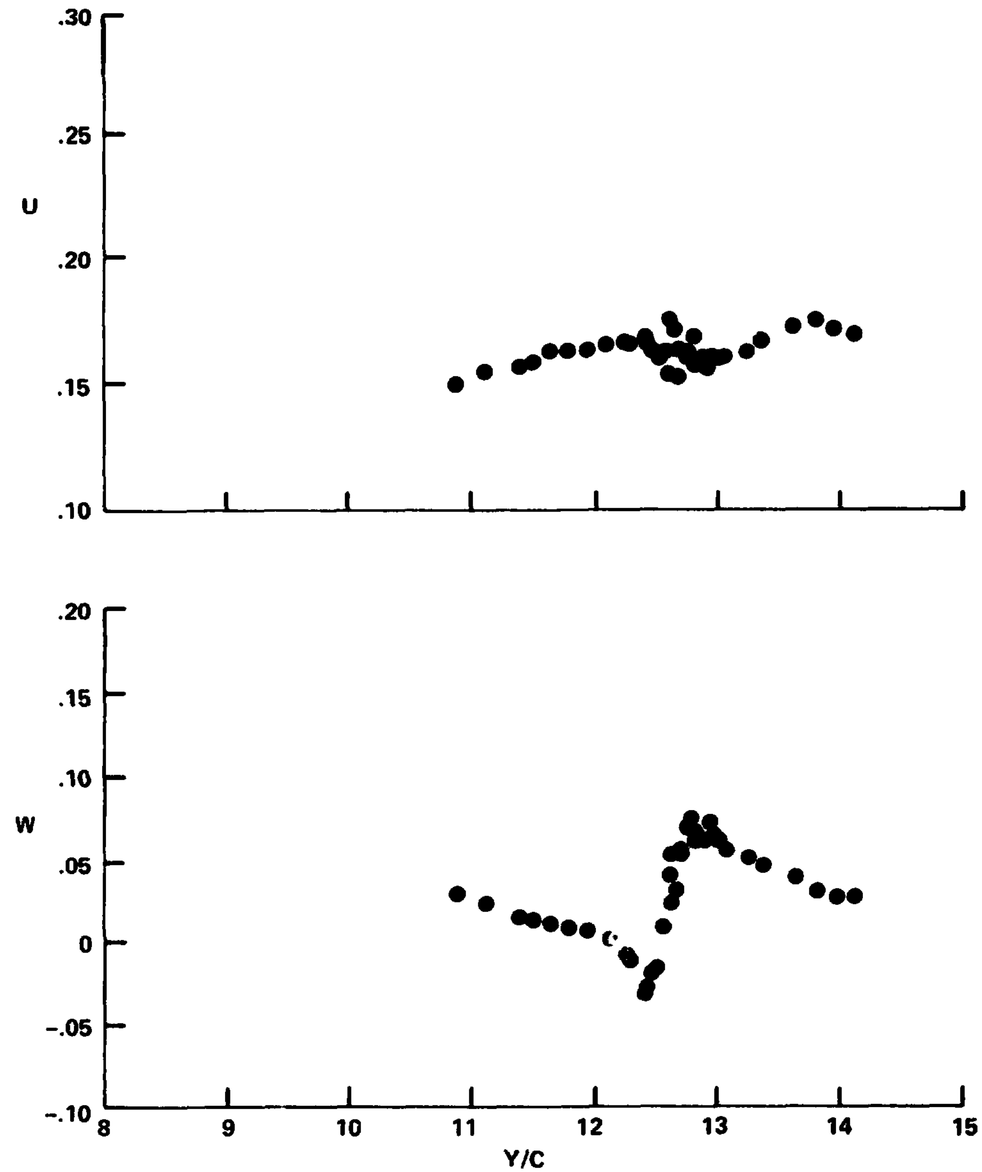

8-17. Lateral traverse, x/c = 1.99, z/c = −0.31

Figure 8. (Continued)

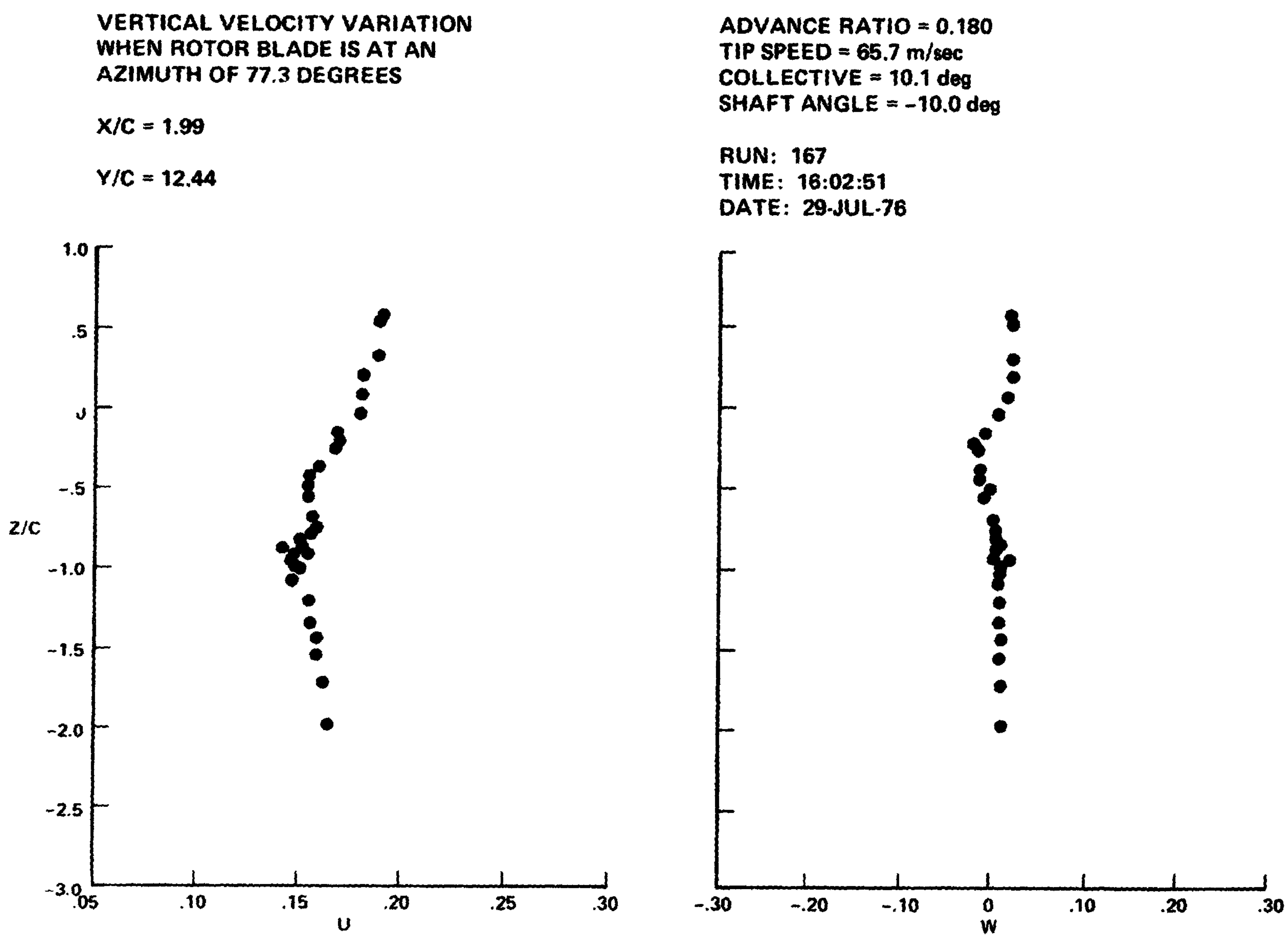

8-18. Vertical traverse, x/c = 1.99, y/c = 12.44

Figure 8. (Continued)

LATERAL VELOCITY VARIATION WHEN ROTOR BLADE IS AT AN AZIMUTH OF 77.3 DEGREES

X/C = 2.48

Y/C = −0.26

ADVANCE RATIO = 0.180

TIP SPEED = 65.7 m/sec

SHAFT ANGLE = −10.0 deg

COLLECTIVE = 10.1 deg

RUN: 172

TIME: 18:26:24

DATE: 29-JUL-76

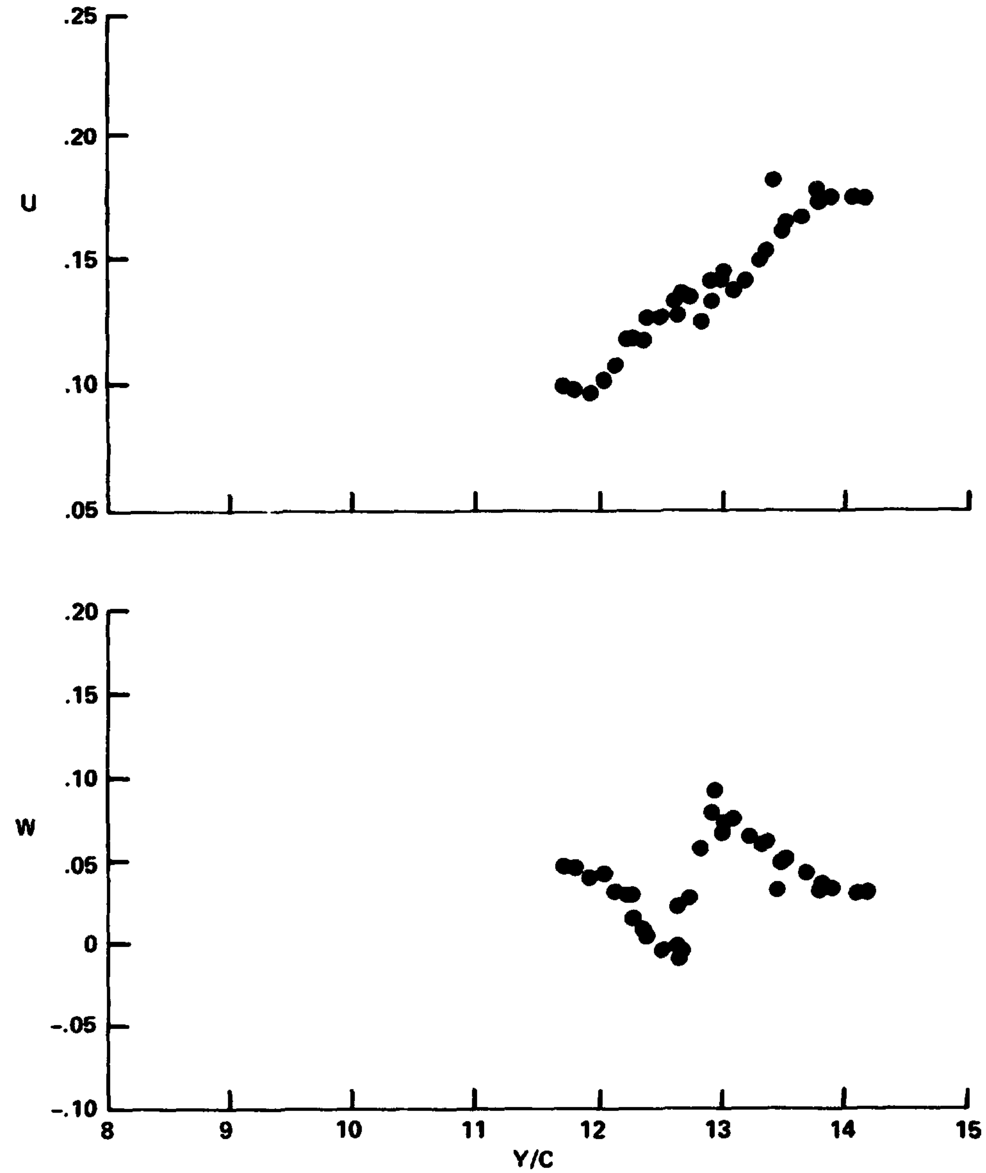

8-19. Lateral traverse, x/c = 2.48, z/c = −0.26

Figure 8. (Continued)

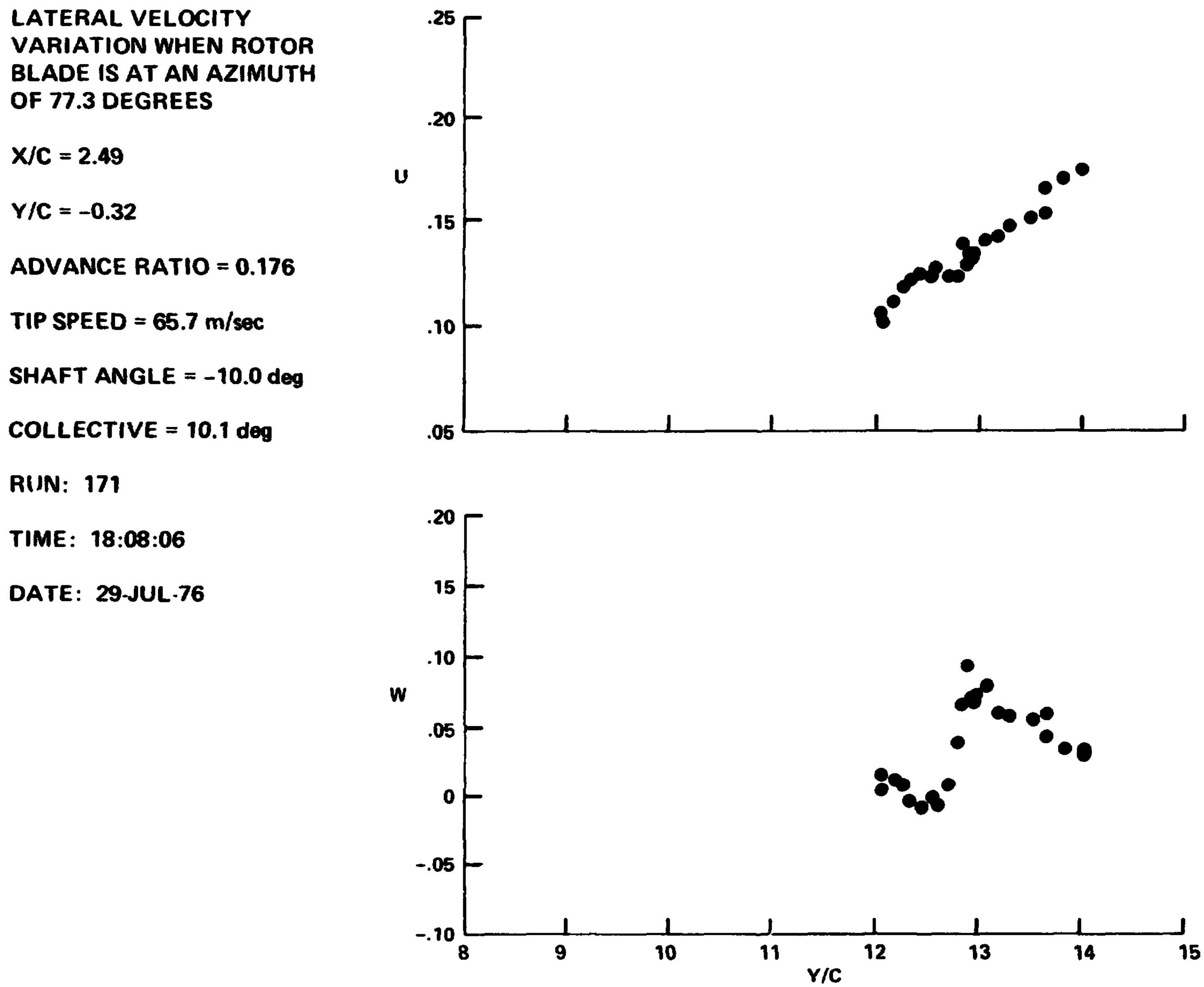

8-20. Lateral traverse, x/c = 2.49, z/c = -0.32

Figure 8. (Continued)

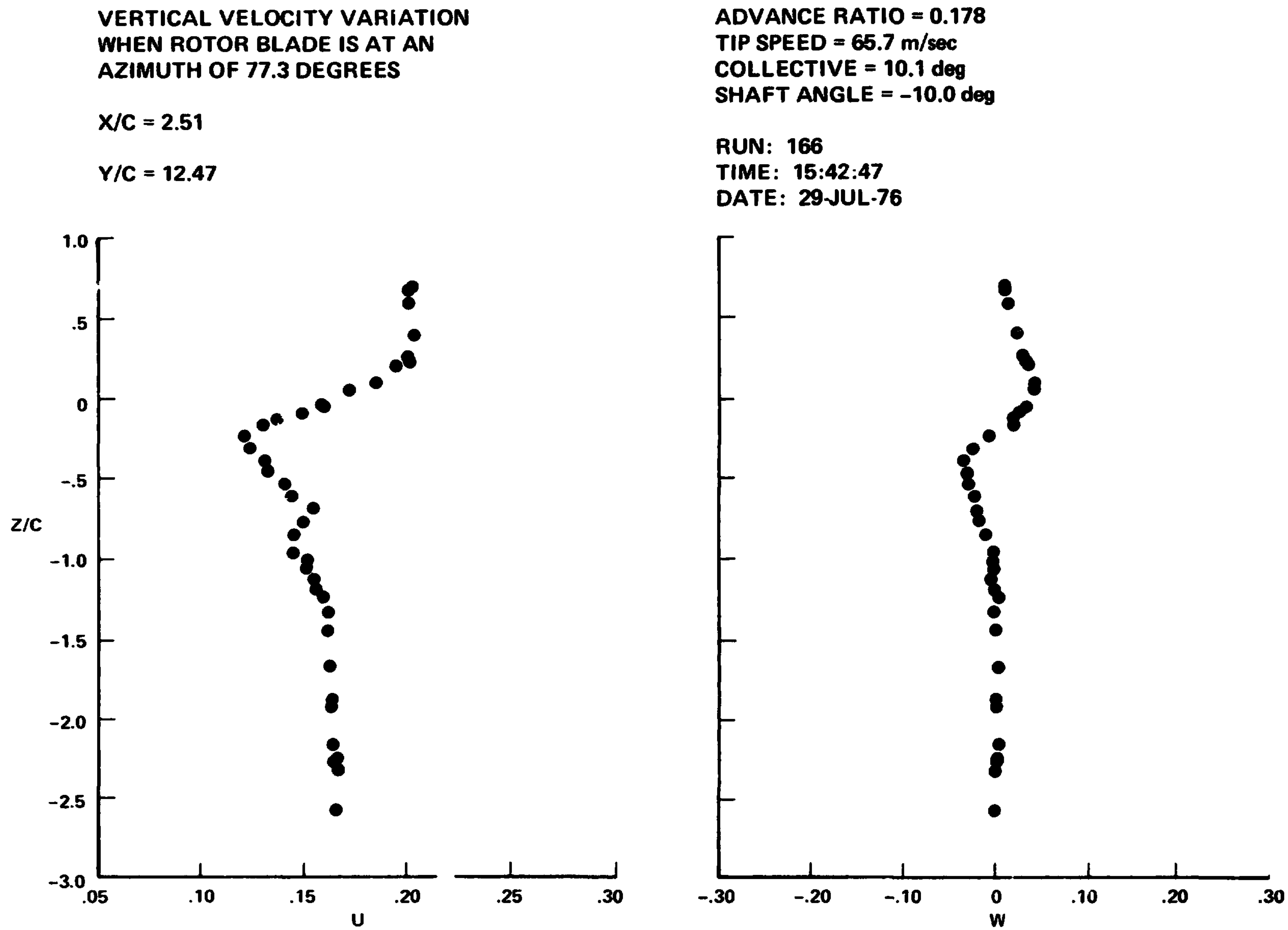

C-21. Vertical traverse, x/c = 2.51, y/c = 12.47

Figure 8. (Continued)

LATERAL VELOCITY VARIATION WHEN ROTOR BLADE IS AT AN AZIMUTH OF 77.3 DEGREES

X/C = 4.28

Z/C = −0.12

ADVANCE RATIO = 0.179

TIP SPEED = 65.7 m/sec

SHAFT ANGLE = −10.0 deg

COLLECTIVE = 10.1 deg

RUN: 182

TIME: 14:48:40

DATE: 30-JUL-76

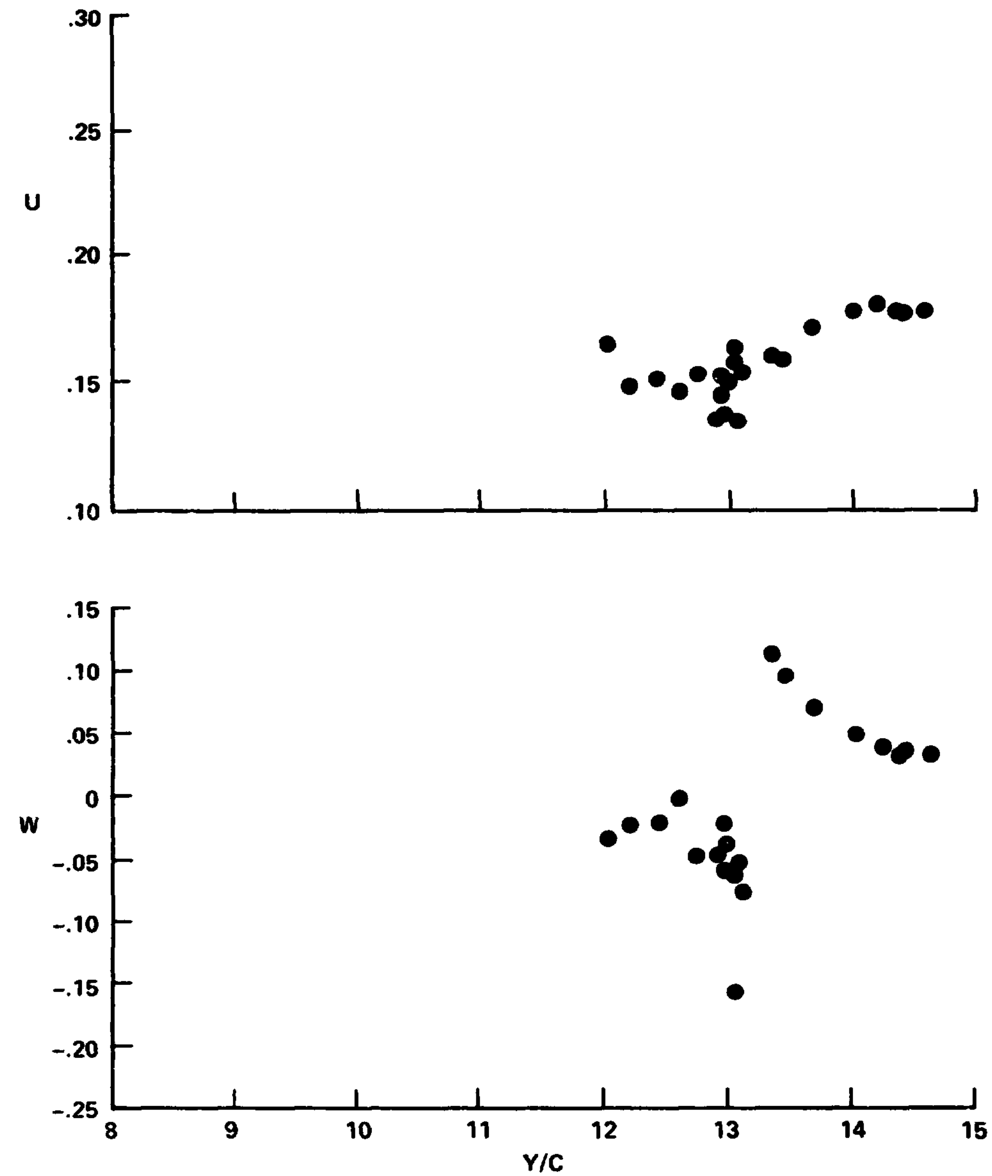

'2. Later'l erse, x/c = 4.28, z/c = −0.12

Figure 8. (Continued)

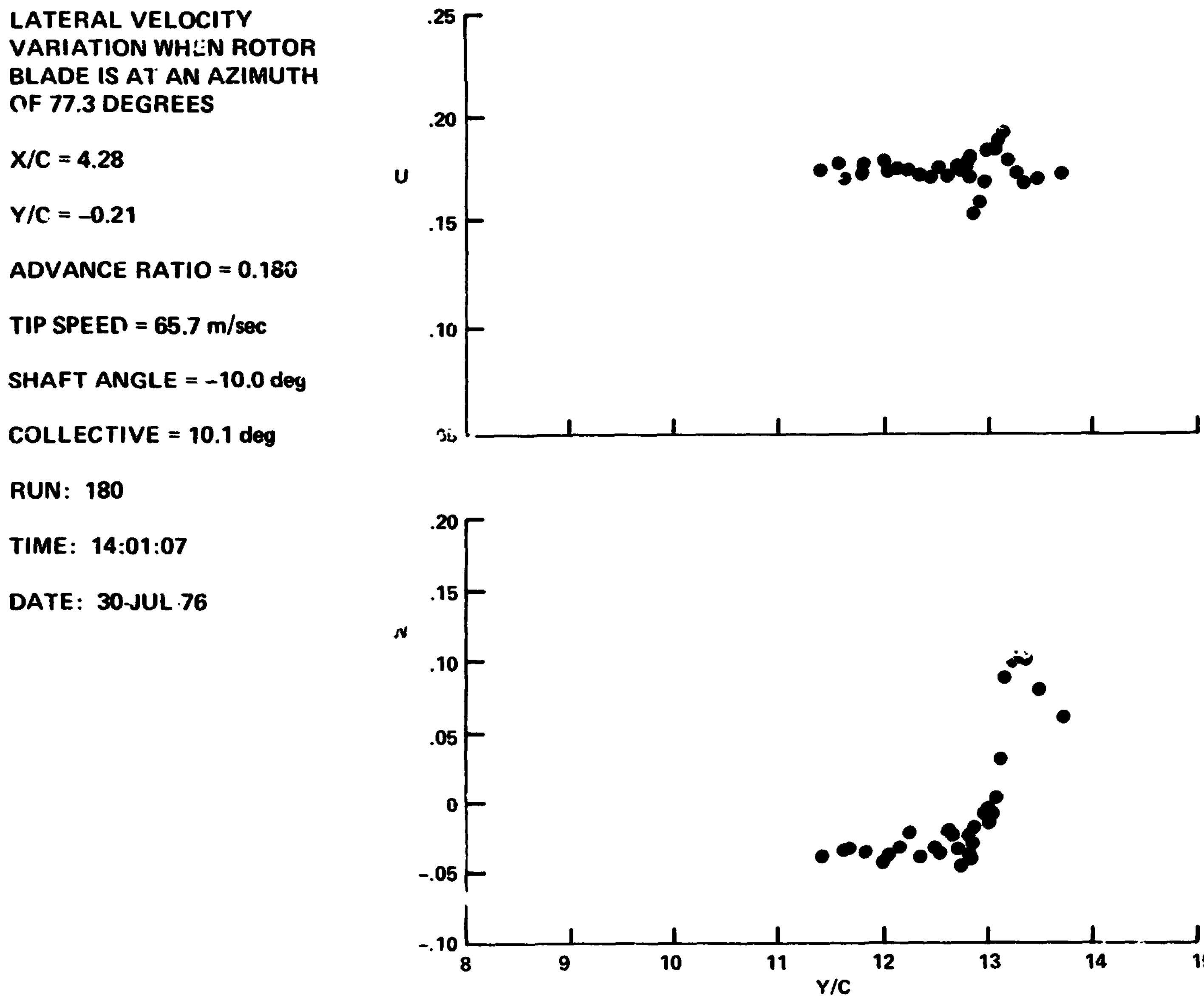

8-23. Lateral traverse, x/c = 4.28, z/c = –0.21

Figure 8. (Continued)

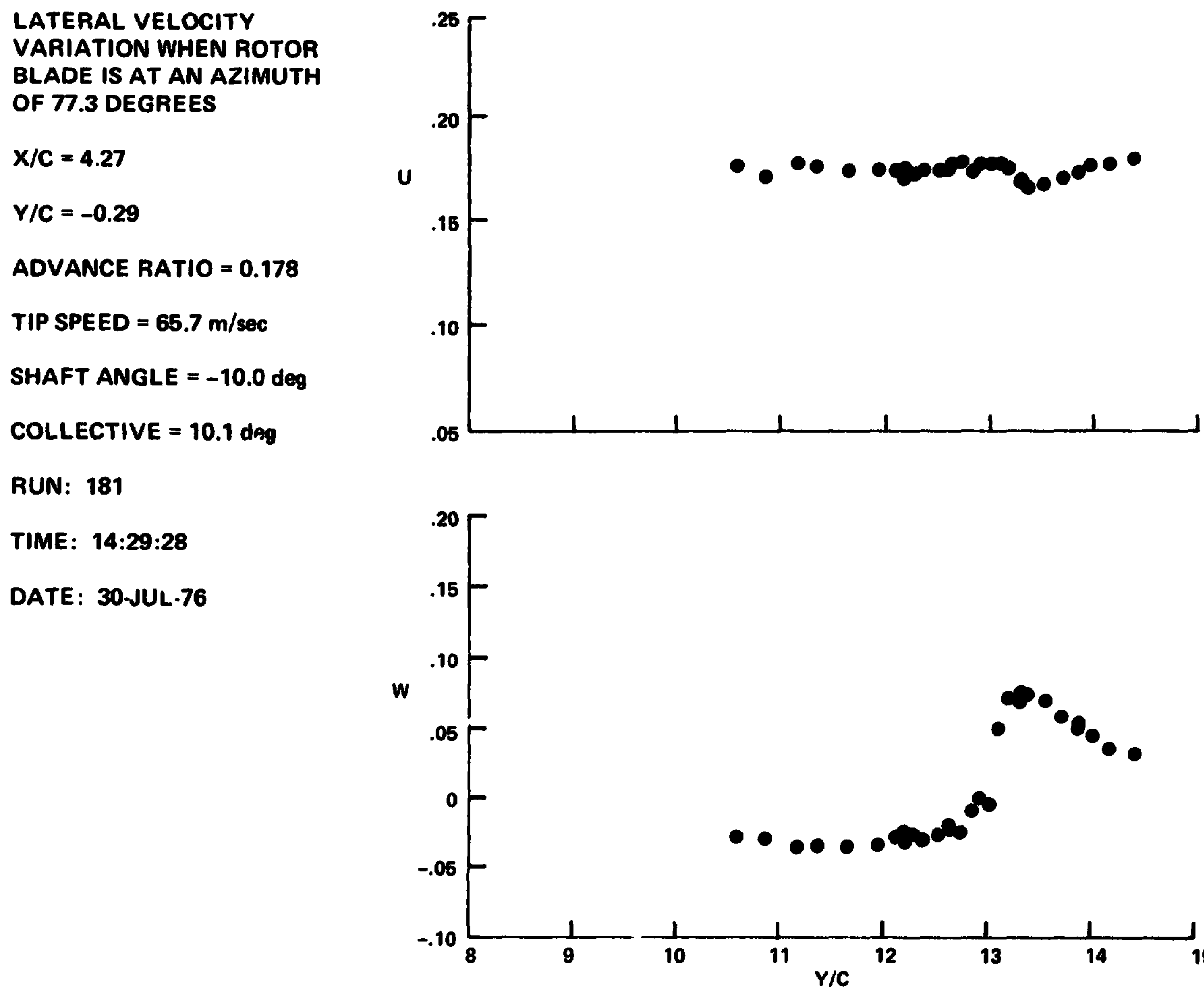

8-24. Lateral traverse, x/c = 4.27, z/c = -0.29

Figure 8. (Continued)

LATERAL VELOCITY
VARIATION WHEN ROTOR
BLADE IS AT AN AZIMUTH
OF 77.3 DEGREES

X/C = 4.28

Y/C = –0.30

ADVANCE RATIO = 0.180

TIP SPEED = 65.7 m/sec

SHAFT ANGLE = –10.0 deg

COLLECTIVE = 10.1 deg

RUN: 173

TIME: 18:53:07

DATE: 29-JUL-76

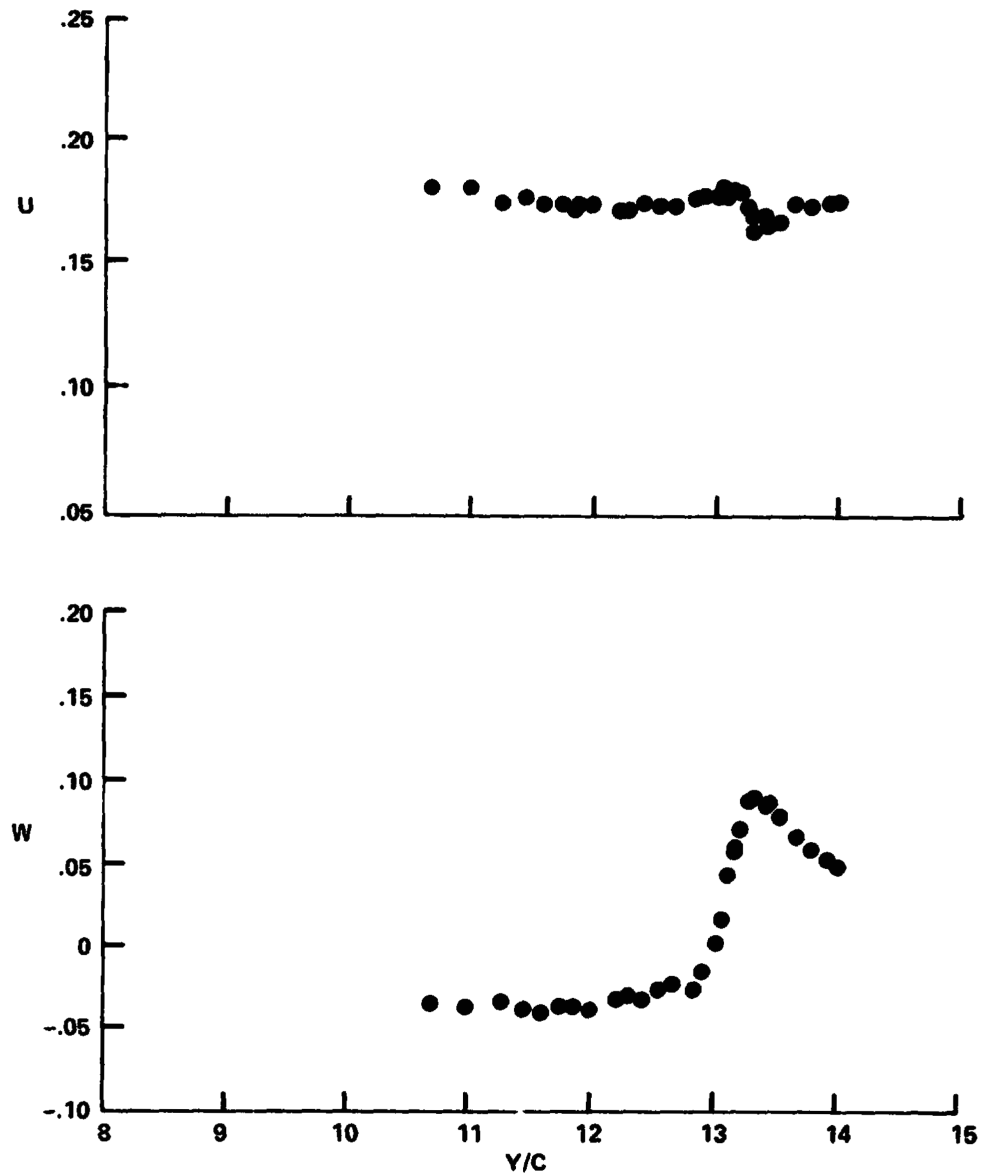

8-25. Lateral traverse, x/c = 4.28, z/c = –0.30

Figure 8. (Continued)

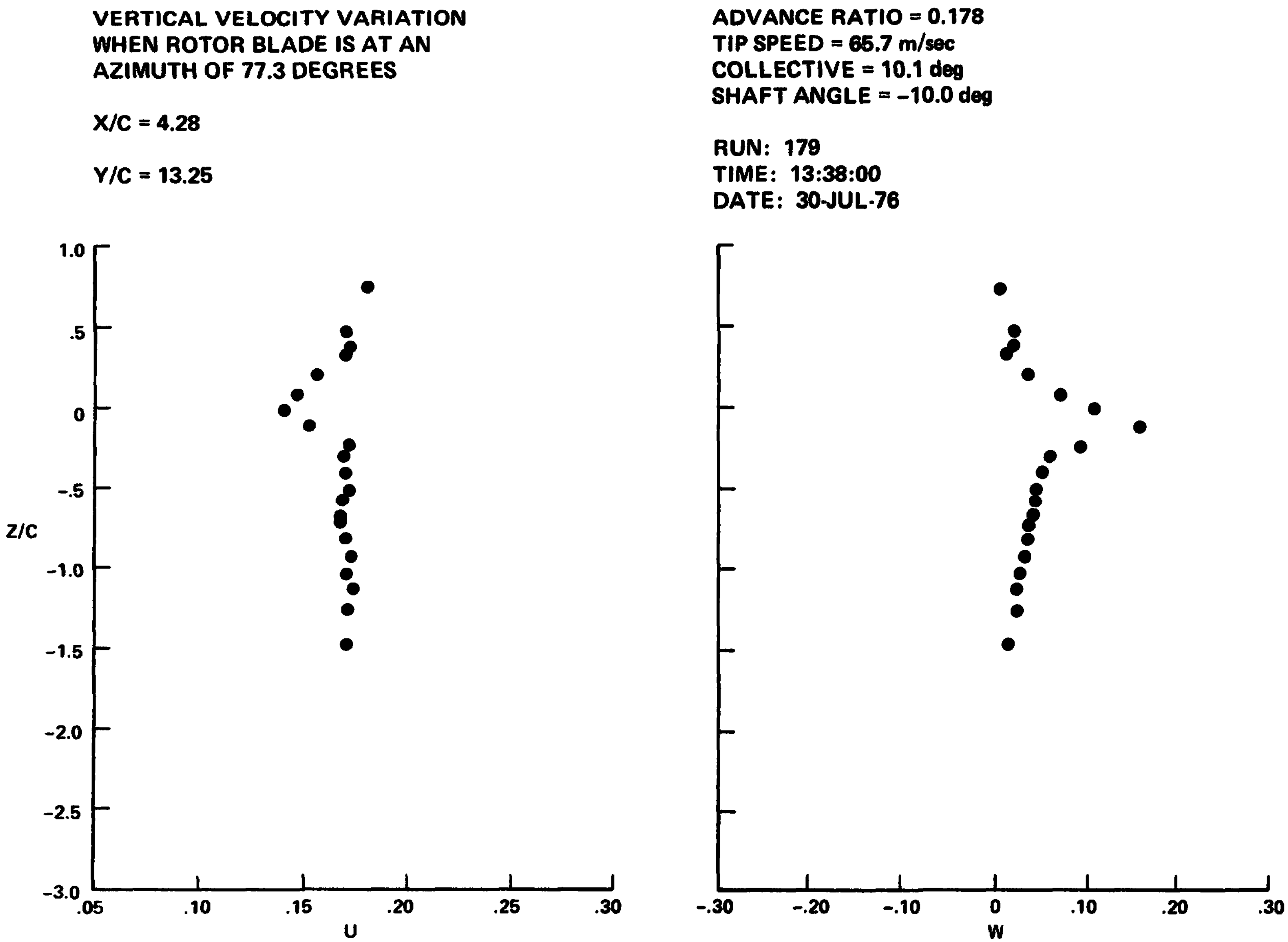

8-26. Vertical traverse, x/c = 4.28, y/c = 13.25

Figure 8. (Concluded)

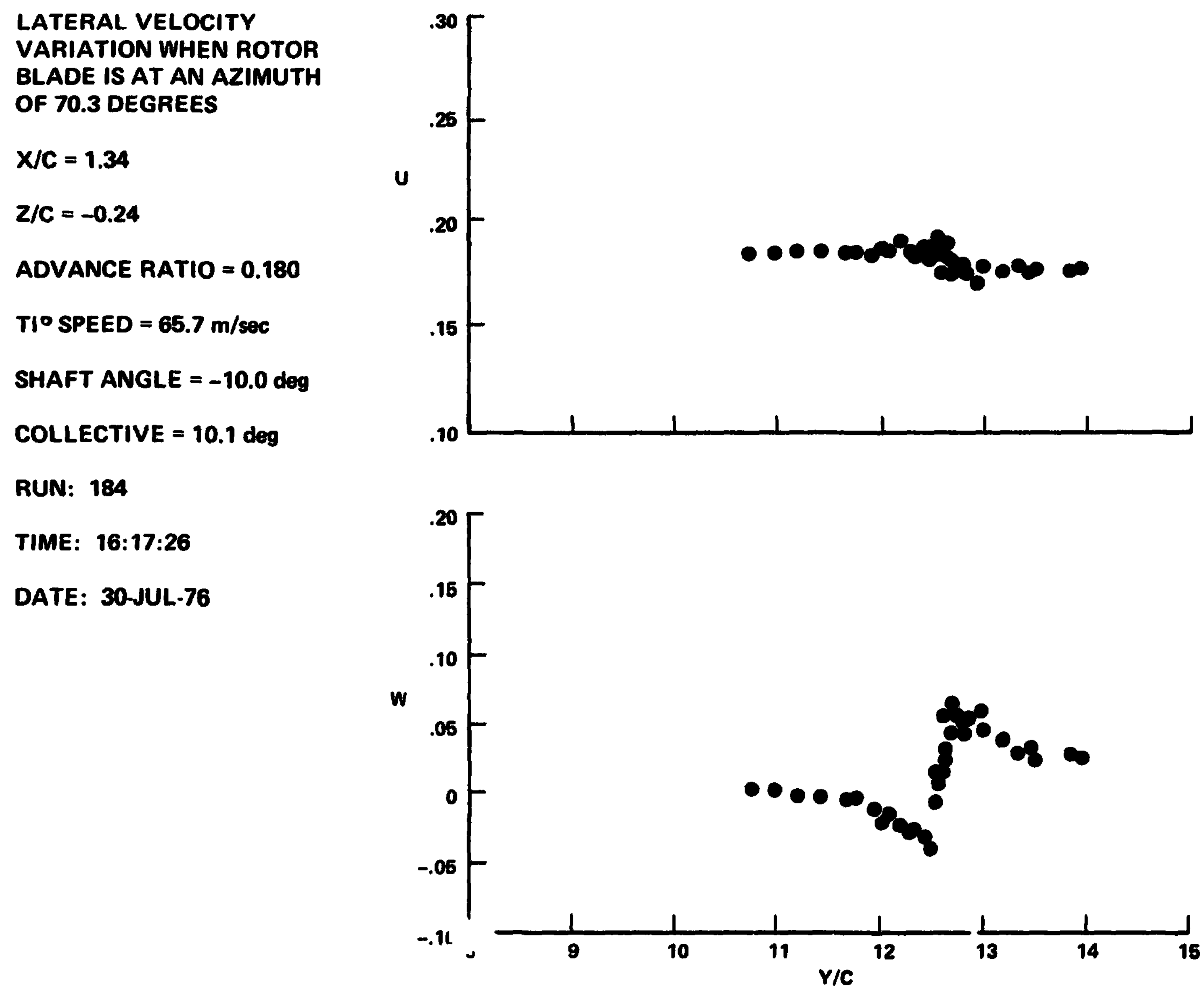

9-1. Lateral traverse, x/c = 1.34, z/c = -0.24

Figure 9. Flowfield velocities from the -11° twist blades, $V/\Omega R = 0.18$, $\theta_{0.75R} = 10.1^{\circ}$, $\psi = 70.3^{\circ}$, N = 600.

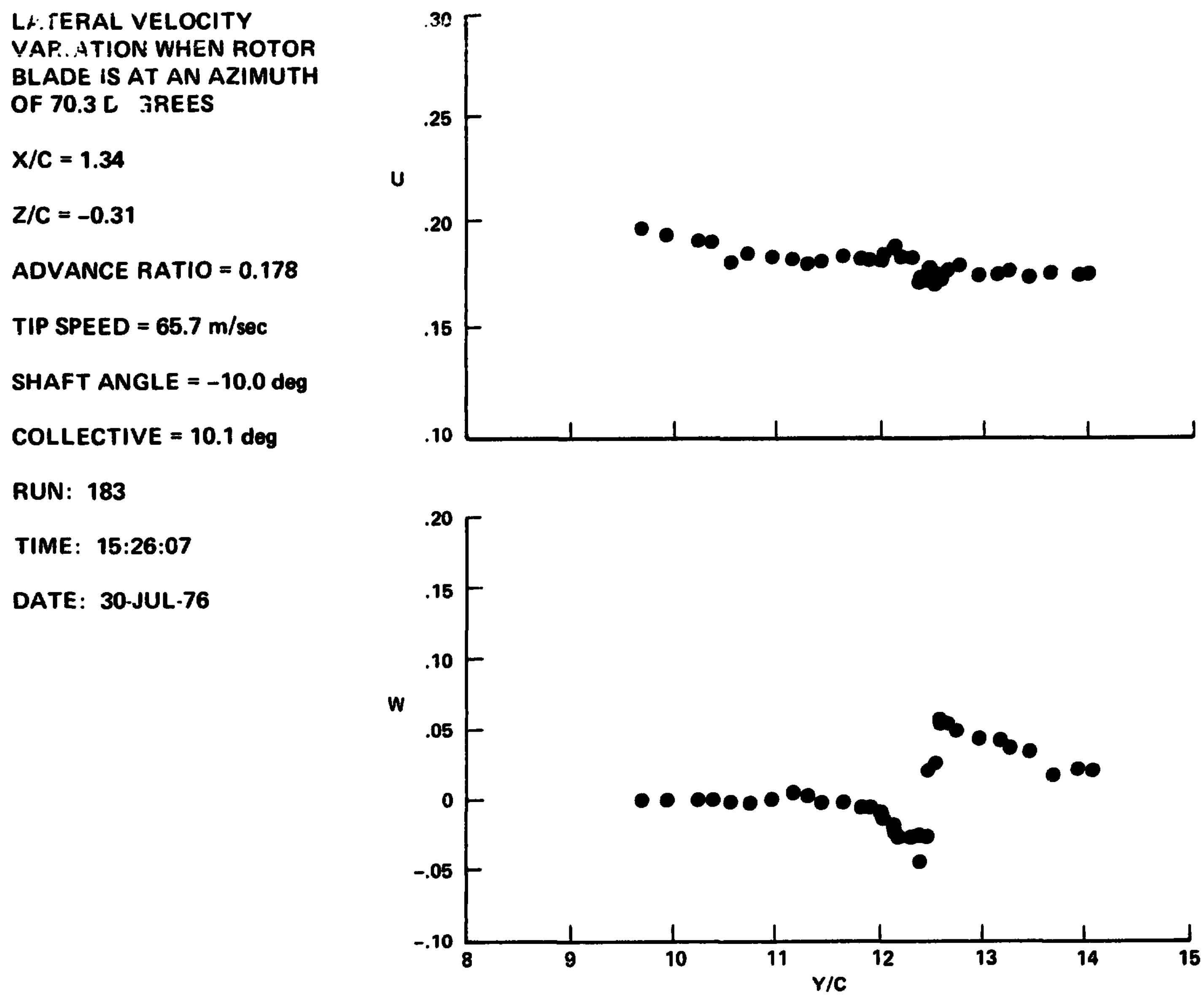

9-2. Lateral traverse, x/c = 1.34, z/c = −0.31

Figure 9. (Continued)

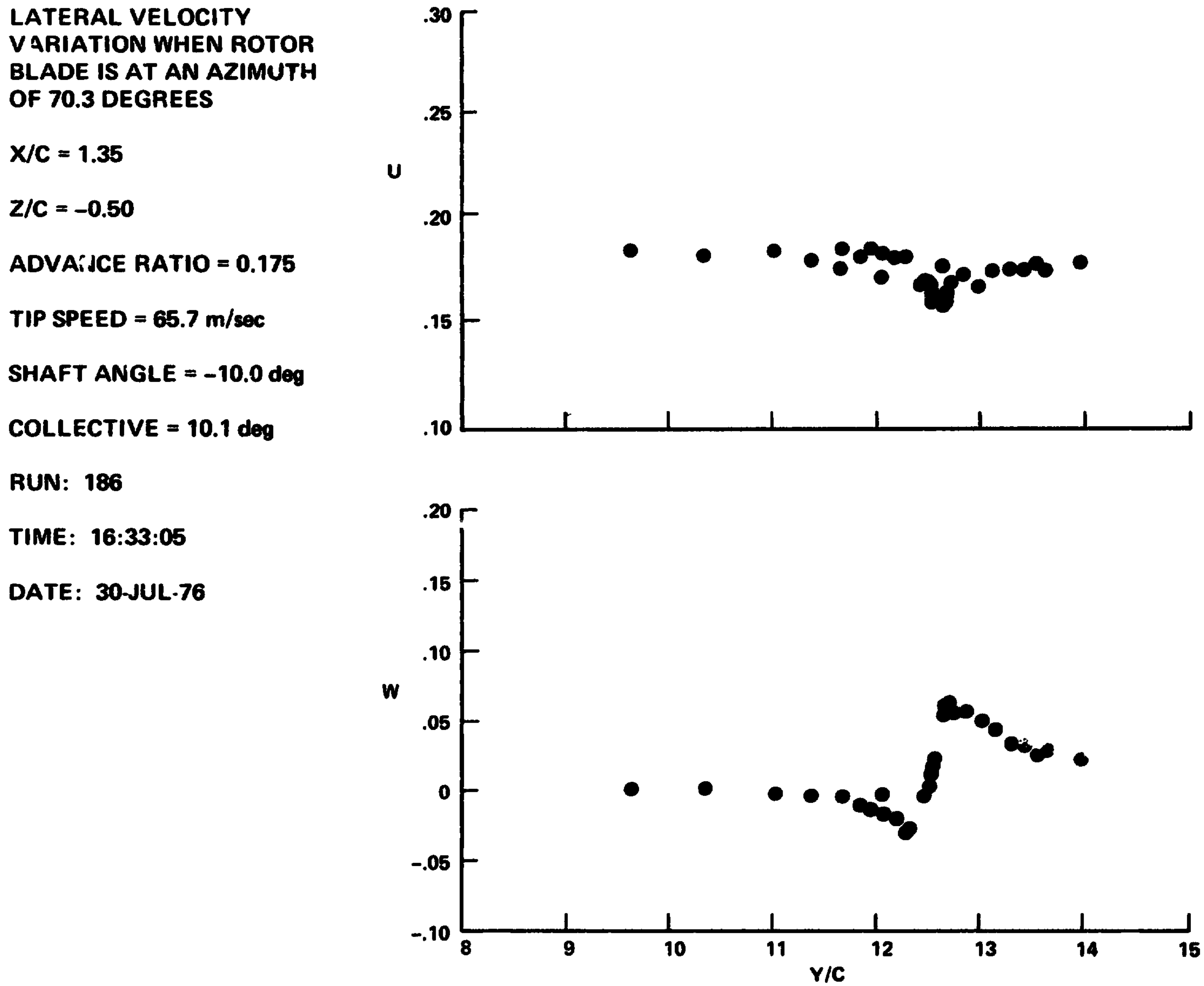

9-3. Lateral traverse, x/c = 1.34, z/c = -0.50

Figure 9. (Continued)

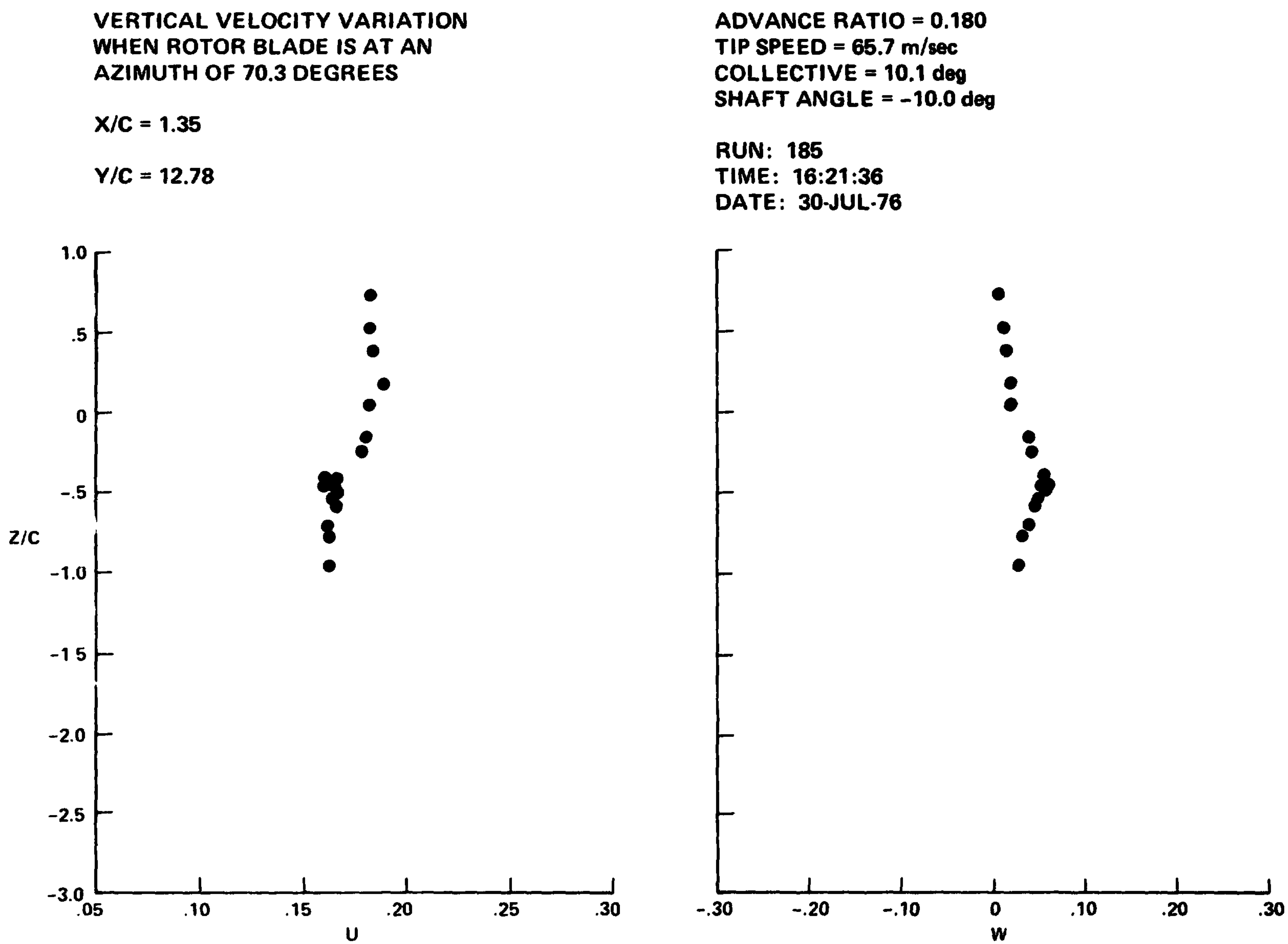

9-4. Vertical traverse, x/c = 1.34, y/c = 12.78

Figure 9. (Continued)

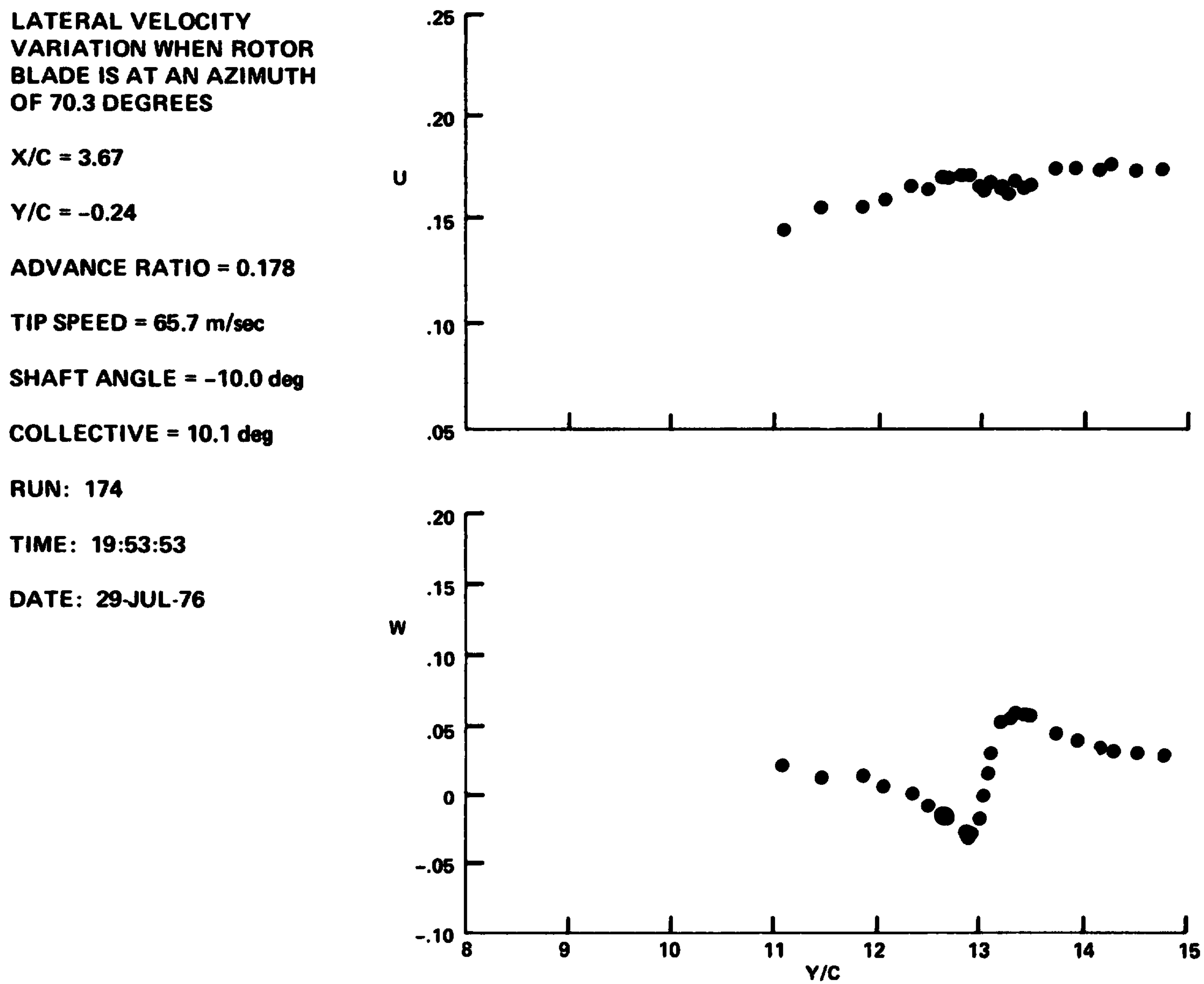

9-5. Lateral traverse, x/c = 3.67, z/c = -0.24

Figure 9. (Continued)

LATERAL VELOCITY
VARIATION WHEN ROTOR
BLADE IS AT AN AZIMUTH
OF 70.3 DEGREES

X/C = 4.01

Y/C = −0.20

ADVANCE RATIO = 0.180

TIP SPEED = 65.7 m/sec

SHAFT ANGLE = −10.0 deg

COLLECTIVE = 10.1 deg

RUN: 175

TIME: 09:46:26

DATE: 30-JUL-76

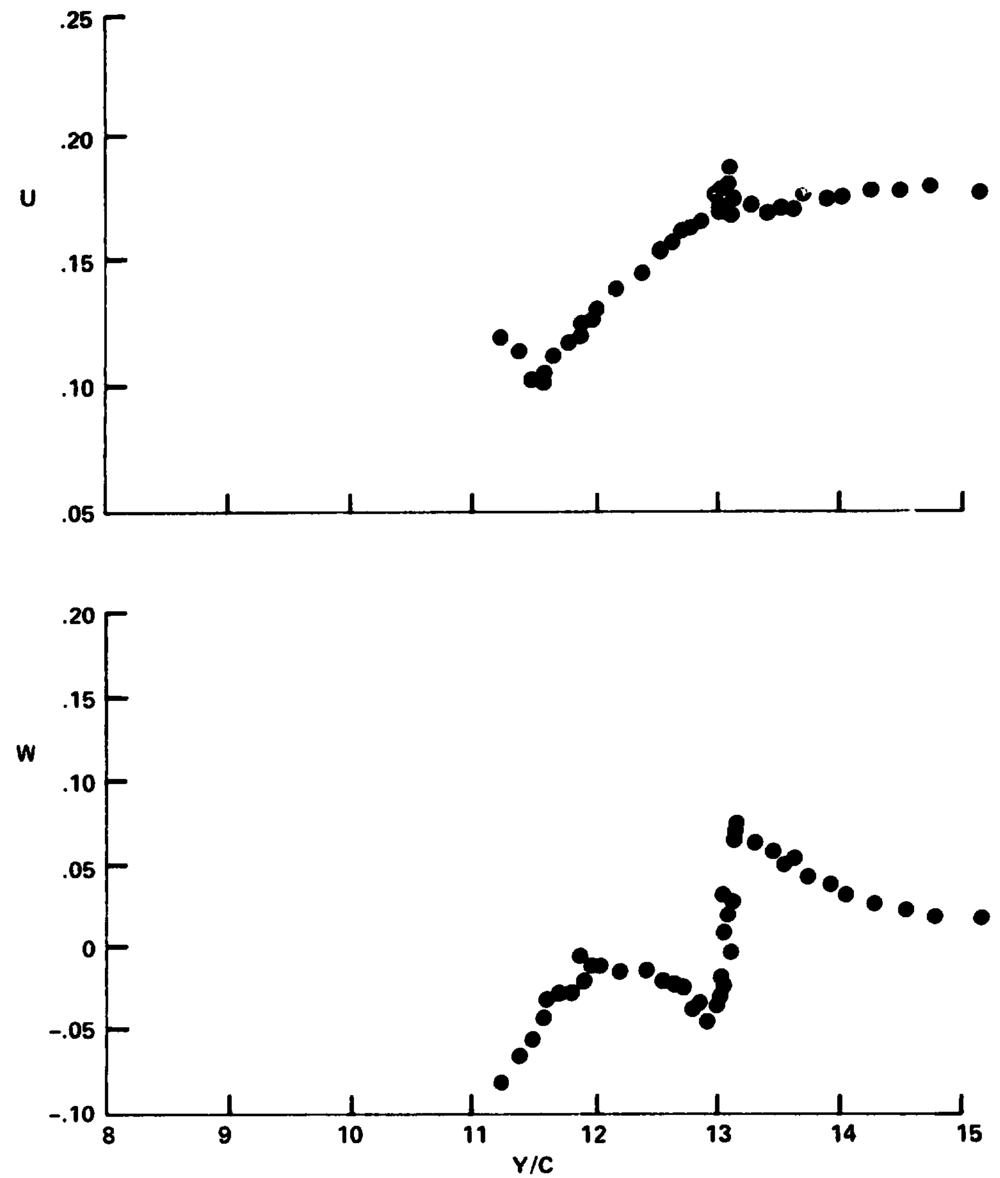

9-6. Lateral traverse, x/c = 4.01, z/c = −0.20

Figure 9. (Continued)

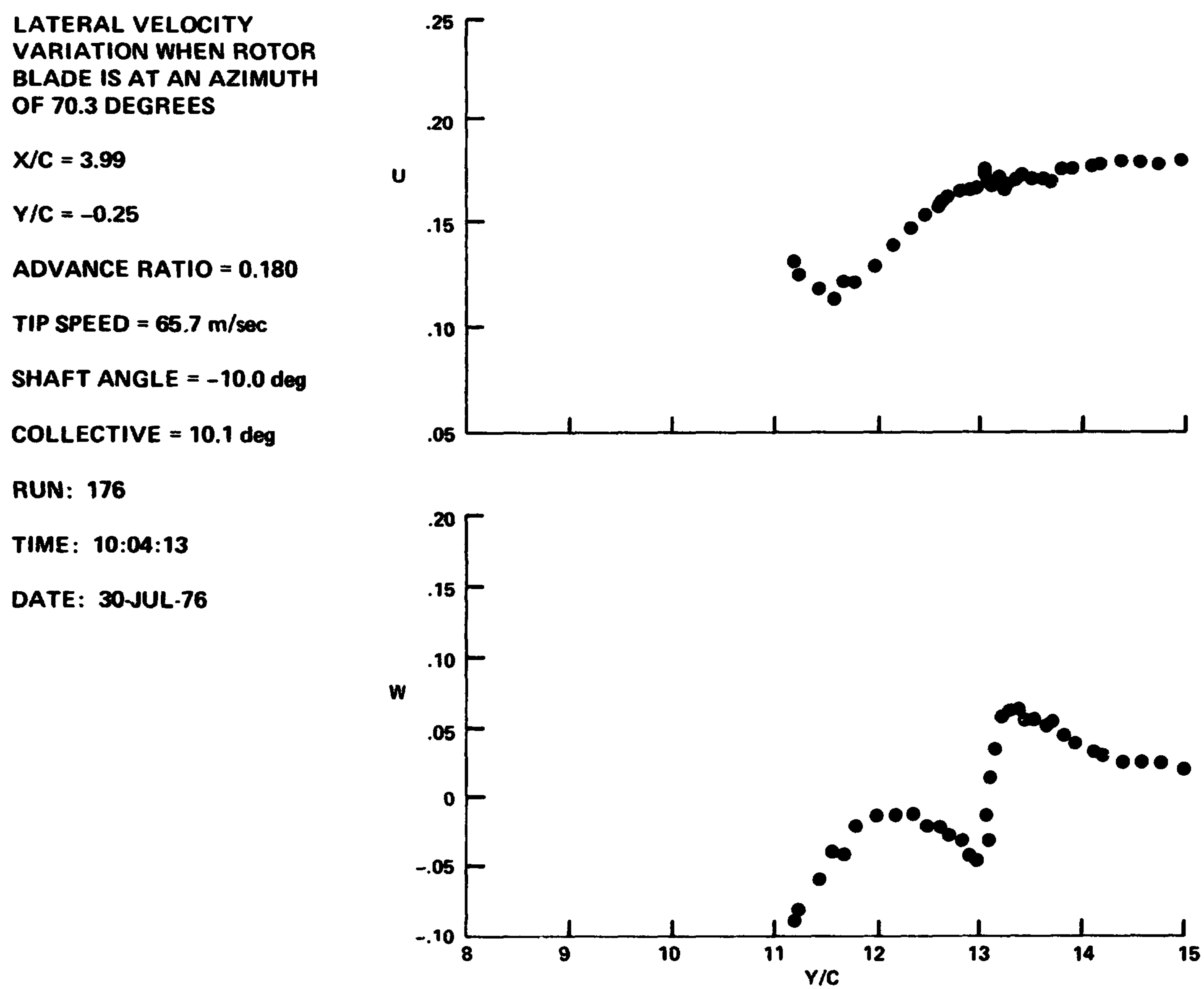

9-7. Lateral traverse, x/c = 3.99, z/c = -0.25

Figure 9. (Concluded)

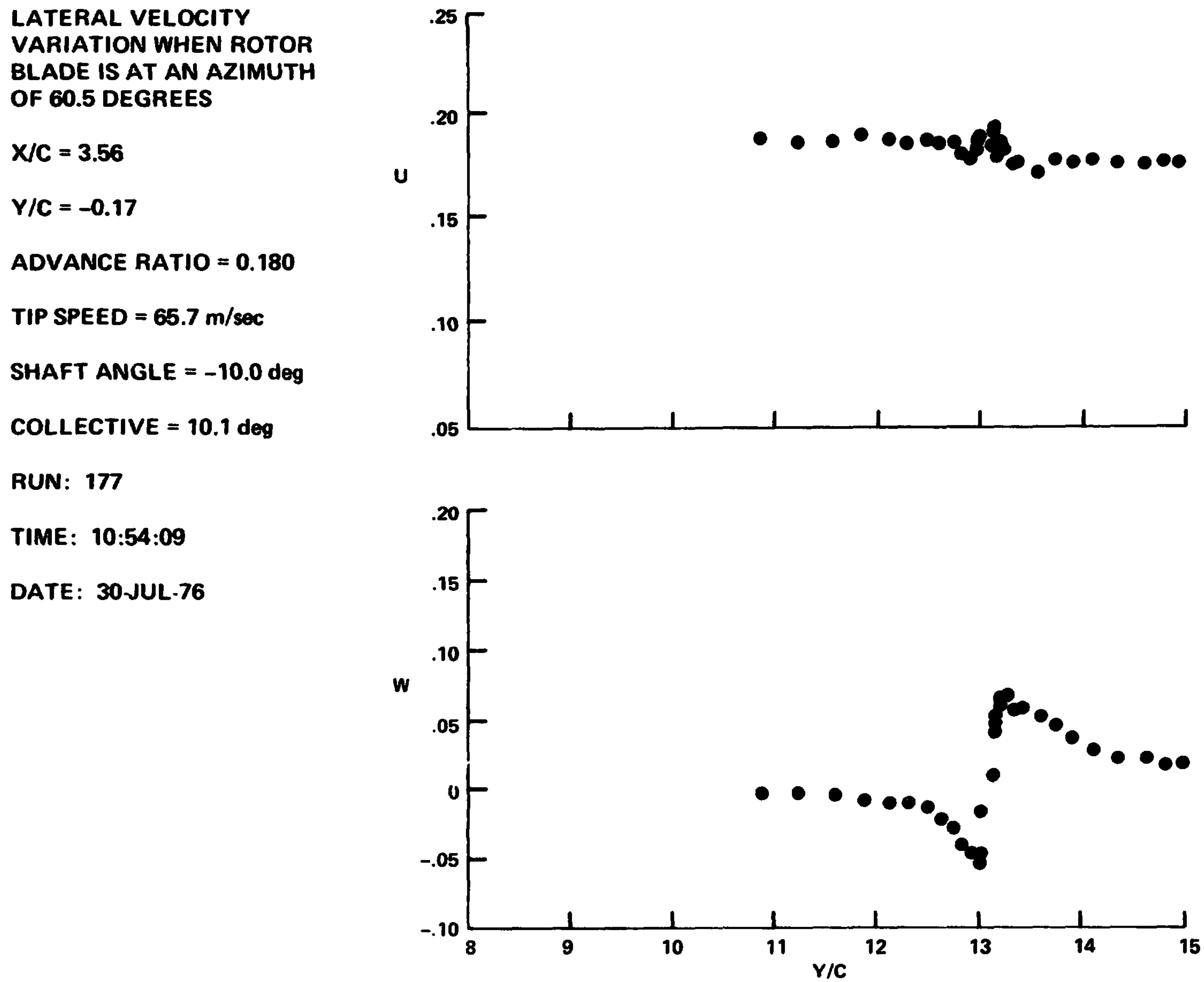

10-1. Lateral traverse, $x/c = 3.56$, $z/c = -0.17$

Figure 10. Flowfield velocities from the -11° twist blades, $V/\Omega R = 0.18$, $\theta_{0.75R} = 10.1^{\circ}$, $\psi = 60.5^{\circ}$, $N = 600$.

LATERAL VELOCITY VARIATION WHEN ROTOR BLADE IS AT AN AZIMUTH OF 60.5 DEGREES

X/C = 3.57

Y/C = -0.2υ

ADVANCE RATIO = 0.181

TIP SPEED = 65.7 m/sec

SHAFT ANGLE = -10.0 deg

COLLECTIVE = 10.1 deg

RUN: 178

TIME: 11:05:54

DATE: 30-JUL-76

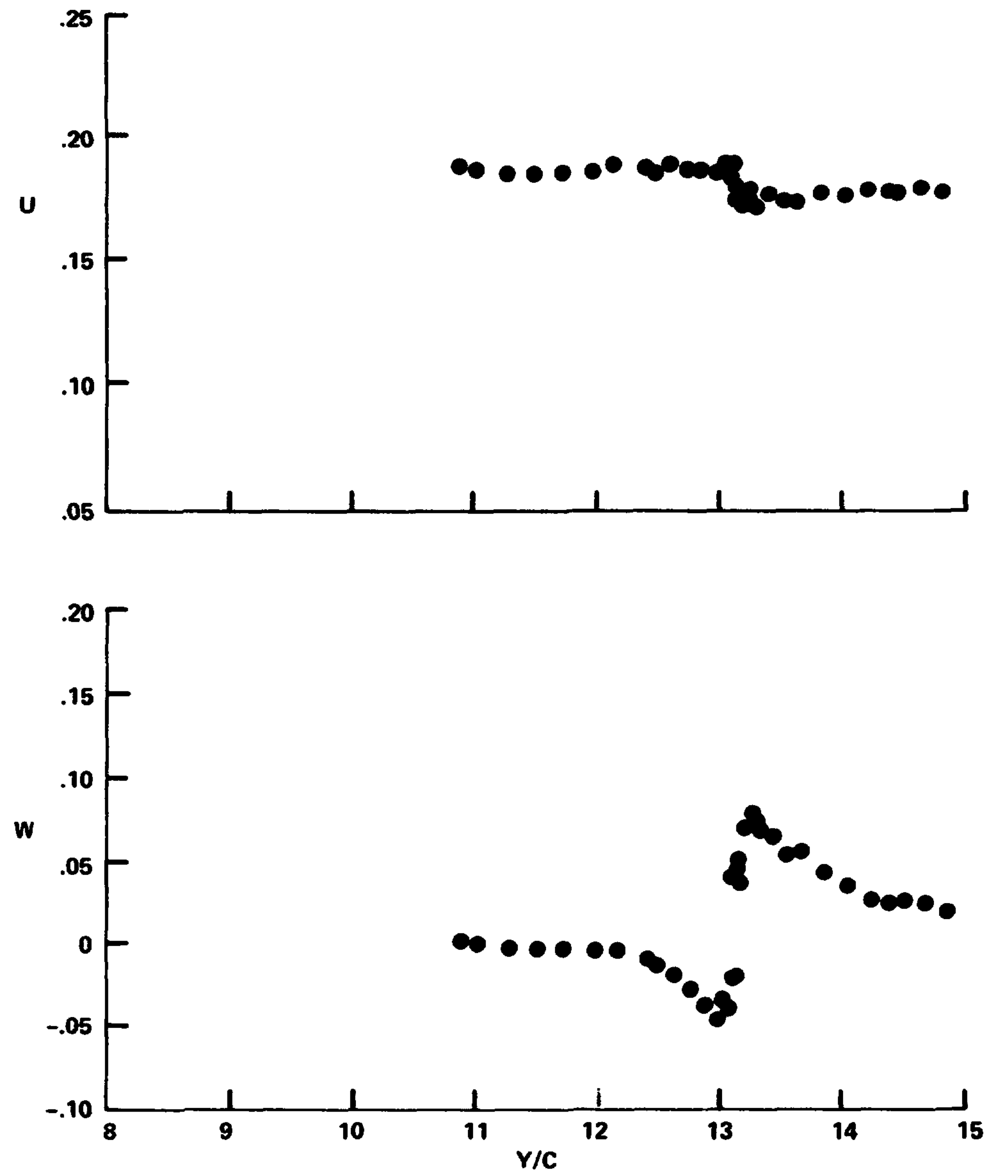

10-2. Lateral traverse, x/c = 3.57, z/c = -0.20

Figure 10. (Concluded)

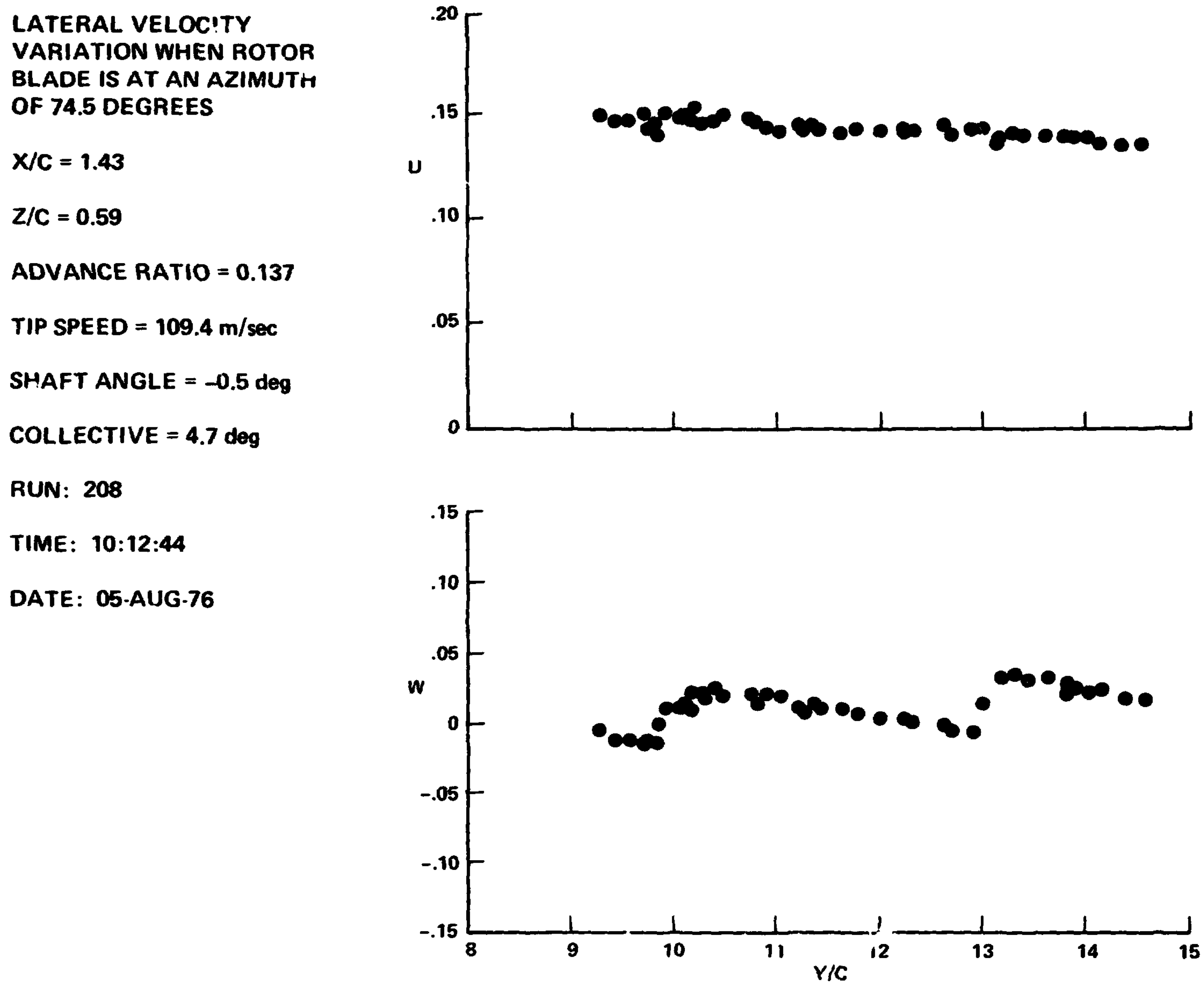

11-1. Lateral traverse, x/c = 1.43, z/c = 0.59

Figure 11. Flowfield velocities from the -11^o twist blades, $V/\Omega R = 0.137$, $\theta_{0.75R} = 4.67^o$, $\psi = 74.5^o$, N = 1000.

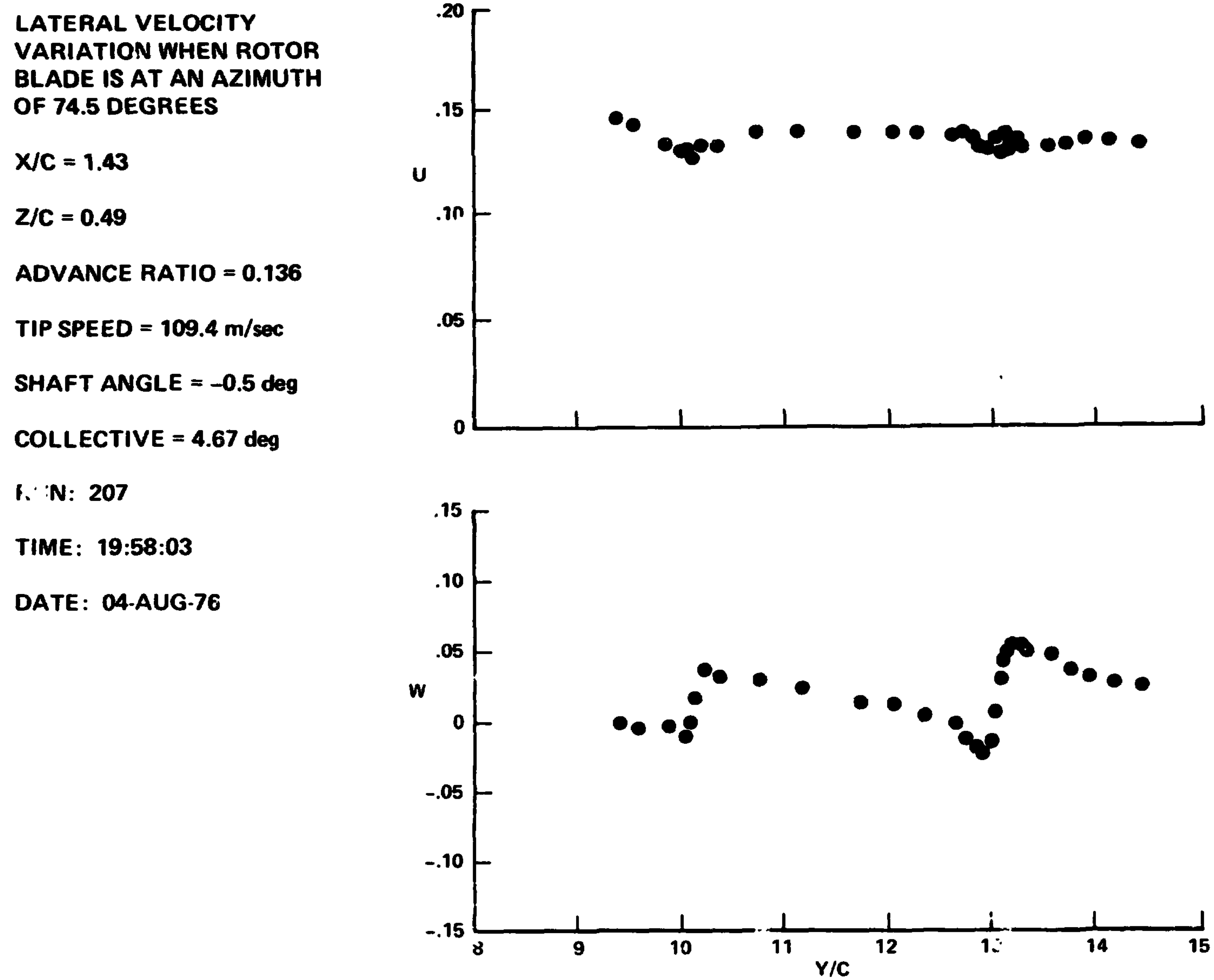

11-2. Lateral traverse, $x/c = 1.43$, $z/c = 0.49$

Figure 11. (Continued)

LATERAL VELOCITY VARIATION WHEN ROTOR BLADE IS AT AN AZIMUTH OF 74.5 DEGREES

X/C = 1.43

Z/C = 0.31

ADVANCE RATIO = 0.137

TIP SPEED = 109.4 m/sec

SHAFT ANGLE = −0.5 deg

COLLECTIVE = 4.67 deg

RUN: 206

TIME: 19:51:40

DATE: 04-AUG-76

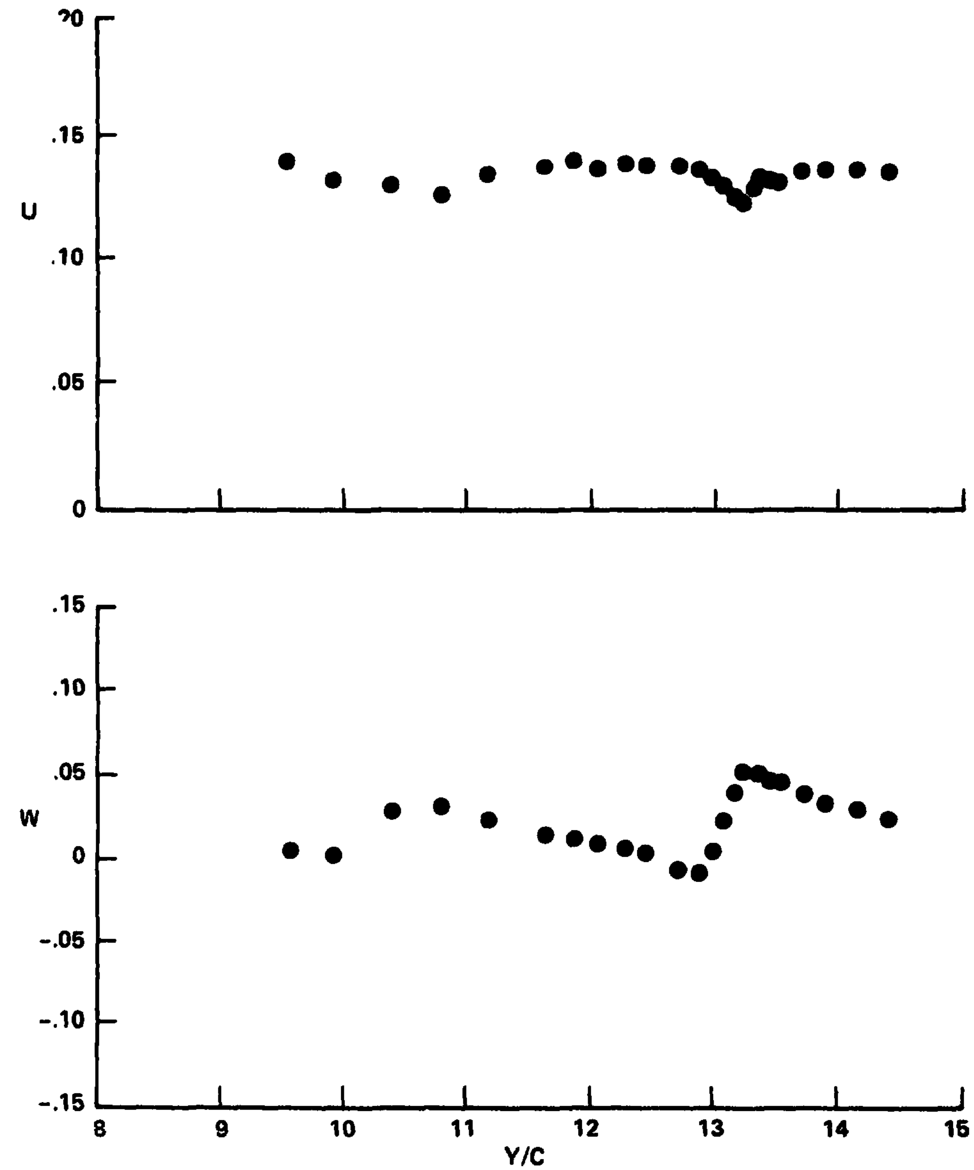

11-3. Lateral traverse, x/c = 1.43, z/c = 0.31

Figure 11. (Continued)

LATERAL VELOCITY VARIATION WHEN ROTOR BLADE IS AT AN AZIMUTH OF 74.5 DEGREES

X/C = 1.43

Z/C = 0.21

ADVANCE RATIO = 0.137

TIP SPEED = 109.4 m/sec

SHAFT ANGLE = –0.5 deg

COLLECTIVE = 4.67 deg

RUN: 205

TIME: 19:44:38

DATE: 04-AUG-76

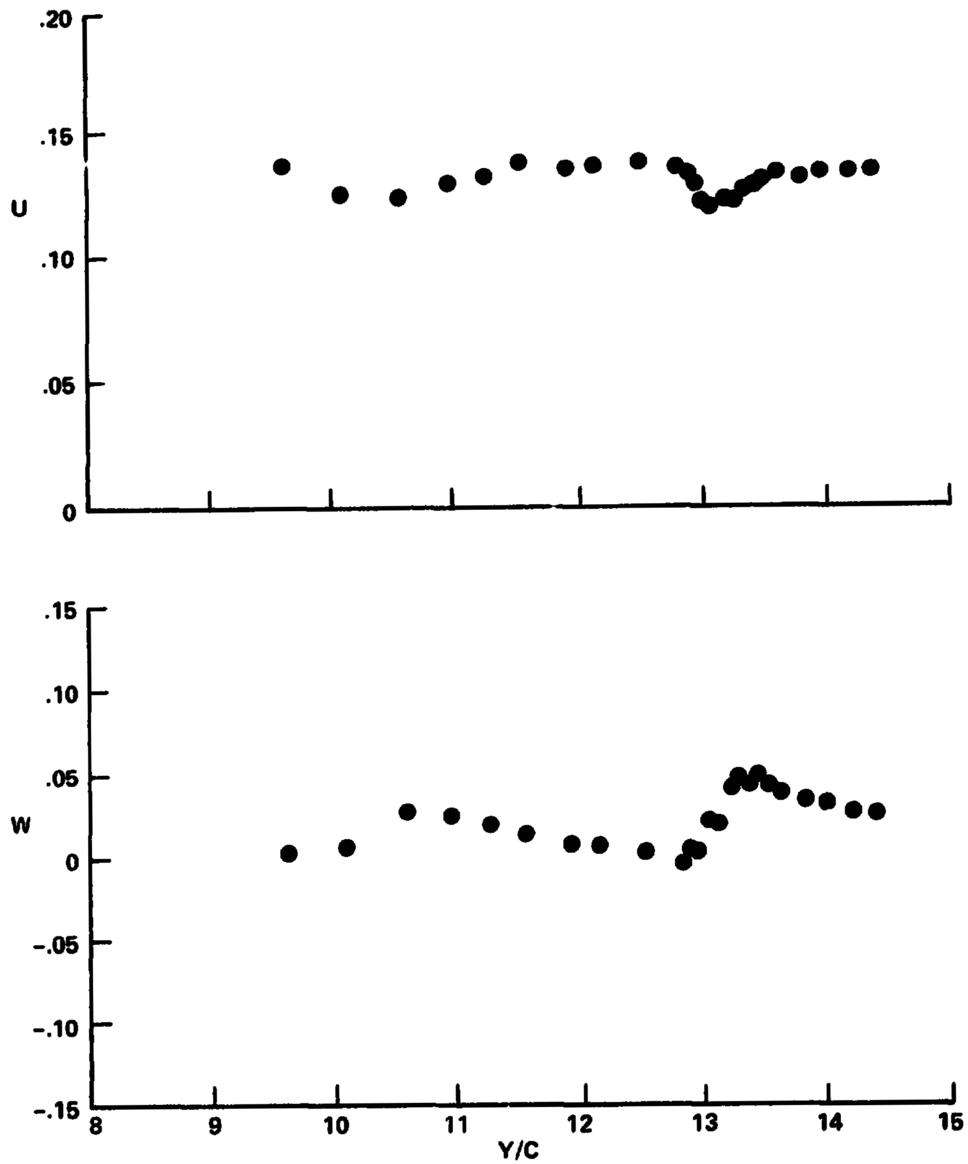

11-4. Lateral traverse, x/c = 1.43, z/c = 0.21

Figure 11. (Continued)

LATERAL VELOCITY VARIATION WHEN ROTOR BLADE IS AT AN AZIMUTH OF 74.5 DEGREES

X/C = 1.41

Z/C = 0.01

ADVANCE RATIO = 0.137

TIP SPEED = 109.4 m/sec

SHAFT ANGLE = −0.5 deg

COLLECTIVE = 4.67 deg

RUN: 204

TIME: 19:32:45

DATE: 04-AUG-76

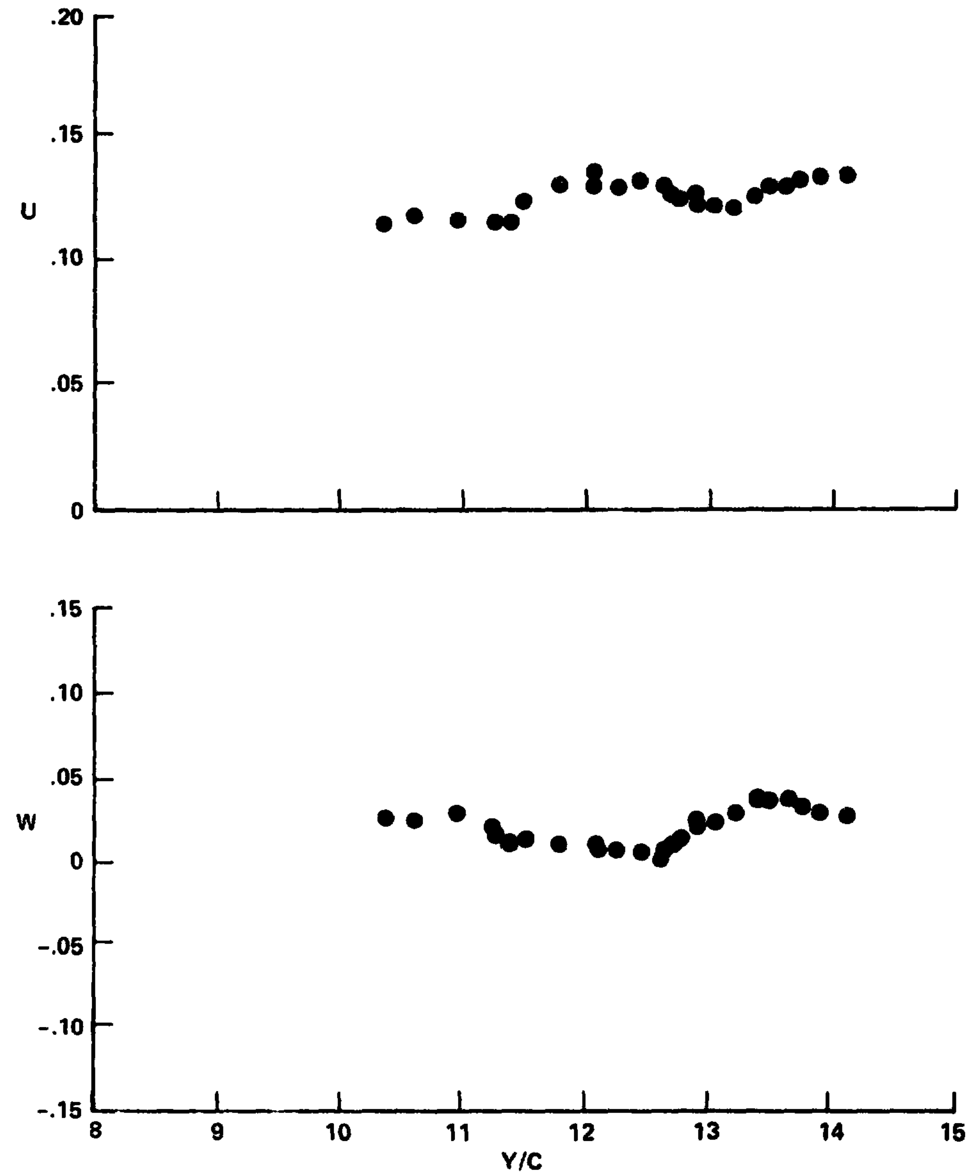

11-5. Lateral traverse, x/c = 1.41, z/c = 0.01

Figure 11. (Continued)

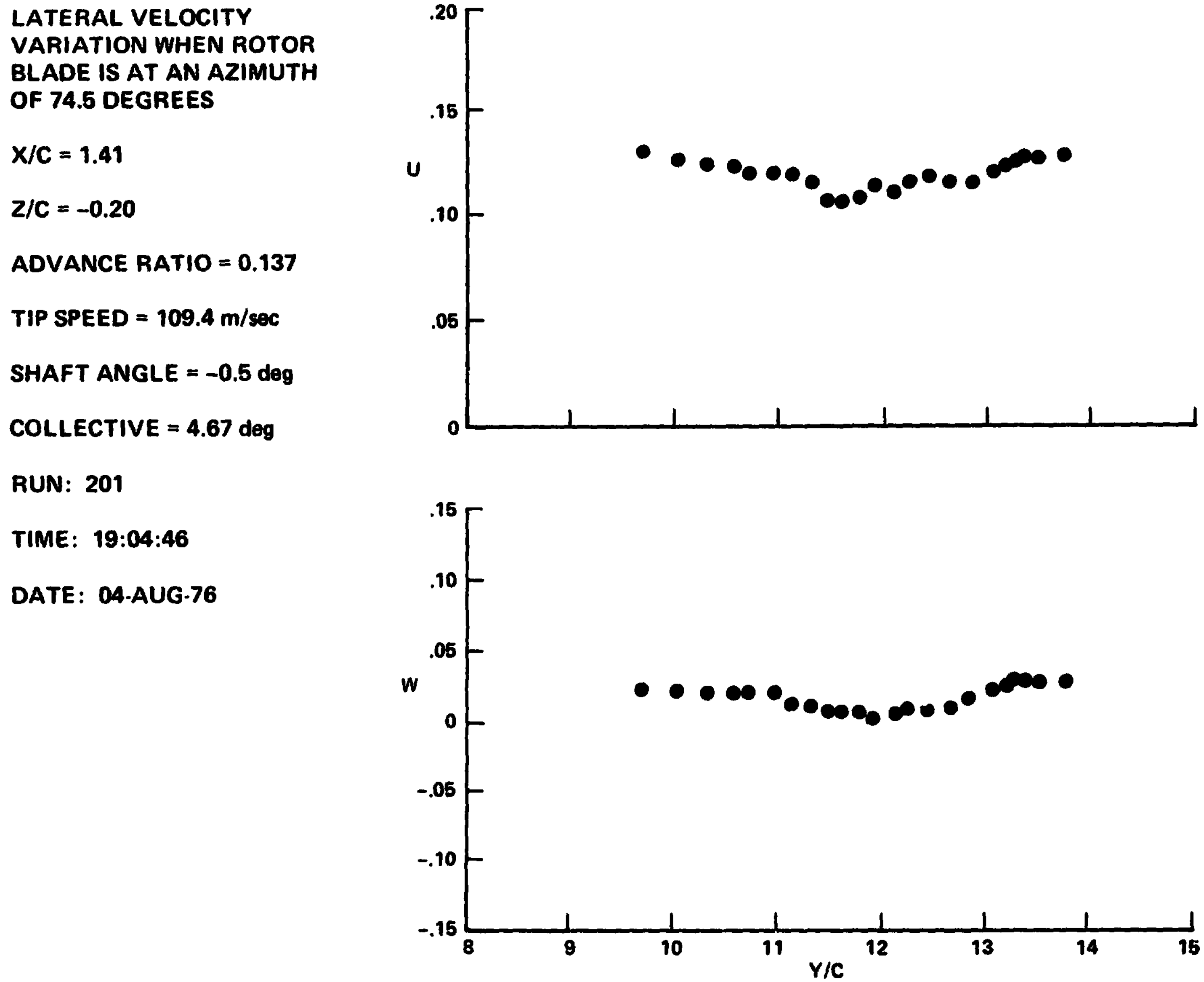

11-6. Lateral traverse, x/c = 1.41, z/c = –0.20

Figure 11. (Continued)

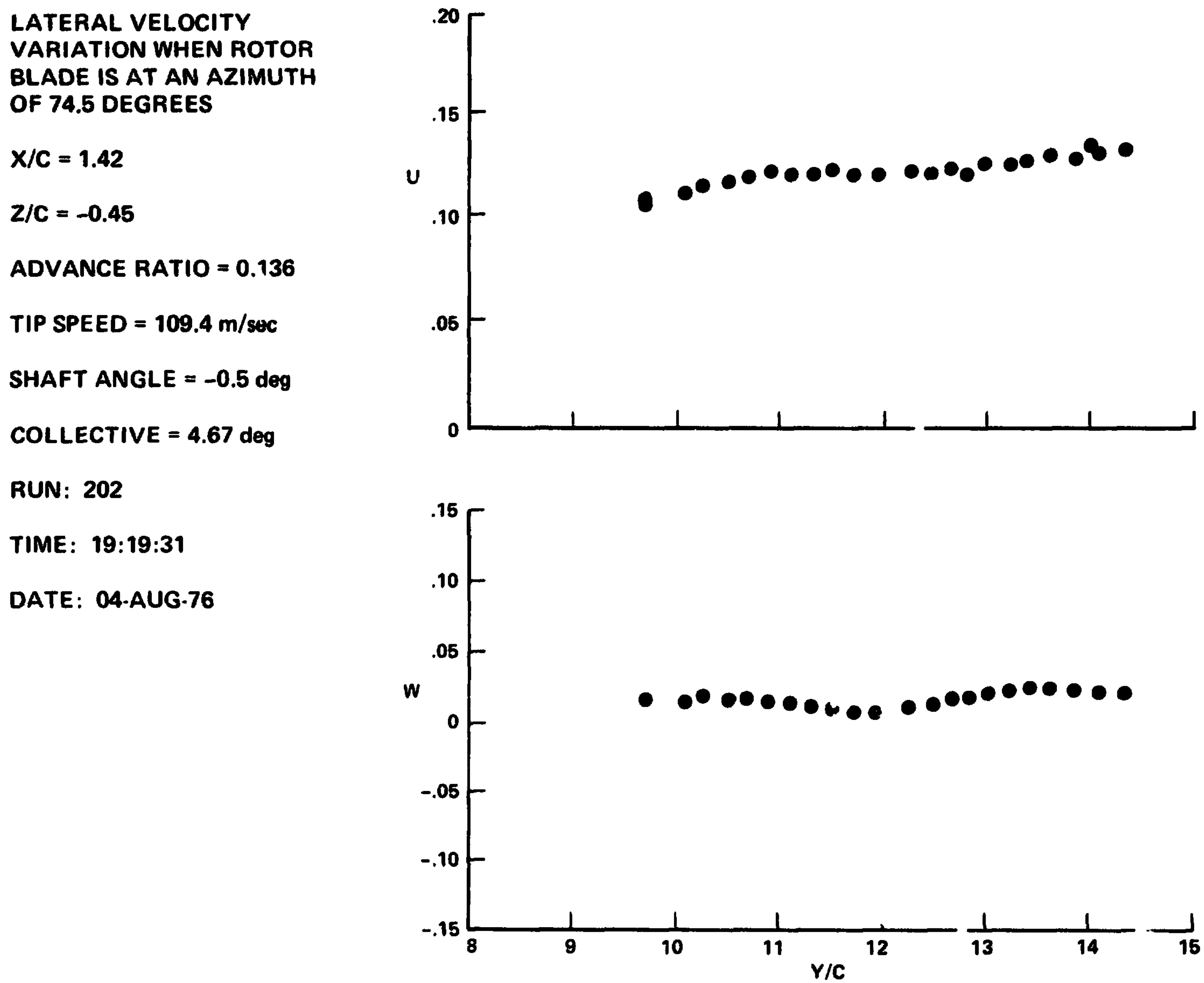

11-7. Lateral traverse, x/c = 1.42, z/c = -0.45

Figure 11. (Continued)

LATERAL VELOCITY VARIATION WHEN ROTOR BLADE IS AT AN AZIMUTH OF 74.5 DEGREES

X/C = 1.41

Z/C = -0.59

ADVANCE RATIO = 0.137

TIP SPEED = 109.4 m/sec

SHAFT ANGLE = -0.5 deg

COLLECTIVE = 4.67 deg

RUN: 203

TIME: 19:27:24

DATE: 04-AUG-76

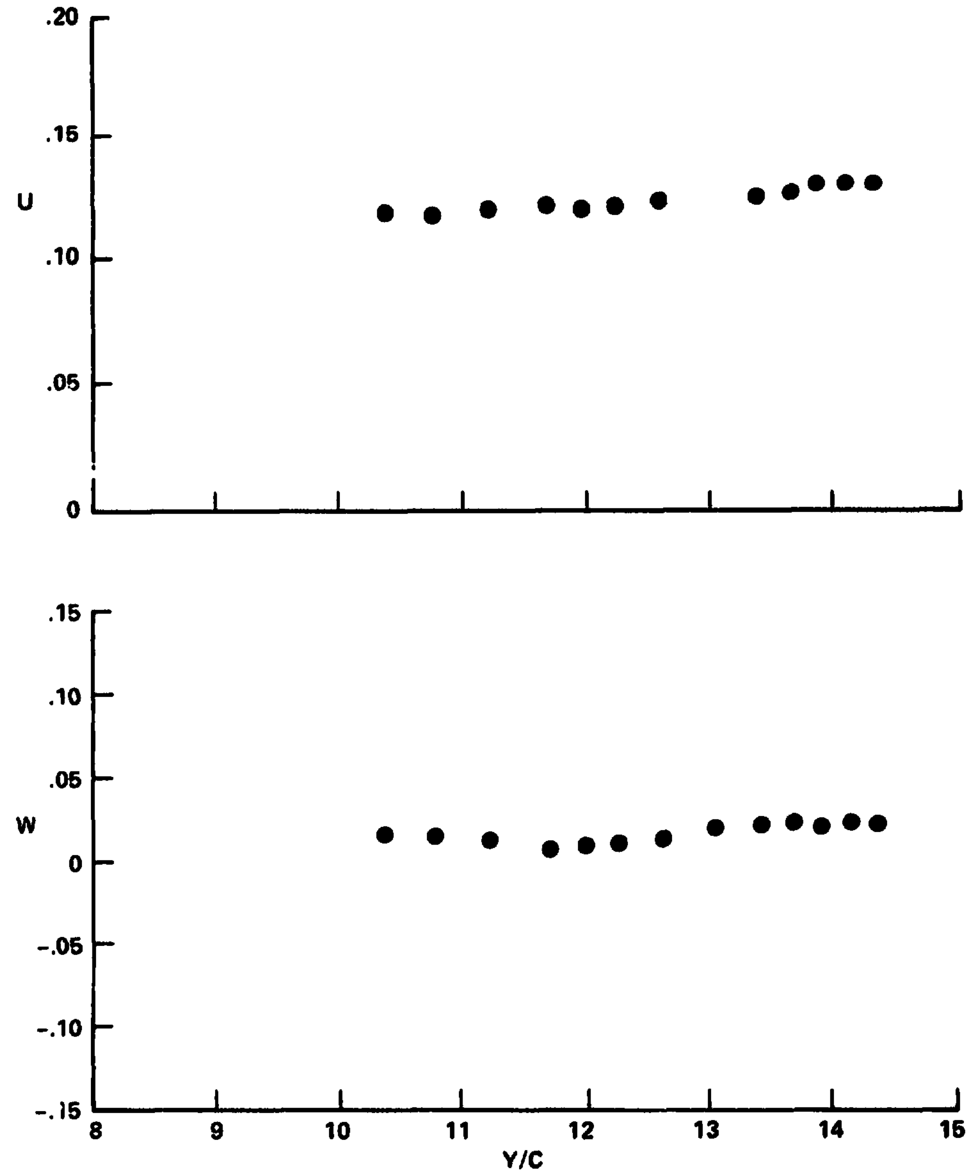

11-8. Lateral traverse, x/c = 1.41, z/c = -0.59

Figure 11. (Concluded)

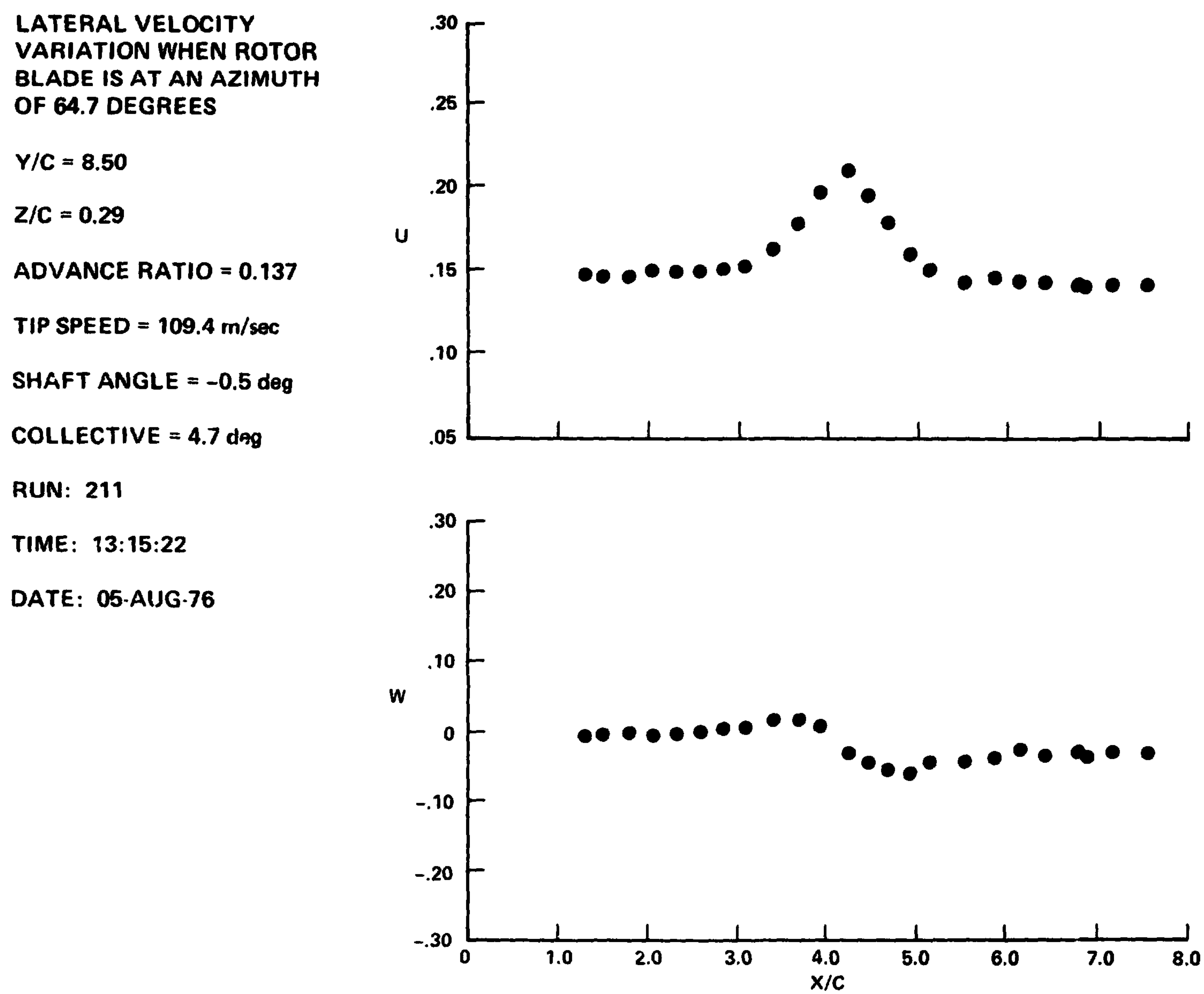

12-1. Streamwise traverse, y/c = 8.50, z/c = 0.29

Figure 12. Flowfield velocities from the -11° twist blades, $V/\Omega R = 0.137$, $\theta_{0.75R} = 4.67^{\circ}$, $\psi = 64.7^{\circ}$, $N = 1000$.

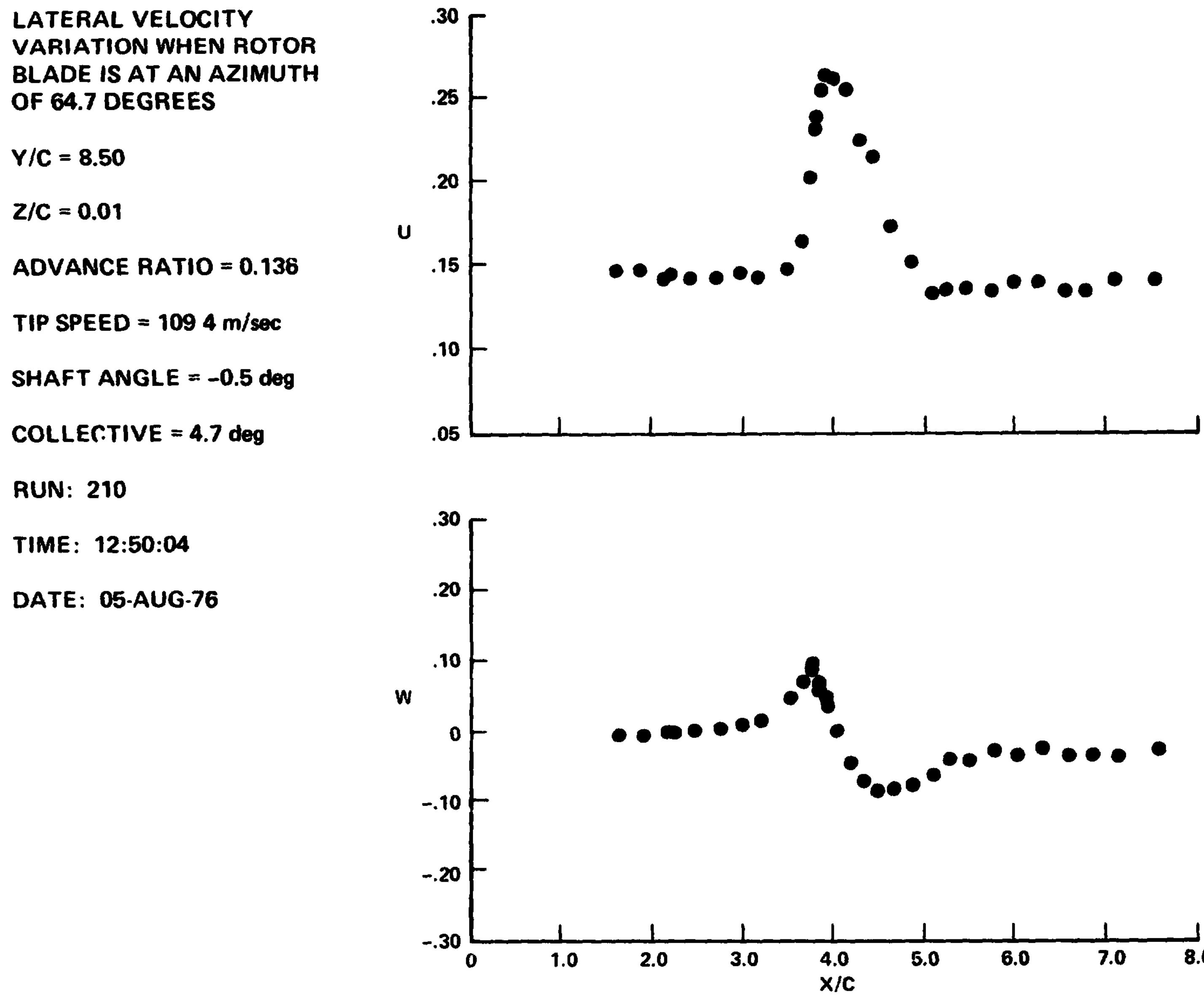

12-2. Streamwise traverse, y/c = 8.50, z/c = 0.01

Figure 12. (Continued)

LATERAL VELOCITY VARIATION WHEN ROTOR BLADE IS AT AN AZIMUTH OF 64.7 DEGREES

Y/C = 8.49

Z/C = -0.16

ADVANCE RATIO = 0.137

TIP SPEED = 109.4 m/sec

SHAFT ANGLE = -0.5 deg

COLLECTIVE = 4.7 deg

RUN: 212

TIME: 13:35:42

DATE: 05-AUG-76

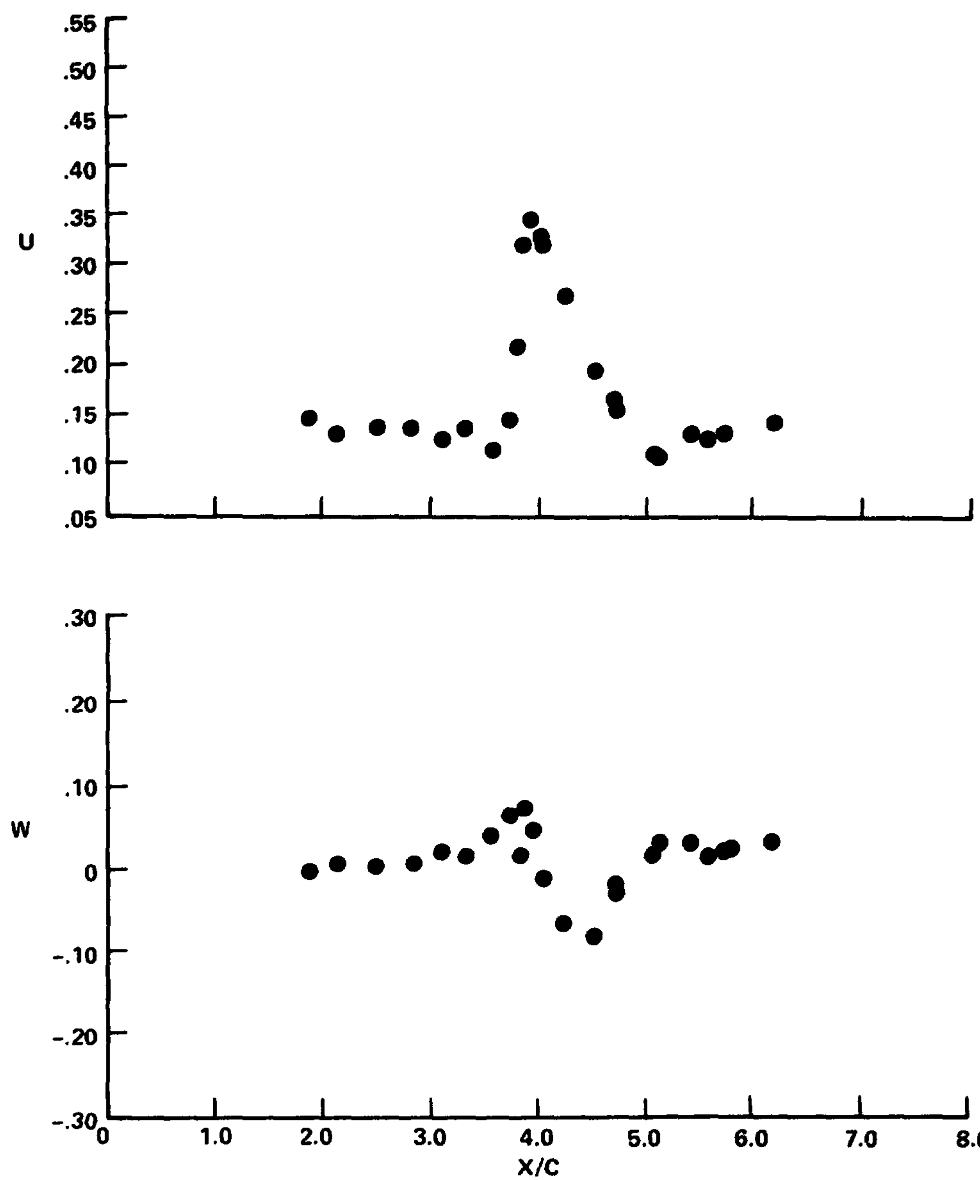

12-3. Streamwise traverse, y/c = 8.50, z/c = -0.16

Figure 12. (Continued)

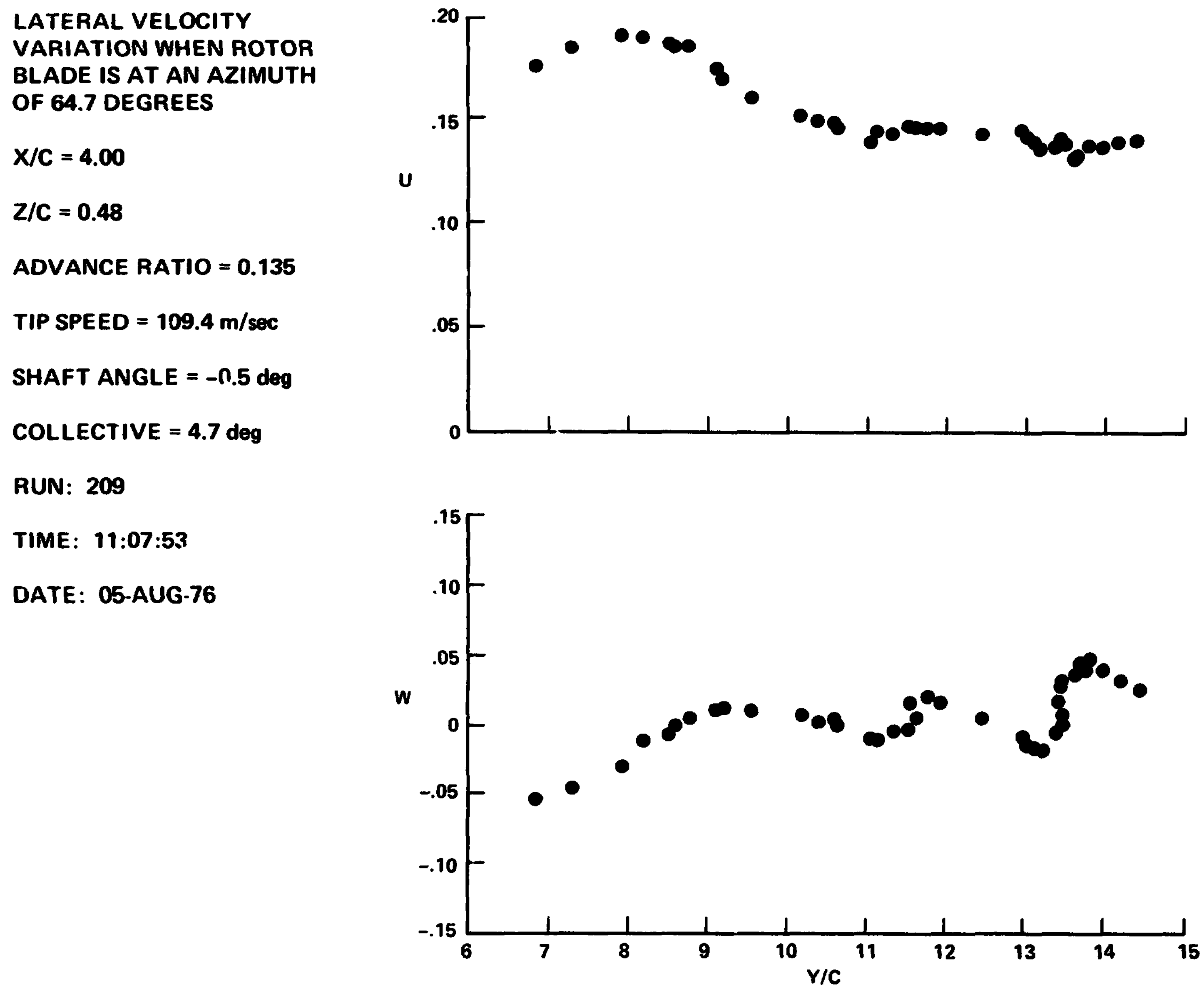

12-4. Lateral traverse, x/c = 4.00, z/c = 0.48

Figure 12. (Concluded)

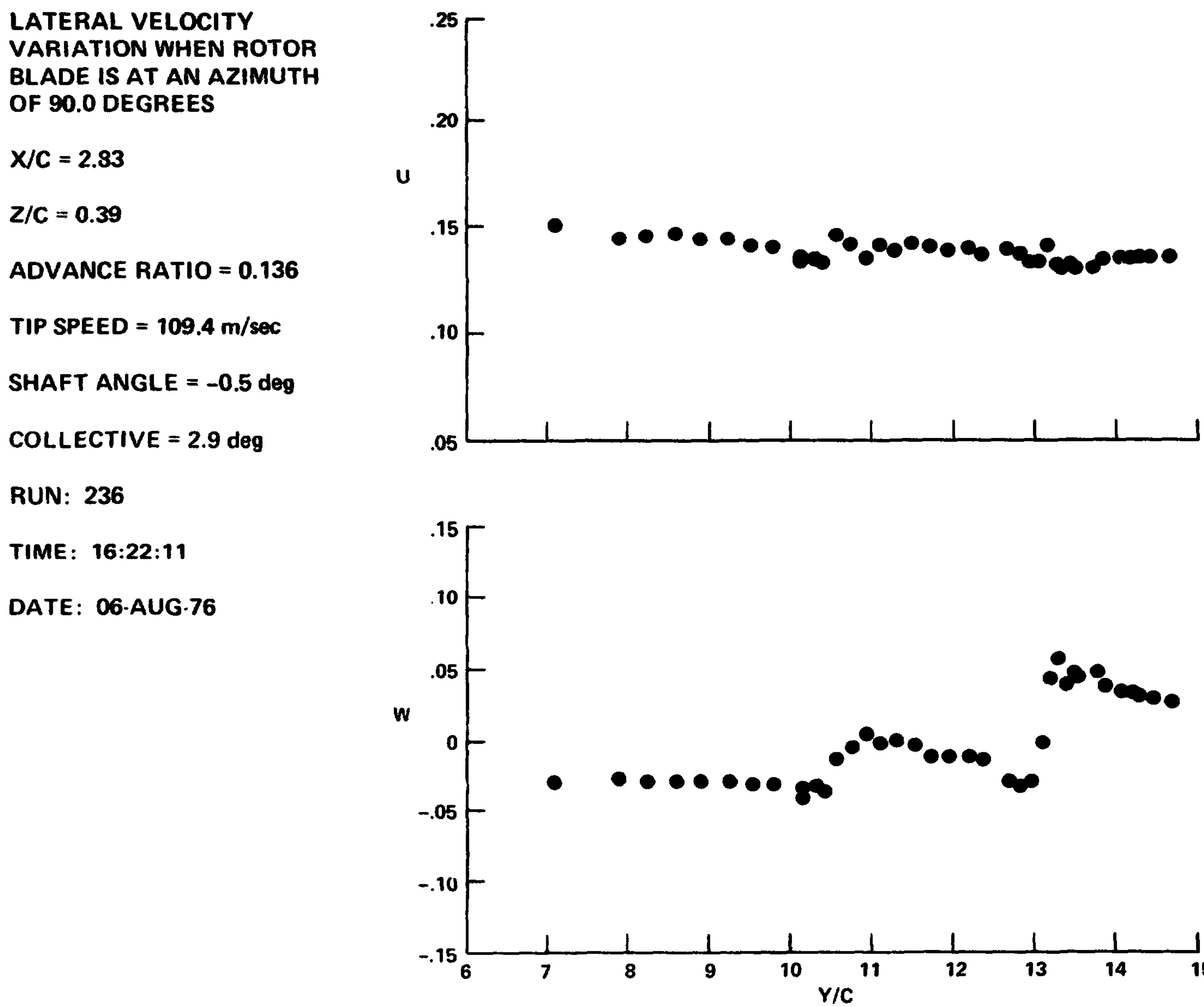

13-1. Lateral traverse, x/c = 2.83, z/c = 0.39

Figure 13. Flowfield velocities from the -11^{o} twist blades, $V/\Omega R = 0.137$, $\theta_{0.75R} = 2.97^{o}$, $\psi = 90^{o}$, N = 1000.

LATERAL VELOCITY VARIATION WHEN ROTOR BLADE IS AT AN AZIMUTH OF 90.0 DEGREES

X/C = 2.83

Z/C = 0.30

ADVANCE RATIO = 0.138

TIP SPEED = 109.4 m/sec

SHAFT ANGLE = –0.5 deg

COLLECTIVE = 2.9 deg

RUN: 235

TIME: 16:15:15

DATE: 06-AUG-76

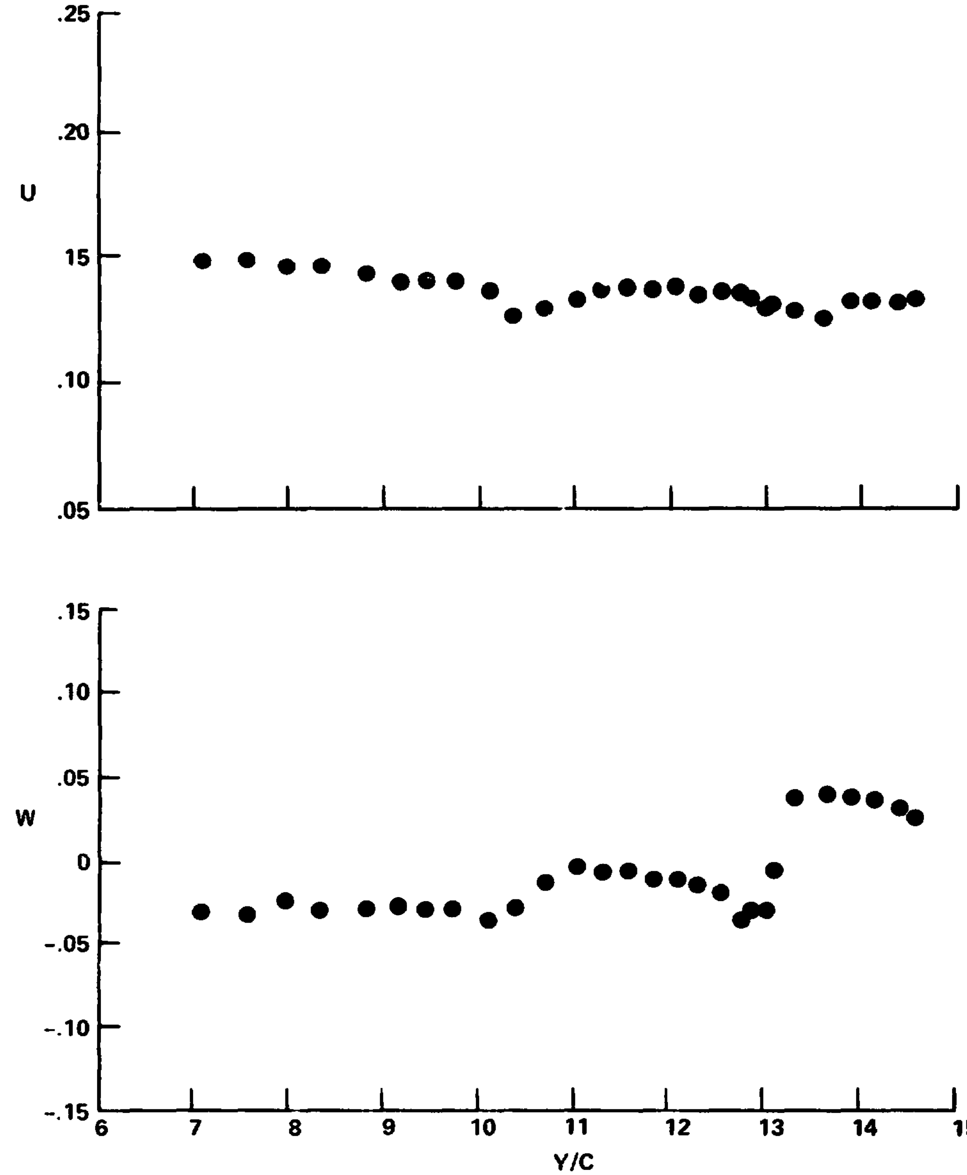

13-2. Lateral traverse, x/c = 2.83, z/c = 0.30

Figure 13. (Continued)

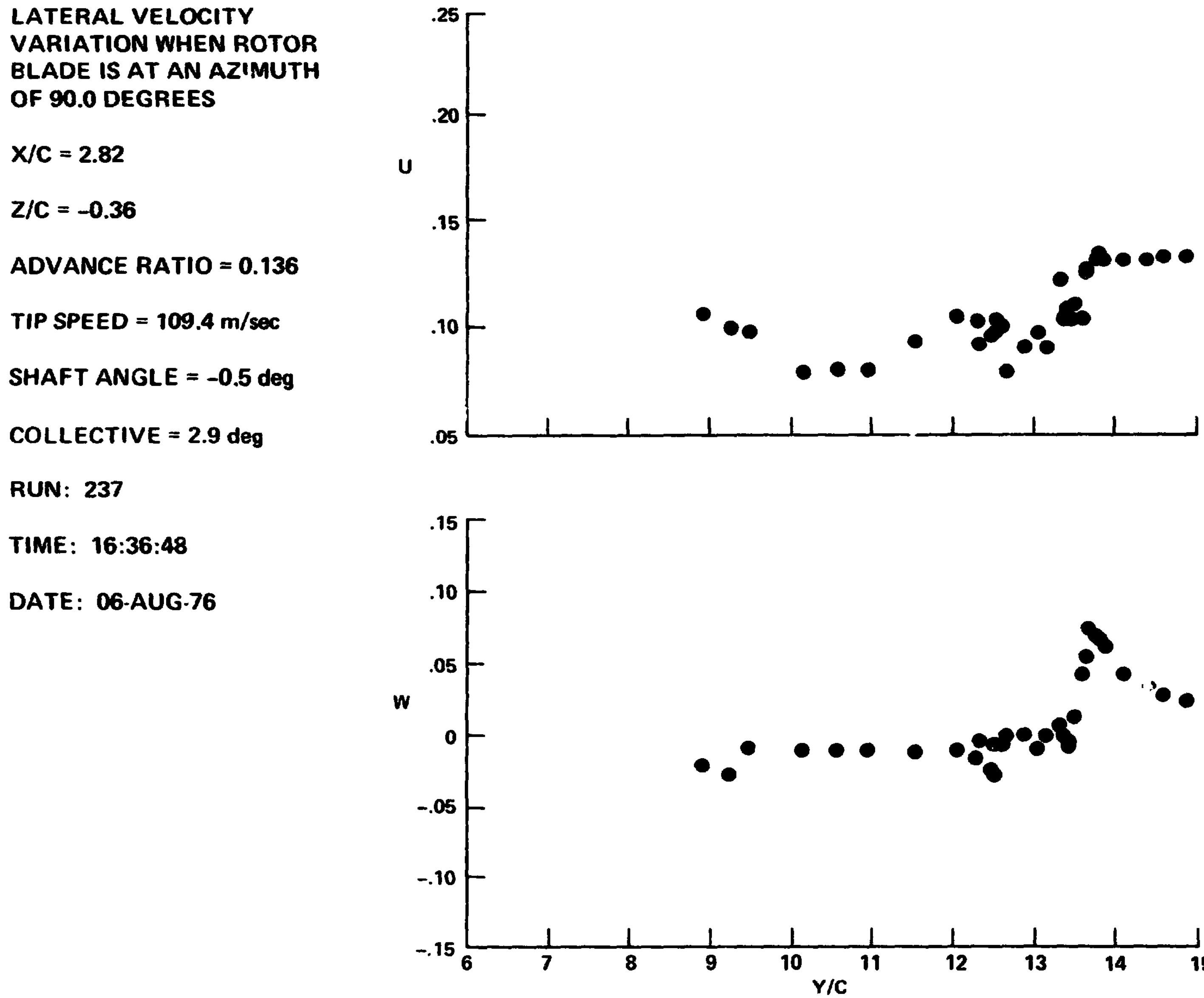

13-3. Lateral traverse, x/c = 2.83, z/c = -0.36

Figure 13. (Concluded)

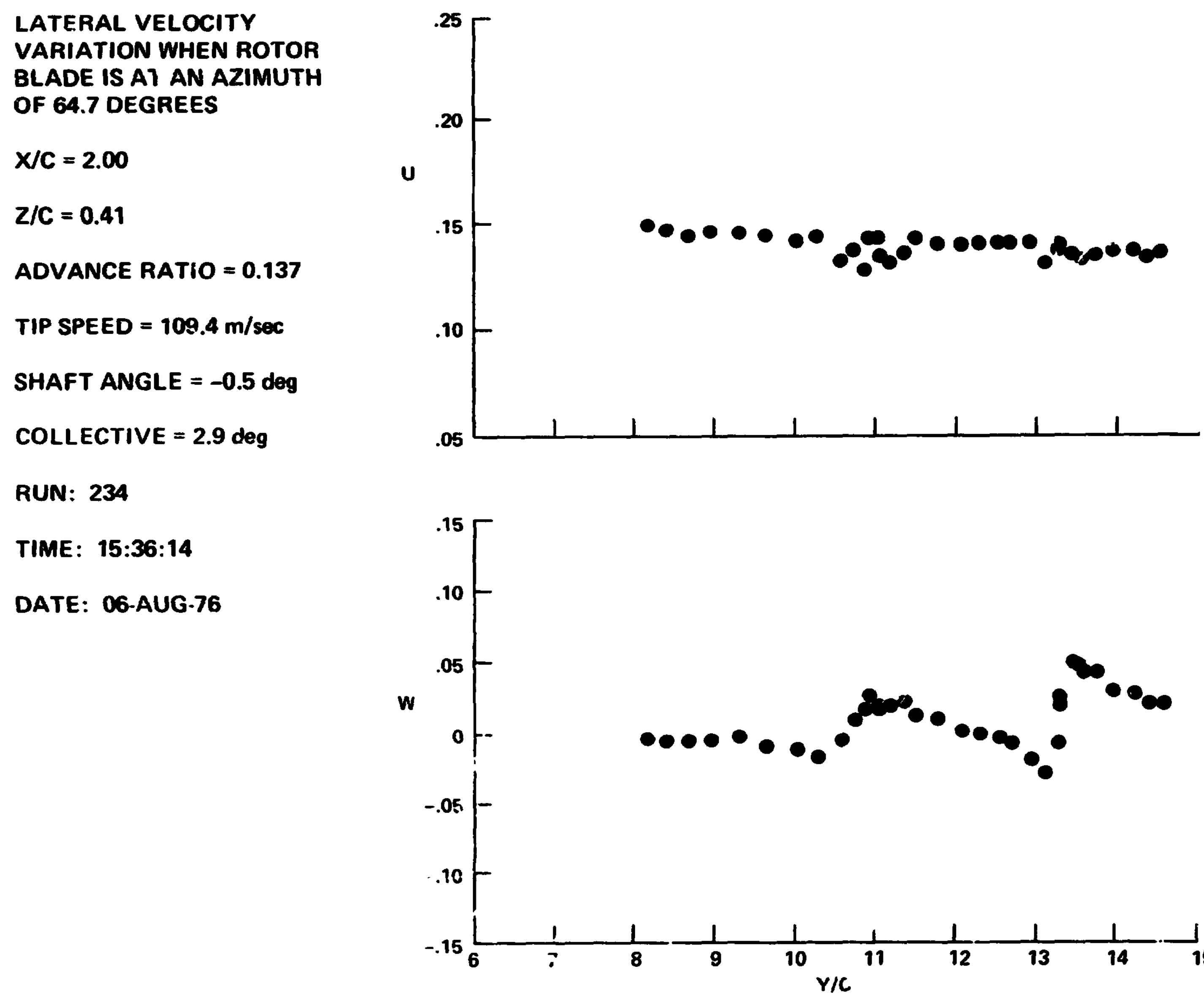

14-1. Lateral traverse, x/c = 2.00, z/c = 0.41

Figure 14. Flowfield velocities from the -11° twist blades, $V/\Omega R = 0.137$, $\theta_{0.75R} = 2.94^{\circ}$, $\psi = 64.7^{\circ}$, N = 1000.

LATERAL VELOCITY VARIATION WHEN ROTOR BLADE IS AT AN AZIMUTH OF 64.7 DEGREES

X/C = 2.00

Z/C = 0.34

ADVANCE RATIO = 0.138

TIP SPEED = 109.4 m/sec

SHAFT ANGLE = –0.5 deg

COLLECTIVE = 2.9 deg

RUN: 232

TIME: 15:13:28

DATE: 06-AUG-76

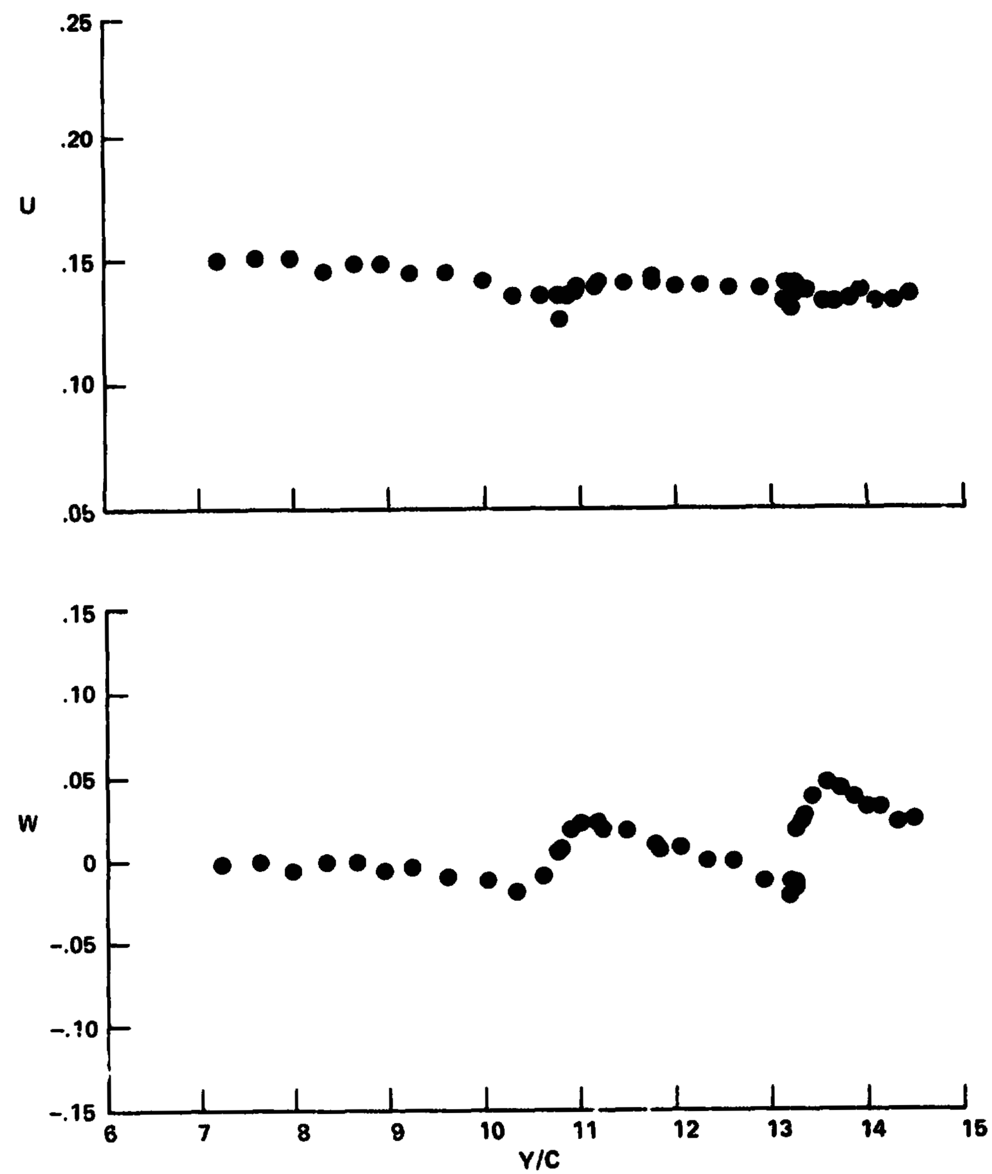

14-2. Lateral traverse, x/c = 2.00, z/c = 0.34

Figure 14. (Continued)

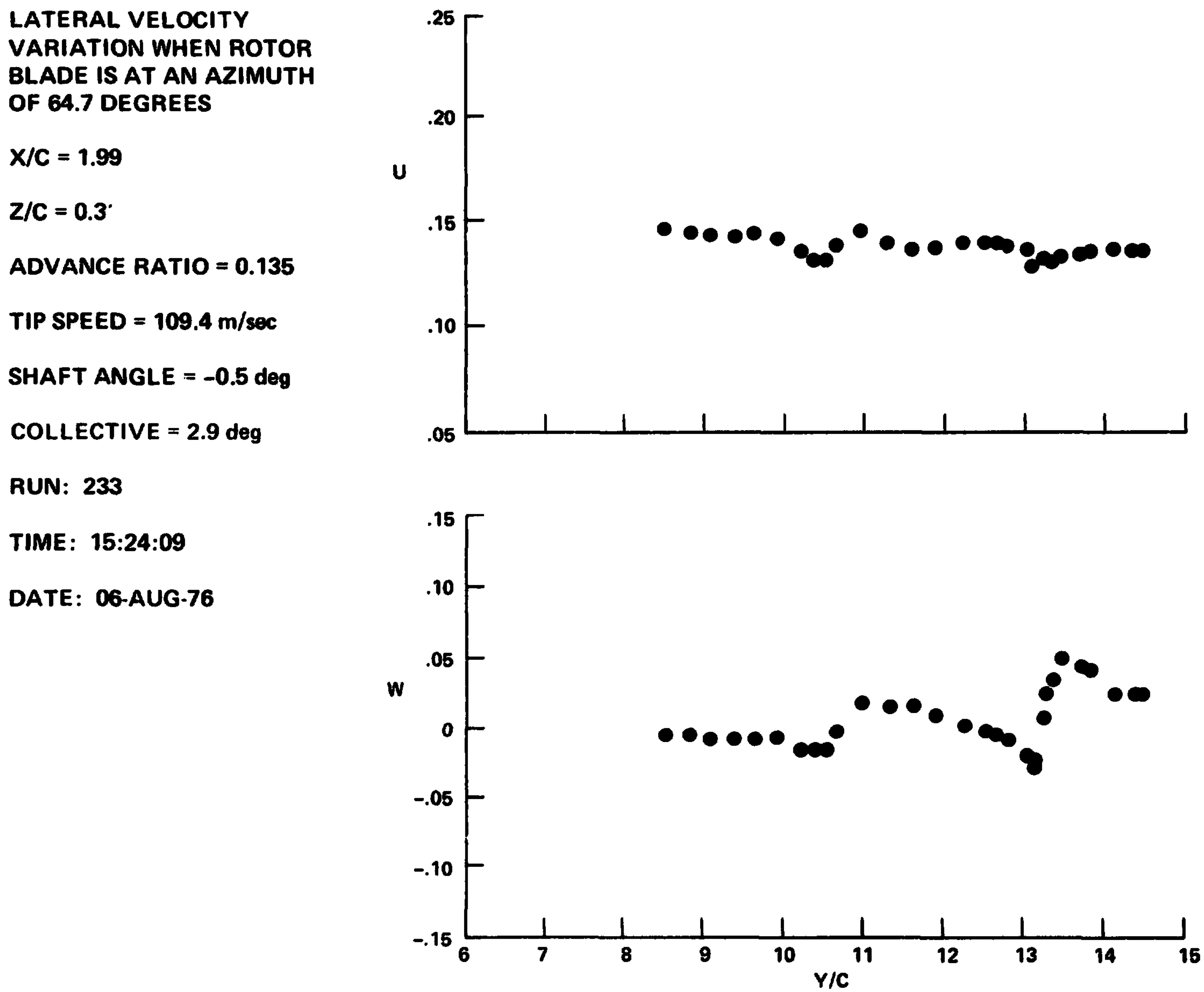

14-3. Lateral traverse, x/c = 2.00, z/c = 0.31

Figure 14. (Continued)

LATERAL VELOCITY
VARIATION WHEN ROTOR
BLADE IS AT AN AZIMUTH
OF 64.7 DEGREES

X/C = 4.00

Z/C = 0.51

ADVANCE RATIO = 0.137

TIP SPEED = 109.4 m/sec

SHAFT ANGLE = −0.5 deg

COLLECTIVE = 2.9 deg

RUN: 226

TIME: 18:39:05

DATE: 05-AUG-76

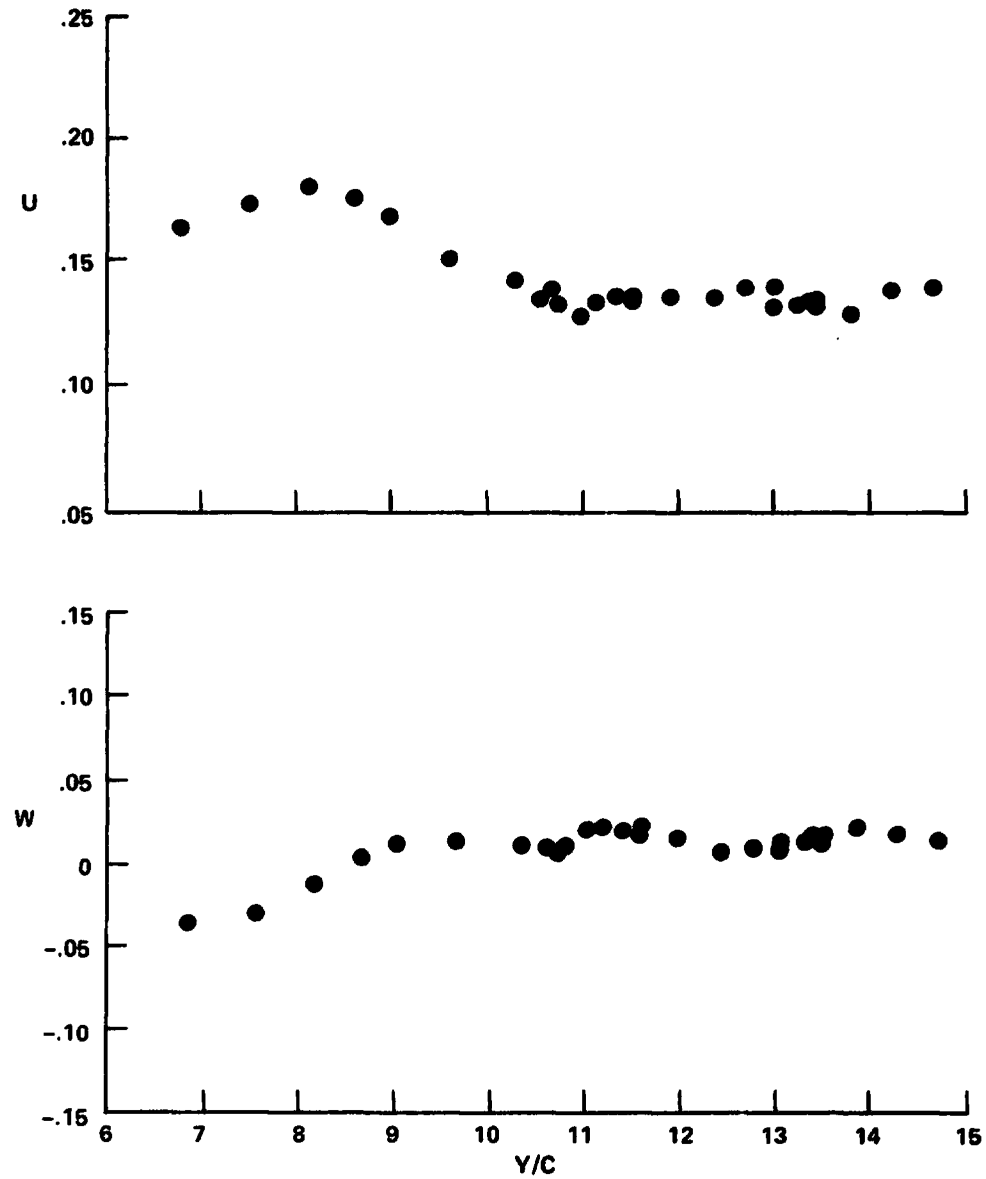

14-4. Lateral traverse, x/c = 4.00, z/c = 0.51

Figure 14. (Continued)

LATERAL VELOCITY VARIATION WHEN ROTOR BLADE IS AT AN AZIMUTH OF 64.7 DEGREES

X/C = 4.00

Z/C = 0.35

ADVANCE RATIO = 0.136

TIP SPEED = 109.4 m/sec

SHAFT ANGLE = -0.5 deg

COLLECTIVE = 2.9 deg

RUN: 228

TIME: 14:52:28

DATE: 06-AUG-76

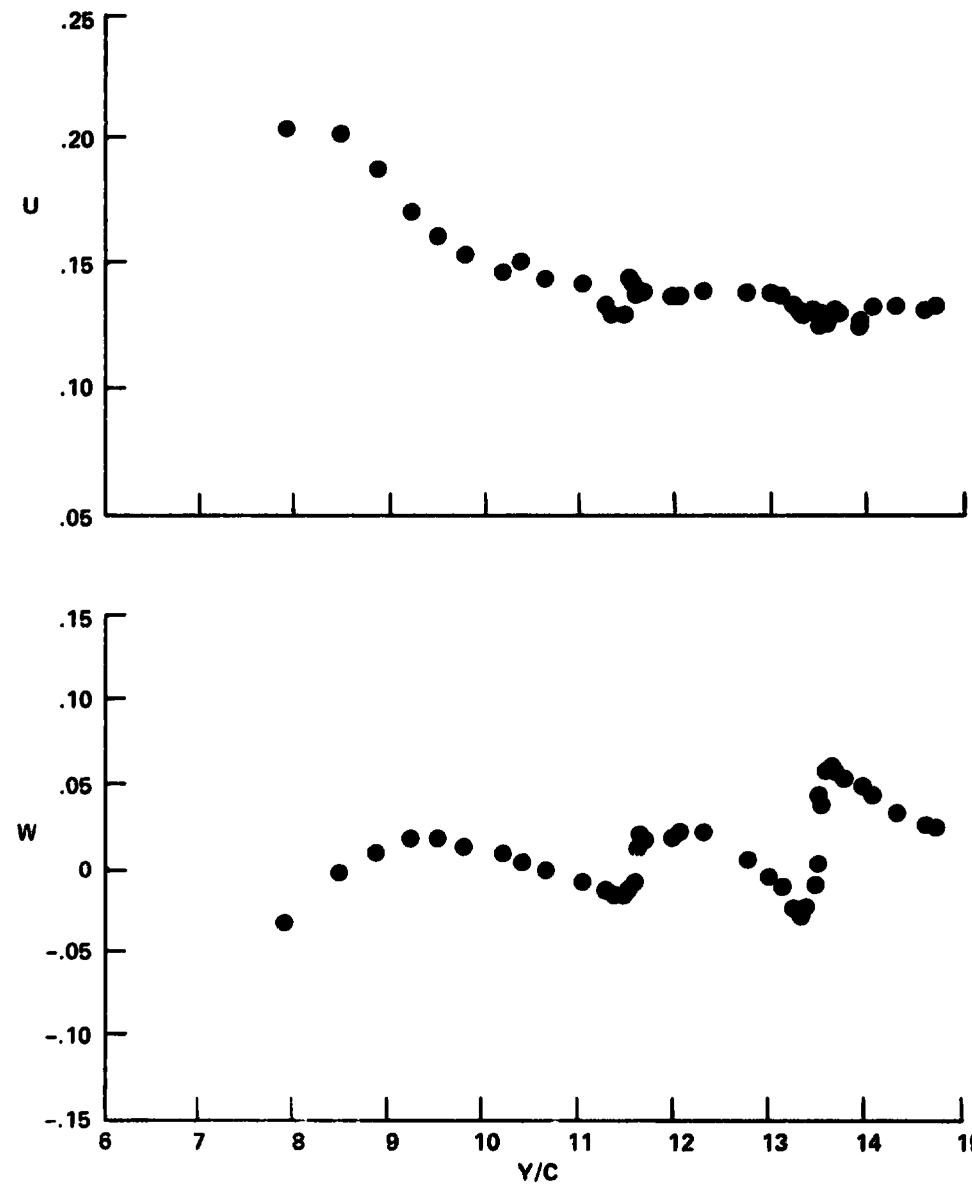

14-5. Lateral traverse, x/c = 4.00, z/c = 0.35

Figure 14. (Continued)

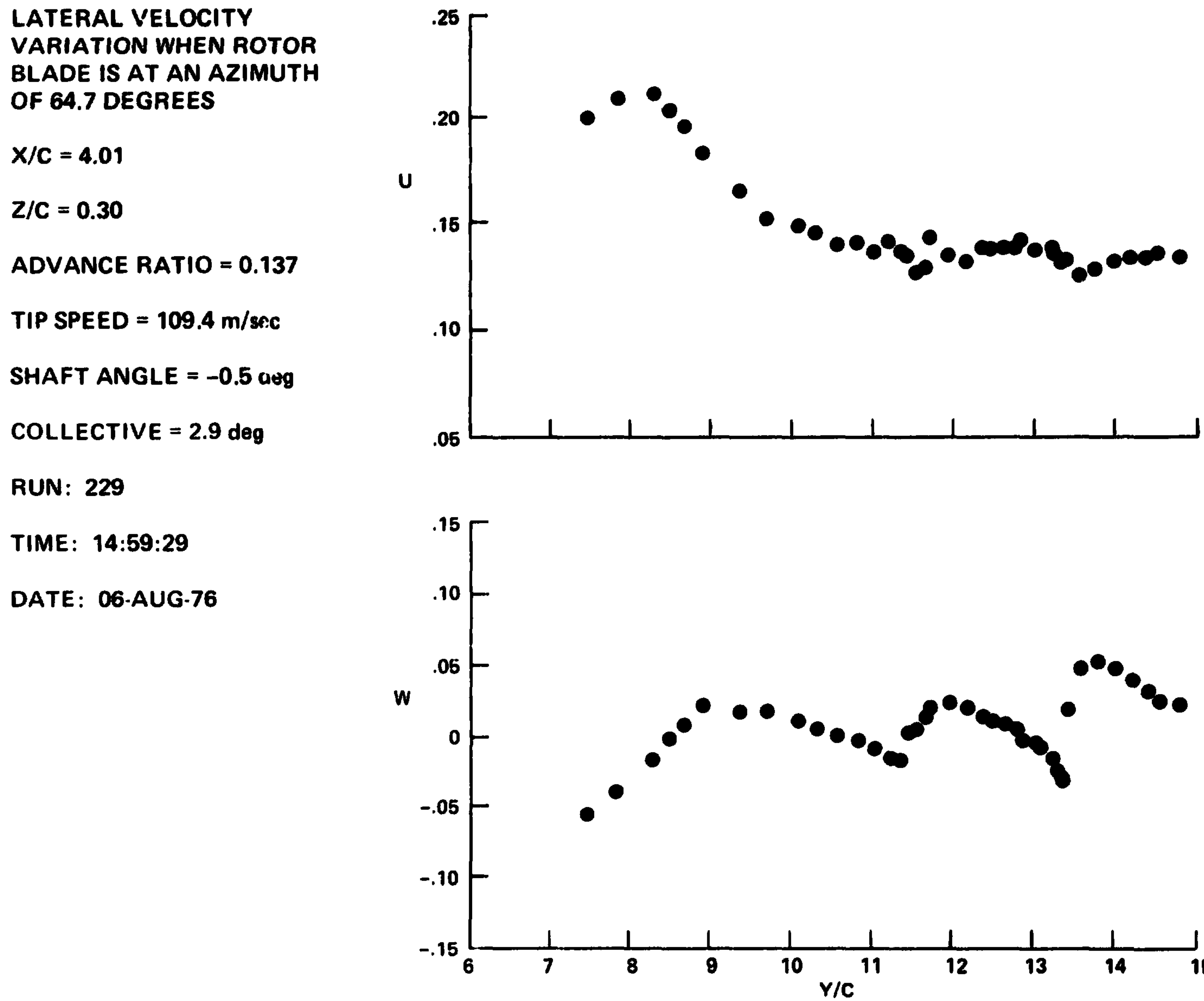

14-6. Lateral traverse, x/c = 4.00, z/c = 0.30

Figure 14. (Continued)

LATERAL VELOCITY VARIATION WHEN ROTOR BLADE IS AT AN AZIMUTH OF 64.7 DEGREES

X/C = 4.00

Z/C = 0.26

ADVANCE RATIO = 0.136

TIP SPEED = 109.4 m/sec

SHAFT ANGLE = -0.5 deg

COLLECTIVE = 2.9 deg

RUN: 230

TIME: 14:49:58

DATE: 06-AUG-76

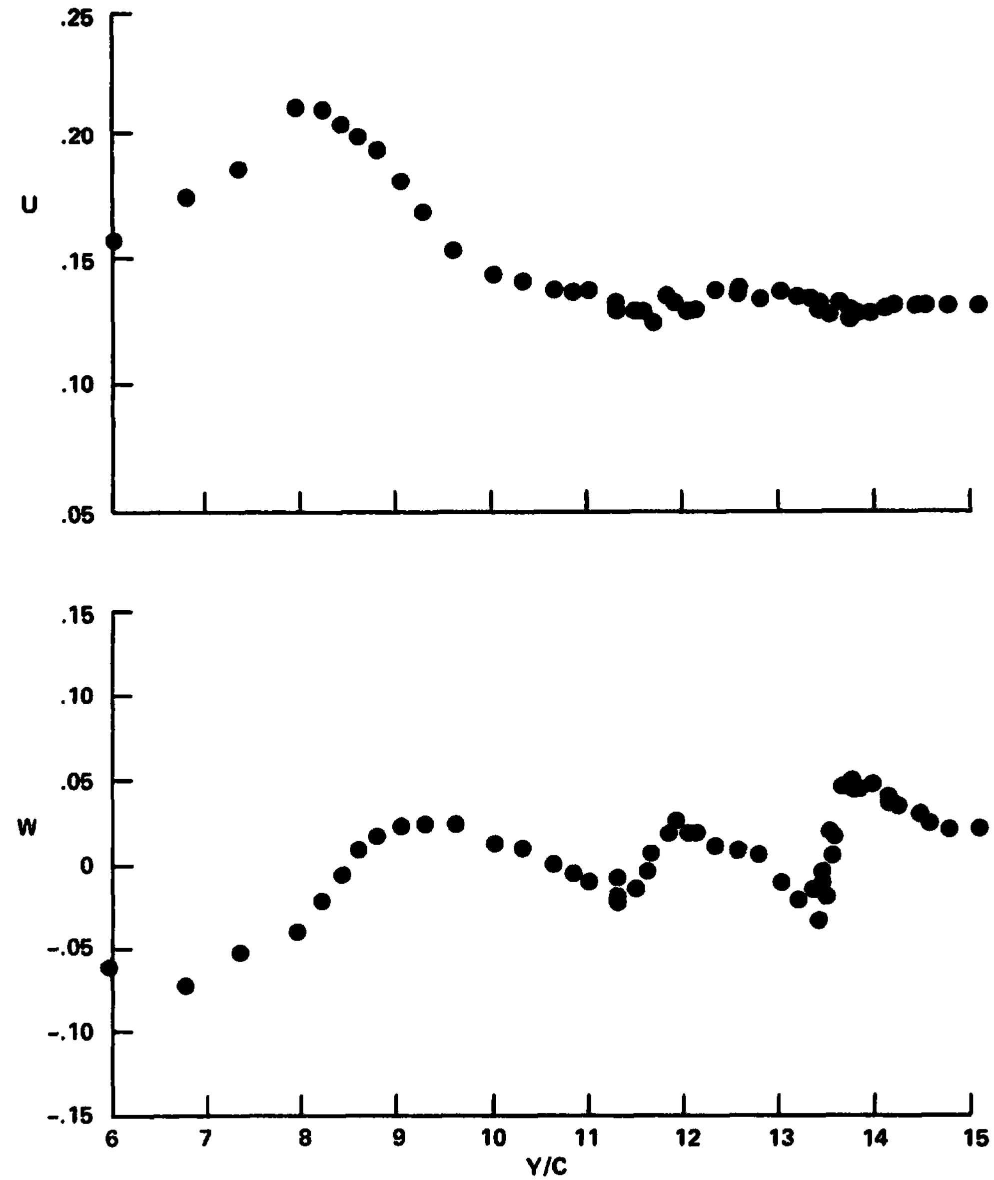

14-7. Lateral traverse, x/c = 4.00, z/c = 0.26

Figure 14. (Continued)

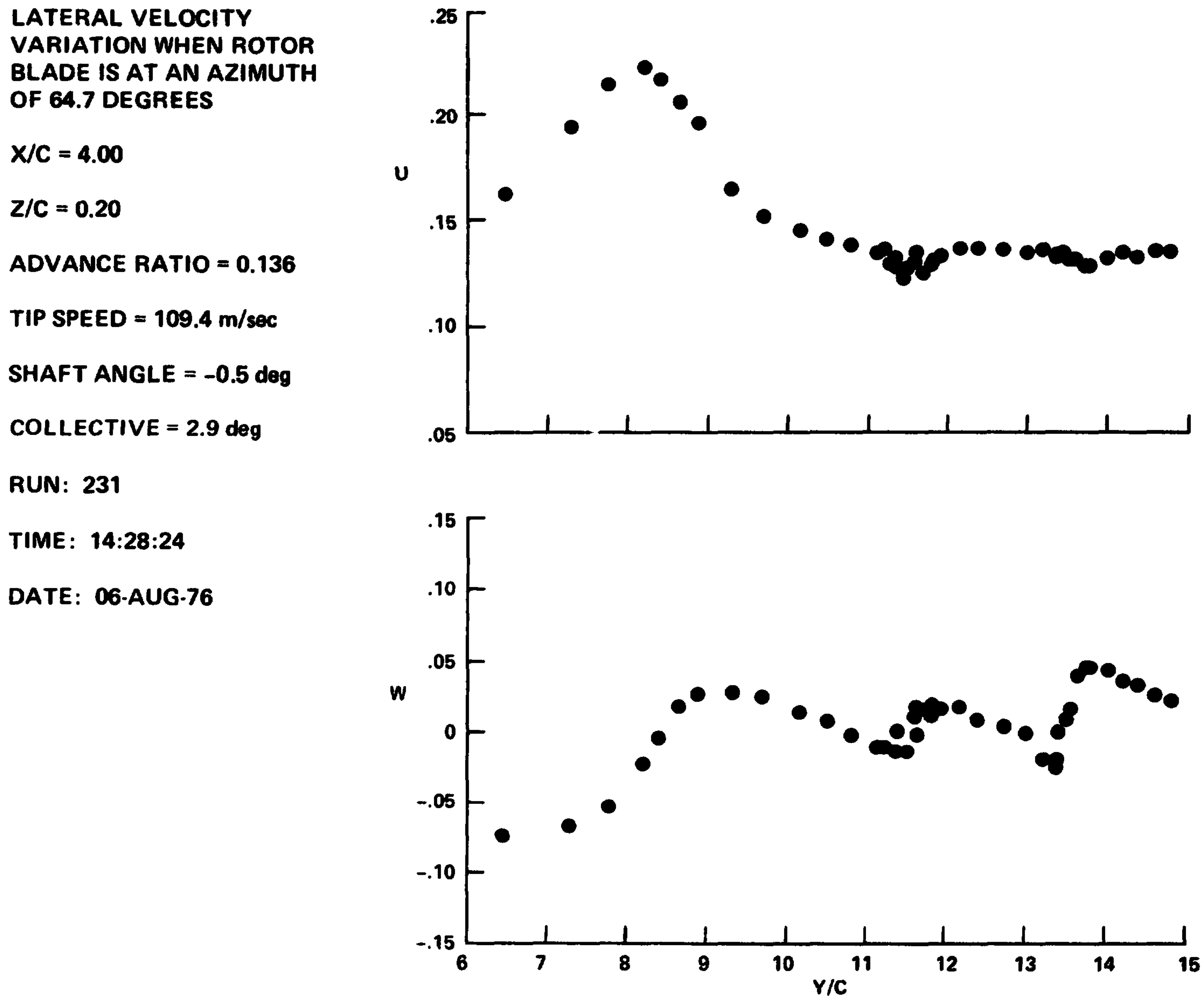

14-8. Lateral traverse, x/c = 4.00, z/c = 0.20

Figure 14. (Continued)

LATERAL VELOCITY VARIATION WHEN ROTOR BLADE IS AT AN AZIMUTH OF 64.7 DEGREES

X/C = 4.01

Z/C = –0.01

ADVANCE RATIO = 0.137

TIP SPEED = 109.4 m/sec

SHAFT ANGLE = –0.5 deg

COLLECTIVE = 2.9 deg

RUN: 227

TIME: 18:50:54

DATE: 05-AUG-76

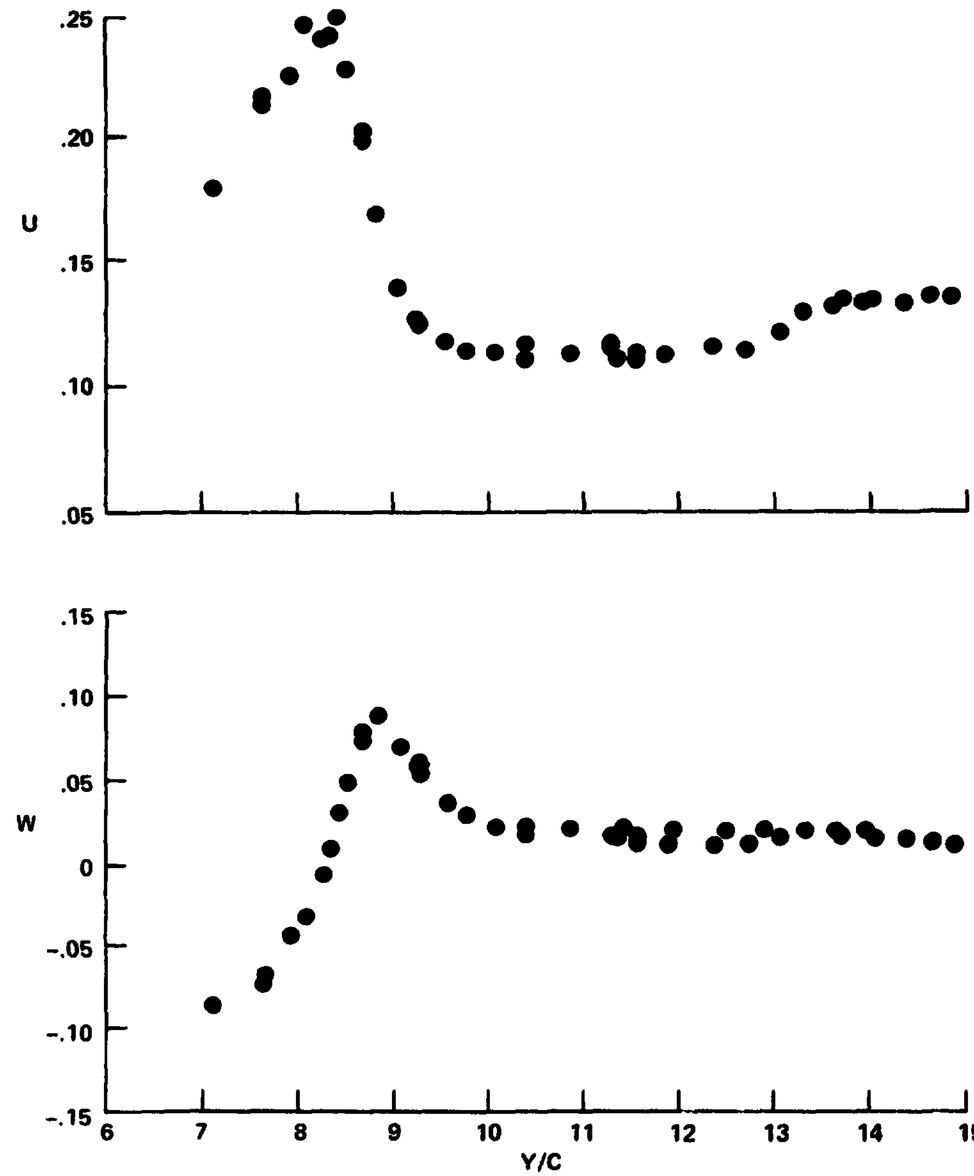

14-9. Lateral traverse, x/c = 4.00, z/c = -0.01

Figure 14. (Concluded)

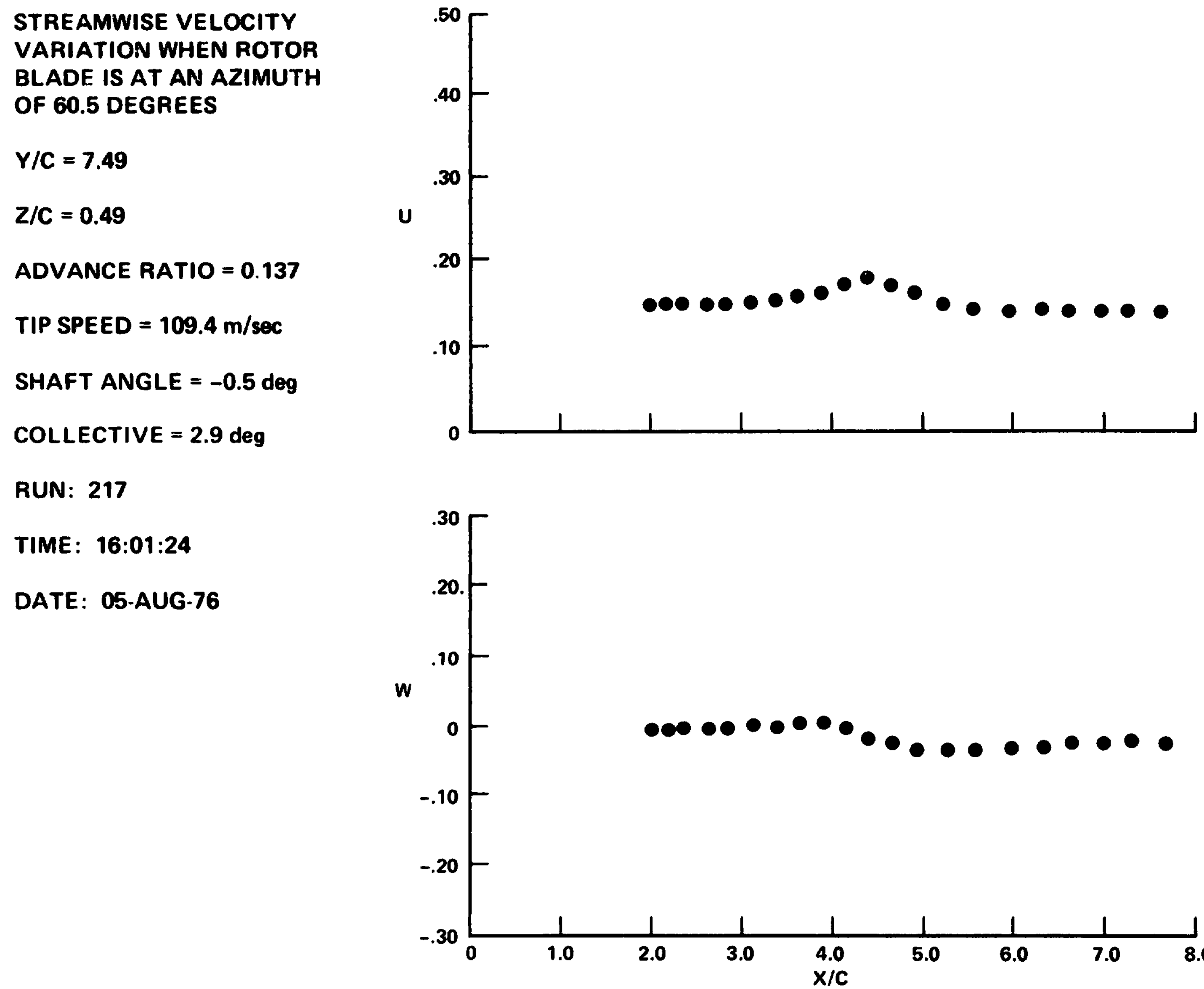

15-1. Streamwise traverse, y/c = 7.50, z/c = 0.49

Figure 15. Flowfield velocities from the -11° twist blades, $V/\Omega R = 0.137$, $\theta_{0.75R} = 2.94^\circ$, $\psi = 60.5^\circ$, N = 1000.

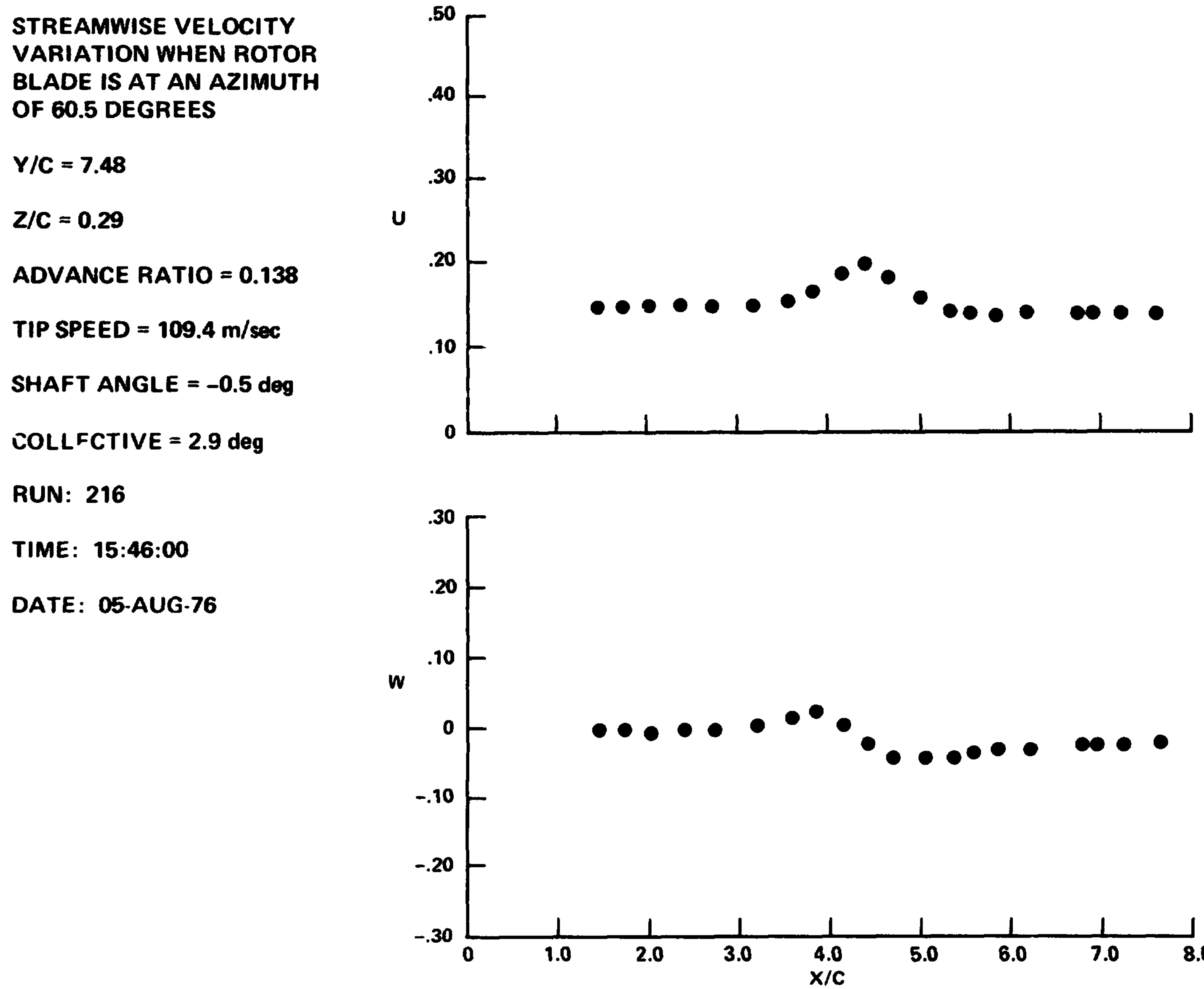

15-2. Streamwise traverse, y/c = 7.50, z/c = 0.29

Figure 15. (Continued)

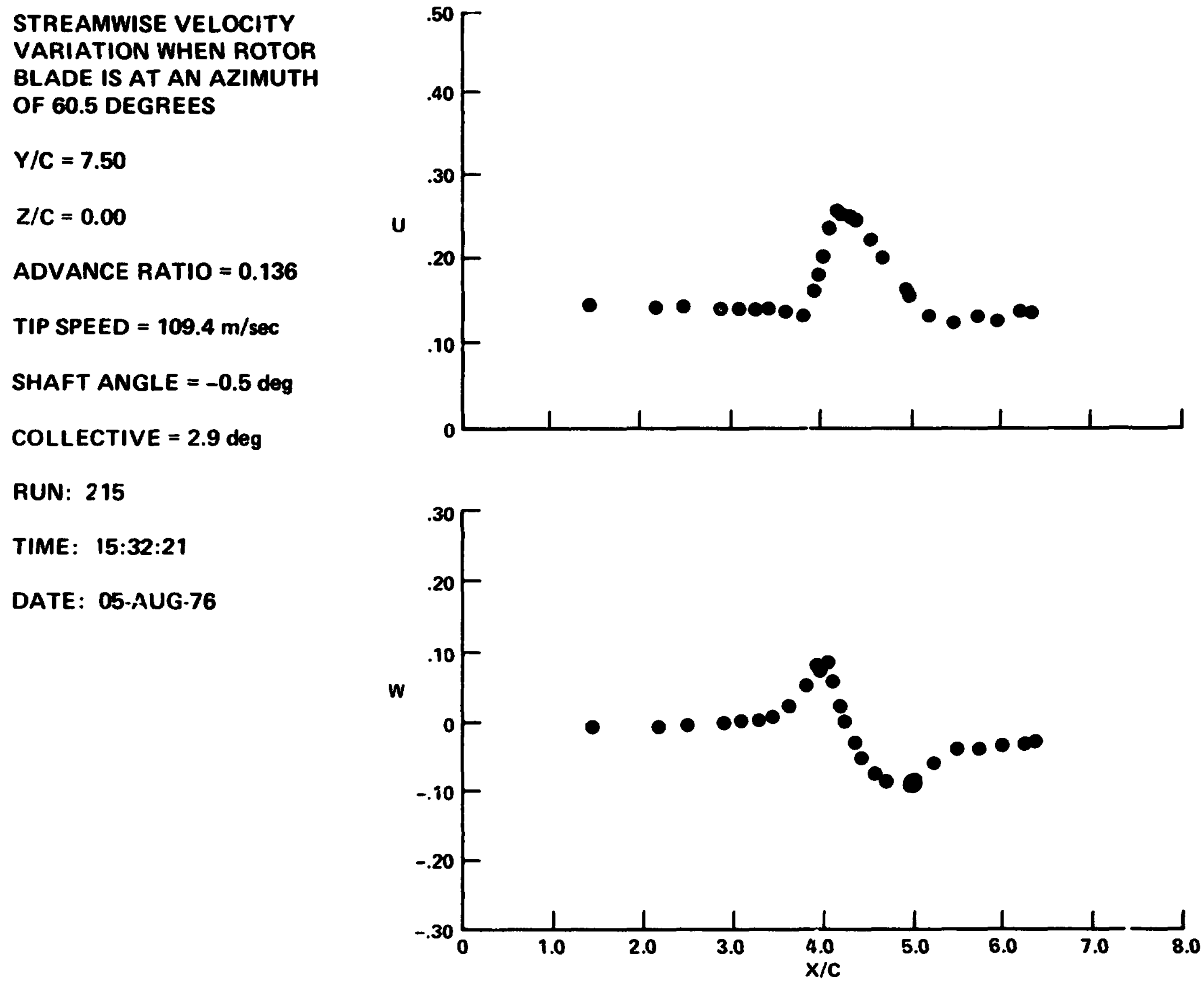

15-3. Streamwise traverse, y/c = 7.50, z/c = 0.00

Figure 15. (Continued)

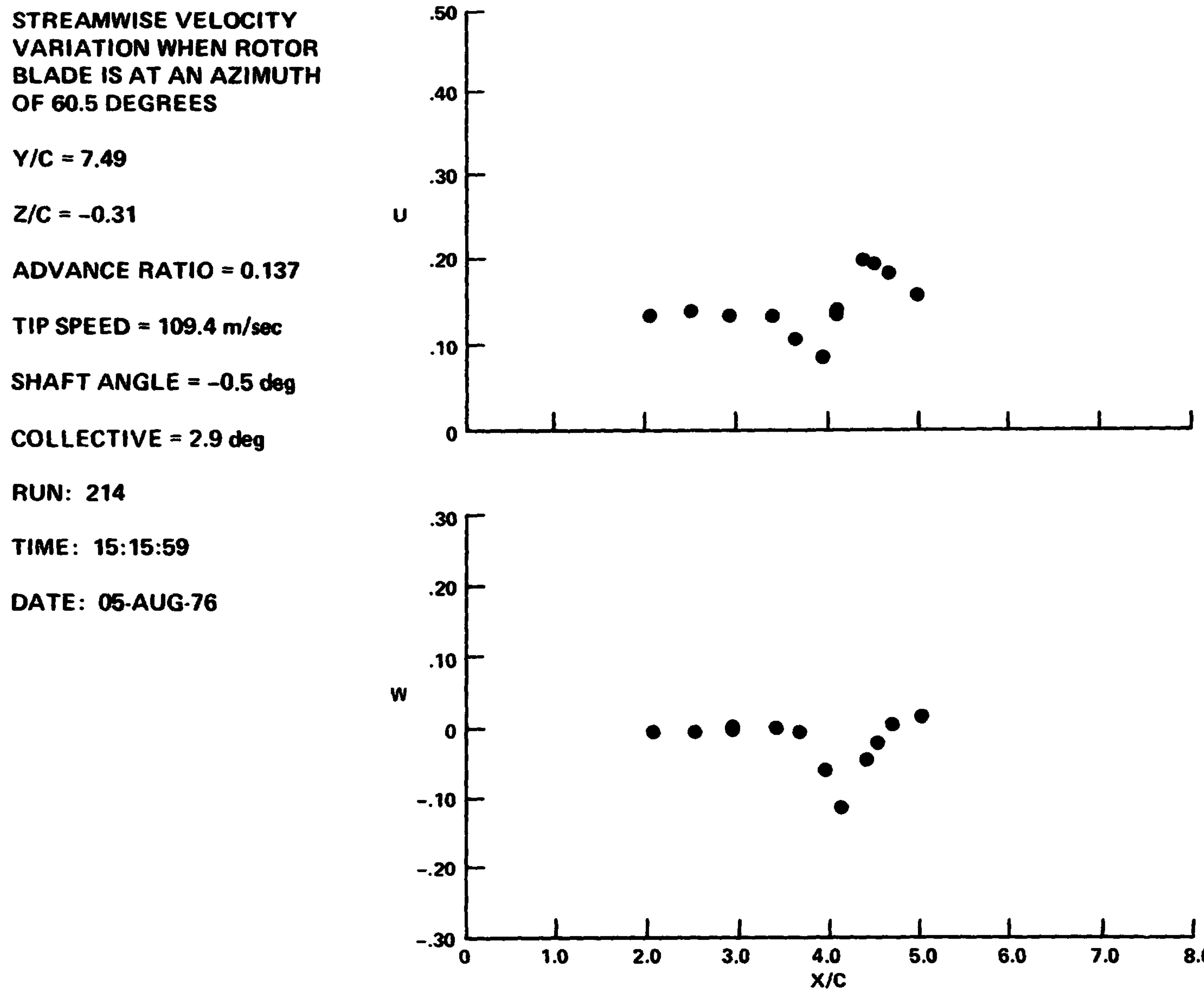

15-4. Streamwise traverse, y/c = 7.50, z/c = -0.31

Figure 15. (Continued)

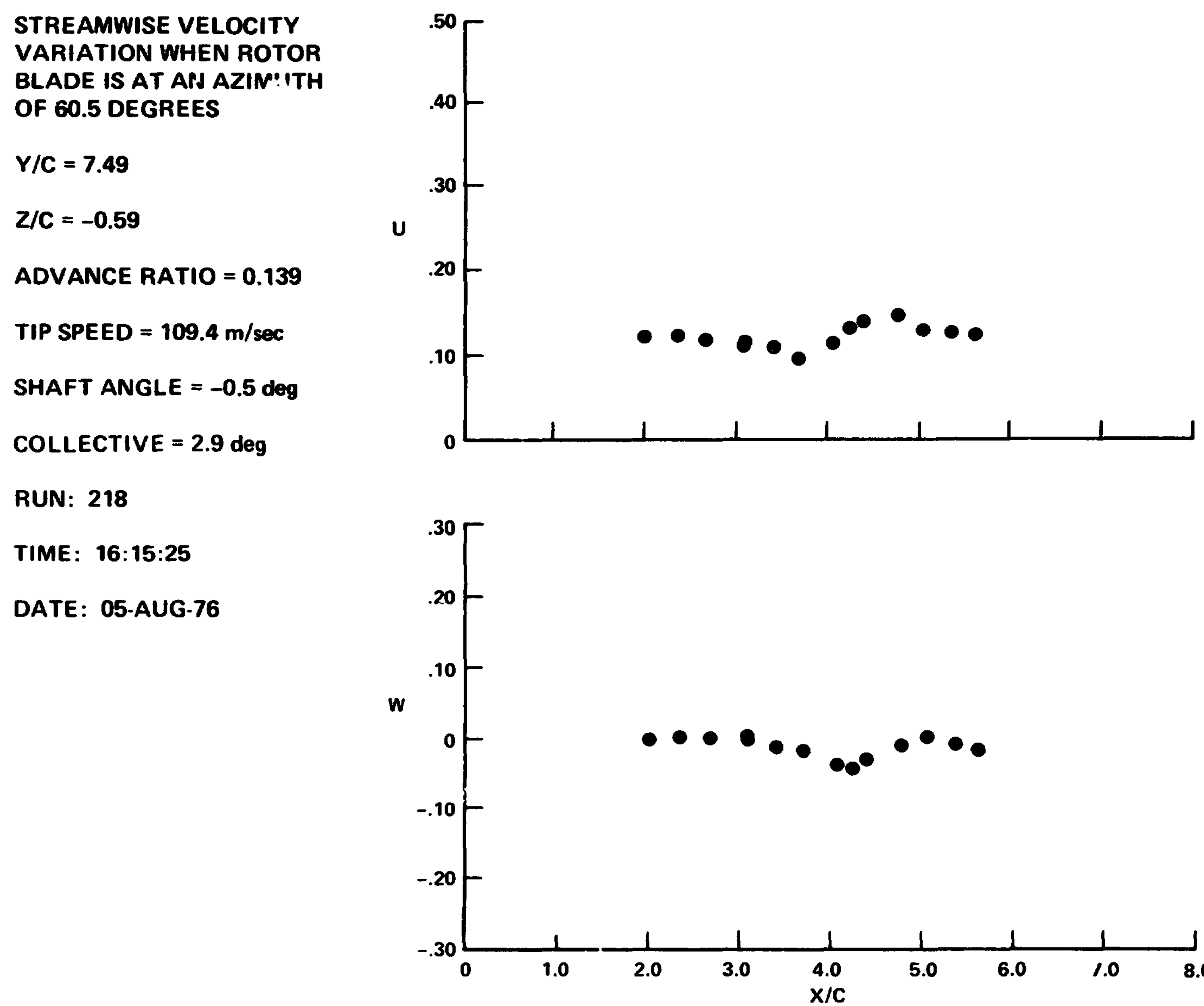

15-5. Streamwise traverse, y/c = 7.50, z/c = –0.59

Figure 15. (Continued)

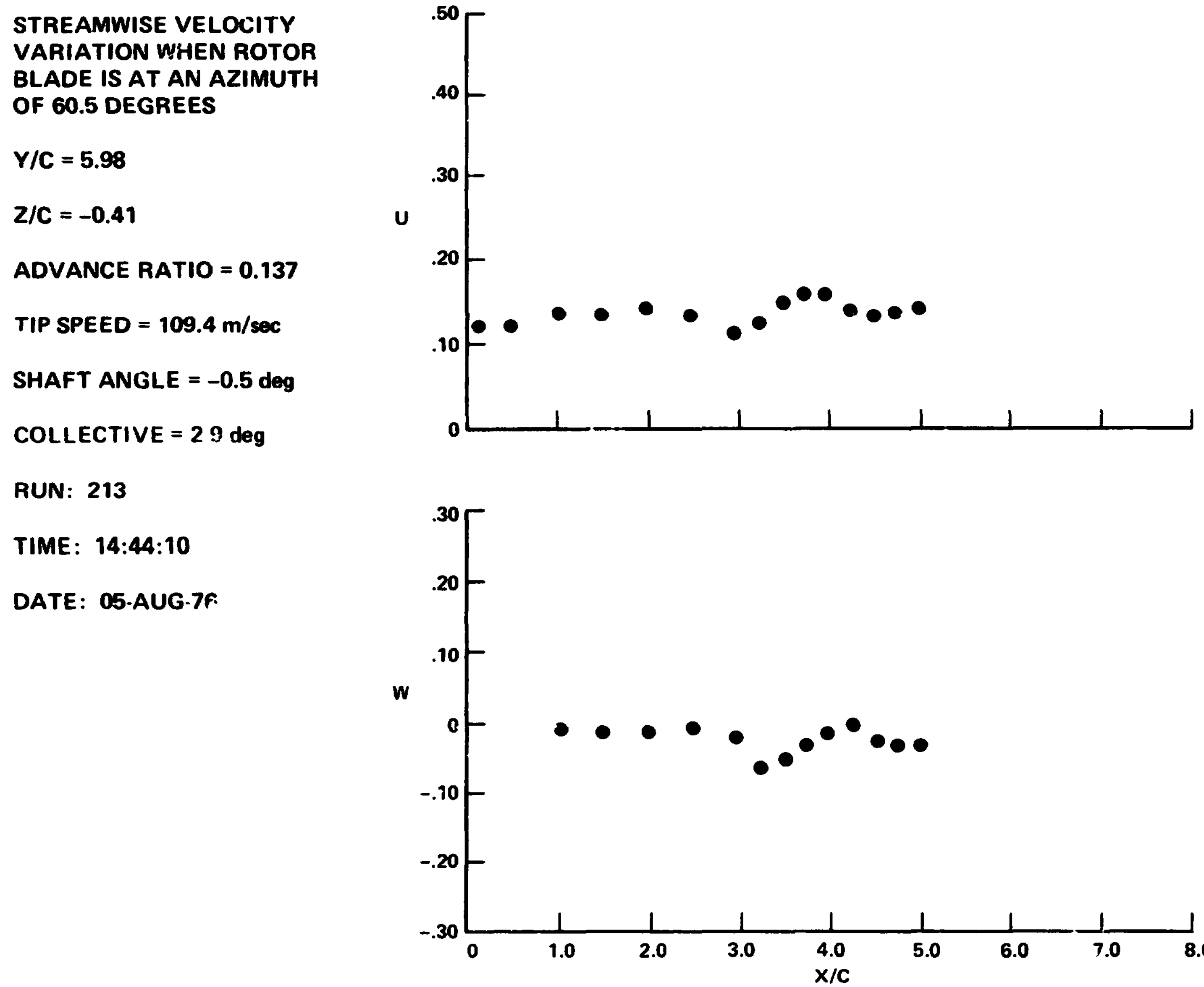

15-6. Streamwise traverse, $y/c = 7.50$, $z/c = -0.79$

Figure 15. (Continued)

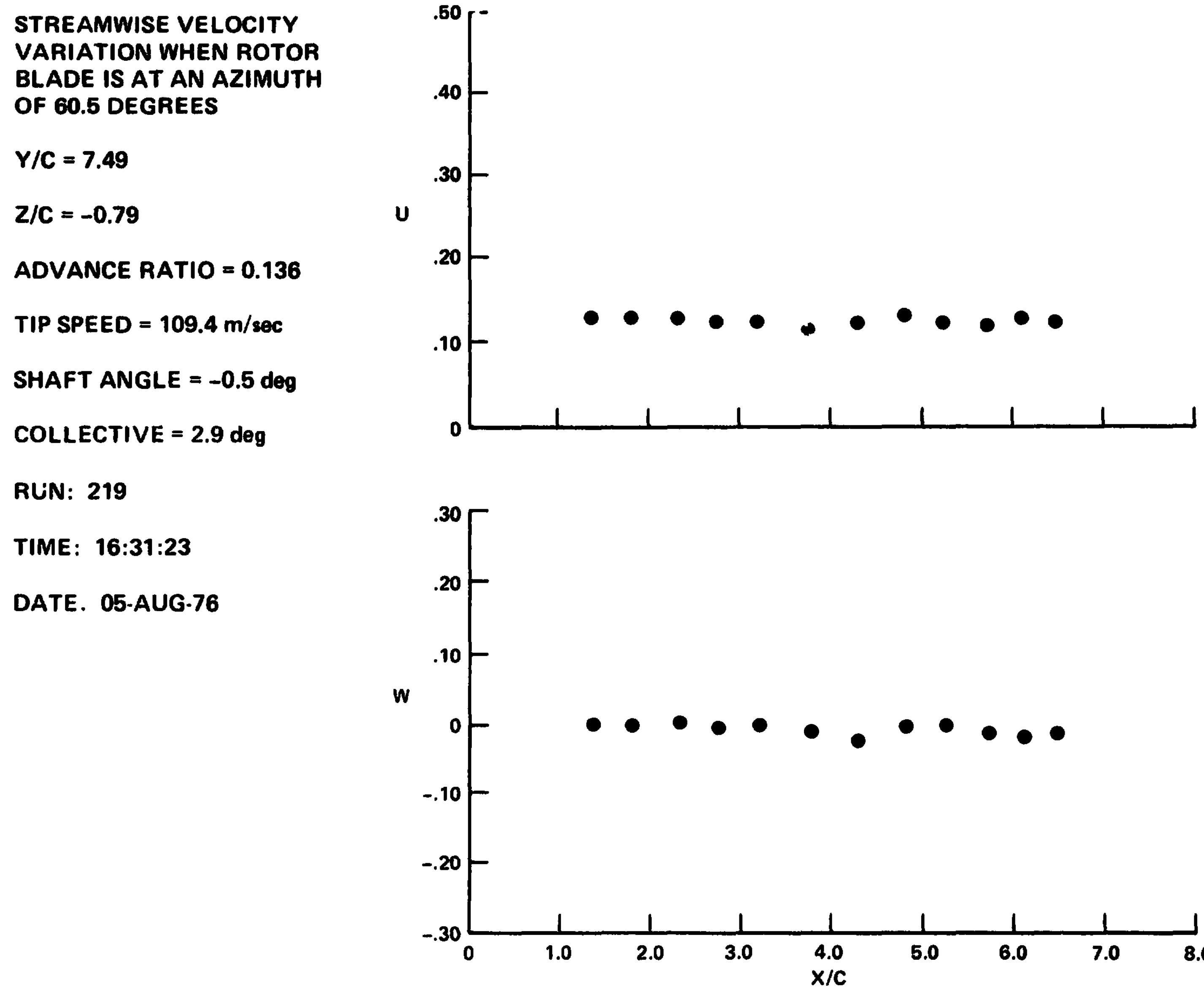

15-7. Streamwise traverse, y/c = 5.98, z/c = -0.41

Figure 15. (Concluded)

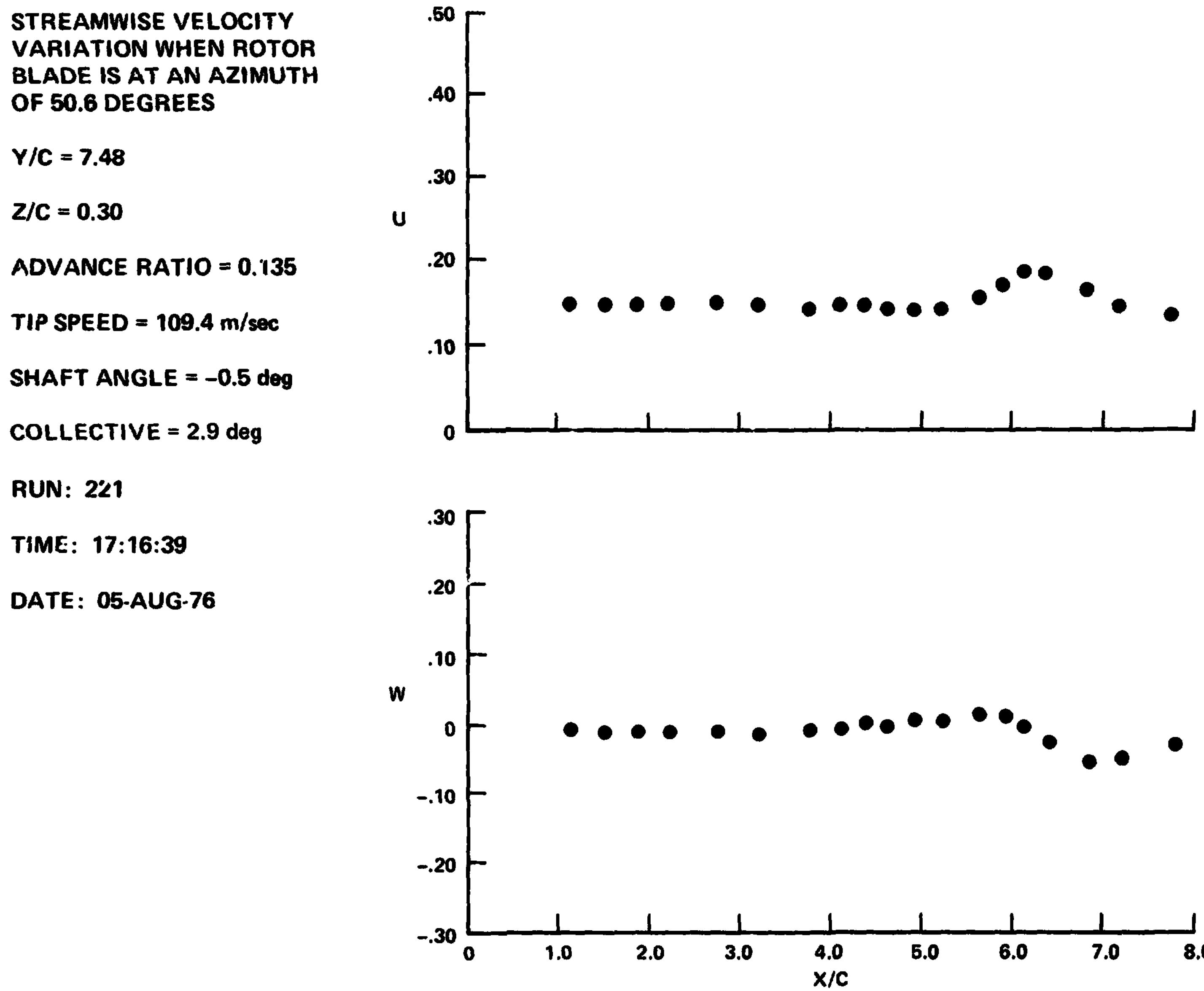

16-1. Streamwise traverse, $y/c = 7.49$, $z/c = 0.30$

Figure 16. Flowfield velocities from the -11° twist blades, $V/\Omega R = 0.137$, $\theta_{0.75R} = 2.94^{\circ}$, $\psi = 50.6^{\circ}$, $N = 1000$.

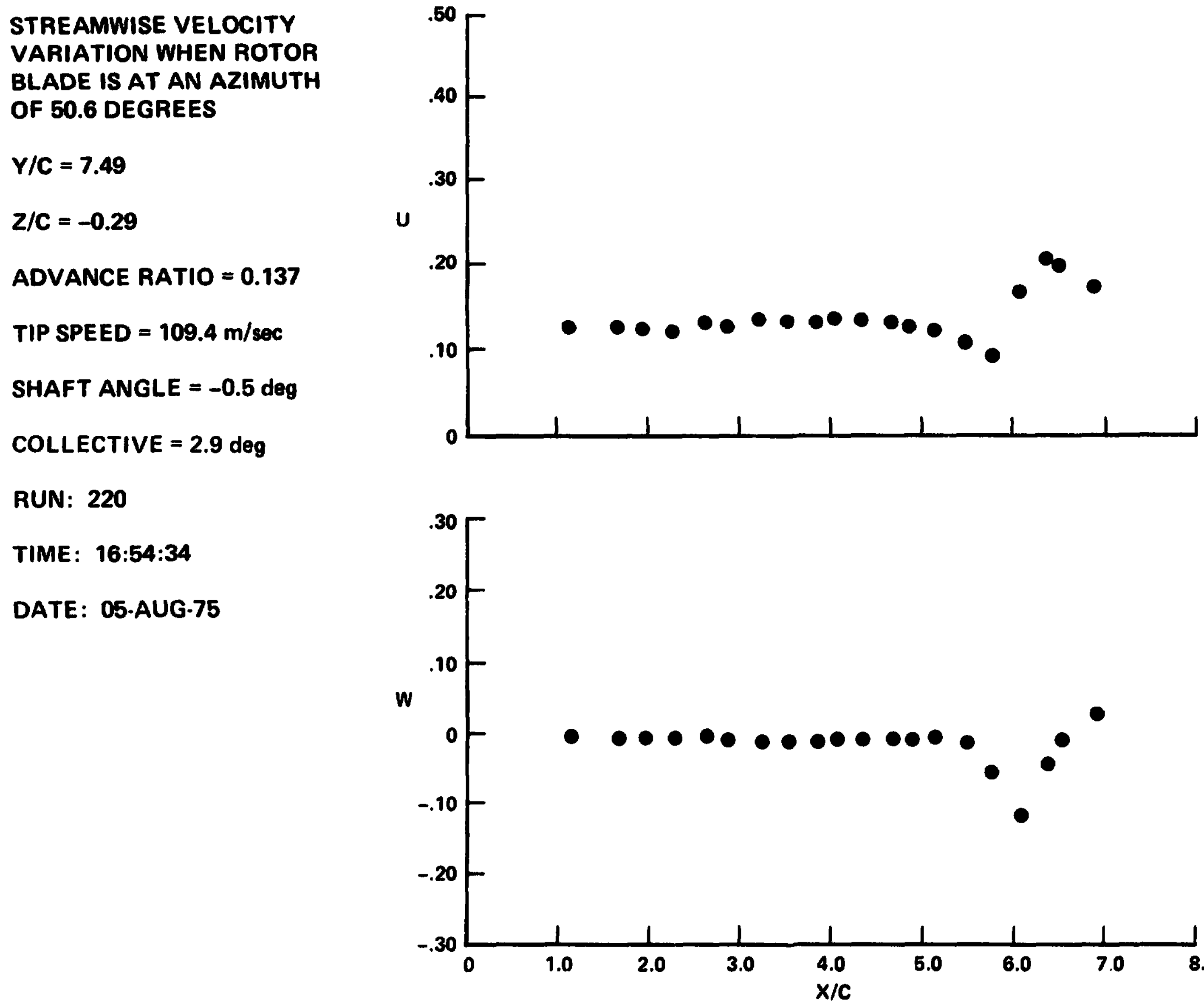

16-2. Streamwise traverse, y/c = 7.49, z/c = -0.01

Figure 16. (Continued)

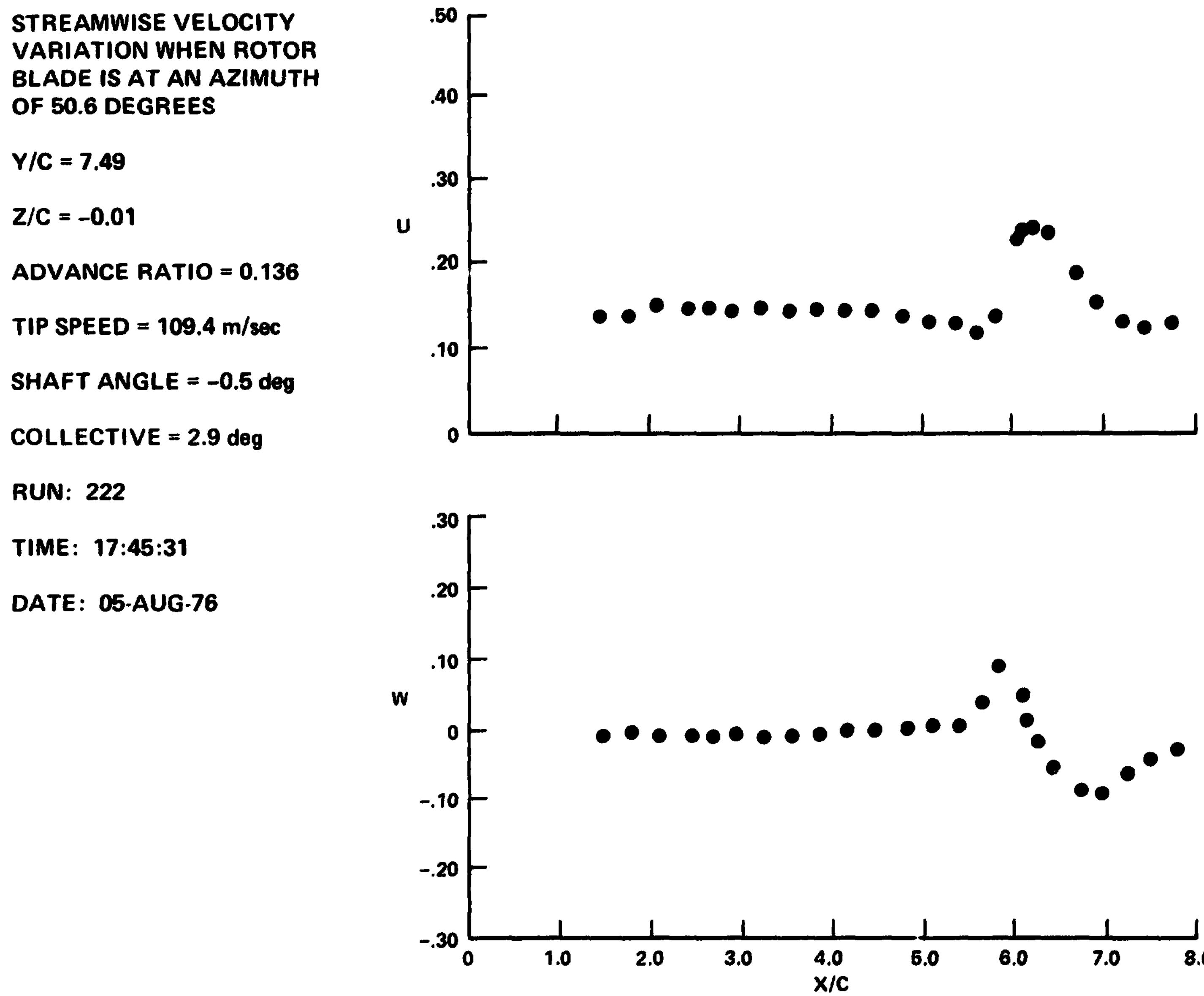

16-3. Streamwise traverse, y/c = 7.49, z/c = -0.29

Figure 16. (Continued)

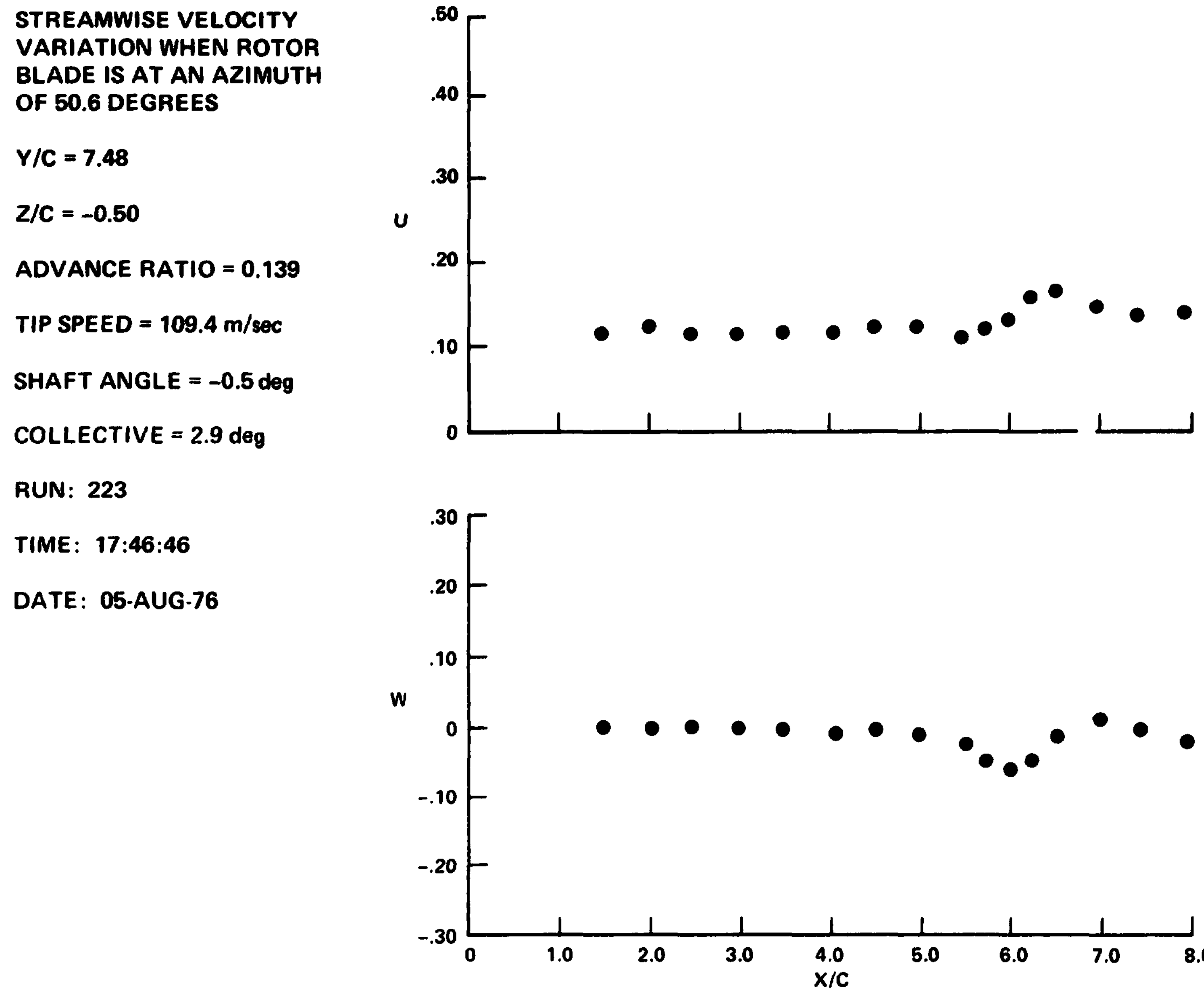

16-4. Streamwise traverse, y/c = 7.49, z/c = -0.50

Figure 16. (Continued)

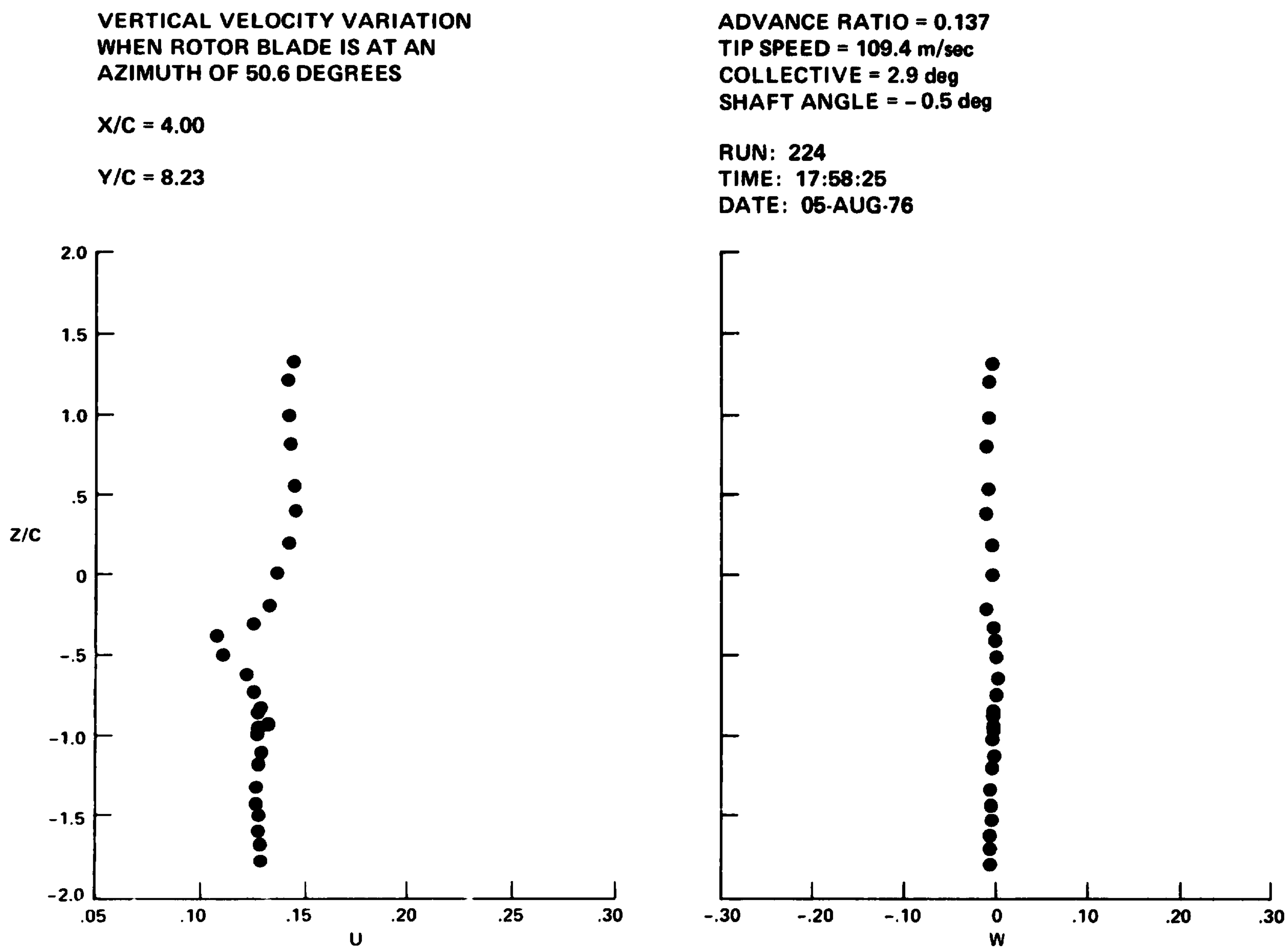

16-5. Vertical traverse, x/c = 4.00, y/c = 8.23

Figure 16. (Concluded)